

Vanillin and Syringaldehyde from Side Streams of Pulp and Paper Industries and Biorefineries

Dissertation presented to Faculdade de Engenharia da Universidade do Porto for the
PhD degree in Chemical and Biological Engineering

by

Carina Andreia Esteves da Costa

Supervisor: Prof. Dr. Alírio Egídio Rodrigues
Co-supervisor: Dr. Paula Cristina de Oliveira Rodrigues Pinto



Laboratory of Separation and Reaction Engineering - Laboratory of Catalysis and Materials
Department of Chemical Engineering, Faculty of Engineering, University of Porto

March, 2017

FEUP, LSRE-LCM - Universidade do Porto

© Carina Andreia Esteves da Costa, 2017

All rights reserved

This thesis was financially supported by Fundação para a Ciência e a Tecnologia (Portugal) through the PhD grant SFRH/BD/89570/2012. This work was also financially supported by: Project POCI-01-0145-FEDER-006984 – Associate Laboratory LSRE-LCM funded by FEDER through COMPETE2020 - Programa Operacional Competitividade e Internacionalização (POCI) – and by national funds through FCT - Fundação para a Ciência e a Tecnologia.



ACKNOWLEDGEMENTS

Começar por agradecer ao orientador desta tese, o Professor Alírio Rodrigues, que me permitiu fazer parte deste grupo que é o LSRE-LCM. A ele agradeço todo o apoio e acompanhamento ao longo deste período. Um obrigado por me continuar a acolher!

Um enorme obrigado de coração à Dr. Paula Pinto. Ela que me transmitiu este interesse especial pelo mundo da lenhina. Obrigada por todos os valores que me transmitiste; ensinaste-me o verdadeiro significado da palavra resiliência. Trabalhar contigo foi uma ótima experiência e se a isso juntar a pessoa maravilhosa e amiga que és então só peço para te ter sempre por perto, quer na vida pessoal quer na profissional.

Devo também um grande agradecimento a todos os amigos e colegas do laboratório, em especial aqueles que ajudam a tornar os dias mais cinzentos, com resultados negros e falta de ânimo num dia mais feliz (um obrigado especial às meninas!). Um beijinho especial à Inês, a minha metade profissional; agradecer por seres uma companheira de trabalho com quem é tão fácil trabalhar e por seres uma pessoa tão querida.

Aos meus amigos mais especiais, aqueles que estão sempre por perto e que sabem tão bem provocar-me os sorrisos mais espontâneos ou as lágrimas mais sinceras. Não os quero nomear, mas todos eles sabem que fazem parte do meu coração, são eles os primeiros com quem partilho as boas notícias ou a quem recorro nas dificuldades.

Um agradecimento especial a toda a minha família. Em especial aos meus pais para quem até os piores resultados são dignos de publicação. Para eles nunca haverá agradecimento suficiente face ao seu apoio incondicional. À minha irmã, por me ensinar que não há limite para opiniões e reclamações; é muito bom ter-te sempre por perto e pronta a ajudar (obrigada pelos vetores) ;)

Ao Pedro, sem querer entrar em banalismsos e frases feitas, dizer-te apenas que a nossa relação é o meu resultado mais fidedigno e que juntos e muito felizes esperamos de coração cheio a nossa pequena réplica (um carinho especial para ele/a).

ABSTRACT

The work developed in this thesis intends to study the production of vanillin and syringaldehyde by oxidative depolymerization of lignins from lignin-rich side streams of pulp and paper industry and/or biorefineries. Researches worldwide confirm the importance of lignin in the scenario of the integration of biorefinery concept and the efforts are focused in the study of alternatives as sources of chemicals. Lignin is an aromatic biopolymer naturally abundant with high potential for valorization. One of the routes is the production of vanillin and syringaldehyde by lignin oxidation with O₂, an environmental friendly process. Vanillin is a phenolic compound with increasing demand in international market. Syringaldehyde is not hitherto produced from lignin; however, as vanillin, it is a valuable starting chemical for the pharmaceutical industry, and could be produced from lignin as well. However, lignin complexity and structural diversity within the same molecule is delaying a more generalized exploitation of its functionality comparatively, for example, to cellulose.

The characterization and comparative evaluation of lignins from different biomass species, different morphological parts of the same species and submitted to different delignification processes were accomplished in this thesis. Lignin-rich side streams and isolated lignins were studied through their composition in inorganic material and sugars. Characterization was accomplished by nitrobenzene oxidation, ¹³C, ³¹P, ¹H and HSQC NMR and FTIR spectroscopy. Data on lignin structure, particularly key characteristics such as H:G:S ratio, degree of condensation, and β-O-4 content, allowed inferring about its potential as raw-material to produce aldehydes, such as vanillin and syringaldehyde. All the lignins were classified according to a radar classification tool built with selected descriptors, simplifying the evaluation and discussion of the impact of the delignification process, species, and morphologic part on lignin structure. This comparative study about lignin potential represents an essential tool for the further selection of lignins and/or processes to a possible route of valorization within a lignocellulosic-based biorefinery.

The evaluation of the potential of selected lignins for production of functionalized aldehydes by oxidative depolymerization was also performed. Industrial *Eucalyptus globulus* sulfite liquor and kraft liquors (collected at different stages of processing before the recovery boiler) were evaluated according to their potential for the production of syringaldehyde and vanillin by

oxidation with O₂ in alkaline medium. Oxidations were performed in a jacketed batch reactor with controlled temperature, total and O₂ partial pressure, and with defined values of NaOH and lignin concentration by direct reaction of pulping liquors and reaction of kraft lignins isolated from liquors. An ethanol organosolv lignin from tobacco stalks was also submitted to oxidation and the effect of selected reaction conditions (initial lignin concentration, temperature and partial pressure of O₂) was studied in order to achieve the best conditions to reach the maximum yields of phenolic monomers. The kinetic study of products formation from this lignin was attained and the results led to the evaluation of its potential as source of vanillin and syringaldehyde.

In a further stage, an industrial kraft liquor was subjected to ultrafiltration using tubular ceramic membranes aiming the fractionation of lignin according to its molecular weight. The composition and characterization of each resulting fraction and the respective isolated lignin was accessed by means of different analytical techniques. The structural information accomplished led to a complete study about the functionality and reactivity of each ultrafiltration fraction in view of their valorization as source of added-value products and valuable chemicals in the context of a second generation biorefinery.

All the work developed in this thesis opens good perspectives from the point of view of pulp and paper industry, aiming for diversification of products and side-streams valorization.

RESUMO

O trabalho desenvolvido nesta tese tem como principal objetivo estudar o processo de produção de vanilina e seringaldeído através da despolimerização oxidativa de lenhinas obtidas a partir de correntes processuais de indústrias de pasta e papel e/ou biorrefinarias. Existe um vasto número de estudos que confirmam a relevância da lenhina e a importância da sua integração no âmbito das biorrefinarias como fonte de produtos alternativos aos obtidos na indústria petroquímica. A lenhina é um polímero aromático naturalmente abundante e com elevado potencial de valorização. Uma das suas possíveis vias de valorização é a produção de vanilina e seringaldeído por oxidação com O₂. A vanilina é um composto fenólico com um crescente interesse no mercado internacional. O seringaldeído, apesar de atualmente não ser produzido diretamente a partir da lenhina é, tal como a vanilina, um importante produto químico com elevado interesse na indústria farmacêutica. Contudo, a complexidade da lenhina e a sua diversidade estrutural dificultam o estudo da sua funcionalidade e reatividade com vista à sua valorização como fonte de fenólicos de valor acrescentado.

Lenhinas obtidas a partir de diferentes espécies de biomassa, diferentes partes morfológicas da mesma espécie e diferentes processos de deslenhificação foram caracterizadas e avaliadas nesta tese. As lenhinas foram estudadas considerando a sua composição em material inorgânico e açúcares. A caracterização foi efetuada por oxidação com nitrobenzeno, RMN de ¹³C, ³¹P, ¹H e HSQC e também FTIR. A informação estrutural obtida, especialmente características como a razão H:G:S, o grau de condensação e o conteúdo em estruturas β-O-4, permitem inferir acerca do potencial das lenhinas como matéria-prima para produção de aldeídos, como a vanilina e o seringaldeído. Todas as lenhinas foram classificadas e avaliadas através de radares, usando como descritores as suas principais características estruturais. Este tipo de representação simplifica a avaliação e discussão do impacto que o processo de deslenhificação, a espécie e a parte morfológica representam na estrutura da lenhina. Este estudo, centrado no potencial das lenhinas, representa uma ferramenta essencial para a seleção de lenhinas e/ou processos considerando uma possível via de valorização no âmbito das biorrefinarias lenhocelulósicas.

O estudo do potencial de lenhinas para produção de aldeídos funcionalizados através da despolimerização oxidativa foi outro dos objetivos desta tese. Licores *Eucalyptus globulus* obtidos através de processos industriais sulfito e kraft foram avaliados de acordo com a sua propensão para

produzir vanilina e seringaldeído por oxidação com O₂ em meio alcalino. As oxidações dos licores e das lenhinas isoladas foram efetuadas num reator batch com condições controladas de temperatura, pressão total e pressão parcial de O₂ e valores definidos de concentração de NaOH e lenhina. Uma lenhina de tabaco obtida a partir do processo organosolv com etanol foi também submetida a oxidação e o efeito da concentração inicial de lenhina, temperatura e pressão parcial de O₂ foi estudado com o objetivo de encontrar as condições que permitem atingir os rendimentos máximos de fenólicos. O estudo cinético da formação dos produtos de oxidação desta lenhina foi também efetuado e os resultados permitiram uma avaliação do seu potencial como fonte de vanilina e seringaldeído.

Numa última etapa, licor kraft industrial foi submetido a ultrafiltração através de membranas cerâmicas tubulares visando o fracionamento da lenhina de acordo com o seu peso molecular. A composição e caracterização de cada fração obtida e das respectivas lenhinas isoladas foram avaliadas através de diferentes métodos e técnicas analíticas. A informação estrutural obtida permitiu o estudo sobre a funcionalidade e reatividade de cada fração do processo de ultrafiltração com vista à sua valorização como fonte de produtos de valor acrescentado no contexto das biorrefinarias.

Todo o trabalho desenvolvido nesta tese é um importante contributo que abre novas perspectivas no âmbito das indústrias de pasta e de papel visando a diversificação dos seus produtos e valorização das correntes processuais.

ABBREVIATIONS

A - constant in the Arrhenius equation

A_m - membrane surface area

Ara - arabinose

ATZ - alumina-titania-zirconia

BSTFA - N,O-bis-(trimethylsilyl)-trifluoroacetamide

BTX - benzene, toluene, xylene

C - carbon

CA - coumarates

$CDCl_3$ - deuterated chloroform

$Corn_{root}$ - roots of corn

$Corn_{stalk}$ - stalks of corn

$Cotton_{root}$ - roots of cotton

$Cotton_{stalk}$ - stalks of cotton

DC - degree of condensation

DMF - dimethylformamide

DMS - dimethyl sulfide

DMSO - dimethyl sulfoxide

$DMSO-d_6$ - deuterated dimethyl sulfoxide

DP - degradation products

E_a - activation energy

EKL - industrial kraft liquor of eucalyptus wood collected after the evaporation stage

EKL_{lig} - lignin isolated by mild acidolysis from EKL liquor

FA - ferrulates

FTIR - Fourier transform infrared spectroscopy

G - guaiacyl

Gal - galactose

GC-FID - gas chromatography with flame ionization detector

GC-MS - gas chromatography mass spectrometry

Glc - glucose

GPC - gel permeation chromatography

H - *p*-hydroxyphenyl

H₂SO₄ - sulfuric acid

HCl - hydrogen chloride

HPLC - high performance liquid chromatography

HSQC - heteronuclear single quantum coherence

HTKL - industrial kraft liquor of eucalyptus wood collected after heat treatment just before the recovery furnace

HTKL_{lig} - lignin isolated by mild acidolysis from HTKL liquor

Hy - *p*-hydroxybenzaldehyde

J - permeate flux (m³.s⁻¹.m⁻²)

J_w - water permeate flux

KBr - potassium bromide

k_{degrad} - degradation rate constant

KL - industrial kraft liquor of eucalyptus wood collected at the outlet of kraft digester (thin liquor)

KL_{lig} - lignin isolated by mild acidolysis from KL liquor

k_{oxid} - production rate constant

LCorn_{root} - lignin isolated by mild acidolysis from corn roots

LCorn_{stalk} - lignin isolated by mild acidolysis from corn stalks

LCotton_{root} - lignin isolated by mild acidolysis from cotton roots

LCotton_{stalk} - lignin isolated by mild acidolysis from cotton stalks

LEg_{bark} - lignin isolated by mild acidolysis from eucalyptus bark

LEg_{Kraft} - lignin isolated and further purified from industrial kraft liquor of eucalyptus wood

LEg_{Org} - lignin produced by ethanol organosolv process of eucalyptus wood

LEg_{wood} - lignin isolated by mild acidolysis from eucalyptus wood

LiCl - lithium chloride

LLC - lignin-carbohydrate complexes

L_p - membrane permeability coefficient

LP_{5kDa} - lignin isolated by mild acidolysis from the permeate obtained from 5 kDa membrane

LR_{15kDa} - lignin isolated by mild acidolysis from the retentate obtained from 15 kDa membrane

LR_{50kDa} - lignin isolated by mild acidolysis from the retentate obtained from 50 kDa membrane

LR_{5kDa} - lignin isolated by mild acidolysis from the retentate obtained from 5 kDa membrane

LS - eucalyptus lignosulfonate

LSCane_{root} - lignin isolated by mild acidolysis from sugarcane roots

LSCane_{stalk} - lignin isolated by mild acidolysis from sugarcane stalks

LTobO_{but} - lignin produced by butanol organosolv process of tobacco stalks

LTobO_{ethan} - lignin produced by ethanol organosolv process of tobacco stalks

LTob_{root} - lignin isolated by mild acidolysis from tobacco roots

LTobSE - lignin produced by steam explosion process of tobacco stalks

LTob_{stalk} - lignin isolated by mild acidolysis from tobacco stalks

M - molecular mass

Man - mannose

Mn - number-average molecular weight

Mw - weight-average molecular weight

N - nitrogen

NaBH₄ - sodium borohydride

NaOH - sodium hydroxide

NCS - non-condensed structures

NMR - nuclear magnetic resonance

NO - nitrobenzene oxidation

O₂ - oxygen

OCH₃ - methoxyl groups

OH_{ph} - phenolic groups

P_{5kDa} - permeate obtained from 5 kDa membrane

PHBA - *p*-hydroxy benzoic acids

*p*O₂ - oxygen partial pressure

ppu - phenylpropane unit

*Q*_{*p*} - permeate flowrate

R - universal gas constant

R_{15kDa} - retentate obtained from 15 kDa membrane

R_{50kDa} - retentate obtained from 50 kDa membrane

R_{5kDa} - retentate obtained from 5 kDa membrane

Rha - rhamnose

*R*_{*m*} - membrane hydraulic resistance coefficient (m⁻¹)

S - syringyl

SA - syringic acid

SCane_{root} - roots of sugarcane

SCane_{stalk} - stalks of sugarcane

sccpm - standard cubic centimeter per minute

SL - industrial spent liquor from magnesium-based acidic sulfite pulping of eucalyptus wood collected after the evaporation step (referred as sulfite liquor)

SO - acetosyringone

SPE - solid phase extraction

Sy - syringaldehyde

T - temperature

TDS - total dissolved solids

TiO₂-Al₂O₃ - titanium dioxide-aluminium oxide

TMP - transmembrane pressure (Pa)

TMS - chlorotrimethylsilane

Tob_{root} - roots of tobacco

Tob_{stalk} - stalks of tobacco

V - vanillin

VA - vanillic acid

VCF - volume concentration factor

VO - acetovanillone

VR - volume reduction

Xyl - xylose

ZrO₂ - zirconium dioxide

μ_0 - viscosity of water at 25 °C

Table of Contents

1	INTRODUCTION	1
1.1	Relevance and motivation	2
1.2	Objectives	3
1.3	Outline	4
1.4	References	5
2	STATE OF THE ART	7
2.1	Pulp and paper industries and biorefineries	7
2.2	Lignin valorization	8
2.3	Lignin chemistry and structure.....	10
2.3.1	Lignin characterization: techniques and methods.....	13
2.4	Lignin depolymerization	14
2.4.1	Vanillin and syringaldehyde.....	15
2.4.2	Lignin oxidation in alkaline medium	16
2.4.2.1	Kinetic study of oxidation products	18
2.5	Lignin fractionation by ultrafiltration.....	20
2.6	The integrated process for vanillin production.....	22
2.7	References	23
3	CHARACTERIZATION AND COMPARATIVE EVALUATION OF HARDWOOD LIGNINS	35
3.1	Introduction	36
3.2	Experimental section: materials and methods	36
3.2.1	<i>E. globulus</i> lignin samples.....	36
3.2.2	Lignin isolation by mild acidolysis	37
3.2.3	Kraft lignin purification.....	37
3.2.4	Preliminary analysis of lignins	37

3.2.4.1 Inorganics content.....	37
3.2.4.2 Carbohydrate content.....	38
3.2.4.3 Elemental analysis	39
3.2.5 Structural characterization of <i>E. globulus</i> lignins	39
3.2.5.1 Nitrobenzene oxidation (NO)	39
3.2.5.2 ¹³ C NMR	40
3.2.5.3 ³¹ P NMR	40
3.2.5.4 ¹ H NMR.....	41
3.3 Composition of <i>E. globulus</i> lignins	41
3.4 Structural characterization of <i>E. globulus</i> lignins	42
3.4.1 Analysis by NO.....	42
3.4.2 ¹³ C NMR	43
3.4.3 ³¹ P NMR.....	48
3.4.4 ¹ H NMR	51
3.5 Empirical formula and molecular mass of ppu.....	53
3.6 Assessing correlations between structural features and NO yields.....	54
3.6.1 DC, S:G:H ratio and correlations with NO results.....	54
3.6.2 Syringyl/guaiacyl ratio (S/G): comparison between methodologies.....	57
3.7 Radar tool for lignins evaluation.....	58
3.7.1 Radar classification of <i>E. globulus</i> lignins from different delignification processes	59
3.7.2 Radar classification of lignins from different morphologic parts of <i>E. globulus</i>	61
3.8 Conclusions.....	61
3.9 References.....	62
4 CHARACTERIZATION AND COMPARATIVE EVALUATION OF INDUSTRIAL CROPS LIGNINS	67
4.1 Introduction	68
4.2 Experimental section: materials and methods	68
4.2.1 Industrial crops and lignins: samples description	68
4.2.2 Lignin content	69
4.2.3 Inorganic and carbohydrates content	69
4.2.4 Nitrobenzene oxidation.....	69
4.2.5 2D-NMR spectral analysis: HSQC spectra	70
4.2.6 FTIR.....	70
4.3 Structural characterization of stalks, roots and isolated lignins	70

4.3.1 Composition of stalks, roots and isolated lignins	70
4.3.2 Analysis by NO	72
4.3.3 ¹³ C NMR.....	74
4.3.4 HSQC spectra of corn stalks lignin	80
4.3.5 ³¹ P NMR	84
4.3.6 FTIR.....	86
4.4 Structural characterization of tobacco lignins.....	87
4.4.1 <i>N. tabacum</i> lignins: description and composition.....	87
4.4.2 Analysis by NO	89
4.4.3 ¹³ C NMR.....	89
4.5 Radar classification of industrial crops lignins.....	92
4.6 Radar classification of tobacco lignins.....	94
4.7 Conclusions	96
4.8 References	97
5 LIGNINS OXIDATION IN ALKALINE MEDIUM.....	103
5.1 Introduction	104
5.2 Experimental section: materials and methods.....	104
5.2.1 Sulfite and kraft liquors and lignins: description.....	104
5.2.2 Lignins isolation.....	105
5.2.3 Characterization of pulping liquors and lignins	105
5.2.3.1 Total dissolved solids and ash content	105
5.2.3.2 Carbohydrate content	105
5.2.3.3 Nitrobenzene oxidation	106
5.2.4 Oxidation experiments	106
5.2.5 Extraction and analysis of the oxidation products	107
5.3 Oxidation of lignin from eucalyptus pulping liquors	107
5.3.1 Composition of pulping liquors and lignins	107
5.3.2 Characterization of liquors and lignins by NO	109
5.3.3 Oxidation of liquors and isolated lignins with O ₂ in alkaline medium.....	110
5.3.4 Conclusions	115
5.4 Oxidation of ethanol organosolv lignin from tobacco stalks	116
5.4.1 Influence of oxidation conditions on the phenolics products yield	117
5.4.1.1 Lignin initial concentration	117
5.4.1.2 Partial pressure of O ₂	119
5.4.1.3 Initial temperature.....	120

5.5 Kinetics of phenolics production from tobacco lignin oxidation	122
5.5.1 Kinetic study of LTobO _{ethan} oxidation	124
5.5.2 Effect of initial lignin concentration	124
5.5.1 Effect of oxygen partial pressure	126
5.5.2 Effect of initial temperature	128
5.5.3 Conclusions.....	129
5.6 Experimental validation of the radar classification of tobacco lignins.....	130
5.7 References.....	131
6 LIGNIN FRACTIONATION BY ULTRAFILTRATION	135
6.1 Introduction	136
6.2 Experimental section: materials and methods	136
6.2.1 Kraft liquor	136
6.2.2 Ultrafiltration equipment and experimental set-up	137
6.2.3 Composition of fractions and isolated lignins.....	138
6.2.4 Nitrobenzene oxidation.....	138
6.2.5 NMR analysis	138
6.2.6 Gel permeation chromatography (GPC)	138
6.3 Ultrafiltration process	139
6.3.1 Water membrane permeability.....	139
6.3.2 Permeate flux	140
6.3.3 Membrane fouling and cleaning.....	143
6.4 Composition and structure of fractions and isolated lignins	144
6.4.1 Composition of ultrafiltration fractions	144
6.4.2 Composition of isolated lignins	146
6.4.3 Nitrobenzene oxidation of isolated lignins.....	147
6.4.4 NMR analysis of isolated lignins	148
6.4.4.1 ¹³ C NMR	148
6.4.4.2 ³¹ P NMR	151
6.4.5 Molecular weight distribution of isolated lignins by GPC.....	153
6.5 Radar classification of isolated lignins from ultrafiltration fractions.....	155
6.6 Conclusions.....	156
6.7 References.....	157
7 FINAL CONCLUSIONS AND SUGGESTIONS FOR FUTURE WORK.....	161

7.1 Final conclusions.....	162
7.2 Suggestions for future work.....	163
7.2.1 Lignin as a polymer component	164
7.2.2 Future research lines.....	166
7.3 References	167

List of Figures

Figure 1 - Average distribution of the main biomass constituents: cellulose, hemicellulose, and lignin (FitzPatrick et al., 2010; Ragauskas et al., 2014).....	8
Figure 2 – Lignin production and potential lignin derived product market and value (Gosselink, 2011).	9
Figure 3 - <i>p</i> -Coumaryl (1), coniferyl (2), and sinapyl (3) alcohols.	10
Figure 4 – Main structural moieties of native and technical lignins (Pandey and Kim, 2011).	11
Figure 5 - Structure of vanillin (4-hydroxy-3-methoxybenzaldehyde) and syringaldehyde (4-hydroxy-3,5-dimethoxybenzaldehyde)	15
Figure 6 – Flow sheet of the integrated process for production of value-added aldehydes and polymers from kraft lignin in a biorefinery concept (Borges da Silva et al., 2009).	23
Figure 7 - Quantitative ¹³ C NMR spectra of (a) LEgOrg, (b) LEgKraft, (c) LEgwood, and (d) LEgbark (in DMSO-d ₆ ; * solvent peak (Hugo et al., 1997)).....	44
Figure 8 - Expanded δ 165-95 ppm region of quantitative ¹³ C NMR spectrum of (a) LEgOrg, (b) LEgKraft, (c) LEgwood, and (d) LEgbark (in DMSO-d ₆).....	45
Figure 9 - Quantitative ³¹ P NMR spectra (δ 155-130 ppm) of phosphitylated lignins (a) LEgOrg, (b) LEgKraft, (c) LEgwood, and (d) LEgbark (in CDCl ₃).....	49
Figure 10 - ¹ H NMR spectra, in CDCl ₃ , of acetylated lignins (a) LEgOrg, (b) LEgKraft, (c) LEgwood and (d) LEgbark. (* CDCl ₃ ; ** dichloromethane; *** methanol: contaminants from the acetylation process (Hugo et al., 1997)).....	52
Figure 11 - Plot of NO yield versus DC values obtained for <i>E. globulus</i> lignins.	56
Figure 12 - Plot of β-O-4 content versus DC values obtained for <i>E. globulus</i> lignins.	56
Figure 13 - Plot of NO yield versus S/G, from ³¹ P NMR, obtained for <i>E. globulus</i> lignins.	58
Figure 14 - Radar classification for eucalyptus wood lignins produced by different processes.	60
Figure 15 - Radar classification for acidolysis lignins obtained from wood and bark of eucalyptus.	61
Figure 16 - Yields of monomeric phenolic products obtained by NO of stalks (S) and roots (R) and the respective isolated lignins (L) from corn, cotton, sugarcane, and tobacco, reported on lignin basis.	73
Figure 17 - Quantitative ¹³ C NMR spectra of (a) LCorn _{stalk} , (b) LCotton _{stalk} , (c) LSCane _{stalk} , and (d) LTob _{stalk} (in DMSO-d ₆ ; * solvent peak (Hugo et al., 1997); C - carbohydrates contamination).	75
Figure 18 - Quantitative ¹³ C NMR spectra (a) LCorn _{root} , (b) LCotton _{root} , (c) LSCane _{roots} , and (d) LTob _{root} (in DMSO-d ₆ ; * solvent peak (Hugo et al., 1997); C - carbohydrates contamination).....	76

Figure 19 - Quantitative ^{13}C NMR spectra of LCotton _{stalk} before (a) and after (b) purification (in DMSO- d_6 ; * solvent peak (Hugo et al., 1997)).	79
Figure 20 - Quantitative ^{13}C NMR spectra of LSCane _{root} before (a) and after (b) purification (in DMSO- d_6 ; * solvent peak (Hugo et al., 1997); C - carbohydrates contamination).	79
Figure 21 - Side-chain (∂_C/∂_H 50-90/2.5-5.5) and aromatic/unsaturated (∂_C/∂_H 90-160/6.0-8.0) regions in the HSQC NMR spectrum of corn stalks lignin (see Table 23 for signal assignments).	81
Figure 22 - Quantitative ^{31}P NMR spectra (δ 155-130 ppm) of phosphitylated lignins: (a) LCorn _{stalk} , (b) LCotton _{stalk} , (c) LSCane _{stalk} , and (d) LTob _{stalk} (in CDCl_3).	85
Figure 23 - FTIR absorption spectra of (a) LCorn _{stalk} , (b) LCotton _{stalk} , (c) LSCane _{stalk} , (d) LTob _{stalk} , (e) LCorn _{root} , (f) LCotton _{root} , (g) LSCane _{root} , and (h) LTob _{root} .	86
Figure 24 - Quantitative ^{13}C NMR spectra of (a) LTobO _{but} , (b) LTobO _{ethan} , (c) LTobSE, and (d) LTob _{stalk} (DMSO- d_6 ; * solvent peak (Hugo et al., 1997)).	91
Figure 25 - Radar classification for stalks lignins from corn, cotton, sugarcane, and tobacco.	93
Figure 26 - Radar classification for roots lignins from corn, cotton, sugarcane, and tobacco.	94
Figure 27 - Radar classification for tobacco lignins produced by different processes.	95
Figure 28 - Experimental setup for batch oxidation of lignins and pulping liquors.	106
Figure 29 – Yields of monomeric phenolic products obtained by NO of pulping liquors (A) and lignins (B).	109
Figure 30 – Time evolution of monomeric products (V, VA, VO, Hy, Sy, SA, and SO) and pH of reaction medium during the oxidation of <i>E. globulus</i> pulping liquors KL (A and B), EKL (C and D), HTKL (E and F), and SL (G and H). General conditions: solids concentration 60 g/L, $\text{pH} \geq 13.8$, $p\text{O}_2 = 3$ bar, $P_{\text{total}} = 9.8$ bar.	111
Figure 31 - Time evolution of monomeric products (V, VA, VO, Hy, Sy, SA, and SO) and pH of reaction medium during the oxidation of isolated lignins KLLig (A and B), EKLLig (C and D), HTKLLig (E and F) from <i>E. globulus</i> kraft liquors. General conditions: solids concentration 60 g/L, $\text{pH} \geq 13.8$, $p\text{O}_2 = 3$ bar, $P_{\text{total}} = 9.8$ bar, $T_{\text{initial}} = 393$ K.	112
Figure 32 – Time evolution of temperature and O_2 uptake during the oxidation of liquors and lignins: KL (A), KLLig (B), EKL (C), EKLLig (D), HTKL (E), HTKLLig (F), and SL (G). General conditions: lignin concentration 60 g/L, $\text{pH} \geq 13.8$, $p\text{O}_2 = 3$ bar, $P_{\text{total}} = 9.8$ bar, $T_{\text{initial}} = 120$ °C.	113
Figure 33 - Yields of Sy, SA, V, and VA produced in the oxidation of pulping liquors and lignins with O_2 in alkaline medium (lignin concentration 60 g/L, $\text{pH} \geq 13.8$, $p\text{O}_2 = 3$ bar, $P_{\text{total}} = 9.8$ bar, $T_{\text{initial}} = 120$ °C).	115
Figure 34 – Time evolution of monomeric products (V, VA, VO, Hy, Sy, SA, and SO) and pH of reaction medium during the oxidation reaction with different initial concentrations of LTobO _{ethan} : 15 g/L (A	

and B), 30 g/L (C and D), and 60 g/L (E and F). General conditions: $T_{\text{initial}} = 393 \text{ K}$, $\text{pH} \geq 13.8$, $P_{\text{total}} = 9.8 \text{ bar}$, and $p\text{O}_2 = 3 \text{ bar}$	118
Figure 35 – Time evolution of monomeric products (V, VA, VO, Hy, Sy, SA, and SO) and pH of reaction medium during the oxidation of LTobO _{ethan} with different partial pressures of oxygen: 2 bar (A and B), 3 bar (C and D), and 4 bar (E and F). General conditions: lignin concentration 60 g/L, $T_{\text{initial}} = 393 \text{ K}$, $\text{pH} \geq 13.8$, and $P_{\text{total}} = 9.8 \text{ bar}$	120
Figure 36 – Time evolution of monomeric products (V, VA, VO, Hy, Sy, SA, and SO) and pH of reaction medium during the oxidation of LTobO _{ethan} with different initial temperatures of reaction: 393 K (A and B), 413 K (C and D), and 433 K (E and F). General conditions: lignin concentration 60 g/L, $\text{pH} \geq 13.8$, $P_{\text{total}} = 9.8 \text{ bar}$, $p\text{O}_2 = 3 \text{ bar}$	121
Figure 37 – Effect of initial LTobO _{ethan} concentration (15, 30, 60 g/L) on V and Sy concentration during oxidation. General conditions: $T_{\text{initial}} = 393 \text{ K}$, $\text{pH}_{\text{initial}} \geq 13.8$, $P_{\text{total}} = 9.8 \text{ bar}$, $p\text{O}_2 = 3 \text{ bar}$	125
Figure 38 – Initial reaction rate of V and Sy production as a function of initial LTobO _{ethan} concentration.	125
Figure 39 - Effect of partial pressure of O ₂ (2, 3, 4 bar) on V and Sy concentration during LTobO _{ethan} oxidation. General conditions: lignin concentration 60 g/L, $T_{\text{initial}} = 393 \text{ K}$, $\text{pH}_{\text{initial}} \geq 13.8$, $P_{\text{total}} = 9.8 \text{ bar}$	126
Figure 40 - Initial reaction rate of V and Sy production as a function of partial pressure of O ₂	127
Figure 41 - Effect of initial temperature (393, 413, 433 K) on V and Sy concentration during LTobO _{ethan} oxidation. General conditions: lignin concentration 60 g/L, $\text{pH}_{\text{initial}} \geq 13.8$, $P_{\text{total}} = 9.8 \text{ bar}$, $p\text{O}_2 = 3 \text{ bar}$	128
Figure 42 - Initial reaction rate of V and Sy production as a function initial temperature.	129
Figure 43 - Radar classification for LTobO _{but} and LTobO _{ethan} lignins.	130
Figure 44 – Time evolution of monomeric products (V, VA, VO, Hy, Sy, SA, and SO) during the oxidation of LTobO _{ethan} (C and D) and LTobO _{but} (A and B). General conditions: 60 g/L of lignin, 2 M NaOH, $p\text{O}_2 = 3 \text{ bar}$, $P_{\text{total}} = 9.8 \text{ bar}$, $T_{\text{initial}} = 393 \text{ K}$	131
Figure 45 - Experimental set-up for cross-flow ultrafiltration in concentration mode: 1) feed tube, 2) direct drive rotary vane pump, 3) inlet pressure gauge, 4) outlet pressure gauge, 5) tubular membrane, 6) circulating valve; 7) rotameter, and 8) permeate collector tube.....	137
Figure 46 - Water permeate fluxes through the ceramic membranes for different TMP at 25 °C, flowrate set to 210 L.h ⁻¹ and a membrane surface area of 0.008 m ²	140
Figure 47 – Schematic representation of the sequential fractionation of the kraft liquor performed with 5, 15 and 50 kDa membranes.	141
Figure 48 - Permeate flux behavior with operating time obtained for the processing with the 5 kDa (A), 15 kDa (B) and 50 kDa (C) membranes.	142

Figure 49 – Composition of lignin fractions obtained from the processing of kraft liquor with 50, 15 and 5kDa ceramic membranes.	145
Figure 50 - Composition of fractions, in %w/w _{TDS} , and isolated lignins, referred to %w/w _{isolated material} , obtained from the ultrafiltration process of kraft liquor.	146
Figure 51 - Quantitative ¹³ C NMR spectra of (a) LKL, (b) LR _{50kDa} , (c) LR _{15kDa} , (d) LR _{5kDa} , and (e) LP _{5kDa} (in DMSO-d ₆ ; * solvent peak (Hugo et al., 1997)).	149
Figure 52 - Quantitative ³¹ P NMR spectra (δ 155-130 ppm) of phosphitylated lignins: (a) LKL, (b) LR _{15kDa} , (c) LR _{5kDa} , and (d) LP _{5kDa} (in CDCl ₃).	152
Figure 53 – Normalization of molecular weight distribution curves obtained by GPC analyses of isolated lignins; analyses were performed at 70 °C and a flow rate of 0.8 mL.min ⁻¹ using DMF with LiCl 0.5%.	153
Figure 54 - Plot of Mw (g.mol ⁻¹) versus S/G ratio, from ¹³ C NMR, obtained for ultrafiltration fractions and kraft liquor.	154
Figure 55 - Radar classification for lignins isolated from fractions obtained from the ultrafiltration of <i>E. globulus</i> kraft liquor.	156
Figure 56 - Potential applications of lignin as renewable resource from biomass (DMSO - dimethyl sulfoxide; DMS - dimethyl sulfide; BTX - benzene, toluene, xylene) (Lange et al., 2013).	164

List of Tables

Table 1 – Types and occurrence (number per 100 ppu) of major structural moieties in lignins from softwoods and hardwoods (Lin and Dence, 1992; Pinto et al., 2012; Santos R.B. et al., 2013).	12
Table 2 - V and Sy maximum yields, reported to %w/w _{lignin} , obtained from non- catalytic oxidation with O ₂ of different lignin samples and liquors.	17
Table 3 - Main expressions related to the kinetic study of lignin oxidation (Araújo et al., 2010; Fargues et al., 1996a; Fargues et al., 1996b; Mathias, 1993; Santos S.G. et al., 2011).....	19
Table 4 - Ash and carbohydrate contents of lignins, presented in %w/w _{lignin} (dry weight).....	42
Table 5 - Detailed composition of carbohydrate fraction (%w/w _{lignin}) of <i>E. globulus</i> lignins.	42
Table 6 - Yields of monomeric phenolic products obtained by NO of lignins.	42
Table 7 - Assignments and quantification (number per aromatic ring) of the structures/linkages and functional groups identified by ¹³ C NMR.....	46
Table 8 - Assignments and quantification (mmol/g _{lignin}) of phenolic, aliphatic, and carboxylic hydroxyl groups identified by ³¹ P NMR.	50
Table 9 - Assignments and quantification (number per phenylpropane unit) of the linkages and functional groups identified by ¹ H NMR.....	53
Table 10 - Empirical formula and molecular mass (M) of ppu of <i>E. globulus</i> lignins.	54
Table 11 – DC (%) and S:G:H ratio calculated for the <i>E. globulus</i> lignins.....	55
Table 12 - S/G for each <i>E. globulus</i> lignin obtained by NO, ¹³ C and ³¹ P NMR.	57
Table 13 - Main structural characteristics selected as descriptors for radar plots of <i>E. globulus</i> lignins.	59
Table 14 - Residues, morphological part, and designation of each material.	69
Table 15 - Composition (ash, carbohydrates, and lignin, dry weight) of stalks and roots.....	71
Table 16 - Ash and carbohydrates contents as contaminants in isolated lignins (dry weight).....	71
Table 17 - Composition of carbohydrate fraction (%w/w) of lignocellulosic materials and respective isolated lignins.	72
Table 18 - Yields of monomeric phenolic products obtained by NO of stalks, roots and isolated lignins.	73
Table 19 - Assignments and quantification (number per aromatic ring) of the structures/linkages and functional groups identified by ¹³ C NMR in lignins from stalks of corn, cotton, sugarcane, and tobacco.....	77

Table 20 - Assignments and quantification (number per aromatic ring) of the structures/linkages and functional groups identified by ^{13}C NMR in lignins from stalks of corn, cotton, sugarcane, and tobacco.	77
Table 21 - ^{13}C NMR assignments and quantification (number per aromatic ring) of the structures/linkages and functional groups identified in mild acidolysis lignins of cotton stalks and sugarcane roots before and after the dioxane purification.....	80
Table 22 - β -O-4 structures content (number per 100 aromatic rings), S:G:H ratio, and DC calculated for mild acidolysis lignins of cotton stalks and sugarcane roots before and after the dioxane purification.	80
Table 23 - The NMR assignments of major components in the HSQC spectrum of the corn stalks lignin.	82
Table 24 - Assignments and quantification of phenolic and aliphatic hydroxyl groups and carboxylic acids in lignins by ^{31}P NMR.	84
Table 25 - Inorganic compounds and carbohydrate contents of lignins.	88
Table 26 - Detailed composition of carbohydrate fraction (%w/w _{lignin}) of tobacco lignins.	88
Table 27 - Yields of monomeric phenolic products obtained by NO of lignins from tobacco stalks.....	89
Table 28 - Assignments and quantification (number per aromatic ring) of the structures/linkages and functional groups identified by ^{13}C NMR for tobacco lignins.....	90
Table 29 - Main structural characteristics of lignins from stalks and roots of tobacco, corn, cotton, and sugarcane.....	92
Table 30 - Main structural characteristics of tobacco lignins.....	94
Table 31 - Inorganic and carbohydrate contents of <i>E. globulus</i> sulfite and kraft liquors and isolated lignins.	108
Table 32 - Sy and V yields per ton of total dissolved solids.	116
Table 33 - Comparison between the maximum yield (η_{max}) and the respective reaction time to maximum ($t_{\eta_{\text{max}}}$) obtained for V and Sy during the oxidation with different initial concentrations of LTobO _{ethan} . .	117
Table 34 - Comparison between the maximum yield (η_{max}) and the respective reaction time to maximum ($t_{\eta_{\text{max}}}$) obtained for V and Sy during the oxidation of LTobO _{ethan} with different values of $p\text{O}_2$	119
Table 35 - Comparison between the maximum yield (η_{max}) and the respective reaction time to maximum ($t_{\eta_{\text{max}}}$) obtained for V and Sy during the oxidation of LTobO _{ethan} with different initial temperatures of reaction.	122
Table 36 - Experimental conditions for the kinetic study of LTobO _{ethan} oxidation.....	124
Table 37 - Initial and final fluxes of 50, 15 and 5 kDa membranes.	142
Table 38 - Water permeability obtained after and before the ultrafiltration using the 5, 15 and 50 kDa cut-off membranes, at 25 °C and flowrate set to 210 L.h ⁻¹	143

Table 39 - Composition of the kraft liquor and the different fractions (retentates and permeate) obtained from the ultrafiltration process; values presented in %w/w.	144
Table 40 – Contaminants content of isolated lignins, presented as %w/w $W_{\text{isolated material}}$ (dry weight).	146
Table 41 - Yields of monomeric phenolic products obtained by NO of isolated lignins from ultrafiltration fractions.	147
Table 42 - Assignments and quantification (number per aromatic ring) of the structures/linkages and functional groups identified by ^{13}C NMR for isolated lignins from ultrafiltration fractions.	148
Table 43 - β -O-4 structures content (number per 100 aromatic rings), DC and S:G:H ratio found for isolated lignins.	150
Table 44 - Assignments and quantification of phenolic and aliphatic hydroxyl groups and carboxylic acids in lignins by ^{31}P NMR.	151
Table 45 - Weight-average (Mw) and number-average (Mn) molecular weight and polydispersity (Mw/Mn) of isolated lignins analysed by GPC.	154

1 Introduction

This chapter provides a general overview about the relevance and viability of side streams of pulp and paper industries and biorefineries to generate high-added value products. This is an important issue for the development of a pathway for vanillin and syringaldehyde production from renewable resources, which contributes to decrease the dependence on petroleum derivatives. The objectives related to the proposed tasks for this work and the outline of this PhD thesis are also presented.

1.1 RELEVANCE AND MOTIVATION

The recent development in biorefineries has become a worldwide effort to a variety of drivers that include the need of alternative source of chemicals, energy, and environmental concerns. One of the main objectives of biorefineries process is the production of bio-based compounds that can be classified into two major groups: bio-based chemicals/materials and bioenergy carriers (electricity, heat, and biofuels). Moreover, if the integrated process of biorefinery comprises a perspective of both chemicals/materials and energy production this offers a major opportunity for synergies (Dapsens et al., 2012). Biorefinery products stand in competition with petroleum-based products with respect to quality, economic efficiency, and product characteristics. However, to ensure the sustainability of biorefinery operations it is crucial the existence of further studies about the progress of products and processes from biorefineries (Ragauskas et al., 2014). A variety of raw-materials (e.g. wood, straw, organic wastes) can be processed in biorefineries, although the selection of raw-material has to take into account some requirements that include quality, quantity, and moderated costs. Biomass represents a valuable feedstock, with a continuous growth in the field of biorefinery, and its use can reduce the existing dependence on fossil feedstocks. One of the main goals of biorefineries is the processing of lignocellulosic biomass by recycling forest and agricultural wastes. This type of biomass includes essentially cellulose, hemicellulose, and lignin in its composition.

Studies worldwide confirm the importance of lignin in the scenario of the integration of biorefinery concept in the existent or new mills (Kim and Pan, 2010; Lersch, 2011; Michels and Wagemann, 2011; Sjöde et al., 2009) and the efforts to find oil alternatives as sources of chemicals. Lignin represents a renewable feedstock that is composed of aromatics, and this occurrence largely depends on the origin of biomass. This polymer can be used to replace chemical fossils in a wide range of products, from plastics, binders, dispersants, and as precursor for carbon fibers (Arkell et al., 2014; Strassberger et al., 2014).

The present thesis intends to gather the emergent interest in lignin. In 2010, the pulp and paper industry produced about 50 Mtons of low purity lignin. Of this, only 2% was used commercially in the dispersants or binding sectors. The remaining 98% was recovered as fuel. One further complication is that the structure of kraft, organosolv, and sulfite lignins differs between plant sources. Therefore, introducing lignin to new markets will depend strongly on its structure and related properties (Strassberger et al., 2014).

Among all the lignin based products, vanillin and syringaldehyde are two important high added value compounds widely recognized. Vanillin is used as flavouring and fragrance ingredient in food, cosmetic, and as intermediate for the synthesis of several second-generation fine chemicals and pharmaceuticals. About 85% of world supply of vanillin still comes from petrochemical route; the remaining is produced from lignin oxidation and from vanilla beans.

Syringaldehyde is also a precursor for pharmaceutical or chemical industry (Erofeev et al., 1990). However, it is not produced by lignin oxidation, mainly because the lignin traditionally used as raw-material is of softwood type (composed by guaiacyl units) rather than hardwood type (composed by syringyl and guaiacyl units). In fact, by oxidation of hardwood lignin both aldehydes are produced at yields that depend of the process conditions and lignin structure. The implementation at industrial scale depends on the economic sustainability of the process which, in turn, depends largely of the raw material availability and products yield (from reaction to final separation).

1.2 OBJECTIVES

In this thesis the characterization and comparative evaluation of newly lignin sources will be accomplished, as organosolv lignin from a lignocellulosic biorefinery, lignins from herbaceous plants, and fractions of lignins produced in laboratory by ultrafiltration. Lignins isolated from mild acidolysis of several lignocellulosic materials (hardwood and herbaceous plants) were also comprehensively analyzed by selected characterization techniques and methods, assessing the most important structural features of lignin structure.

The first objective of this work includes a comprehensive and comparative analysis of *E. globulus* lignins, revealing the importance of processing on lignin functionality and reactivity as one of the possible tools for the selection of lignins/processes to a valorization route within a lignocellulosic-based biorefinery. The characterization of lignin from stalks and roots of corn, cotton, sugarcane, and tobacco production will be also performed considering their availability and valorization as feedstock.

The oxidation reactions of different lignins and liquors will be the focus of the second objective. The aim is to evaluate the potential of industrial *Eucalyptus globulus* sulfite liquor and kraft liquors (collected at different stages of processing before the recovery boiler) and an organosolv tobacco lignin for the production of syringaldehyde and vanillin by oxidation with O₂ in alkaline medium. Oxidations were performed in a jacketed reactor with controlled temperature, total and O₂ partial pressure, and with defined values of NaOH and lignin concentration.

The third objective is the kinetic evaluation of products formation from one selected lignin evaluating their potential as source of vanillin and syringaldehyde. For the selected lignin, the evaluation of the influence of temperature, initial lignin concentration, and partial pressure of O₂ in the reaction, as also the estimation of the kinetic parameters of oxidation will be achieved. The reaction mixture will be characterized aiming to identify other possible valuable products; the

maximum yields of the low molecular weight products in the oxidation mixture at different oxidation reaction conditions will be attained.

An ultrafiltration process for the fractionation of a selected lignin will be performed and the fourth objective will be achieved. For the lignin fractionation by ultrafiltration sequential membranes with a suitable cut-off will be used and different fractions with different molecular weight values will be obtained. The lignin fractions and the respective isolated lignins will be comprehensively characterized and evaluated.

1.3 OUTLINE

The main goal of the present thesis is to produce vanillin and syringaldehyde by oxidative depolymerization of lignins, achieving the process conditions to take full benefit of the potential of each lignin studied.

A review, based on the most important works published in literature about pulp and paper industries and biorefineries, lignin structure, characterization methods, lignin depolymerization, including process conditions and principal results, will be accomplished in **Chapter 2** (State of the art).

In **Chapter 3** and **Chapter 4** the structural characterization of lignins coming from different process streams and different sources will be discussed. Lignins structure will be studied with reference to uncondensed units obtained by nitrobenzene oxidation, and with reference to functional groups and typical structures/linkages by quantitative ^{13}C , ^{31}P , ^1H , and 2D nuclear magnetic resonance (NMR), and Fourier transform infrared spectroscopy (FTIR). The obtained results will support a comprehensive and comparative analysis of lignins structure, enabling to infer about the importance of processing and biomass source on lignin functionality and reactivity. A comparative approach, using radar classification, highlighting for each material the characteristic features of its lignin will be also established. The main outcomes of these chapters were compiled and analyzed giving origin to three publications:

- Costa, C.A.E., Pinto, P.C.R., Rodrigues, A.E. Evaluation of chemical processing impact on *E. globulus* wood lignin and comparison with bark lignin. *Ind. Crop. Prod.* 2014, 61, 479-491

- Costa, C.A.E., Pinto, P.C.R., Rodrigues, A.E. Radar tool for lignin classification on the perspective of its valorization. *Ind. Eng. Chem. Res.* 2015, 54, 7580-7590.

- Costa, C.A.E., Coleman, W., Dube, M., Rodrigues, A.E., Pinto, P.C.R. Assessment of key features of lignin from lignocellulosic crops: Stalks and roots of corn, cotton, sugarcane, and tobacco. *Ind. Crop. Prod.* 2016, 92, 136-148.

The oxidation reactions with molecular oxygen in alkaline medium applied to different lignins and liquors will be discussed in detail in **Chapter 5** (Lignins oxidation in alkaline medium). This chapter also includes, for one selected lignin, the evaluation of the effect of temperature, lignin concentration, and partial pressure of O₂ in the reaction and the kinetic study of products formation. The data from the oxidation of industrial *Eucalyptus globulus* sulfite liquor and kraft liquors (collected at different stages of processing before the recovery boiler) and the respective isolated lignins led to the evaluation of the potential of each sample for the production of vanillin and syringaldehyde and the results were already published in the following publication:

- Pinto, P.C.R.; Costa, C.E.; Rodrigues, A.E. Oxidation of lignin from *Eucalyptus globulus* pulping liquors to produce syringaldehyde and vanillin. *Ind. Eng. Chem. Res.* 2013, 52, 4421-4428.

In **Chapter 6** a study about the fractionation of *E. globulus* industrial kraft liquor by ultrafiltration will be attained. The composition and characterization of each resulting fraction and the respective isolated lignin will be accessed by means of different analytical techniques, being able to establish the differences in their composition and structural characteristics and subsequently their more adequate commercial application as high added-value products.

Chapter 7 includes the main conclusions of all the work developed in this thesis, as well as some key suggestions for future work.

1.4 REFERENCES

Arkell, A., Olsson, J., Wallberg, O. Process performance in lignin separation from softwood black liquor by membrane filtration. *Chem. Eng. Res. Des.* 2014, 92, 1792-1800.

Dapsens, P.Y., Mondelli, C., Pérez-Ramírez, J. Biobased chemicals from conception toward industrial reality: Lessons learned and to be learned. *ACS Catalysis* 2012, 2, 1487-1499.

Erofeev, Y.V., Afanas'eva, V.L., Glushkov, R.G. Synthetic routes to 3,4,5-trimethoxybenzaldehyde (review). *Pharm. Chem. J.* 1990, 24, 501-510.

Kim, D.-E., Pan, X. Preliminary study on converting hybrid poplar to high-value chemicals and lignin using organosolv ethanol process. *Ind. Eng. Chem. Res.* 2010, 49, 12156-12163.

Lersch, M. 2011. Biorefining at Borregaard – recent developments in the processing of lignocellulosics. *The 3rd Nordic Wood Biorefinery Conference (NWBC 2011)*, 22-24 March, Stokolm, Sweeden. pp. 109-113.

Michels, J., Wagemann, K. 2011. The German lignocellulose feedstock biorefinery project. *The 3rd Nordic Wood Biorefinery Conference (NWBC 2011)*, 22-24 March, Stockholm, Sweeden. pp. 70-75.

Ragauskas, A.J., Beckham, G.T., Biddy, M.J., Chandra, R., Chen, F., Davis, M.F., Davison, B.H., Dixon, R.A., Gilna, P., Keller, M., Langan, P., Naskar, A.K., Saddler, J.N., Tschaplinski, T.J., Tuskan, G.A., Wyman, C.E. Lignin valorization: Improving lignin processing in the biorefinery. *Science* 2014, 344, 1246843.

Sjöde, A., Frölander, A., Lersch, M., Rødsrud, G. 2009. Lignocellulosic biomass conversion by sulfite pretreatment, (Ed.) N. Borregaard Industries Limited.

Strassberger, Z., Tanase, S., Rothenberg, G. The pros and cons of lignin valorisation in an integrated biorefinery. *RSC Advances* 2014, 4, 25310-25318.

2 State of the art

2.1 PULP AND PAPER INDUSTRIES AND BIOREFINERIES

In the second half of the 20th century crude oil was the main raw material for energy, transportation, and chemicals. Technologies for processing crude oil have been developing since 1860s, and today's refineries are highly integrated industrial plants (Strassberger et al., 2014). However, the depleting stocks of fossil fuels and the growing concern over economic and environmental issues have motivated the researches to find renewable and abundant alternatives for the use of petrochemicals (Fernando et al., 2006; Lucia, 2008). Lignocellulosic biomass appears to be a valuable feedstock for the production of second generation biofuels, chemicals, and biomaterials (Azadi et al., 2013; FitzPatrick et al., 2010; Long et al., 2015) and it is becoming a logical and promising alternative to petroleum resources. The main goal of tomorrow's biorefineries will be the processing of lignocellulosic biomass by recycling forest and agricultural residues (Strassberger et al., 2014).

Lignocellulosic biomass is composed of three major components: cellulose, hemicelluloses, and lignin (Figure 1). The concept of a biorefinery that integrates processes and technologies for biomass conversion demands an efficient utilization of all the three components. However, most of the biorefinery schemes are focused on the valorization of cellulose and hemicelluloses, a so-called sugar platform, while lignin remains relatively underutilized to its potential, and is usually considered a low-value residue (Vishtal and Kraslawski, 2011). Most of the low-purity lignin produced in pulp and paper industries is used as low-cost fuel to generate energy for mill operations, and only a small fraction, approximately 1 million ton per year, is used for commercial applications (Holladay et al., 2007; Saito et al., 2014; Strassberger et al., 2014).

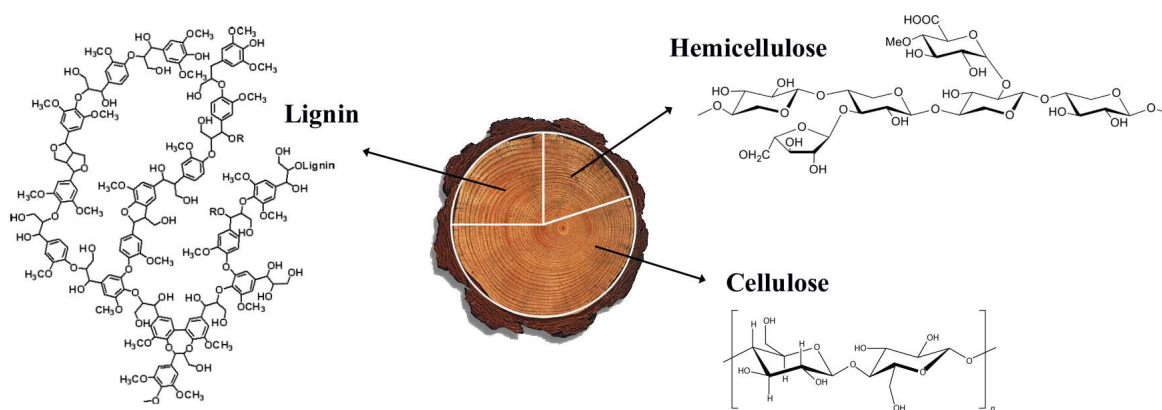


Figure 1 - Average distribution of the main biomass constituents: cellulose, hemicellulose, and lignin (FitzPatrick et al., 2010; Ragauskas et al., 2014).

Numerous studies have pointed out that the inherent properties of lignin could significantly improve the productivity of the biorefinery processes and its potential applications (Azadi et al., 2013; Ragauskas et al., 2014; Strassberger et al., 2014; Vishtal and Kraslawski, 2011; Yuan et al., 2013). However, the application and valorization of this biopolymer largely depends on their structure, purity, and properties.

2.2 LIGNIN VALORIZATION

Lignin plays a significant role in the operational improvement of the emerging lignocellulosic-based biorefinery activity; it is available at large-scale from the side streams of pulp and paper industries, representing a valuable renewable resource (Berlin and Balakshin, 2014; Pinto et al., 2011; Strassberger et al., 2014). The largest volume of lignin produced worldwide comes from wood pulping, with more than 70 million tons occurring annually; the lignin generated is known as liginosulfonate or as kraft depending on the process used, sulfite or kraft pulping respectively.

Kraft process accounts for 80% of the world chemical pulp production (Fahlbusch et al., 2002). Black liquor is a by-product of this process and holds about 12-18 wt% of dry matter content, mainly composed by lignin material (30-45 wt%) and wood carbohydrates (25-35 wt%), as well as formic and acetic acids (10 wt%), wood extractives (3-5 wt%), methanol (1 wt%) and several inorganic elements mainly sodium and sulphur (Rojas et al., 2006; Wallberg et al., 2003). Lignin from pulping liquors, improves significantly the profitability of pulp and paper industries by debottlenecking wood pulp production as a result of increasing the recovery capacity of pulping chemicals and the valorization of the lignin stream. However, pulping operations are highly integrated and dependent on pulping liquor, which is concentrated and burned in the recovery boiler, supporting the energetic integration of some pulp mill operations with the simultaneously recovery of pulping chemicals (Krotschek and Sixta, 2008).

In some mills, part of liquor produced is diverted to increase the pulp production capacity (situations where recovery furnace is limited) or to upgrade its components, mainly lignin. For these reasons, the economic and environmental sustainability of these new industries depends on the successful integration of a route for lignin valorization, since the conversion of this low-value by-product into high-value co-products will help to offset the costs of lignocellulosic-based biorefineries production. In Figure 2 current and potential lignin-product combinations are presented.

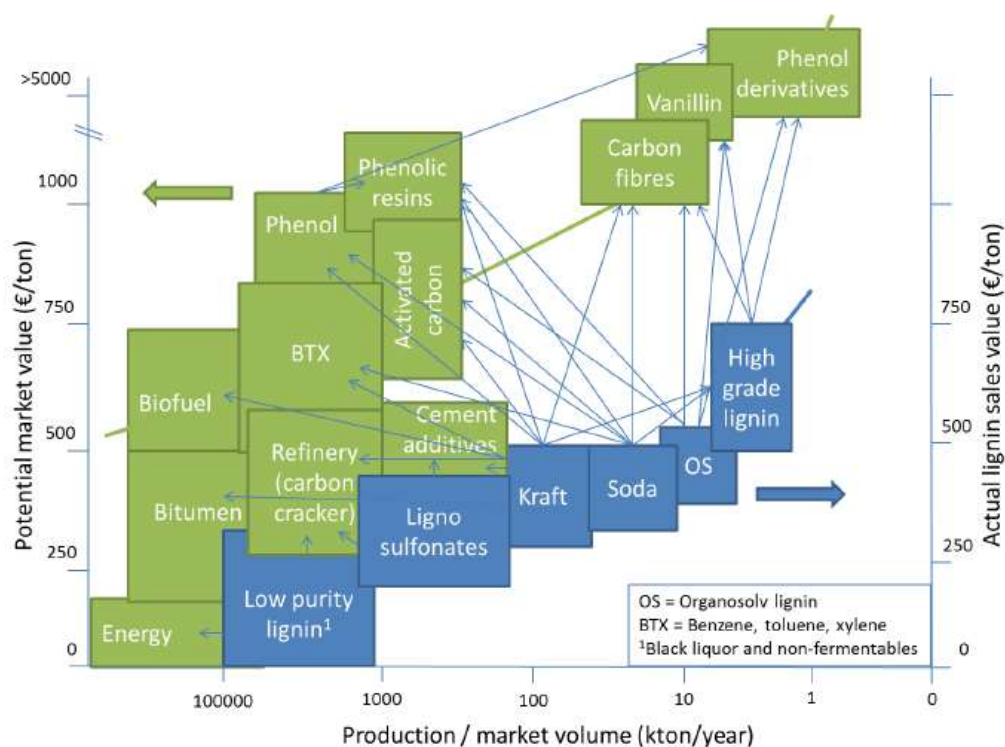


Figure 2 – Lignin production and potential lignin derived product market and value (Gosselink, 2011).

Current and potential applications of lignin have been reviewed extensively, lignin can be a potential source of renewable fuels and potential high added-value products, such as adhesives, dispersants, emulsifiers, concrete additives, foams, resins, and thermoplastics, and also low molecular weight phenolic compounds (Azadi et al., 2013; Berlin and Balakshin, 2014; Borges da Silva et al., 2009; Calvo-Flores and Dobado, 2010; Lora, 2008; Pinto et al., 2012; Ragauskas et al., 2014; Sjöde et al., 2009; Stewart, 2008). Nowadays, Borregaard LignoTech (Norway) is the main world producer (and processor) of lignosulfonates with an annual production of 160,000 solid tons/year, followed by Tempec (Canada). Moreover, Borregaard LignoTech is the only producer of vanillin from lignin (Lersch, 2011).

Both low- and high-value lignin applications are often seen as efficient vehicles to increase the productivity, reduce fossil fuel consumption, and increase the profitability of the industrial plants where lignin is produced as a by-product (Berlin and Balakshin, 2014). However, this is still restricted to a low fraction of the lignin produced around the world, being a challenging task for the

next years due to the increase of lignin availability as a consequence of lignocellulosic biorefineries activity. However, regarding the chemical valorization of lignin it is important to take into account its complexity and heterogeneity, since their reactivity and physico-chemical properties depend strongly on the source, the delignification and isolation process.

2.3 LIGNIN CHEMISTRY AND STRUCTURE

Lignin occurs widely in the middle lamellae and secondary cell walls of higher plants and plays a key role in constructive tissues as a building material, giving it its strength and rigidity and resistance to environmental stresses (Behling et al., 2016). Lignin is one of the principal components of the lignocellulosic materials; this three-dimensional phenolic macromolecule contribute as much as 30% of the weight and 40% of the energy content of lignocellulosic biomass (Azadi et al., 2013). The contents of lignin may vary in softwoods from 18-33% and in hardwoods from 15-35% (Azadi et al., 2013; Buranov and Mazza, 2008; Lin and Dence, 1992; Ragauskas et al., 2014). In non-wood fiber crops the lignin content is generally lower and ranges from below 5%, in cotton and in extracted flax or hemp bast fibres, to around 11-15% for sisal and jute (Gosselink, 2011). In grasses such as cereal straws, bamboo or bagasse the lignin content ranges from 15-25% (Buranov and Mazza, 2008; Monteil-Rivera et al., 2013). Despite the differences found between the major groups of higher plants, lignin content and composition also differs between species and even morphological parts of the same plant (Sjöström, 1993).

Lignin exhibits a complex three-dimensional amorphous structure, arising from the polymerization of its general structural subunit, the phenylpropane unit (ppu). The ppu can comprise several functional groups, being the most frequent ones aromatic methoxyl and phenolic hydroxyl, primary and secondary aliphatic hydroxyl, minor amounts of carbonyl groups (of aldehydes and ketones), and carboxyl groups (Berlin and Balakshin, 2014; Calvo-Flores and Dobado, 2010; Pinto et al., 2012). Coniferyl, sinapyl, and *p*-coumaryl alcohols are the precursors of the main moieties of lignin structure, guaiacyl (G), syringyl (S), and *p*-hydroxyphenyl (H) respectively, and differ between them in the methoxylation of the aromatic nuclei, as depicted in Figure 3.

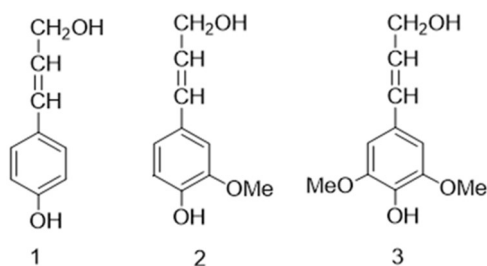


Figure 3 - *p*-Coumaryl (1), coniferyl (2), and sinapyl (3) alcohols.

The ratio between G, S, and H units, the molecular weight and the amount of lignin differs among groups of plants. Softwood lignins primarily contain G units and small proportions of H units and hardwood lignins contain both S and G units, with a minor proportion of H units. Moreover, even in the same group of plants, in this case hardwoods, there is a high variety of proportions between G and S units as detailed in the literature (Santos R.B. et al., 2011). For that reason, the first factor to take into account is the lignin nature, an unalterable factor. Usually, herbaceous plants contain a higher frequency of H units than hardwoods. Therefore, one should expect lower G and S units in these lignins compared with lignins composed exclusively by these units. In addition, lignins from herbaceous plants contain significant amounts of cinnamic and ferulic acid derivatives attached to lignin predominantly via ester linkages with the hydroxyl in C γ of C $_9$ -units (Lin and Dence, 1992). Lignin-carbohydrate complexes (LCC) are also formed in plant cells. The main types of LCC linkages in lignocellulosic materials are believed to be phenyl glycoside bonds, esters, and benzyl ethers (Balakshin et al., 2011).

The exact mechanism of lignin polymerization and biosynthesis has been exhaustively studied in literature and details of this complex pathway can be found in the some review articles (Boerjan et al., 2003; Lewis and Yamamoto, 1990; Ralph et al., 2004). The proportion of each type of linkage in lignin structure depends on the relative contribution of a particular monomer to the polymerization process. The phenylpropane units of lignin are linked through aryl ether bonds (β -O-4, α -O-4, 4-O-5) and carbon-carbon linkages (5-5', β -5, β -1, β - β) (Calvo-Flores and Dobado, 2010; Lin and Dence, 1992). The most abundant dilignol is the β -O-4 type (structure A, Figure 4), accounting for more than 50% of the interunit linkages in lignin (Berlin and Balakshin, 2014; Pinto et al., 2012). Other common lignin interunit linkages include 5-5' (structure B, Figure 4), α -O-4 (structure C, Figure 4), phenylcoumaran (β -5; structure D, Figure 4), resinol (β - β ; structure E, Figure 4), 4-O-5' (structure F, Figure 4), and β -5 (structure G, Figure 4) moieties.

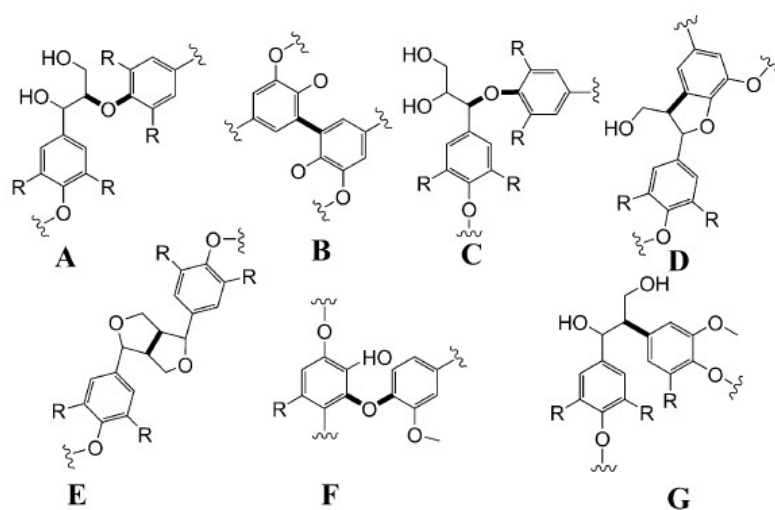


Figure 4 – Main structural moieties of native and technical lignins (Pandey and Kim, 2011).

The occurrence of the most common and important inter-unit linkages identified in hardwood and softwood lignins are shown in Table 1.

Table 1 – Types and occurrence (number per 100 ppu) of major structural moieties in lignins from softwoods and hardwoods (Lin and Dence, 1992; Pinto et al., 2012; Santos R.B. et al., 2013).

Linkages	number/100 ppu	
	Softwood	Hardwood
β -O-4	45-50	50-65
5-5'	10-25	4-10
β -5	9-12	4-6
α -O-4	6-8	4-8
β -1	3-10	5-7
4-O-5'	4-8	6-7
β - β	2-4	3-7

The degree of condensation (DC) is an important lignin characteristic often correlated (negatively) with lignin reactivity. The definition of condensed lignin moieties found in literature is not always clear (Berlin and Balakshin, 2014). Most commonly, the DC is related with the lignin moieties linked with C-C linkages with other lignin units via C₂, or C₆ positions in the aromatic ring of S units, C₂, C₅ or C₆ positions of the aromatic ring of G units, and in the case of H units also C₃ position is available. The most common condensed structures are 5-5', β -5, and 4-O-5' structures (Berlin and Balakshin, 2014). On the other hand, α -aryl ether and β -aryl ether linkages are the most easily cleaved, providing a basis for industrial processes, such as chemical pulping, and several methods in lignin chemical analysis. The other linkages are all more resistant to chemical degradation (Sannigrahi et al., 2010).

G type lignins, contain more resistant linkages as those involving the C₅ of aromatic nuclei (β -5, 5-5' and 4-O-5') than SG lignins due to the availability of the C₅ position for coupling. This could be one of the reasons for the higher condensation degree of softwood lignins than hardwood and herbaceous plants ones; consequently, this fact has implications on lignin reactivity.

As already mentioned, the source of biomass and the delignification process have considerable influence on lignin structure (linkages and functional groups) and consequently on its reactivity toward a further chemical process (Pinto et al., 2011). Hence, the lignin obtained from delignification processes differs from the native one as a result of multiple reactions (Pinto et al., 2012), that predominantly involve condensation and degradation reactions (Berlin and Balakshin, 2014). Considering the delignification process, kraft and organosolv lignins from softwoods (Froass et al., 1998; Pan et al., 2005; Saito et al., 2014; Sannigrahi et al., 2009), hardwoods (Ibarra et al., 2007; Pan et al., 2006; Pinto et al., 2005; Pinto et al., 2002; Wen et al., 2013a; Wen et al.,

2013b) or both (Capanema et al., 2001), and also herbaceous plants (Alriols et al., 2010; El Hage et al., 2010) have been extensively analyzed. All the authors have concluded that the delignification process undergoes structural transformations in lignin. In general, lignins obtained from delignification processes have higher contents of phenolic hydroxyl groups, carboxylic acid groups, and condensed structures, and lower contents of aliphatic hydroxyl groups and β -O-4 structures than the respective native lignins (Fernández-Costas et al., 2014; Ibarra et al., 2007; Lourenço et al., 2012).

2.3.1 Lignin characterization: techniques and methods

A detailed understanding of lignin structure is essential in order to combine efforts toward their valorization into valuable products. Besides all the existing information about lignin structure, this polymer is not described through a simple structural characterization due to its high complexity and diverse possibilities of combination between sub-units in this macromolecule. All of these specifications have implications on lignin reactivity and for this reason it is essential that for lignin characterization several complementary methods have to be applied in order to determine their major structural features.

Over the last decades, both destructive and nondestructive methods have been developed for lignin characterization. The destructive methods include hydrogenolysis, nitrobenzene oxidation, cupric (II) oxidation, permanganate oxidation, ozonation, thioacidolysis, and also derivatization followed by reductive cleavage (Lu and Ralph, 1997; Pepper et al., 1967; Quesada et al., 1999). All of these destructive methods could provide information regarding the structure of lignin through the generation of low-molecular weight compounds. However, all of them only comprise the selective cleavage of a specific fraction of lignin, hindering the study of the whole lignin structure. To overcome this challenge, nondestructive methods are available and enable the identification and quantification of the main structural features of lignin.

The advantage of spectroscopic methods over degradation techniques is their ability to analyze the whole lignin structure and directly detect lignin moieties and/or functional groups. The nondestructive methods include different spectroscopic techniques such as Fourier transform infrared spectroscopy (FTIR), Raman spectroscopy and nuclear magnetic resonance (NMR) (Capanema et al., 2004; Fernández-Costas et al., 2014; Froass et al., 1998; Lin and Dence, 1992; Ralph et al., 1998). NMR techniques comprise ^{13}C , ^{31}P , ^1H , and 2D heteronuclear single quantum coherence (HSQC) NMR, and among all, quantitative ^{13}C NMR is the most widely used method for the evaluation of the main structural features of hardwoods (Evtuguin et al., 2001; Fernández-Costas et al., 2014), softwoods (Capanema et al., 2004; Nimz et al., 1981), and also annual plant (Sun et al., 2004; Xiao et al., 2001) lignins. A combination of quantitative ^{13}C and 2D HSQC NMR

has been also applied to provide comprehensive structural information on lignin from a variety of sources (Capanema et al., 2001; Fernández-Costas et al., 2014).

Extensive data about lignin composition and structure are generated from all of the referred techniques: relative abundance of H, G, and S units, distribution of inter-unit linkages and functional groups, as well as the degree of condensation of this polymer. The assessment and correlation between these key structural features are essential for the evaluation of a lignin relative to its potential as source of value-added compounds. However, the complexity of lignin structure makes difficult to extract comprehensive, focused, and “ready to use” information.

2.4 LIGNIN DEPOLYMERIZATION

The heterogeneous molecular structure of lignin constitutes a valuable source of chemicals, particularly phenolics. However, lignin depolymerization with selective bond cleavage is the major challenge for converting it into value-added chemicals and to accomplish its subsequent valorization. The need of defining structural parameters for the assessment of lignin potential for vanillin (V) and syringaldehyde (Sy) production was previously identified by other authors (Pinto et al., 2011).

Pyrolysis (thermolysis), gasification, hydrogenolysis, chemical oxidation, and hydrolysis under supercritical conditions are the major thermochemical methods studied regarding lignin depolymerization (Azadi et al., 2013; Pandey and Kim, 2011). All the referred depolymerization methods lead to phenolic compounds of low molecular weight of great interest, which are produced with different yields depending on the source of lignin and the reaction conditions.

The oxidative depolymerization of lignin can be performed through different types of oxidants, and the characteristics of each oxidant determine their activity and selectivity in the reaction (Lin and Dence, 1992). Consequently, the oxidant selection is based on the properties that allow obtaining the maximum products yields from lignin oxidation. The high yields reported, considering mainly V and Sy, were obtained by oxidation with molecular oxygen in alkaline medium (Pandey and Kim, 2011; Pinto et al., 2012).

The use of molecular oxygen as oxidant is advantageous when economic and environmental questions are considered (Fargues et al., 1996a). This is an inexpensive and green oxidant, which preserves the lignin aromatic rings during the oxidation reaction. However, when oxygen is used it is important to take into account some limitations: its nonselectivity, the possibility of over oxidation, its low solubility in the reaction medium, and the requirement of high temperatures for activation (Marshall and Sankey, 1951; Pinto et al., 2012; Tromans, 1998). Moreover, it is well known the phenolic units and ring-conjugated structures of lignin became more reactive with oxygen.

The oxidative depolymerization of lignin gives a complex mixture of products highly dependent on the nature of the raw material and the selected reaction conditions. Between them it is possible to find oligomeric products, phenolic, and non-phenolic compounds. However, in most studies, the authors focus their attention on the identification and quantification of specific phenolic compounds of greatest interest that usually include several aldehydes (V and Sy), acids (vanillic acid (VA) and syringic acid (SA)), and ketones (acetovanillone (VO) and acetosyringone (SO)).

2.4.1 Vanillin and syringaldehyde

Vanillin (V, 4-hydroxy-3-methoxybenzaldehyde, Figure 5) is the highest volume aroma chemical produced worldwide. Their numerous advantages: it is a safe compound, aromatic, and it bears two reactive functions that can be chemically modified (the methoxy group being less reactive than the aldehyde and phenol functions), make this compound with potential to be a key renewable aromatic building-block.

V is widely used as flavouring and fragrance ingredient in food, cosmetic and as intermediate for the synthesis of several second-generation fine chemicals and pharmaceuticals (Calvo-Flores and Dobado, 2010). It is produced from different sources, namely petro-based intermediates, woody biomass, and orchid pods. Around 20,000 tons of V are produced per year, 15% of which coming from lignin (around 3,000 tons/y), while the worldwide production of natural V extract is only 40 to 50 tonnes per year, which represents less than 1% of its total production. 85% of the world supply is produced from petro-based intermediates, especially guaiacol. There are different ways to prepare V from guaiacol being the most employed is the Riedel process (Huang et al., 2012). The great advantage of this process is that the glyoxylic acid condensation is highly region-selective towards the para position, which avoids side-products and thus expensive separation reactions. Other advantages of the petrochemical production of V is the production costs, when made from petrochemical sources V costs as little as \$10 per kg, and does not depend of natural conditions to yield considerably amounts, whereas V made in a way that can be labelled as natural can cost hundreds of dollars per kg (Fache et al., 2016).

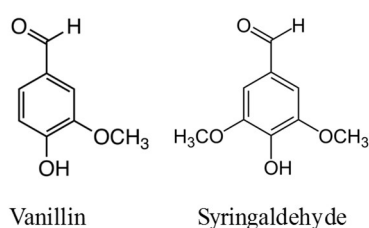


Figure 5 - Structure of vanillin (4-hydroxy-3-methoxybenzaldehyde) and syringaldehyde (4-hydroxy-3,5-dimethoxybenzaldehyde).

Syringaldehyde (Sy, 4-hydroxy-3,5-dimethoxybenzaldehyde, Figure 5) is also a precursor for pharmaceutical or chemical industry (Erofeev et al., 1990) and it has been synthesized from gallic acid, pyrogallol, and V itself (Ibrahim, 2012). Recently, the demand for chemicals from renewable sources has brought new life on the lignin route to produce V. Furthermore, there is an increasing interest also for homologous compounds such as Sy (German Federal Government, 2012; Holladay et al., 2007), for direct applications (Schneider, 1997), or as precursors of fine chemicals and drugs (Erofeev et al., 1990; Ibrahim, 2012; Lee et al., 2009).

Sy can be produced from oxidative depolymerization of lignin from hardwood (Pinto et al., 2011; Villar et al., 2001; Wu et al., 1994) or from annual plants (Sales et al., 2006). In fact, by oxidation of these lignins both aldehydes are produced at yields that depend of the process conditions and lignin structure. Considering its current availability in the side streams of pulp industries and biorefineries, this could be an important approach in view of lignin exploitation for high added value applications. This promising research field was not explored so far. The implementation at industrial scale depends on the economic sustainability of the process which, in turn, depends largely of the raw material availability and products yield (from reaction to final separation).

2.4.2 Lignin oxidation in alkaline medium

In the last decades, several authors have been working on lignin oxidation with O₂ in alkaline conditions in order to develop an effective process of V and Sy production from different sources of lignin (Araújo et al., 2010; Fargues et al., 1996a; Mathias et al., 1995; Mathias and Rodrigues, 1995; Pinto et al., 2013; Sales et al., 2006; Santos S.G. et al., 2011; Tarabanko et al., 2001).

The oxidative depolymerization of lignin involves the cleavage of aromatic rings, aryl ether linkages, and/or other linkages in lignin structure. Products from lignin alkaline oxidation are predominantly aromatic aldehydes or acids depending on the reaction conditions. Among them, V and Sy and other phenolics like *p*-hydroxybenzaldehyde (Hy), VA and SA are the most important and their occurrence plays a decisive role to determine the reaction efficiency (Pinto et al., 2012; Wu et al., 1994). V and Sy yields depend first on lignin type: guaiacyl lignins (G type, typical of softwoods) yield V under oxidative depolymerization, whereas *p*-hydroxyphenyl:guaiacyl:syringyl (H:G:S) lignins (typical of herbaceous plants and hardwoods) are able to produce Sy, Hy, and lower yields of V. Moreover, other interesting mono-phenolic compounds such as guaiacol and syringol are also often mentioned as depolymerization products (Pinto et al., 2012; Vigneault et al., 2007; Wong et al., 2010).

An overview of some representative non-catalytic oxidation studies concerning the raw material, the reaction conditions, and yields of V and Sy are gathered in Table 2.

Table 2 - V and Sy maximum yields, reported to %w/w_{lignin}, obtained from non-catalytic oxidation with O₂ of different lignin samples and liquors.

	Oxidation conditions	maximum yield		Ref.
		V	Sy	
Hardwood	Organosolv beech lignin $T_{\text{initial}} = 393 \text{ K};$ $p\text{O}_2 = 3.0 \text{ bar}; P_{\text{total}} \approx 9.7 \text{ bar};$ $[\text{lignin}] = 60 \text{ g/L}; [\text{NaOH}] = 2.0 \text{ mol/L}$	1.2	2.5	(Pinto et al., 2011)
	<i>E. globulus</i> sulfite liquor $T_{\text{initial}} = 403\text{-}423 \text{ K};$ $p\text{O}_2 = 6.0 \text{ bar}; P_{\text{total}} = 6.0 \text{ bar};$ $[\text{liquor}] = 5 \text{ g/L}; [\text{NaOH}] = 0.75 \text{ mol/L}$	2-3	5-7	(Santos S.G. et al., 2011)
	Aspen wood $T_{\text{initial}} = 443\text{-}473 \text{ K}; P_{\text{total}} = 2\text{-}13 \text{ bar};$ $[\text{lignin}] = 21.8 \text{ g/L};$ $[\text{NaOH}] = 2.0 \text{ mol/L}$	7.8	19.7	(Tarabanko and Petukhov, 2003)
Softwood	Pinus kraft lignin (Westvaco Co) $T_{\text{initial}} = 383\text{-}427 \text{ K};$ $p\text{O}_2 = 1.2\text{-}5.0 \text{ bar}; P_{\text{total}} \approx 9.7 \text{ bar};$ $[\text{lignin}] = 30\text{-}120 \text{ g/L};$ $[\text{NaOH}] = 2.0 \text{ mol/L}$	10.8	---	(Fargues et al., 1996a)
	Softwood kraft lignin (mainly spruce) isolated by LignoBoost process $T_{\text{initial}} = 393 \text{ K};$ $p\text{O}_2 = 3.0 \text{ bar}; P_{\text{total}} \approx 9.7 \text{ bar};$ $[\text{lignin}] = 60 \text{ g/L}; [\text{NaOH}] = 2.0 \text{ mol/L}$	3.1	--	(Pinto et al., 2011)
	Indulin AT, Borregaard) $T_{\text{initial}} = 396 \text{ K};$ $p\text{O}_2 = 4.0 \text{ bar}; P_{\text{total}} = 9.0 \text{ bar};$ $[\text{lignin}] = 60 \text{ g/L}; [\text{NaOH}] = 2.0 \text{ mol/L}$	3.3	--	(Araújo et al., 2010)
	Pinus kraft lignin (Westvaco Co) $T_{\text{initial}} = 393 \text{ K};$ $p\text{O}_2 = 3.0 \text{ bar}; P_{\text{total}} \approx 9.7 \text{ bar};$ $[\text{lignin}] = 60 \text{ g/L}; [\text{NaOH}] = 2.0 \text{ mol/L}$	4.4	--	(Pinto et al., 2011)
	Pinus kraft lignin (Westvaco Co and Portucel) $T_{\text{initial}} = 372\text{-}414 \text{ K};$ $p\text{O}_2 = 1.8\text{-}6.5 \text{ bar}; P_{\text{total}} = 4.8\text{-}10 \text{ bar};$ $[\text{lignin}] = 30\text{-}120 \text{ g/L};$ $[\text{NaOH}] = 1\text{-}4 \text{ mol/L}$	10.5	--	(Mathias, 1993; Mathias and Rodrigues, 1995)

The values, found in the literature, do not exceed 10.8 %w/w_{lignin} in the case of V and 19.7 %w/w_{lignin} for Sy (Fargues et al., 1996a; Mathias and Rodrigues, 1995; Pinto et al., 2011; Santos S.G. et al., 2011; Tarabanko and Petukhov, 2003). The oxidation of lignin to produce V and Sy has been demonstrated at high pH (almost 14) and high temperatures (higher than 373 K) with molecular oxygen (with a partial pressure equal or higher than 3 bar). The limitation of this process is the low solubility of oxygen in the reaction medium of sodium hydroxide (NaOH) and lignin in the high operational temperatures (Pinto et al., 2012).

A study about the improvement of the process conditions of oxidative cleavage of an aspen wood lignin into aromatic aldehydes (V and Sy) was developed by Tarabanko and Petukhov (Tarabanko and Petukhov, 2003). In this work a mechanism for the formation of aromatic aldehydes from lignin oxidative depolymerization was described, which starts from the formation of phenoxy radical and is accomplished by the formation of V through the cleavage of substituted coniferyl aldehyde. The proposed mechanism allow inferring that the selectivity of the oxidation process could be achieved using more severe reaction conditions, in order to increase the yield of

aromatic aldehydes from lignin (Tarabanko and Petukhov, 2003). Villar et al. (Villar et al., 2001) attributed the low yield of aldehydes obtained from oxidation to the condensed nature of lignins and to the decomposition to lower-molecular weight acids.

The oxidation with catalysts (mainly transition metal salts) has been referred to increase the yields of the products (Sippola and Krause, 2005; Wu et al., 1994; Zakzeski et al., 2010a; Zakzeski et al., 2010b). However, Fargues et al. (Fargues et al., 1996a) observed that the addition of copper and cobalt catalysts didn't affect much the conversion and aldehyde yields, which is in contrast to the results of Xiang and Lee (Xiang and Lee, 2001) who found a mixture of Cu^{2+} and Fe^{3+} to be an effective catalyst increasing the yield of aldehydes from 7.9 to 11.1 wt%. Wu and Heitz (Wu and Heitz, 1995) and Zhang et al. (Zhang et al., 2009) also reported the effectiveness of catalysts in increasing the yield of aldehydes.

2.4.2.1 Kinetic study of oxidation products

Since the goal of alkaline oxidation is to achieve the maximum conversion into phenolic compounds, mainly V and Sy, several studies are focused in the discussion of the effect of reaction conditions in products yields obtained from lignin or spent liquors oxidation (Araújo et al., 2010; Dardelet et al., 1985; Fargues et al., 1996a; Mathias and Rodrigues, 1995). Besides the several kinetic studies of oxidation products from different lignins sources, as far as is concerned, there are no kinetic studies about oxidation products from kraft *E. globulus* lignin.

The accurate selection of the oxidation conditions is important not only to obtain the maximum yields of intermediary products, but also to avoid the oxidation of the produced aldehydes into organic acids such as formic, acetic, lactic, oxalic, syringic, vanillic, and *p*-hydroxybenzoic (Sales et al., 2006). However, the best process conditions for high yields on V and Sy should be determined for each lignin. Several authors studied the dependency of these phenolic compounds yield on temperature, reaction time, oxygen partial pressure ($p\text{O}_2$), initial lignin concentration, and alkaline condition (Araújo, 2008; Fargues et al., 1996a; Mathias, 1993; Pinto et al., 2012; Sales et al., 2006; Santos S.G. et al., 2011). It was observed that, in general, all the parameters have a positive effect on the net conversion as well as the products yields.

Fargues and co-workers (Fargues et al., 1996a; Fargues et al., 1996b) studied the process optimization of the production of V from the oxidation of a kraft *Pinus spp.* lignin. The kinetic study was carried out to measure reaction orders with respect to lignin, oxygen, and alkalinity, as well as the influence of temperature on the kinetic rate constants. They proved the dependency of the kinetic constant of V production with the temperature, and also show that the V produced is also degraded by oxidation whose importance depends on the pH and the temperature of the solution. The authors also found a maximum yield of V when oxidation reaction was performed

with lignin concentration of 60 g/l, temperature of 393 K, in alkaline medium containing NaOH at 80 g/l under pO_2 of 4 bar.

Araújo and co-workers (Araújo et al., 2010) observed that whatever is the lignin source, the variation of pH is the most important condition in the oxidation reaction: lower values of pH increase the rate of V degradation, reducing its yield. The mathematical model, used by these authors, to describe V production depends on the lignin source, and the temperature and O_2 pressure should be adjusted for the different reactions taking into account that the final yields are the equilibrium between improving the V conversion and minimizing its oxidation.

The main expressions used in literature for the kinetic study of phenolics production from lignin oxidation are depicted in Table 3.

Table 3 - Main expressions related to the kinetic study of lignin oxidation (Araújo et al., 2010; Fargues et al., 1996a; Fargues et al., 1996b; Mathias, 1993; Santos S.G. et al., 2011).

Kinetic study of V production from lignin oxidation, considering also the production of some degradation compounds from V	$\text{lignin} \xrightarrow{r_{\text{oxid}}} \text{V} \xrightarrow{r_{\text{degrad}}} \text{DP}$	V - vanillin; DP - degradation products;
	$r_{\text{oxid}} = k [\text{lignin}]^n pO_2^m$	k_{oxid} – V production rate constant; pO_2 – partial pressure of O_2 ; [lignin] – initial lignin concentration;
	$r_{\text{degrad}} = k [\text{V}]^a pO_2^b$	k_{degrad} – V degradation rate constant; A – constant in the Arrhenius equation
	$r_{\text{oxid}} = A \exp\left(-\frac{E_a}{RT}\right) [\text{lignin}]^n pO_2^m$	E_a - activation energy; R – universal gas constant; T - temperature (K)

Santos and co-workers (Santos S.G. et al., 2011) studied the major products obtained from the oxidation of an eucalyptus lignosulfonate (LS) and the kinetics of their formation. The oxidation reactions were performed with molecular O_2 , in alkaline medium, and in the temperature range of 403-423 K. The authors observed that oxidation of LS leads to a predominant formation of Sy and V among low molecular weight aromatic oxidation products. The kinetic results proved that the rate constant of Sy formation was more than twice that for V, and that Sy also suffered faster degradation (about 5 times) than V, under the same conditions. They also suggested that aromatic aldehydes in LS oxidation, under alkaline conditions, are formed via different mechanisms than aromatic acids, and that their yields are drastically affected by carbohydrates, which should be eliminated from sulfite spent liquor before oxidation (Santos S.G. et al., 2011). Fargues and co-workers (Fargues et al., 1996a) referred that, in lignin oxidation reactions, pO_2 should not be too high, and the effect of pO_2 is on the rate of products formation with no influence on yields. Nevertheless, the pO_2 should be controlled to avoid further oxidation of V (Collis, 1954; Fargues et al., 1996b). Changes in total pressure from 5 to 14 bar do not affect the products yields (Fargues et al., 1996a).

Some authors also referred that the reaction time and temperature should also be controlled to avoid degradation of the aldehydes produced leading to the formation of acids (Fargues et al., 1996a; Mathias, 1993). On the other hand, it is also stated in the literature that higher temperatures allow obtaining higher V yields in a shorter reaction time. Considering that V yield has a maximum with regard to the reaction severity, the rate of degradation of this compound is also higher (Pinto et al., 2012; Santos S.G. et al., 2011). Sales and co-workers studied lignin degradation reactions and aromatic aldehydes formation using a kinetic model quantified by a complex reaction network (Sales et al., 2006). Under the selected reaction conditions of temperature (in the range of 373-413 K) and pO_2 (between 2 and 10 bar) the kinetic evolution of a sugarcane lignin oxidation and products formation was investigated. The authors demonstrated that moderate pO_2 and short reaction times must be employed in order to obtain the maximum yields of intermediate oxidation products, such as V, Sy, and Hy, and to avoid that the produced aldehydes are oxidized into organic acids, since the lignin consumption is a faster reaction step.

Another important process parameter for aldehydes production is the pH value of the mixture. pH should stay higher than 12 in order to keep the high alkalinity during the reaction and consequently for the total ionization of phenolic groups and conversion to reactive quinonemethide. During the lignin oxidation process, the yield of V decreases when the pH value begins to decrease. Indeed, high alkali concentrations ($pH > 12$) reduce V degradation whereas at lower pH values (<11.5), an accentuated decrease in V yield is observed (Fargues et al., 1996a; Pinto et al., 2012). This phenomenon was attributed to the protonation of reaction intermediates, more basic than the phenolics produced (vanillin $pK_a = 7.4$) (Fargues et al., 1996a; Pinto et al., 2012; Tarabanko and Petukhov, 2003).

2.5 LIGNIN FRACTIONATION BY ULTRAFILTRATION

Due to the inherent heterogeneity of lignin structure and composition a variety of lignin fractionation methodologies have been proposed in the literature (Pinto et al., 2012). The molecular weight of lignin can vary between 1,000 Da and 300,000 Da within the same sample, and fractionation has become one of the most effective methods to obtain and characterize specific lignin fractions (Tolbert et al., 2014; Toledano et al., 2010a). Fractionation methods led to relatively homogeneous lignin fractions, which makes possible to understand more easily its composition, structure, and its use as source of phenolic compounds (Cui et al., 2014). Moreover, lignin fractionation methodologies can also be performed with the aim of lignin purification, since some methods allow removing contaminants, as carbohydrates and inorganic material. In the literature, there are three main methods applied for lignin fractionation, which include sequential organic solvent extraction, selective precipitation, and membrane ultrafiltration (Cui et al., 2014; Toledano et al., 2010a).

Membrane fractionation have been widely studied in the last years; the simple and effective separation, the concentration and purification of products, in small and medium scale process, makes this an interesting method to apply in several applications, as polymer formulations, or to obtain low molecular weight compounds (Alriols et al., 2010). The effectiveness of this fractionating method depends on the type of selected membrane and its pore-size or cut-off (Alriols et al., 2010; Toledano et al., 2010b). Considering the variety in the membrane types and in the operating conditions and, therefore, the field of application, there are four different types of membrane fractionation: microfiltration, ultrafiltration, nanofiltration, and reverse osmosis. However, all of them present important drawbacks related with the fouling and cleaning cycle associated to the membrane.

Membrane processes show all the advantages to be a key separation unit in biorefineries and pulp and paper industries due to their excellent fractionation capability, reduced consumption of chemicals, and low energy requirement (Abels et al., 2013; Jönsson et al., 2008). The use of ultrafiltration membranes in pulp and paper industries have as main applicability the treatment of bleach plant effluent and the fractionation and concentration of spent liquors (García et al., 2009). This process allows the selective extraction of lignin fractions from the black liquor solutions; the obtained fractions vary in composition, chemical structure, and properties. In literature, it is demonstrated that lignin fractions obtained from membranes with low molecular weight cut-off show a higher amount of phenolic hydroxyl groups and an increase in the content of α -oxidized aromatics and carboxylic groups (Keyoumu et al., 2004; Sevastyanova et al., 2014).

Several authors studied the application of membrane technology for the concentration and recovery of different lignin fractions with specific molecular weight. The main objective is to obtain different fractions able to be used in the synthesis of different high value-added products, as chemical reactants, resins and biocomposites, and antioxidant agents (Abels et al., 2013; Borges da Silva et al., 2009). In these studies, different operating conditions and types of membranes were considered. Toledano and co-workers processed black liquor resulting from alkaline treatment of *Miscanthus sinensis* using ultrafiltration (Toledano et al., 2010a; Toledano et al., 2010b). Ceramic membranes with cut-offs of 5, 10, and 15 kDa were used and lignin fractions with different molecular weights were obtained. The authors concluded that the fractionation process applied affects lignin properties, since ultrafiltered fractions show low contents of contaminants, as LCC (Toledano et al., 2010a; Toledano et al., 2010b). However, concerning β -O-4 and β -5, guaiacyl, syringyl, ferulates and *p*-coumaric acid contents they didn't find significant differences between fractions.

Liu and co-workers studied the use of organic and inorganic membranes to separate lignin from cellulose fraction in black liquor solutions (Liu et al., 2004). The authors have performed batch experiments using black liquor from straw, with a transmembrane pressure of 200 kPa at 303 K, and the results showed that approximately 80% lignin retention was achieved with

microfiltration membranes and 90% lignin retention with ultrafiltration membranes. However, to prove the high effectiveness of ultrafiltration membranes it is necessary to develop comparative studies with others fractionation methods. Toledano and co-authors presented two methods to fractionate lignin resulting from the black liquor of the pulping process of *Miscanthus sinensis* (Toledano et al., 2010b). The first method was the selective precipitation, which is achieved by the gradual acidification with concentrated sulfuric acid (H_2SO_4) of the black liquor, getting different precipitates according to the pH, and the second one the ultrafiltration, which uses ceramic membranes of different cut-off (5, 10 and 15 kDa) to obtain different liquors containing lignins with specific molecular weight. Different lignin fractions were obtained by both methods, and the characterization results showed that the fractionation process applied affects the properties of the obtained lignin. Ultrafiltered fractions are less contaminated by LCC than the fractions obtained by selective precipitation. Ultrafiltration process also allowed controlling the molecular weight of the obtained fractions.

Besides the large applicability of membranes fractionation in small scale, also pilot scale experiments were already performed. Keyoumu and co-workers used ceramic membranes to perform the continuous separation of defined low molecular weight lignin fractions from softwood and hardwood kraft black liquors on a pilot scale (Keyoumu et al., 2004). The membranes used had Mw cut-offs of 1, 5, and 15 kDa, and the authors proved that nano and ultrafiltration of black liquors appear to be a technically feasible way to remove organic material from the pulp mill effluent. More than 40% of the lignin degradation products obtained in the permeate had a Mw less than 1 kDa. The results also showed that the lignins isolated from this permeate are highly phenolic and have relatively uniform molecular weight distributions.

2.6 THE INTEGRATED PROCESS FOR VANILLIN PRODUCTION

The general concept of the integrated process for V production includes reaction and separation steps for producing V and lignin-based polyurethanes from kraft lignin (Borges da Silva et al., 2009). A simplified representation of the integrated process regarding the production and recovery of value-added aldehydes from lignin-containing raw materials proposed by the research group of LSRE-LCM, working with lignin based biorefining since 90's, is shown in Figure 6.

The strategy is to combine reaction engineering and efficient separation processes for converting lignin from pulping spent liquors into value-added aldehydes. A portion of the by-product streams is processed to extract lignin (acidification/precipitation, ultrafiltration or LignoBoost process). The subsequent processes are based on three main steps. The first step consists on the alkaline lignin oxidation with O_2 in a structured bubble column reactor (Araújo et al., 2009). Then, the reactor stream follows to an ultrafiltration process leading to the separation of high molecular weight fraction of degraded lignin from the lower molecular weight species, which goes

preferentially to the permeate. The permeate flows through a packed bed on acid resin in H^+ form to protonate the phenolates (Zabkova et al., 2007). At the end, there is a refine process using crystallization process.

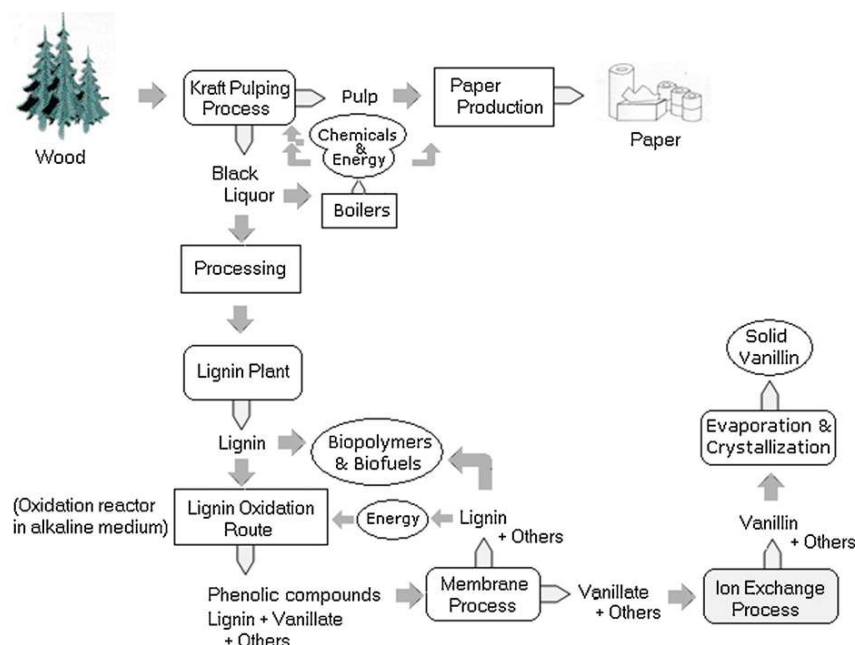


Figure 6 – Flow sheet of the integrated process for production of value-added aldehydes and polymers from kraft lignin in a biorefinery concept (Borges da Silva et al., 2009).

The production of lignin-based polyurethanes elastomers and foams could be also explored. The high molecular weight fraction retained in the ultrafiltration process can be considered as raw-material for lignin-based polyurethanes. The production of polymers from lignin is undoubtedly an attractive approach since it can take advantage of its functional groups and macromolecular properties. This application has been the topic of intense research and materials with quite promising properties were already obtained (Cateto et al., 2009; Cateto et al., 2008).

This complete process (reaction and separation) is easily integrated in a pulp and paper industrial plant, considering the possibility of part of the lignin from side streams (spent liquor) be deviated for the production of high added-value chemicals and not only burned to generate energy in pulp mills. Moreover, this process perfectly fits into the scope of new emerging lignocellulosic-based biorefineries to valorize lignin.

2.7 REFERENCES

Abels, C., Carstensen, F., Wessling, M. Membrane processes in biorefinery applications. *J. Membr. Sci.* 2013, 444, 285-317.

- Alriols, M.G., García, A., Llano-Ponte, R., Labidi, J. Combined organosolv and ultrafiltration lignocellulosic biorefinery process. *Chem. Eng. J.* 2010, 157, 113-120.
- Araújo, J.D. 2008. Production of vanillin from lignin present in the Kraft black liquor of the pulp and paper industry, in: *LSRE, Department of Chemical Engineering, Faculty of Engineering University of Porto*. Porto.
- Araújo, J.D.P., Grande, C.A., Rodrigues, A.E. Structured packed bubble column reactor for continuous production of vanillin from kraft lignin oxidation. *Catal. Today* 2009, 147, S330-S335.
- Araújo, J.D.P., Grande, C.A., Rodrigues, A.E. Vanillin production from lignin oxidation in a batch reactor. *Chem. Eng. Res. Des.* 2010, 88, 1024-1032.
- Azadi, P., Inderwildi, O.R., Farnood, R., King, D.A. Liquid fuels, hydrogen and chemicals from lignin: A critical review. *Renew. Sust. Energ. Rev.* 2013, 21, 506-523.
- Balakshin, M., Capanema, E., Gracz, H., Chang, H.m., Jameel, H. Quantification of lignin-carbohydrate linkages with high-resolution NMR spectroscopy. *Planta* 2011, 233, 1097-1110.
- Behling, R., Valange, S., Chatel, G. Heterogeneous catalytic oxidation for lignin valorization into valuable chemicals: what results? What limitations? What trends? *Green Chemistry* 2016.
- Berlin, A., Balakshin, M. 2014. Chapter 18 - Industrial lignins: analysis, properties, and applications. in: *Bioenergy Research: Advances and Applications*, (Eds.) V.K. Gupta, M.G. Tuohy, C.P. Kubicek, J. Saddler, F. Xu, Elsevier. Amsterdam, pp. 315-336.
- Boerjan, W., Ralph, J., Baucher, M. Lignin biosynthesis *Annu. Rev. Plant Biol.* 2003, 54, 519-546.
- Borges da Silva, E.A., Zabkova, M., Araujo, J.D., Cateto, C.A., Barreiro, M.F., Belgacem, M.N., Rodrigues, A.E. An integrated process to produce vanillin and lignin-based polyurethanes from kraft lignin. *Chemical Engineering Research & Design* 2009, 87, 1276-1292.
- Buranov, A.U., Mazza, G. Lignin in straw of herbaceous crops. *Ind. Crop. Prod.* 2008, 28, 237-259.
- Calvo-Flores, F.G., Dobado, J.A. Lignin as renewable raw material. *ChemSusChem* 2010, 3, 1227-1235.

- Capanema, E.A., Balakshin, M.Y., Chen, C.L., Gratzl, J.S., Gracz, H. Structural analysis of residual and technical lignins by ^1H - ^{13}C correlation 2D NMR-spectroscopy. *Holzforchung* 2001, 55, 302-308.
- Capanema, E.A., Balakshin, M.Y., Kadla, J.F. A comprehensive approach for quantitative lignin characterization by NMR spectroscopy. *J. Agric. Food. Chem.* 2004, 52, 1850-1860.
- Cateto, C.A., Barreiro, M.F., Rodrigues, A.E., Belgacem, M.N. Optimization study of lignin oxypropylation in view of the preparation of polyurethane rigid foams. *Ind. Eng. Chem. Res.* 2009, 48, 2583-2589.
- Cateto, C.A., Barreiro, M.F., Rodrigues, A.E., Brochier-Salon, M.C., Thielemans, W., Belgacem, M.N. Lignins as macromonomers for polyurethane synthesis: A comparative study on hydroxyl group determination. *J. Appl. Polym. Sci.* 2008, 109, 3008-3017.
- Collis, B.C. 1954. Manufacture of vanillin from lignin, Monsanto, Chemicals. United States.
- Cui, C., Sun, R., Argyropoulos, D.S. Fractional precipitation of softwood kraft lignin: Isolation of narrow fractions common to a variety of lignins. *ACS Sustainable Chemistry & Engineering* 2014, 2, 959-968.
- Dardelet, S., Froment, P., Lacoste, N., Robert, A. Aldéhyde syringique: Possibilités de production à partir de bois feuillus. *Revue - A.T.I.P.* 1985, 39, 267-274.
- El Hage, R., Brosse, N., Sannigrahi, P., Ragauskas, A. Effects of process severity on the chemical structure of *Miscanthus* ethanol organosolv lignin. *Polym. Degrad. Stab.* 2010, 95, 997-1003.
- Erofeev, Y.V., Afanas'eva, V.L., Glushkov, R.G. Synthetic routes to 3,4,5-trimethoxybenzaldehyde (review). *Pharm. Chem. J.* 1990, 24, 501-510.
- Evtuguin, D.V., Neto, C.P., Silva, A.M.S., Domingues, P.M., Amado, F.M.L., Robert, D., Faix, O. Comprehensive study on the chemical structure of dioxane lignin from plantation *Eucalyptus globulus* wood. *J. Agric. Food. Chem.* 2001, 49, 4252-4261.
- Fache, M., Boutevin, B., Caillol, S. Vanillin production from lignin and its use as a renewable chemical. *ACS Sustainable Chemistry & Engineering* 2016, 4, 35-46.
- Fahlbusch, K.-G., Hammerschmidt, F.-J., Panten, J., Pickenhagen, W., Schatkowski, D., Bauer, K., Garbe, D., Surburg, H. 2002. Flavors and fragrances. 7th Edition ed. in: *Ullmann's encyclopedia of industrial chemistry*, Wiley-VCH. Weinheim, Germany.

- Fargues, C., Mathias, A., Rodrigues, A. Kinetics of vanillin production from kraft lignin oxidation. *Ind. Eng. Chem. Res.* 1996a, 35, 28-36.
- Fargues, C., Mathias, A., Silva, J., Rodrigues, A. Kinetics of vanillin oxidation. *Chem. Eng. Technol.* 1996b, 19, 127-136.
- Fernández-Costas, C., Gouveia, S., Sanromán, M.A., Moldes, D. Structural characterization of Kraft lignins from different spent cooking liquors by 1D and 2D Nuclear Magnetic Resonance spectroscopy. *Biomass Bioenergy* 2014, 63, 156-166.
- Fernando, S., Adhikari, S., Chandrapal, C., Murali, N. Biorefineries: Current status, challenges, and future direction. *Energ. Fuel* 2006, 20, 1727-1737.
- FitzPatrick, M., Champagne, P., Cunningham, M.F., Whitney, R.A. A biorefinery processing perspective: Treatment of lignocellulosic materials for the production of value-added products. *Bioresour. Technol.* 2010, 101, 8915-8922.
- Froass, P.M., Ragauskas, A.J., Jiang, J. Nuclear magnetic resonance studies. 4. Analysis of residual lignin after kraft pulping. *Ind. Eng. Chem. Res.* 1998, 37, 3388-3394.
- García, A., Toledano, A., Serrano, L., Egüés, I., González, M., Marín, F., Labidi, J. Characterization of lignins obtained by selective precipitation. *Sep. Purif. Technol.* 2009, 68, 193-198.
- German Federal Government. 2012. Biorefineries roadmap, (Ed.) Agency for renewable resources (FNR), Druckerei Schlesener KG. Berlin.
- Gosselink, R.J.A. 2011. Lignin as a renewable aromatic resource for the chemical industry, in: *Wageningen University*.
- Holladay, J.E., Bozell, J.J., White, J.F., Johnson, D. 2007. Results of screening for potential candidates from biorefinery lignin. Pacific Northwest National Laboratory and National Renewable Energy Laboratory.
- Huang, W.-B., Du, C.-Y., Jiang, J.-A., Ji, Y.-F. Concurrent synthesis of vanillin and isovanillin. *Res. Chem. Intermed.* 2012, 39, 2849-2856.
- Ibarra, D., Chávez, M.I., Rencoret, J., Del Río, J.C., Gutiérrez, A., Romero, J., Camarero, S., Martínez, M.J., Jiménez-Barbero, J., Martínez, A.T. Lignin modification during *Eucalyptus globulus* kraft pulping followed by totally chlorine-free bleaching: A two-dimensional

- nuclear magnetic resonance, fourier transform infrared, and pyrolysis–gas chromatography/mass spectrometry study. *J. Agric. Food. Chem.* 2007, 55, 3477-3490.
- Ibrahim, M.N.M., Sriprasanthi, R. B., Shamsudeen, S., Adam, F., and Bhawani, S. A. . A concise review of the natural existance, synthesis, properties, and applications of syringaldehyde. *BioRes.* 2012, 7.
- Jönsson, A.S., Nordin, A.-K., Wallberg, O. Concentration and purification of lignin in hardwood kraft pulping liquor by ultrafiltration and nanofiltration. *Chem. Eng. Res. Des.* 2008, 86, 1271-1280.
- Keyoumu, A., Sjö Dahl, R., Henriksson, G., Ek, M., Gellerstedt, G., Lindström, M.E. Continuous nano- and ultra-filtration of kraft pulping black liquor with ceramic filters: A method for lowering the load on the recovery boiler while generating valuable side-products. *Ind. Crop. Prod.* 2004, 20, 143-150.
- Krotschek, A.W., Sixta, H. 2008. Recovery. in: *Handbook of Pulp*, (Ed.) H. Sixta, Vol. 2, Wiley-VCH Verlag GmbH&Co. KGaA. Weinheim, Germany, pp. 967-994.
- Lee, C.Y., Sharma, A., Cheong, J.E., Nelson, J.L. Synthesis and antioxidant properties of dendritic polyphenols. *Bioorg. Med. Chem. Lett.* 2009, 19, 6326-6330.
- Lersch, M. 2011. Biorefining at Borregaard – recent developments in the processing of lignocellulosics. *The 3rd Nordic Wood Biorefinery Conference (NWBC 2011)*, 22-24 March, Stokolm, Sweeden. pp. 109-113.
- Lewis, N.G., Yamamoto, E. Lignin: Occurrence, biogenesis and biodegradation. *Annu. Rev. Plant Physiol. Plant Mol. Biol.* 1990, 41, 455-496.
- Lin, S.Y., Dence, C.W. *Methods in lignin chemistry*; Springer-Verlag, 1992.
- Liu, G., Liu, Y., Ni, J., Shi, H., Qian, Y. Treatability of kraft spent liquor by microfiltration and andultrafiltration. *Desalination* 2004, 160, 131-141.
- Long, S.P., Karp, A., Buckeridgec, M.S., Murphyf, D.J., Onwona-Agyemang, S., Vonshakh, A. 2015. Feedstocks for biofuels and bioenergy. in: *Bioenergy and sustainability: Bridging the gaps.* , (Eds.) Souza G.M., Victoria R.L., Joly C.A., Verdade L.M., Scientific Committee on Problems of the Environment (SCOPE). Paris, pp. 302-336.

- Lora, J. 2008. Industrial commercial lignins: Sources, properties and applications. 1^o ed. in: *Monomers, Polymers and Composites from Renewable Resources*, (Eds.) M.N. Belgacem, A. Gandini, Elsevier. Oxford.
- Lourenço, A., Gominho, J., Marques, A.V., Pereira, H. Variation of lignin monomeric composition curing kraft pulping of *Eucalyptus globulus* heartwood and sapwood. *J. Wood Chem. Technol.* 2012, 33, 1-18.
- Lu, F., Ralph, J. Derivatization followed by reductive cleavage (DFRC method), a new method for lignin analysis: protocol for analysis of DFRC monomers. *J. Agric. Food. Chem.* 1997, 45, 2590-2592.
- Lucia, L.A. Lignocellulosic biomass: A potential feedstock to replace petroleum. *BioResources* 2008, 3, 981-982.
- Marshall, H.B., Sankey, A.C. 1951. Method of producing vanillin, Ontario Paper Company, Ltd United States.
- Mathias, A.L. 1993. Produção de vanilina a partir da lenhina: Estudo cinético e do processo (in Portuguese language), in: *LSRE, Department of Chemical Engineering*, Faculty of Engineering University of Porto. Porto.
- Mathias, A.L., Lopretti, M.I., Rodrigues, A.E. Chemical and biological oxidation of *Pinus-Pinaster* lignin for the production of vanillin. *J. Chem. Technol. Biotechnol.* 1995, 64, 225-234.
- Mathias, A.L., Rodrigues, A.E. Production of vanillin by oxidation of *Pine* kraft lignins with oxygen. *Holzforschung* 1995, 49, 273-278.
- Monteil-Rivera, F., Phuong, M., Ye, M., Halasz, A., Hawari, J. Isolation and characterization of herbaceous lignins for applications in biomaterials. *Ind. Crop. Prod.* 2013, 41, 356-364.
- Nimz, H.H., Robert, D., Faix, O., Nembr, M. Carbon-¹³NMR spectra of lignins, 8. Structural differences between lignins of hardwoods, softwoods, grasses and compression wood. *Holzforschung* 1981, 35, 16-26.
- Pan, X., Arato, C., Gilkes, N., Gregg, D., Mabee, W., Pye, K., Xiao, Z., Zhang, X., Saddler, J. Biorefining of softwoods using ethanol organosolv pulping: Preliminary evaluation of process streams for manufacture of fuel-grade ethanol and co-products. *Biotechnol. Bioeng.* 2005, 90, 473-481.

- Pan, X., Gilkes, N., Kadla, J., Pye, K., Saka, S., Gregg, D., Ehara, K., Xie, D., Lam, D., Saddler, J. Bioconversion of hybrid poplar to ethanol and co-products using an organosolv fractionation process: Optimization of process yields. *Biotechnol. Bioeng.* 2006, 94, 851-861.
- Pandey, M.P., Kim, C.S. Lignin depolymerization and conversion: A review of thermochemical methods. *Chem. Eng. Technol.* 2011, 34, 29-41.
- Pepper, J.M., Casselman, B.W., Karapally, J.C. Lignin oxidation. Preferential use of cupric oxide. *Can. J. Chem.* 1967, 45, 3009-3012.
- Pinto, P.C., Borges da Silva, E.A., Rodrigues, A.E. Insights into oxidative conversion of lignin to high-added-value phenolic aldehydes. *Ind. Eng. Chem. Res.* 2011, 50, 741-748.
- Pinto, P.C., Evtuguin, D.V., Neto, C.P. Effect of structural features of wood biopolymers on hardwood pulping and bleaching performance. *Ind. Eng. Chem. Res.* 2005, 44, 9777-9784.
- Pinto, P.C., Evtuguin, D.V., Neto, C.P., Silvestre, A.J.D., Amado, F.M.L. Behavior of *Eucalyptus globulus* lignin during kraft pulping II. Analysis by NMR, ESI/MS and GPC. *J. Wood Chem. Technol.* 2002, 22, 109 - 125.
- Pinto, P.C.R., Borges da Silva, E.A., Rodrigues, A.E. 2012. Lignin as source of fine chemicals: Vanillin and syringaldehyde. in: *Biomass Conversion*, (Eds.) C. Baskar, S. Baskar, R.S. Dhillon, Springer Berlin Heidelberg, pp. 381-420.
- Pinto, P.C.R., Costa, C.E., Rodrigues, A.E. Oxidation of lignin from *Eucalyptus globulus* pulping liquors to produce syringaldehyde and vanillin. *Ind. Eng. Chem. Res.* 2013, 52, 4421-4428.
- Quesada, J., Rubio, M., Gomez, D. Ozonation of lignin rich solid fractions from corn stalks. *J. Wood Chem. Technol.* 1999, 19, 115-137.
- Ragauskas, A.J., Beckham, G.T., Biddy, M.J., Chandra, R., Chen, F., Davis, M.F., Davison, B.H., Dixon, R.A., Gilna, P., Keller, M., Langan, P., Naskar, A.K., Saddler, J.N., Tschaplinski, T.J., Tuskan, G.A., Wyman, C.E. Lignin valorization: Improving lignin processing in the biorefinery. *Science* 2014, 344, 1246843.
- Ralph, J., Hatfield, R.D., Piquemal, J., Yahiaoui, N., Pean, M., Lapierre, C., Boudet, A.M. NMR characterization of altered lignins extracted from tobacco plants down-regulated for lignification enzymes cinnamylalcohol dehydrogenase and cinnamoyl-CoA reductase. *Proceedings of the National Academy of Sciences* 1998, 95, 12803-12808.

- Ralph, J., Lundquist, K., Brunow, G., Lu, F., Kim, H., Schatz, P., Marita, J., Hatfield, R., Ralph, S., Christensen, J., Boerjan, W. Lignins: natural polymers from oxidative coupling of 4-hydroxyphenyl- propanoids. *Phytochem. Rev.* 2004, 3, 29-60.
- Rojas, O.J., Song, J., Bullón, J., Argyropoulos, D.S. Lignin separation from kraft black liquors by tangential ultrafiltration. *Chimica e l'Industria (Italy)* 2006, 88.
- Saito, T., Perkins, J.H., Vautard, F., Meyer, H.M., Messman, J.M., Tolnai, B., Naskar, A.K. Methanol fractionation of softwood kraft lignin: Impact on the lignin properties. *ChemSusChem* 2014, 7, 221-228.
- Sales, F.G., Maranhão, L.C.A., Lima Filho, N.M., Abreu, C.A.M. Kinetic evaluation and modeling of lignin catalytic wet oxidation to selective production of aromatic aldehydes. *Ind. Eng. Chem. Res.* 2006, 45, 6627-6631.
- Sannigrahi, P., Ragauskas, A.J., Miller, S.J. Lignin structural modifications resulting from ethanol organosolv treatment of *Loblolly Pine*. *Energ. Fuel* 2009, 24, 683-689.
- Sannigrahi, P., Ragauskas, A.J., Tuskan, G.A. Poplar as a feedstock for biofuels: A review of compositional characteristics. *Biofuels, Bioproducts and Biorefining* 2010, 4, 209-226.
- Santos R.B., Capanema, E.A., Balakshin, M.Y., Chang, H.M., Jameel, H. Effect of hardwoods characteristics on kraft pulping process: Emphasis on lignin structure. *BioResources* 2011, 6, 3623-3637.
- Santos R.B., Hart, P., Jameel, H., Chang, H. Wood based lignin reactions important to the biorefinery and pulp and paper industries. *BioResources* 2013, 8, 1456-1477.
- Santos S.G., Marques, A.P., Lima, D.L.D., Evtuguin, D.V., Esteves, V.I. Kinetics of eucalypt lignosulfonate oxidation to aromatic aldehydes by oxygen in alkaline medium. *Ind. Eng. Chem. Res.* 2011, 50, 291-298.
- Schneider, P., Damhus, T. 1997. Enhancer such as acetosyringone, Novo Nordisk A/S. Denmark.
- Sevastyanova, O., Lange, H., Crestini, C., Dobele, G., Helander, M., Chang, L., Lindström, M.E. 2014. Selective isolation of technical lignin from the industrial side-streams - structure and properties. *NWBC - Nordic Wood Biorefinery Conference*, Stockholm.
- Sippola, V.O., Krause, A.O.I. Bis(o-phenanthroline)copper-catalysed oxidation of lignin model compounds for oxygen bleaching of pulp. *Catal. Today* 2005, 100, 237-242.

- Sjöde, A., Frölander, A., Lersch, M., Rødsrud, G. 2009. Lignocellulosic biomass conversion by sulfite pretreatment, (Ed.) N. Borregaard Industries Limited.
- Sjöström, E. Wood chemistry: Fundamentals and applications; Academic Press: London, 1993.
- Stewart, D. Lignin as a base material for materials applications: Chemistry, application and economics. *Ind. Crop. Prod.* 2008, 27, 202-207.
- Strassberger, Z., Tanase, S., Rothenberg, G. The pros and cons of lignin valorisation in an integrated biorefinery. *RSC Advances* 2014, 4, 25310-25318.
- Sun, X.F., Xu, F., Sun, R.C., Wang, Y.X., Fowler, P., Baird, M.S. Characteristics of degraded lignins obtained from steam exploded wheat straw. *Polym. Degrad. Stab.* 2004, 86, 245-256.
- Tarabanko, V., Petukhov, D. Study of mechanism and improvement of the process of oxidative cleavage of lignins into the aromatic aldehydes. *Chemistry for Sustainable Development* 2003, 11, 655-667.
- Tarabanko, V.E., Pervishina, E.P., Hendogina, Y.V. Kinetics of aspen wood oxidation by oxygen in alkaline media. *React. Kinet. Catal. Lett.* 2001, 72, 153-162.
- Tolbert, A., Akinosho, H., Khunsupat, R., Naskar, A.K., Ragauskas, A.J. Characterization and analysis of the molecular weight of lignin for biorefining studies. *Biofuels, Bioproducts and Biorefining* 2014, 8, 836-856.
- Toledano, A., García, A., Mondragon, I., Labidi, J. Lignin separation and fractionation by ultrafiltration. *Sep. Purif. Technol.* 2010a, 71, 38-43.
- Toledano, A., Serrano, L., Garcia, A., Mondragon, I., Labidi, J. Comparative study of lignin fractionation by ultrafiltration and selective precipitation. *Chem. Eng. J.* 2010b, 157, 93-99.
- Tromans, D. Oxygen solubility modeling in inorganic solutions: concentration, temperature and pressure effects. *Hydrometallurgy* 1998, 50, 279-296.
- Vigneault, A., Johnson, D.K., Chornet, E. Base-catalyzed depolymerization of lignin: Separation of monomers. *The Canadian Journal of Chemical Engineering* 2007, 85, 906-916.
- Villar, J.C., Caperos, A., Garcia-Ochoa, F. Oxidation of hardwood kraft-lignin to phenolic derivatives with oxygen as oxidant. *Wood Sci. Technol.* 2001, 35, 245-255.
- Vishtal, A.G., Kraslawski, A. Challenges in industrial applications of technical lignins. *2011* 2011, 6, 3547-3568.

- Wallberg, O., Jönsson, A.-S., Wimmerstedt, R. Ultrafiltration of kraft black liquor with a ceramic membrane. *Desalination* 2003, 156, 145-153.
- Wen, J.-L., Xue, B.-L., Sun, S.-L., Sun, R.-C. Quantitative structural characterization and thermal properties of birch lignins after auto-catalyzed organosolv pretreatment and enzymatic hydrolysis. *J. Chem. Technol. Biotechnol.* 2013a, 88, 1663-1671.
- Wen, J.L., Sun, S.L., Yuan, T.Q., Xu, F., Sun, R.C. Structural elucidation of lignin polymers of *Eucalyptus* chips during organosolv pretreatment and extended delignification. *J. Agric. Food. Chem.* 2013b, 61, 11067-11075.
- Wong, Z., Chen, K., Li, J. Formation of vanillin and syringaldehyde in an oxygen delignification process. *Bioresour. Technol.* 2010, 5, 1509-1516.
- Wu, G., Heitz, M. Catalytic mechanism of Cu^{2+} and Fe^{3+} in alkaline O_2 oxidation of lignin. *J. Wood Chem. Technol.* 1995, 15, 189-202.
- Wu, G., Heitz, M., Chornet, E. Improved alkaline oxidation process for the production of aldehydes (vanillin and syringaldehyde) from steam-explosion hardwood lignin. *Ind. Eng. Chem. Res.* 1994, 33, 718-723.
- Xiang, Q., Lee, Y.Y. Production of oxychemicals from precipitated hardwood lignin. *Appl. Biochem. Biotechnol.* 2001, 91-93, 71-80.
- Xiao, B., Sun, X.F., Sun, R. Chemical, structural, and thermal characterizations of alkali-soluble lignins and hemicelluloses, and cellulose from maize stems, rye straw, and rice straw. *Polym. Degrad. Stab.* 2001, 74, 307-319.
- Yuan, T.-Q., Xu, F., Sun, R.-C. Role of lignin in a biorefinery: Separation characterization and valorization. *J. Chem. Technol. Biotechnol.* 2013, 88, 346-352.
- Zabkova, M., Borges da Silva, E.A., Rodrigues, A.E. Recovery of vanillin from kraft lignin oxidation by ion-exchange with neutralization. *Sep. Purif. Technol.* 2007, 55, 56-68.
- Zakzeski, J., Bruijninx, P.C.A., Jongerius, A.L., Weckhuysen, B.M. The catalytic valorization of lignin for the production of renewable chemicals. *Chem. Rev.* 2010a, 110, 3552-3599.
- Zakzeski, J., Jongerius, A.L., Weckhuysen, B.M. Transition metal catalyzed oxidation of Alcell lignin, soda lignin, and lignin model compounds in ionic liquids. *Green Chemistry* 2010b, 12, 1225-1236.

Zhang, J., Deng, H., Lin, L. Wet aerobic oxidation of lignin into aromatic aldehydes catalysed by a perovskite-type oxide: $\text{LaFe}_{1-x}\text{Cu}_x\text{O}_3$ ($x=0, 0.1, 0.2$). *Molecules* 2009, 14, 2747-2757.

3

Characterization and comparative evaluation of hardwood lignins

The production of fuels, added-value chemicals, and materials from lignocellulosic biomass has becoming noticeable in the recent years, leading to an intense demand on feedstocks. In this perspective, forest and industrial by-products are sustainable sources for exploitation.

In this chapter, *E. globulus* lignins produced by mild acidolysis of wood and bark, and industrial lignins (kraft and organosolv) were characterized by several NMR techniques, including ^{13}C , ^{31}P and ^1H NMR. The first goal was to evaluate the impact of the delignification process on the structure of *E. globulus* lignin (functional groups and linkages) and to find the main structural features related with the ability to produce phenolic aldehydes, such as vanillin and syringaldehyde, as a possible route for lignin valorization. The second goal was to report the structure of lignin from *E. globulus* bark, presenting the comparison with the lignin from the respective wood. The results are discussed in a comparative approach, using radar classification, highlighting for each material the characteristic features of lignins.

This chapter is based on the following publications:

- Costa, C.A.E.; Pinto, P.C.R.; Rodrigues, A.E. Evaluation of chemical processing impact on *E. globulus* wood lignin and comparison with bark lignin. *Ind. Crop. Prod.* 2014, 61, 479-491.
- Costa, C.A.E.; Pinto, P.C.R.; Rodrigues, A.E. Radar tool for lignin classification on the perspective of its valorization. *Ind. Eng. Chem. Res.* 2015, 54, 7580–7590.

3.1 INTRODUCTION

Eucalyptus species represent the main raw-material for the pulp industry in South America, Portugal and Spain. In Portugal, about 7 million m³ of debarked *Eucalyptus globulus* wood per year is used in pulp production for high performance paper. The logs are debarked at mill site and the bark is mainly used as fuel to energy supply for mill operations. Some chemical aspects of *E. globulus* bark and wood are similar (Miranda et al., 2013; Mota et al., 2012) and suitable for a valorization route compatible with the biorefinery concept, integrated in the existing pulp mills. In pulp and paper industries, lignin represents a by-product exceeding 50 million tons per year (Gosselink et al., 2004). However, most of the lignin produced is used as low-cost fuel to generate energy for mill operations (along with pulping chemicals recovery), and only a small fraction, approximately 1 million ton per year, is used for commercial applications (Holladay et al., 2007; Saito et al., 2014), mostly in liginosulfonate form. The increase demand for platform chemicals from renewables feedstocks is one of the driven forces for the creation of lignocellulosic-based biorefineries, which are currently emerging all over the world. The economic sustainability of these new industries depends on the successful integration of a route for lignin valorization which is related with the characteristics of the lignin produced. The source of biomass and the delignification process have considerable influence on the structure of this biopolymer (linkages and functional groups) and consequently on its reactivity toward a further chemical process (Pinto et al., 2011). Hence, the lignin obtained from delignification processes differs from the native one as a result of multiple reactions (Pinto et al., 2012), that predominantly involve condensation and degradation reactions (Berlin and Balakshin, 2014). This chapter presents a comprehensive and comparative analysis of *E. globulus* lignins, revealing the importance of processing on lignin functionality and reactivity as one of the possible tools for the selection of lignins/processes to a valorization route within a lignocellulosic-based biorefinery.

3.2 EXPERIMENTAL SECTION: MATERIALS AND METHODS

3.2.1 *E. globulus* lignin samples

Four lignins resulting from *E. globulus* were studied: a lignin produced by the organosolv process of *E. globulus* wood (LEgOrg) (kindly supplied by Lignol Innovations, Canada), a lignin isolated and further purified from *E. globulus* industrial kraft liquor (LEgKraft), and lignins isolated from wood (LEg_{wood}) and bark (LEg_{bark}) by mild acidolysis using dioxane and hydrogen chloride (HCl), as described in the following section.

3.2.2 Lignin isolation by mild acidolysis

Wood and bark were submitted to mild acidolysis for lignin isolation. About 25 g of dried material (fraction 40–60 mesh, pre-extracted with ethanol/toluene) was placed in a 1 L three necked flask fitted with a reflux condenser and a nitrogen bubbler. The solvent, 250 mL of dioxane/water (9:1, v/v) mixture containing 1.82 g of HCl equivalent to 0.2 M, was slowly added. The reaction mixture, under nitrogen, was heated with a heating mantle and refluxed at 90-95 °C for a period of 40 min. Then, the mixture was allowed to cool in a nitrogen atmosphere to around 50 °C. The liquid phase was filtered off and the solid residue was subjected to the next extraction with 200 mL of the acidic dioxane/water solution for a period of 30 min, as described above. This process was repeated two more times, collecting each liquid phase. The last extraction was performed during 30 min with 150 mL of dioxane/water without addition of HCl. Each portion of extract was concentrated separately and then the concentrates were combined and lignin was precipitated by addition of the dioxane solution in cold water. The isolated lignin was separated by centrifugation, washed with water until neutral pH and freeze-dried.

3.2.3 Kraft lignin purification

Before characterization, kraft lignin was submitted to further purification by dissolution in dioxane. About 30 g of kraft lignin were dissolved in 400 mL of dioxane and left over-night at room temperature and moderate stirring. The dioxane non-soluble fraction, enriched in contaminants, was removed off and washed thoroughly with dioxane. The dioxane-soluble fraction, enriched in lignin, and the washing dioxane was slowly added to cold water for precipitation. The precipitate was recovered by centrifugation, washed with water and freeze-dried, giving origin to LEgKraft.

3.2.4 Preliminary analysis of lignins

3.2.4.1 Inorganics content

The inorganic content of lignins and residues was gravimetrically quantified; about 100 mg of each lignin was placed in a crucible and incinerated in a muffle furnace at 600 °C during 6.5 h. Each determination was made in triplicated.

3.2.4.2 Carbohydrate content

For carbohydrate analysis, lignins were submitted to acid methanolysis. This method assures an efficient cleavage of the glycosidic linkages between neutral monosaccharides and uronic acids with low degradation. However, acid methanolysis does not promote the complete cleavage of cellulose, and for this reason only the quantification of non-cellulosic polysaccharides fraction could be achieved (calculated as homopolymer) (Mota et al., 2012).

Lignins (10-15 mg) were submitted to acid methanolysis in 2 mL of 2 M HCl methanolic solution, prepared by dilution of a commercial solution of 3 M HCl with anhydrous methanol. The methanolysis reaction was performed at 100 °C, during 4 h. After cooling, 100 µL of pyridine were added to the methanolysates to neutralize the remaining HCl, followed by the addition of 1.00 mL of sorbitol methanolic solution 0.1 mg/mL (internal standard); the resulting mixture was carefully evaporated under reduced pressure. Then, the dried methanolysates were dissolved in 150 µL of pyridine, 150 µL of N,O-bis-(trimethylsilyl)-trifluoroacetamide (BSTFA) and 50 µL of chlorotrimethylsilane (TMS), maintaining the reaction mixture at 80 °C for 30 min, to convert the partially methylated monosaccharides to trimethylsilylated derivatives. The products were identified by gas chromatography mass spectrometry (GC-MS) and quantified by gas chromatography with flame ionization detector (GC-FID).

For quantification, the products were analyzed by GC-FID on a DANI GC 1000 chromatograph, with a capillary column ValcoBond VB1 (30 m × 0.32 mm I.D., 0.25 µm film thickness), using the following temperature program: 100-175 °C at 4 °C/min and 175-290 °C at 12 °C/min. The temperature of the detector and the injector were kept at 290 °C and 260 °C, respectively. External calibration was performed with standards for each monosaccharide: rhamnose, xylose, galacturonic acid, glucose, galactose, manose, and arabinose; glucuronic acid was the standard used for 4-O-methyl-glucuronic acid quantification. The GC-MS analyses were performed in a Trace Gas Chromatograph 2000 Series equipped with a Finnigan Trace MS mass spectrometer (EI), using helium as carries gas (35 cm/s). The chromatographic conditions, including the column, were the same as described for GC-FID with a transfer-line temperature of 290 °C and split ratio of 1:100.

Methanolysis of polysaccharides leads to the cleavage of the glycoside bonds with the production of the α - and β -anomers and pyranose and furanose ring forms of the monosaccharides. The identification was performed based on the number of glycoside peaks, their relative retention time and signal intensity proportion (Bleton et al., 1996; Doco et al., 2001), and mass spectra of trimethylsilyl methyl glycoside derivatives using spectral data reported in the literature (Bleton et al., 1996; Doco et al., 2001) and standards.

3.2.4.3 Elemental analysis

Carbon (C), hydrogen (H), sulfur (S) and nitrogen (N) contents were determined using a Thermo Scientific Flash 2000 Organic Elemental Analyser. The percentage of oxygen (O) was calculated by difference, i.e. by subtracting the C, H, S, and N percentages from 100.

3.2.5 Structural characterization of *E. globulus* lignins

3.2.5.1 Nitrobenzene oxidation (NO)

Analysis by NO provides the yields and types of simple phenolic aldehydes and acids (Hy, V, Sy, VA, SA) obtained through the cleavage of linkages between monolignols in the non-condensed fraction of lignin. G-type units yield V, while S-type units give Sy as major products. H units yield Hy. VA and SA are usually minor products from G and S units, respectively.

Lignins were submitted to alkaline NO. About 30 mg of each sample was dissolved in 7.00 mL of 2 M NaOH aqueous solution in a teflon vessel and, after adding 0.45 mL of nitrobenzene the vessel was placed into a stainless steel reactor and heated up to 170 °C for 4 h. Each oxidation experiment was made in triplicate. The oxidized material was then extracted with chloroform in a separating funnel (four times, 5 mL each) to remove nitrobenzene and its reduction products. After the first extraction, the aqueous phase was acidified (pH 2) with a few drops of H₂SO₄ solution (12 M), and then extracted four times with chloroform (5 mL each). The four extracts were combined and dried over anhydrous sodium sulfate. The solvent was evaporated under reduce pressure, the dried sample was dissolved in methanol and made up to 10 mL with methanol. The solution was then filtered and analyzed by high performance liquid chromatography (HPLC) in a Knauer HPLC system equipped with a Smartline 5000 online degasser, a Smartline 1000 quaternary pump, and a 2500 UV detector was used. The analytical column was a ChromSep SS (250 × 3.0 mm, 5 μm) with a ChromSpher 5 C18 (Chrompack) guard column. The detection wavelength was set at 280 nm. Chromatograms were run at room temperature and at 0.4 mL/min. The volume of the injection loop was 20 μL. A preliminary study on HPLC operating conditions was carried out to obtain a good compromise between retention and run time for the separation of all the compounds.

The separation was performed using an elution gradient due to the different polarities of the compounds. Formic acid (pKa 3.75) was added to ensure a low pH and to prevent the ionization of carboxylic groups and, thus, peak tailing. The mobile phase used for analysis was a binary eluent: eluent A, 95:5 (v/v) water:methanol containing 0.1% (v/v) formic acid; eluent B, 5:95 (v/v) water:methanol with 0.1% (v/v) formic acid. Eluents were filtered through a 0.20 μm pore size filter (Millipore). The gradient program was 0-3 min 90% A, 10% B; 7 min 80% A, 20% B; 7-20

min 80% A, 20% B; 40 min 40% A, 60% B; 43 min 100% B. Standard solutions and samples were filtered before injection using a 0.2 μm disposable filter (Millipore).

Eight standard solutions were prepared with all seven compounds (V, VA, VO, Sy, SA, SO, Hy) dissolved in methanol to an individual final concentration ranging from 0.3 to 4 mg/mL. These solutions were diluted to 0.5-20 $\mu\text{g}/\text{mL}$ with 95:5 (v/v) water-methanol, containing 0.1% (v/v) formic acid, for HPLC calibration. Each standard solution was prepared in triplicate. NO and HPLC analysis were performed in duplicated.

3.2.5.2 ^{13}C NMR

^{13}C NMR provides important information about the carbons in different structural and chemical environments in lignin structure. The quantitative data from ^{13}C NMR led to the calculation of basic parameters which summarizes the main structural characteristics of lignins: β -O-4 structures content, DC, S/G, and S:G:H ratio (Balakshin et al., 2015; Capanema et al., 2005).

Quantitative ^{13}C NMR spectra were recorded using a Bruker AVANCE III 400 spectrometer operating at 400 MHz, at 318 K, during 72 h. About 170 mg of dried lignin was dissolved in 0.5 mL deuterated dimethyl sulfoxide (DMSO- d_6). Quantitative conditions used for ^{13}C NMR signal acquisition were: simple 1D pulse sequence, relaxation delay of 12 s, 1400 scans, and 1D sequence with power gated coupling using 90° flip angle.

3.2.5.3 ^{31}P NMR

Quantitative ^{31}P NMR method allows determining each type of hydroxyl groups present in the lignin structure. The S, G and H free phenolic groups, as well as carboxylic, aliphatic and condensed structures carrying free phenolic groups can be quantitatively identified using this technique (Argyropoulos et al., 2009; Granata and Argyropoulos, 1995; Heitner et al., 2010; Pu et al., 2011). Hydroxyl groups, specifically free phenolic groups, are one of the most important structural characteristic that affects physical and chemical properties of lignin. These functional groups have a great influence in lignin reactivity concerning the cleavage of inter-unit linkages and/or oxidative degradation (Lai and Guo, 1991), and also when it is applied as macro monomer, as in the synthesis of compounds, like polyurethanes (Cateto et al., 2008).

The dry lignin was accurately weighted (about 40 mg) in a sample vial, dissolved in 400 μL (1.6:1,v/v) of pyridine and deuterated chloroform (CDCl_3) and left at room temperature overnight with continuous stirring. Cholesterol (200 μL , 19 mg/mL) and chromium (III) acetyl-acetonate (50

μL , 11.4 mg/mL) are used as internal standard (IS) and relaxation reagent, respectively, as recommended by (Argyropoulos et al., 2009). After 2 h, 100 μL of phosphitylating reagent (2-chloro-4,4,5,5-tetramethyl-1,3,2-dioxaphospholane) is added and the mixture was transferred into a 5-mm-OD NMR tube. Before adding the phosphitylating reagent, it was checked that the lignin was completely dissolved in the solvent mixture. The phosphitylated lignins were analyzed by ^{31}P NMR spectroscopy using a Bruker AVANCE III 400 spectrometer operating at 400 MHz, at 298 K. The spectrum was acquired during 30 min with 10 s relaxation time, 45° pulse angle, and 4 s pulse delay.

3.2.5.4 ^1H NMR

Prior to ^1H NMR analysis the lignins were acetylated. Lignin samples were subjected to acetylation in order to enhance their solubility in organic solvents, used in NMR techniques. This reaction implies the substitution of all the hydroxylic functions by new acetyl groups.

Lignins (20 mg) were dissolved in 0.1 mL of an acetic anhydride/pyridine solution (4.7:4.0, v/v) for 24 hours, at 315 K. Then the mixture was diluted with 1.0 mL of methanol and 8.0 mL of dichloromethane and left for 30 minutes, after which 5 mL of a HCl 7% solution were added. The mixture was poured into a separatory funnel of 50 mL and the aqueous phase of the mixture was removed. The addition of 5.0 mL of HCl 7% solution and the removal of the aqueous phase was repeated two times. One more wash with distilled water was performed and after that the organic phase was removed, dried with sodium sulfate anhydrous, and evaporated under reduced pressure.

The ^1H NMR spectrum of acetylated hardwood lignins in CDCl_3 solution, with a minimum concentration of 5 %w/v, was acquired using a Bruker AVANCE III 400 spectrometer, operating at 400 MHz, at room temperature. The acquisition parameters used were: 12 μs pulse width (90°), 2 s relaxation delay, and 200-250 scans. The acquisition time was about 2 h and CDCl_3 was used as internal standard.

3.3 COMPOSITION OF *E. GLOBULUS* LIGNINS

The inorganics and carbohydrate content of eucalyptus lignins are depicted in Table 4. The ash content of all the lignins is lower than 1%, and carbohydrate amount is lower than 3%. In the case of kraft lignin, the purification procedure leads to a final product with rather low content of ashes and carbohydrates.

Table 4 - Ash and carbohydrate contents of lignins, presented in %w/w_{lignin} (dry weight).

	lignins			
	LEgOrg	LEgKraft	LEgwood	LEgbark
Inorganic compounds (%w/w _{lignin})	0.11±0.01	< 0.01	1.0±0.04	0.34±0.01
Carbohydrates (%w/w _{lignin})	1.4±0.04	1.0±0.03	1.8±0.05	2.7±0.08

The content of the main sugar residues found in *E. globulus* lignins is depicted in Table 5. Xylose was the main sugar residue found followed by glucose and galactose; minor quantities of rhamnose, arabinose, and mannose were also detected.

Table 5 - Detailed composition of carbohydrate fraction (%w/w_{lignin}) of *E. globulus* lignins.

	Glc	Xyl	Ara	Gal	Rha	Man
LEgOrg	0.20	0.28	0.10	0.12	0.02	0.09
LEgKraft	0.07	0.21	0.07	0.10	0.01	0.04
LEgwood	0.19	0.27	0.11	0.14	0.02	0.06
LEgbark	0.13	0.31	0.15	0.64	0.02	0.01

*Glc – glucose; Xyl – xylose; Ara – arabinose; Gal – galactose; Rha – rhamnose; Man - mannose.

3.4 STRUCTURAL CHARACTERIZATION OF *E. GLOBULUS* LIGNINS

3.4.1 Analysis by NO

The NO results for the yields and types of simple phenolic aldehydes obtained for LEgOrg, LEgKraft, LEgwood, and LEgbark, are depicted in Table 6. The main products of hardwood lignins after NO are V and Sy, derived from G and S units, respectively. NO yields are higher for LEgwood and LEgbark lignins, and follow the sequence LEgwood≈LEgbark>LEgOrg>LEgKraft.

Table 6 - Yields of monomeric phenolic products obtained by NO of lignins.

lignin	products, % w/w_{lignin}*					
	Hy	V	Sy	VA	SA	total yield
LEgOrg	0.52	4.98	18.6	0.13	2.25	26.5
LEgKraft	0.20	3.67	13.3	0.53	3.31	21.0
LEgwood	0.04	4.38	24.6	0.46	1.60	31.1
LEgbark	0.04	4.40	25.6	0.37	2.52	32.9

* reported to nonvolatile solids weight after deducting ashes and carbohydrates

The results confirm that lignins produced by mild acidolysis have higher content of non-condensed structures, being probably closer to that of native lignin (Evtuguin et al., 2001; Lin and Dence, 1992). On the other hand, kraft and organosolv lignins have a higher content of condensed

structures, which are more resistant to degradative oxidation. Among the lignins obtained by delignification processes it is visible that LEgKraft present a higher content of these structures than LEgOrg. High total yield of NO is indicative of advantageous structural characteristic with high relevance for lignin valorization, specifically considering the production of V and Sy. LEgKraft showed the highest relative content of VA and SA, which is indicative of a high content of structures with carbonyl group at C α (benzyl carbon) (Gierer et al., 1977) in this lignin, which could be a disadvantage in the oxidative reactions aiming to obtain aldehydes. The proportion of H structures represents less than 2% of the total yield on oxidation products for all the lignin samples.

Concerning Sy/V molar ratio, the values found in this work for mild acidolysis lignins (4.9 and 4.7, for wood and bark respectively) are higher than the values found for *E. globulus* wood growth in China, 3.7 (Xie and Yasuda, 2004) and for other *Eucalyptus* species (S/G ratio: 2.7-4) (Ohra-aho et al., 2013), both obtained by direct analysis of the sawdust. However, Sy/V of this work is close to that obtained by other authors for plantation *E. globulus* wood (4.6) (Evtuguin et al., 2001). NO has been applied for characterization purposes of isolated lignin (Erdocia et al., 2014; Evtuguin et al., 2001; Pinto et al., 2002a) and native lignin (directly in the sawdust) (Ohra-aho et al., 2013; Xie and Yasuda, 2004) or to estimate the maximum yield on functionalized phenolics that is possible to produce by oxidative depolymerization (Pinto et al., 2011; Tarabanko and Petukhov, 2003). In this last perspective, it has been suggested that the yield of oxidation with O₂ in alkaline medium is about 40–50% of NO yield (Pinto et al., 2011; Tarabanko et al., 1995).

Pinto et al. (2002a) studied the behavior of *E. globulus* lignins during kraft process. The authors reported a decrease of NO yield along the kraft pulping with a final value of 19.8% (about 36% of initial wood lignin yield), a value close to that found for LEgKraft (21.1%). This decrease on yield is related with the increase of condensed structures resulting from the reaction of lignin in kraft conditions, which is in accordance with the decrease observed also between LEg_{wood} and LEgKraft. In general, hardwood lignins and lignins obtained by processes involving low temperature and soft conditions (such as mild acidolysis) led to higher yields toward NO. The low impact of mild acidolysis (Lin and Dence, 1992) on native lignin structure allows obtaining a reference lignin for comparison with the industrial processed ones.

3.4.2 ¹³C NMR

The quantitative ¹³C NMR spectra of LEgOrg, LEgKraft, LEg_{wood}, and LEg_{bark} lignins with the main assignments identified are shown in Figure 7. Figure 8 is an amplification of the resonance region corresponding to the aromatic carbons (δ 100–160 ppm), the most important in the ¹³C NMR lignin analysis.

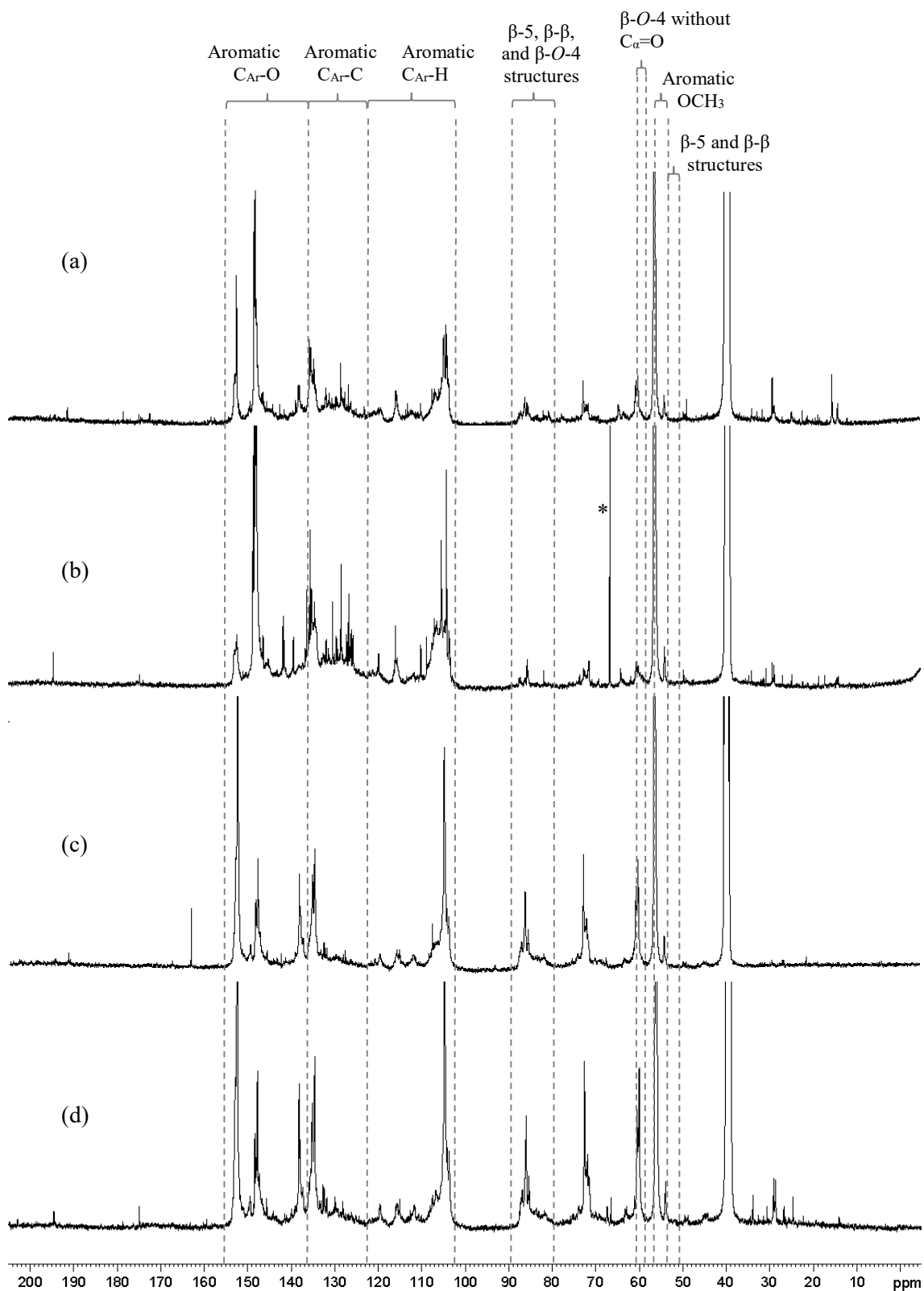


Figure 7 - Quantitative ^{13}C NMR spectra of (a) LEgOrg, (b) LEgKraft, (c) LEgwood, and (d) LEgbark (in DMSO-d_6 ; * solvent peak (Hugo et al., 1997)).

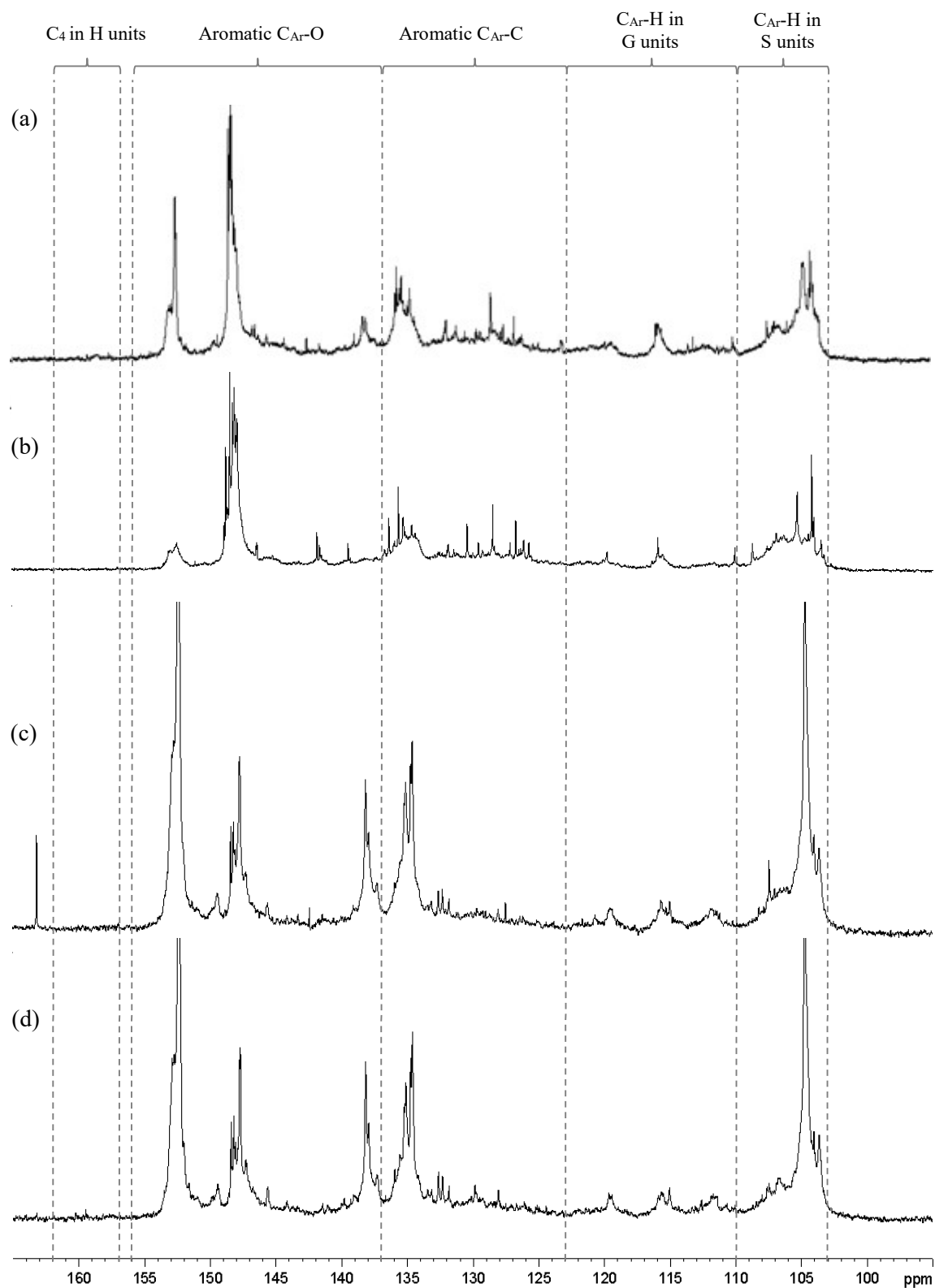


Figure 8 - Expanded δ 165-95 ppm region of quantitative ^{13}C NMR spectrum of (a) LEOrg, (b) LEOkraft, (c) LEOwood, and (d) LEObark (in DMSO-d_6).

The matching of carbon chemical shifts of each functional group present in lignin structure was made based on reference spectra and data available on literature (Capanema et al., 2004;

Evtuguin et al., 2001; Landucci, 1985; Lin and Dence, 1992; Xia et al., 2001). The ^{13}C NMR results, presented in Table 7, are reported as the ratio of the integral of a given carbon signal to one-sixth of the integral of aromatic carbons (Ar).

Table 7 - Assignments and quantification (number per aromatic ring) of the structures/linkages and functional groups identified by ^{13}C NMR.

assignments (spectroscopic range)	amount (number/Ar)			
	LEgOrg	LEgKraft	LEg _{wood}	LEg _{bark}
C_β in β -5 and β - β structures (δ 51.0-53.8 ppm)	0.10	0.07	0.06	0.11
Aromatic OCH_3 (δ 54.3-57.3 ppm)	1.40	1.38	1.75	1.53
C_γ in β -O-4 structures without $\text{C}\alpha=\text{O}$ (δ 59.3-60.8 ppm)	0.26	0.10	0.46	0.44
C_γ in β -5 and β -O-4 structures with $\text{C}\alpha=\text{O}$; C_γ in β -1 (δ 62.5-63.8 ppm)	0.07	0.03	0.07	0.08
$\text{C}\alpha$ in β -O-4 structures; C_γ in pinoresinol/syringaresinol and β - β structures (δ 70.0-76.0 ppm)	0.34	0.17	0.71	0.69
C_β in β -O-4 structures; $\text{C}\alpha$ in β -5 and β - β structures (δ 80.0-90.0 ppm)	0.44	0.16	0.82	0.76
Aromatic $\text{C}_{\text{Ar}}\text{-H}$ (δ 103.0–123.0 ppm)	1.95	1.83	2.05	2.06
Aromatic $\text{C}_{\text{Ar}}\text{-C}$ (δ 123.0–137.0 ppm)	1.75	1.86	1.27	1.41
Aromatic $\text{C}_{\text{Ar}}\text{-O}$ (δ 137.0–156.0 ppm)	2.30	2.30	2.68	2.53
C_4 in H units (δ 157.0–162.0 ppm)	0.00	0.00	0.00	0.07
CHO in benzaldehyde structures (δ 191.0–192.0 ppm)	0.04	0.02	0.03	0.02
CHO in cinnamaldehyde structures (δ 193.5–194.5 ppm)	0.04	0.02	0.02	0.04

The integral of the δ 103–162 ppm region was set as the reference, assuming that it includes six aromatic carbons (Capanema et al., 2004; Lin and Dence, 1992). The aromatic region of the lignin ^{13}C NMR spectra is usually used for the quantification of different types of aromatic carbons: tertiary ($\text{C}_{\text{Ar}}\text{-H}$), quaternary oxygenated ($\text{C}_{\text{Ar}}\text{-O}$) and non-oxygenated ($\text{C}_{\text{Ar}}\text{-C}$) (Capanema et al., 2004). Also, the content of S, G and H units can be evaluated from this region, δ 103–162 ppm. The number of tertiary aromatic carbons of S units (between 1.18/Ar and 1.49/Ar) was estimated in the spectrum region of 103–110 ppm, while for G units (in the range of 0.56/Ar–0.77/Ar) the integral at δ 110–123 ppm was considered. The amount of H units was estimated from the signal at δ 157–162 ppm, assigned to C_4 in the corresponding structures (Evtuguin et al., 2001). H units were detected for LEg_{bark} while for the other lignins no signal of this type of units was found, indicating that its content is negligible. An increase in the number of aromatic carbons $\text{C}_{\text{Ar}}\text{-C}$ and a slight decrease in the number of aromatic $\text{C}_{\text{Ar}}\text{-H}$ were found in the order LEg_{wood}, LEgOrg and LEgKraft. This trend is related with the increase of the condensed structures content in the same order. The increase of condensation in lignins results mainly from the accumulation of the original moieties as well as $\text{C}_{\text{Ar}}\text{-C}_{\text{Ar}}$ and $\text{C}_{\text{Ar}}\text{-O-C}_{\text{Ar}}$ coupling in the delignification or isolation process.

Comparatively to wood lignin, LEgOrg and LEgKraft present a higher content of resistant structures, more pronounced for the kraft lignin.

From the integral at δ 80–90 ppm it is possible to estimate the total amount of β -O-4 structures; however, this region of integration also includes β -5 and β - β structures. The net content of β -O-4 structures was calculated by the subtraction of the amount of β -5 and β - β structures (δ 51.0–53.8 ppm) from the integral of δ 80.0–90.0 ppm (Balakshin et al., 2015; Capanema et al., 2005). For this structure, values of 0.76/Ar, 0.65/Ar, 0.34/Ar, and 0.09/Ar were obtained for LEg_{wood}, LEg_{bark}, LEgOrg, and LEgKraft, respectively. The results indicate that kraft and organosolv lignins show a lower content of β -O-4 structures than lignins produced by mild acidolysis. The decrease during kraft and organosolv process is a consequence of the cleavage of aryl-ether structures, one of the main reactions occurring in the delignification process that led to important changes in lignin structure. This phenomenon can be verified in the ^{13}C NMR spectra of lignin samples (Figure 7) in the increasing order: mild acidolysis, organosolv and kraft lignin. Taking the region of aromatic $\text{C}_{\text{Ar}}\text{-O}$ it is possible to observe a decrease of the signal at δ 152 ppm, that corresponds to etherified C_3 and C_5 in S units (mainly in β -O-4 structures), and an increase of the signal at δ 148 ppm, due to the resonance of C_4 in G units of β - β structures, C_3 and C_5 in non-ether S units, C_3 in non-ether G units, and C_4 in G units with conjugated $\text{C}=\text{C}$ bonds (Wen et al., 2013a; Wen et al., 2013b). Also the signal near to δ 138 ppm, that represents C_4 in etherified S units, shows a considerable decrease in the same order. This observation is also related with the degradation of β -O-4 structures, as already stated by Wen et al. (2013b), for kraft and organosolv lignins, in higher extension for kraft ones. For lignins produced by kraft process at laboratory scale, Pinto and their co-authors (Pinto et al., 2002b) obtained a content of these structures of 0.33/Ar for a purified *E. globulus* kraft lignin, which is rather high comparatively to the value of this work, for the industrial kraft lignin (0.10/Ar). For a birch organosolv lignin a content of β -O-4 structures of 0.42/Ar was found (Wen et al., 2013a), while for an organosolv lignin from *E. grandis* \times *E. urophyllathe* content of β -O-4 structures obtained was 0.29/Ar, representing 39% of the initial content (0.75/Ar, based on mild acidolysis lignin) (Wen et al., 2013b). These values are considerable higher, than the values the values found in this work, where the final content of β -O-4 structures represents about 22% of the mild acidolysis lignin.

The lowest content of OCH_3/Ar found for LEgKraft and for LEgOrg comparatively with the wood lignin reflects the demethoxylation that occurs during the delignification process, usually referred for the kraft one (Pinto et al., 2002a), but already noticed for organosolv process (Wen et al., 2013b). OCH_3 contents in *E. globulus* lignin samples are within the values reported in earlier studies of other hardwood lignins. Santos and their co-workers found values of OCH_3/C_9 between 1.4 and 1.9 for milled wood lignins from ten different hardwood species, among them *E. globulus* milled wood lignin presented the highest content (Santos R.B. et al., 2012). Also Capanema et al. (2005) presents values of OCH_3/C_9 for hardwood milled wood lignins characterized by different

authors and the obtained values vary from 1.4 to 1.6. In fact, a particular characteristic of *E. globulus* lignins is the higher OCH₃ content found comparatively with those obtained for other types of hardwood lignins (Evtuguin et al., 2001; Pinto et al., 2005), due to the higher S/G ratio of the former.

The content of β -O-4 structures with C α =O is calculated based on the resonance at δ 62.5–63.8 ppm; however, this region of integration also contains β -5 structures. The contents of this type of structures are low for all the lignins (between 0.03/Ar and 0.08/Ar). Similar values of these structures were obtained for an *E. globulus* lignin produced by wood mild acidolysis (0.04/Ar) and also for a purified kraft lignin of the same specie (0.08/Ar) (Pinto et al., 2002b). As stated before, the content of H units found in LEg_{wood} is negligible, while for LEg_{bark} about 7% of these units were found. In accordance, the content of OCH₃ in LEg_{bark} is lower comparatively to LEg_{wood}, reflecting the presence of the three structural units H, G and S and not only G and S as in wood. LEg_{bark} contains higher C_{Ar}-C, similar C_{Ar}-H and lower C_{Ar}-O contents comparatively to wood lignin, suggesting that bark lignin has a higher frequency of condensed structures per aromatic ring. For the other types and contents of interunit linkages and functional groups obtained from ¹³C NMR no significant differences were found between LEg_{wood} and LEg_{bark}. These statements are in agreement with studies already published about the characterization of wood and bark lignins obtained from softwood species (Huang et al., 2011; Solár et al., 1988). These authors also confirm the lower presence of OCH₃ and the higher content of condensed structures in bark lignins. A detailed comparison between the lignins produced by wood and bark mild acidolysis provide important information in order to optimize the use of bark lignins for the production of aromatic aldehydes by oxidation. With the ¹³C NMR data, and by comparison with lignin obtained by mild acidolysis it is possible to notice that the kraft and organosolv lignins are the product of an intense modification during the respective delignification process, more pronounced for kraft one.

3.4.3 ³¹P NMR

Table 8 summarizes the results of quantitative ³¹P NMR analysis of phosphitylated lignin samples, LEgOrg, LEgKraft, LEg_{wood}, and LEg_{bark}, the respective spectra are shown in Figure 9.

The concentration of each hydroxyl functional group (in mmol/g_{lignin}) was calculated on the basis of the content of internal standard, cholesterol (δ 145.2 ppm), and its integrated peak area was normalized to 1.

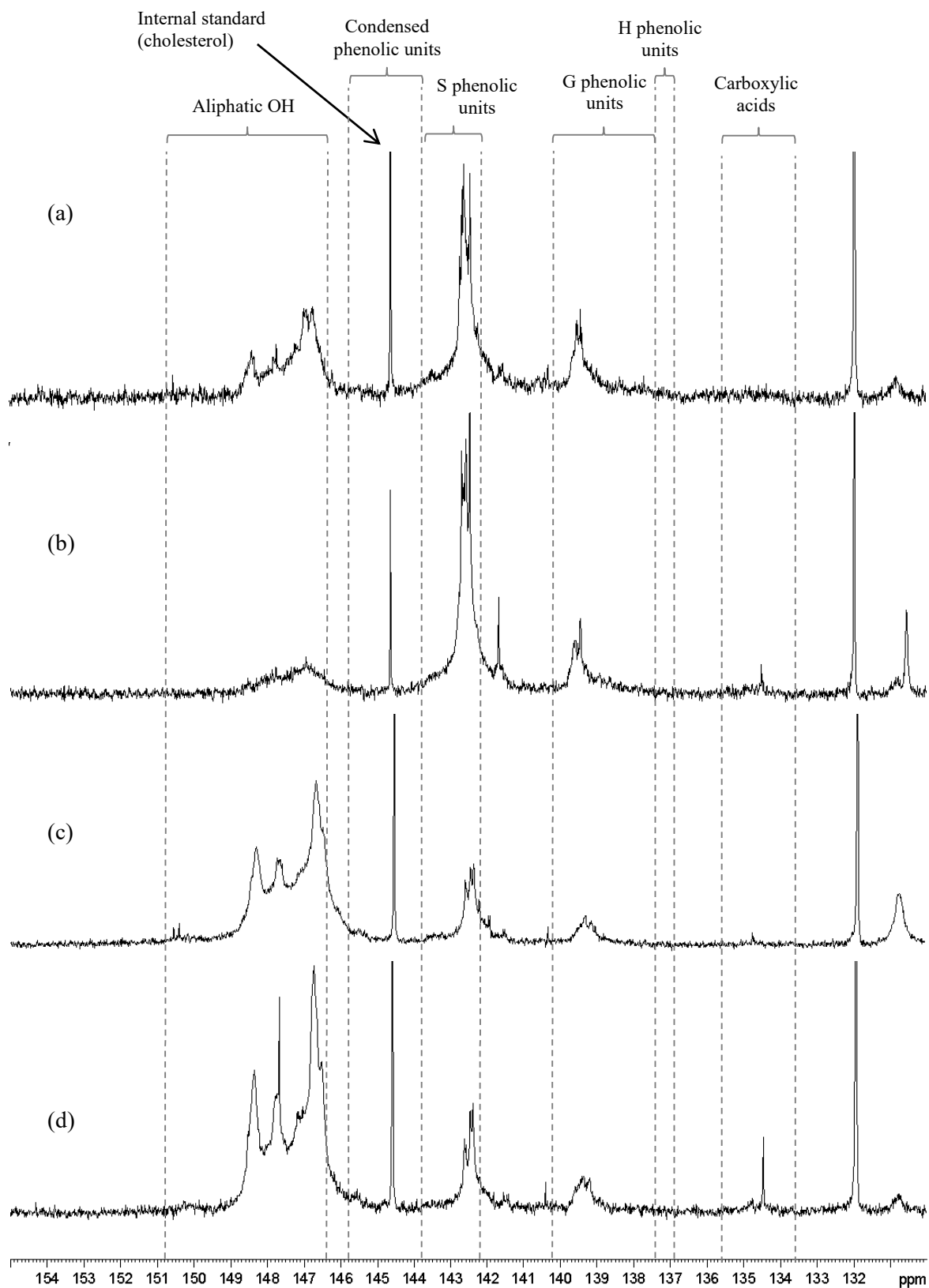


Figure 9 - Quantitative ^{31}P NMR spectra (δ 155-130 ppm) of phosphitylated lignins (a) LEOrg, (b) LEgKraft, (c) LEgwood, and (d) LEgbark (in CDCl_3).

Table 8 - Assignments and quantification (mmol/g_{lignin}) of phenolic, aliphatic, and carboxylic hydroxyl groups identified by ³¹P NMR.

Assignments	amount (mmol/g _{lignin})			
	LEgOrg	LEgKraft	LEgwood	LEgbark
Aliphatic OH (δ 146.4-150.8 ppm)	1.39	1.61	3.12	4.12
Carboxylic acids (δ 135.6-133.6 ppm)	0.02	0.00	0.16	0.24
Total phenolic units	2.66	7.25	1.60	1.79
Condensed phenolic units (δ 145.8-143.8; 142.2-140.2 ppm)	0.70	1.29	0.47	0.49
Non-condensed phenolic units				
S phenolic units (δ 143.8-142.2 ppm)	1.47	4.72	0.72	0.78
G phenolic units (δ 140.2-137.4 ppm)	0.47	1.24	0.41	0.52
H phenolic units (δ 137.4-136.9 ppm)	0.00	0.00	0.00	0.00

The content of aliphatic OH groups in LEgOrg and LEgKraft is about 36–46% lower than LEgbark and LEgwood. These groups are mainly comprised of primary and secondary OH groups located on C γ and C α of the phenylpropane side chain of lignin structure (Froass et al., 1998). The loss of aliphatic OH groups during the delignification processes is related with the degradation of side-chains of ppu, since these lignins were subjected to more drastic conditions than in acidolysis (Ibarra et al., 2007).

Different authors applied ³¹P NMR to study the chemical transformations of hardwood lignins during organosolv and kraft processes with different severity grades, and also found a decrease of aliphatic OH groups during de delignification (Pinto et al., 2002b; Wen et al., 2013b). This fact could be related with the loss of γ -hydroxymethyl groups, as formaldehyde, and OH groups on the side chain of ppu to form β -1 linkages, as previously described by Hallac and co-workers (Hallac et al., 2010).

³¹P NMR comparison between industrial lignins (kraft and organosolv) and mild acidolysis lignin also shows that the delignification process causes an increase in phenolic OH units present in lignin structure, which is in accordance with the decrease of β -O-4 structures, as well as the decrease of etherified structures already discussed for ¹³C NMR. An increase in free phenolic OH units leads to an increase in lignin solubility, what can be advantageous regarding the production and recovery of added-value aldehydes from lignin (Pinto et al., 2012). Minor amounts of carboxylic OH groups were obtained for mild acidolysis lignins, while for LEgOrg and LEgKraft these types of assignments are not detected. For the condensed structures carrying free OH groups the total content found was between 0.47/g_{lignin} and 1.29/g_{lignin} of the total phenolic units content. Kraft and organosolv lignins, as well as lignins produced by wood and bark mild acidolysis, showed different condensed moieties in their structures, such as 5-5', β -5 and β -1. However, the formation of additional condensed linkages during the pulping process is evident, mainly for kraft process, originating a lignin with a higher content of this type of structures (Nanayakkara et al., 2011). Other authors (Sannigrahi et al., 2009; Wen et al., 2013b) also noticed that both softwood

and hardwood organosolv lignins show an increase in condensed phenolic units comparatively to the corresponding milled wood lignin, from 0.02/ppu to 0.11/ppu for softwood and from 0.05/ppu to 0.09/ppu in the case of hardwood lignins.

With respect to kraft process, Pinto et al. (2002b) found an increase in the total phenolic OH content with the progressive increase of kraft delignification applied to an *E. globulus* lignin. Granata and Argyropoulos (1995) found the same behavior for a softwood kraft lignin; the authors also observed that the delignification process increases the content of condensed structures caring free phenolic OH groups. Among the OH groups in different structures identified by ^{31}P NMR, lignins produced by wood and bark mild acidolysis presented similar results, including the distribution of non-condensed phenolic units in H, G and S units. However, a slight difference is reported for aliphatic OH content, which is higher for LEg_{bark} than for LEg_{wood} . This difference is probably the effect of the higher content of carbohydrate in the bark than in wood lignin (Table 4) rather than a structure-related effect.

From the ^{31}P NMR analysis it is possible to conclude that the main modifications induced by organosolv and kraft processes were the decrease in the content of aliphatic OH groups and an overall increase of phenolic groups, in particular for units involved in condensed structures, more evident for kraft lignin, $\text{LEg}_{\text{Kraft}}$.

3.4.4 ^1H NMR

^1H NMR spectroscopy allowed obtaining additional data about lignin structure. ^1H NMR spectrum of each *E. globulus* lignin is presented in Figure 10.

Semi-quantitative determination of structural elements identified by ^1H NMR (Table 9) were made by C_9 using the resonance of OCH_3 , at δ 3.5–4.0 ppm, as reference, and the signal assignments from the literature (Chen and Robert, 1988; Fukagawa et al., 1991; Lundquist, 1992; Nose et al., 1995). The comparison between the results from the different spectroscopy techniques was performed assuming that the numbers of structural elements calculated per C_6 or C_9 are similar. This is true if the side chain still contains three carbons; however, for some lignins, mainly the kraft ones, this assumption could not be true due to the already described elimination of lateral chain.

The results obtained from ^1H NMR are in accordance with the structural features already stated for ^{13}C and ^{31}P NMR: kraft and organosolv lignins present a lower content of aliphatic OH and more phenolic OH groups, resulting from aryl-ether cleavage (depicted in Table 9 as β -O-4 structures without $\text{C}\alpha=\text{O}$, at δ 5.9-6.2 ppm), than mild acidolysis lignins.

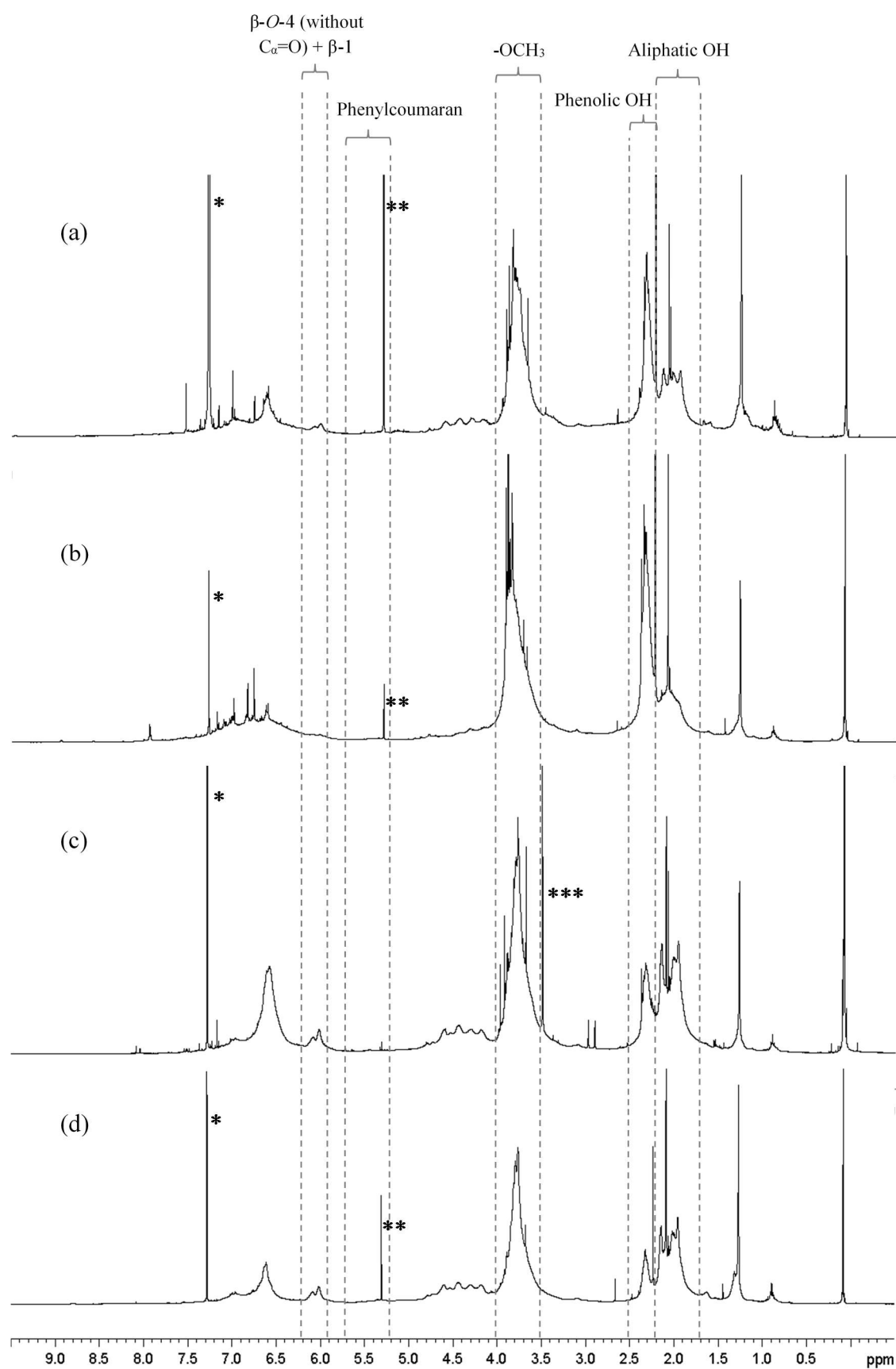


Figure 10 - ^1H NMR spectra, in CDCl_3 , of acetylated lignins (a) LEgOrg, (b) LEgKraft, (c) LEg_{wood} and (d) LEg_{bark}. (* CDCl_3 ; ** dichloromethane; *** methanol: contaminants from the acetylation process (Hugo et al., 1997)).

Table 9 - Assignments and quantification (number per phenylpropane unit) of the linkages and functional groups identified by ^1H NMR.

Assignments (spectroscopic range)	amount (number per ppu)			
	LEgOrg	LEgKraft	LEgwood	LEgbark
-CH ₂ - and -CH ₃ (δ 1.5-0.7 ppm)	0.44	0.23	0.29	0.44
Aliphatic OH (δ 2.2-1.7 ppm)	0.61	0.45	1.05	1.15
Phenolic OH (δ 2.5-2.2 ppm)	0.71	0.78	0.52	0.42
β - β (δ 3.2-3.0 ppm)	0.23	0.07	0.19	0.17
Phenylcoumaran (δ 5.7-5.2 ppm)	0.18	0.15	0.22	0.23
β -O-4 (without C α =O) and β -1 (δ 6.2-5.9 ppm)	0.25	0.19	0.47	0.42
H in aromatic ring (δ 8-6.2 ppm)	2.04	2.11	3.20	2.04

The amount of β - β structures, calculated based on the resonance at δ 3.2–3.0 ppm, is lower for LEgKraft comparatively to LEgOrg and mild acidolysis lignins due to a more intense involvement of the lateral chain in the kraft delignification process. A lower content of aliphatic OH was also found for this sample. Aliphatic OH groups decrease along the delignification process due to the degradation of the side chain of ppu, as already stated by ^{31}P NMR. The results from ^1H NMR also show that bark lignin have a higher frequency of free aliphatic OH, CH₂ and CH₃ groups comparatively to wood one. These differences could be due to carbohydrates contamination (as stated before for aliphatic OH) and due to the presence of aliphatic extractives of bark, which are more abundant in bark than in wood (Freire et al., 2002). Another difference between these lignins is the lower content of C-H in aromatic ring for LEgbark comparatively to LEgwood. This fact is attributed to a slight higher condensation degree of bark lignin, as previously stated by the higher content of C_{Ar}-C linkages quantified by ^{13}C NMR.

3.5 EMPIRICAL FORMULA AND MOLECULAR MASS OF PPU

Based on OCH₃ and phenolic groups (OH_{ph}) content, calculated by ^1H NMR, and elemental analysis the empirical formula of lignin samples as well as the molecular mass (M) of ppu were calculated and presented in Table 10.

Besides the content on OH_{ph} and OCH₃ groups, the formula indicates the average proportion of C:H:O in the ppu of each lignin. Elemental analysis results were corrected for the content of carbohydrates. Comparing the results obtained for lignins produced by wood and bark mild acidolysis, it is possible to observe that LEgwood shows a slight increase in the value of M. This fact is related with the higher contents of OCH₃ and OH_{ph} obtained for this lignin sample, as stated before. The results show a low content of H and O per ppu, observed for LEgOrg and LEgKraft, which could be related with a high frequency of C-C linkages (condensed structures) formed during the delignification process, as noticed in section 3.4.2 (^{13}C NMR results). Lignin samples presented

contents of OCH₃/ppu between 1.4 and 1.7, and the decrease of OCH₃ from wood to organosolv and kraft lignins confirm the demethoxylation.

Table 10 - Empirical formula and molecular mass (M) of ppu of *E. globulus* lignins.

lignin	empirical formula	M (g/mol)
LEgOrg	C ₉ H _{7.9} O _{1.6} (OH _{ph}) _{0.59} (OCH ₃) _{1.34}	193
LEgKraft	C ₉ H _{7.7} O _{0.9} S _{0.3} (OH _{ph}) _{0.78} (OCH ₃) _{1.38}	196
LEgwood	C ₉ H _{8.5} O _{2.5} (OH _{ph}) _{0.52} (OCH ₃) _{1.74}	219
LEgbark	C ₉ H _{9.1} O _{2.3} (OH _{ph}) _{0.31} (OCH ₃) _{1.53}	207

Considering the content of OH_{ph}/ppu, LEgKraft presents the highest value indicating an extensive cleavage of β-O-4 structures. Organosolv process has a more preserving effect on these structures. The molecular mass of a ppu of lignins produced by wood and bark mild acidolysis are in the range of 207-219 g/mol, decreasing to 193-196 g/mol after delignification process (Table 10). Another consideration which can be used to distinguish kraft lignin is the presence of organic sulfur in this structure, as thiol groups. Sulfur free lignins are more appealing from the point of view of lignin valorization than lignins that present organic sulfur in their structures.

3.6 ASSESSING CORRELATIONS BETWEEN STRUCTURAL FEATURES AND NO YIELDS

3.6.1 DC, S:G:H ratio and correlations with NO results

DC includes the lignin moieties with C-C linkages with other lignin units through C₂ or C₆ positions of the aromatic ring of S units, C₂, C₅ or C₆ positions of the aromatic ring of G units, and in the case of H units also C₃ position is available. The most common condensed moieties in lignin structure are 5-5', β-5, and 4-O-5' structures (Berlin and Balakshin, 2014). ¹³C NMR results (Table 7) allow calculating the DC value as well as the relative content of S:G:H. In these calculations it is assumed that one aromatic ring (Ar) is equivalent to ppu. To estimate the DC is necessary to calculate the theoretical amount of C_{Ar-H} atoms from the S:G:H ratio. However, a few ways for the estimation of the amounts of G, S and H units have been presented. Some authors (Capanema et al., 2005; Landucci, 1985) showed that the most accurate method to estimate the G:S:H ratio in lignin is based on the content of OCH₃/Ar; however this method is not suitable for lignins that suffer demethoxylation during the delignification process. For this reason the quantification of each structural unit was performed based on the integral of the respective ¹³C NMR spectrum as previously reported (Capanema et al., 2005; Evtuguin et al., 2001):

$$S = \text{Integral}_{103-110}/2$$

$$G = \text{Integral}_{110-123}/3$$

$$H = \text{Integral}_{157-162}$$

The region of δ 103–123 ppm is attributed to aromatic tertiary carbons (C_{Ar-H}). The value for C_{Ar-H} in non-condensed G units is 3, while for S units that value is 2. In the case of H units only two carbons resonate in this region (C_3 and C_5), and for this reason the value for C_{Ar-H} in non-condensed structures involving H units is 2 (Capanema et al., 2004; Capanema et al., 2005; Evtuguin et al., 2001). In this approach, an equal proportion of non-condensed moieties in G and S units was considered; however, this assumption leads to an underestimation of G content, since this moiety is more frequently involved in condensed structures (C_{Ar-C}) than S units, due to the free position at C_5 . In spite of this limitation, the theoretical value of C_{Ar-H} was calculated for the four lignins (Capanema et al., 2005):

$$\text{Theoretical } C_{Ar-H} = (2S + 3G + 2H)$$

The difference between the theoretical and the experimental values, corrected for 100, gives the percentage of condensed moieties in lignin structure. The DC and S:G:H ratio calculated for eucalyptus lignins are depicted in Table 11.

Table 11 – DC (%) and S:G:H ratio calculated for the *E. globulus* lignins.

lignin	DC (%)	S:G:H
LEgOrg	35	70:30:00
LEgKraft	43	74:26:00
LEg _{wood}	15	80:20:00
LEg _{bark}	16	70:23:07

The S:G:H ratio found for all the samples shows a predominance of S units as expected for this type of lignins. Among the studied lignins, LEgKraft presents the highest value of DC, reaching to about three times the value of wood lignin produced by mild acidolysis. In the case of LEgOrg, a DC value more than twice of LEg_{wood} was found. The higher content of condensed structures in kraft than in organosolv lignin demonstrates that lignin undergoes fewer transformations in the organosolv process.

DC is an important parameter for studies about lignin applications since it has a negative impact on lignin reactivity. On the other hand, NO has been used to evaluate the yield of phenolic aldehydes that would be produced in an oxidative process. The plot of NO yields versus DC values show a good correlation (Figure 11), clearly demonstrating that the reactivity of lignin toward NO

decreases with the increases of condensed structures content. If lignin structure has a high content of condensed structures, lower yield of phenolic aldehydes could be achieved.

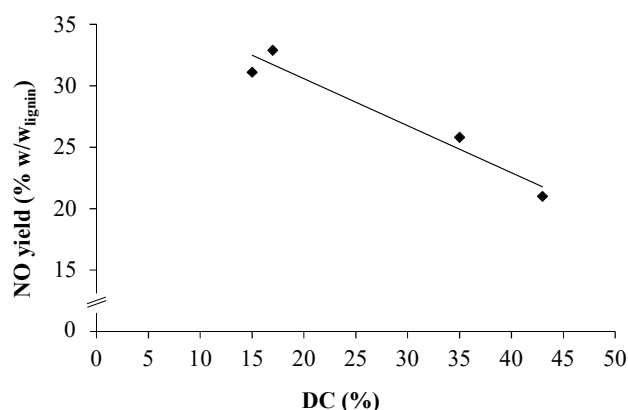


Figure 11 - Plot of NO yield versus DC values obtained for *E. globulus* lignins.

The correlation between β -O-4 structures content, from ^{13}C NMR, and DC values is depicted in Figure 12. The observed trend gives further support to the suggested relation between the content of uncondensed structures and the value of DC obtained for each lignin sample: the higher the total of uncondensed structures, lower is the DC.

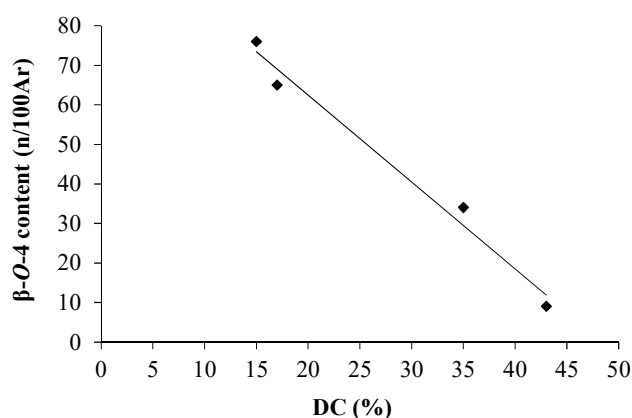


Figure 12 - Plot of β -O-4 content versus DC values obtained for *E. globulus* lignins.

For lignins produced by mild acidolysis, high yields of monomeric phenolic aldehydes were produced by NO and high contents of β -O-4 structures were obtained by ^{13}C NMR. The low DC found indicates a low content of condensed moieties in their structure, probably close to the native lignin in wood and bark. Lignin reactivity is highly related with these structural alterations. The extent of these alterations allows predicting the potential of lignin to produce aldehydes, since it is the cleavage of non-condensed structures in the oxidation process that leads to these compounds. Based on this indication, it is possible to conclude that LEg_{wood} and LEg_{bark} lignins preserved a considerable fraction of its original ether structures (comparing with organosolv and kraft lignins). However, delignification process inevitably led to a change on native characteristics mainly due to

the cleavage of β -O-4 and α -O-4 linkages and condensation reactions. The extent of condensation associated to lignin samples was already studied by other authors. Capanema and co-authors (Capanema et al., 2005) presented values of DC between 18 and 50% for three different milled wood lignins, from different species of *Eucalyptus*. However, if the same type treatment is considered, but with a different lignin source, in this case softwood, values in the range of 38–56% of DC were found (Capanema et al., 2004; Huang et al., 2011). In general, higher values of DC were obtained for softwood lignins. Lignins from softwood species have mainly G units, which have an aromatic carbon in C₅ available to be involved in condensed structures, in opposition to S units. When delignification processes were applied, the obtained wood lignins present DC values that can reach 73% (Liitiä et al., 2002; Sannigrahi et al., 2009).

3.6.2 Syringyl/guaiacyl ratio (S/G): comparison between methodologies

The results obtained by NO, ¹³C, and ³¹P NMR allow determining S/G in lignins. In the case of NO the S/G ratio only considers S and G units involved in non-condensed structures. On the other hand, S and G units determined from ¹³C NMR are present in both etherified and non-etherified moieties of lignin structure. For ³¹P NMR, only S and G units with free phenolic hydroxyl groups were quantified. It is important to note, that the results provided by the three spectroscopic techniques allow identifying important fractions of lignin structure. By NO, ¹³C, and ³¹P NMR uncondensed structures, free phenolic hydroxyl G and S units, and total amount of S and G units can be quantified. The results of S/G ratio calculated are depicted in Table 12.

Table 12 - S/G for each *E. globulus* lignin obtained by NO, ¹³C and ³¹P NMR.

lignin	S/G ratio		
	NO	¹³ C NMR	³¹ P NMR
LEgOrg	4.1	2.3	3.0
LEgKraft	4.0	2.8	3.7
LEg _{wood}	5.4	4.0	1.8
LEg _{bark}	5.9	3.0	1.5

The values of S/G obtained from NO results are higher than those from ¹³C and ³¹P NMR. This is related with the fact that NO only allows the quantification of non-condensed structures. As stated before, S units are more involved in this type of structures, since they have two OCH₃ groups in C₃ and C₅ of aromatic ring that prevent the formation of other type of linkages. LEg_{wood} and LEg_{bark} present high S/G ratio determined from NO yields and ¹³C NMR. However, the S/G ratio determined by ³¹P NMR is lower for these samples. This behavior is related with the kind of S and G units quantified by each technique. As referred before, uncondensed structures are present in

higher quantities in mild acidolysis lignins, so, higher values of S units involved in this type of structures were determined by NO, and consequently a higher S/G ratio is obtained. When the total amount of uncondensed structures, calculated by NO, were plotted against the S/G obtained by ^{31}P NMR, a good correlation (Figure 13) was observed, i.e., the higher the total of uncondensed structures is, lower is the amount of S relative to G units (both with free OH groups).

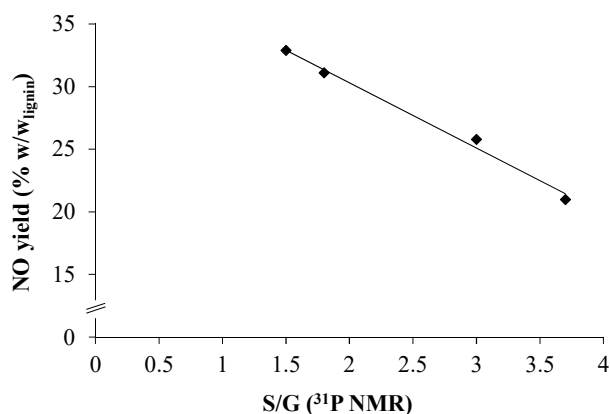


Figure 13 - Plot of NO yield versus S/G, from ^{31}P NMR, obtained for *E. globulus* lignins.

A high content of non-condensed structures means that lignin is more preserved and linkages in this type of structures were not extensively cleaved during the delignification process. For this reason, lower content of S relative to G units, both with free phenolic groups, are reported for kraft and organosolv lignins.

3.7 RADAR TOOL FOR LIGNINS EVALUATION

One of the challenges associated with exploiting lignin is the variability resulting from the type of plant and species, the delignification process, and the subsequent processing, all of which modifies its structure, making a constant and uniform lignin difficult to obtain. This is one aspect to which lignocellulosic processors must pay attention, today and in the future. The evaluation of a lignin relative to its suitability as a source of value-added compounds should combine the assessment of key characteristics such as H:G:S ratio, condensation, and β -O-4 content, and allow a qualitative prediction of the yield expected by oxidative depolymerization under the same range of conditions.

The work presented in this section aims to establish a classification technique for lignins based on their major structural characteristics, as a tool for lignins selection in view of V and/or Sy production. Radar plots representation allows a direct classification of the different lignins by comparison of their key descriptors, reducing the unavoidable complexity of lignin structure to its key aspects, while maintaining the scientific basis of the data sets with quantitative information.

Content of β -O-4 structures, the number of non-condensed structures (NCS) per 100 ppu (determined as 100 - DC), the content of S, and G units, and NO yields on V and Sy (as a measurement of the reactivity of non-condensed fractions of lignin) were the selected descriptors for radar plots. NCS include lignin moieties not involved in C_{Ar}-C and C_{Ar}-O linkages; this is an important structural feature of lignins resulting from the processing of lignocellulosic materials. Native lignins naturally contain condensed structures; however, in the course of delignification, new condensed structures are produced (Balakshin et al., 2015; Gierer, 1985; Sjöström, 1993), decreasing the NSC content. This decrease depends on the impact of delignification process on a particular lignin.

The values of all the parameters selected as key descriptors for radar plots of *E. globulus* lignins are depicted in Table 13.

Table 13 - Main structural characteristics selected as descriptors for radar plots of *E. globulus* lignins.

Lignin	β -O-4 structures (n/100Ar)	NCS (n/100ppu)	S:G:H	S/G
LEgOrg	34	65	70:30:00	2.3
LEgKraft	9	57	74:26:00	2.8
LEg _{wood}	76	85	80:20:00	4.0
LEg _{bark}	65	84	70:23:08	3.0

Radar plots were created using the software Origin Pro 8.6 (OriginLab Corporation, Northampton, USA).

3.7.1 Radar classification of *E. globulus* lignins from different delignification processes

The driving force of *Eucalyptus globulus* wood lignins comparison is to state the effect of different delignification processes on the same hardwood species and to qualify the lignins produced. In a wide scope, this approach allows the evaluation of the consequences of the chosen delignification process or conditions for the same process and, in a last instance, tailoring the process taking into account the lignin produced and the route of valorization.

Radar classification of eucalyptus wood lignins, LEgOrg, LEgKraft and LEg_{wood}, are presented in Figure 14. This representation allows a direct classification of different lignins by comparison of the key descriptors.

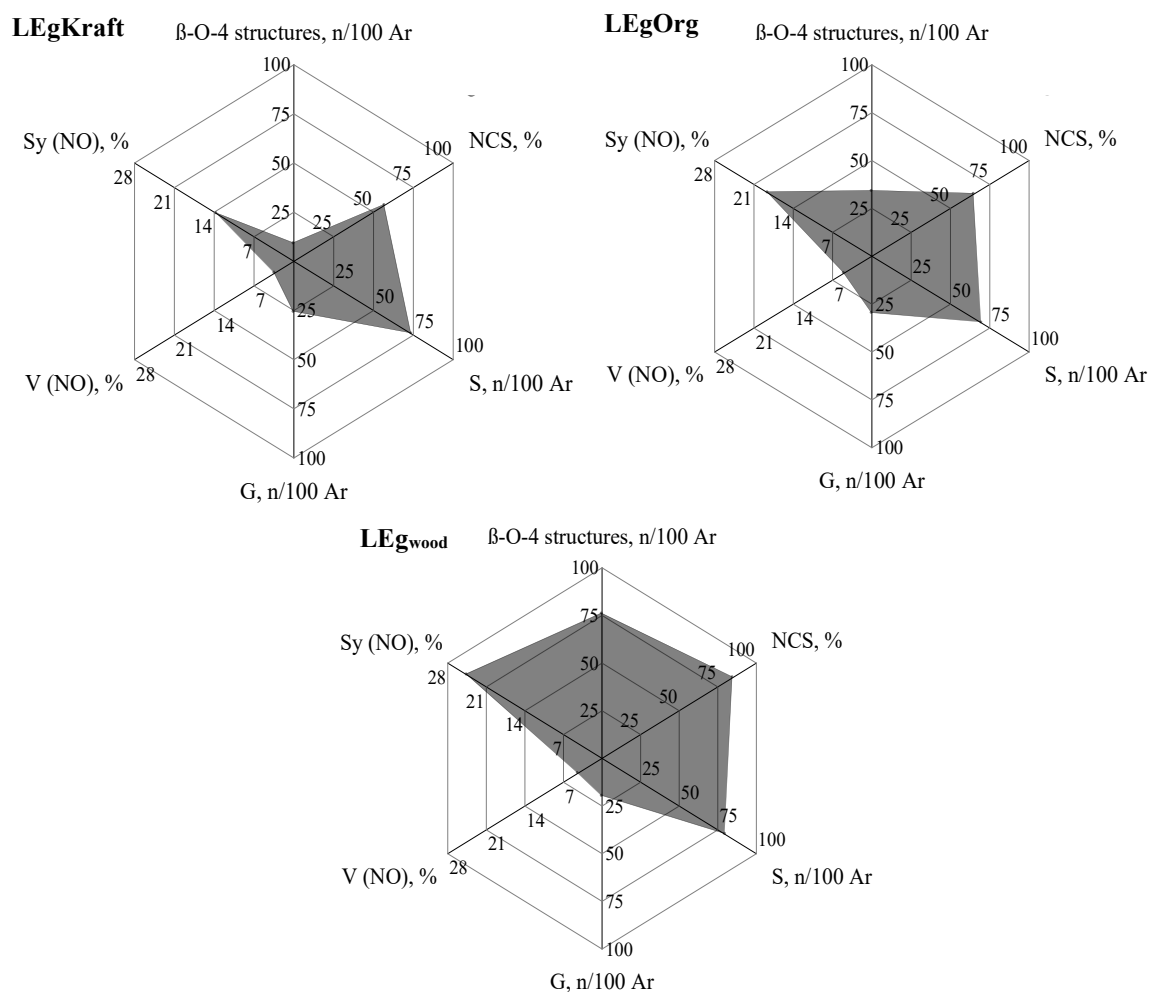


Figure 14 - Radar classification for eucalyptus wood lignins produced by different processes.

Lignin from mild acidolysis, LEg_{wood} , has the highest values for all descriptors. The best ranking of this lignin as a source of phenolic aldehydes is a consequence of the low impact that the mild acidolysis process has on the native lignin structure. Although this process is limited to laboratory scale because of solvent and conditions used, it is widely used for detailed characterization purposes.

The area defined by β -O-4 and NCS (hereafter designated as triangle Δ) in each radar plot provides the first illustration of the amount of lignin degradation effected by processing as compared with lignin isolated by mild acidolysis. The lower area of triangle Δ found for LEg_{kraft} is caused by the kraft process which promotes a higher depolymerization of lignin in bulk and in liquid phase than pulping by organosolv. The differences in the radar plots for lignins from organosolv and kraft processes clearly indicate that the former is a more preserved lignin. The organosolv process stands out as a better choice for wood delignification from the perspective of lignin valorization by means of oxidation to produce Sy and V.

3.7.2 Radar classification of lignins from different morphologic parts of *E. globulus*

Mild acidolysis lignins from wood and bark of eucalyptus trees were characterized in the previous sections, concluding that the lignins of these two morphologic parts showed few differences. In accordance, radar plots depicted in Figure 15 show only slightly lower intensity of descriptors for β -O-4 and S in the case of LEg_{bark}, as reflected by the radar area. In spite of these differences, radar plots allow ranking these lignins as having equivalent potential for oxidation. The S units descriptor, comparing bark and wood, denotes a less reactive lignin toward oxidation, which suggests that it would require different conditions in oxidation with O₂.

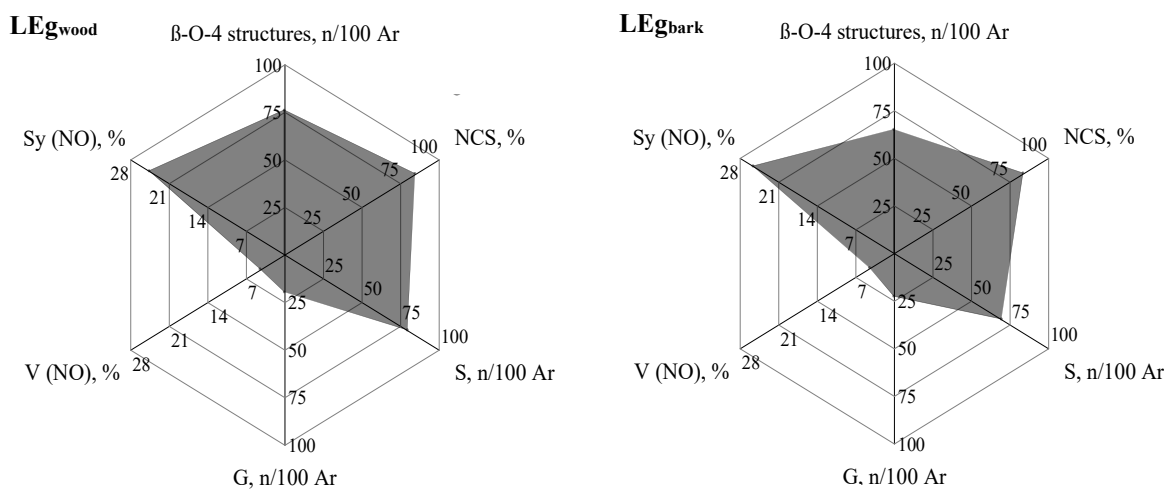


Figure 15 - Radar classification for acidolysis lignins obtained from wood and bark of eucalyptus.

3.8 CONCLUSIONS

The characterization of the different *E. globulus* lignins, allow identifying and quantifying several functional groups and interunit linkages that would be related with the ability to produce functionalized aldehydes. The structural alterations during processing have particular impact on its reactivity and it allows predicting its potential to produce aldehydes by oxidation, namely V and Sy. LEgKraft and LEgOrg have a low content of β -O-4 structures and a high amount of phenolic OH groups, since during kraft and organosolv process β -aryl ether bonds are predominantly cleaved. Another remarkable difference between mild acidolysis (close to native lignins) and the industrial lignins (kraft and organosolv) is the higher DC and the lower NO yield found in the last. Organosolv lignin is the product of fewer transformations as compared to kraft lignin. The DC value of each *E. globulus* lignin proved to have a good correlation with NO yield and total β -aryl ether content (from ¹³C NMR), and the NO yield was also successful correlated with S/G (with free phenolic groups, from ³¹P NMR). LEg_{bark} contains higher C_{Ar}-C, similar C_{Ar}-H, and lower C_{Ar}-O contents comparatively to LEg_{wood}, allow concluding that bark lignin has a higher frequency of

condensed structures. H units were exclusively found in bark lignin. However, LE_{gwood} and LE_{gbark} do not show noteworthy differences for the other types and contents of interunit linkages and functional groups, demonstrating that *E. globulus* lignins structure from wood and bark are similar.

The overall results showed that organosolv or a mild delignification process would be a preferable process to obtain lignin from *E. globulus* wood or bark when the objective is the valorization toward production of functionalized aldehydes. However, the delignification process within a biorefinery should be selected based on the criteria balance between the polysaccharide fraction, the quality of pulp and the lignin characteristics to achieve a complete and sustainable valorization of all components of the lignocellulosic biomass.

3.9 REFERENCES

- Argyropoulos, D.S., Abacherli, A., Rincón, A.G., Arx, U.V. 2009. Quantitative ³¹P nuclear magnetic resonance (NMR) spectra of lignin. in: *Analytical Methods for Lignin Characterisation*, International Lignin Institute.
- Balakshin, M.Y., Capanema, E.A., Santos, R.B., Chang, H., Jameel, H. Structural analysis of hardwood native lignins by quantitative ¹³C NMR spectroscopy. *Holzforschung* 2015, 70, 95-108.
- Berlin, A., Balakshin, M. 2014. Chapter 18 - Industrial lignins: analysis, properties, and applications. in: *Bioenergy Research: Advances and Applications*, (Eds.) V.K. Gupta, M.G. Tuohy, C.P. Kubicek, J. Saddler, F. Xu, Elsevier. Amsterdam, pp. 315-336.
- Bleton, J., Mejanelle, P., Sansoulet, J., Goursaud, S., Tchaplá, A. Characterization of neutral sugars and uronic acids after methanolysis and trimethylsilylation for recognition of plant gums. *J. Chromatogr. A* 1996, 720, 27-49.
- Capanema, E.A., Balakshin, M.Y., Kadla, J.F. A comprehensive approach for quantitative lignin characterization by NMR spectroscopy. *J. Agric. Food. Chem.* 2004, 52, 1850-1860.
- Capanema, E.A., Balakshin, M.Y., Kadla, J.F. Quantitative characterization of a hardwood milled wood lignin by nuclear magnetic resonance spectroscopy. *J. Agric. Food. Chem.* 2005, 53, 9639-9649.
- Cateto, C.A., Barreiro, M.F., Rodrigues, A.E., Brochier-Salon, M.C., Thielemans, W., Belgacem, M.N. Lignins as macromonomers for polyurethane synthesis: A comparative study on hydroxyl group determination. *J. Appl. Polym. Sci.* 2008, 109, 3008-3017.

- Chen, C.L., Robert, D. 1988. Characterization of lignin by ^1H and ^{13}C NMR spectroscopy. in: *Methods Enzymol.*, (Ed.) S.T.K. Willis A. Wood, Vol. Volume 161, Academic Press, pp. 137-174.
- Doco, T., O'Neill, M.A., Pellerin, P. Determination of the neutral and acidic glycosyl-residue compositions of plant polysaccharides by GC-EI-MS analysis of the trimethylsilyl methyl glycoside derivatives. *Carbohydr. Polym.* 2001, 46, 249-259.
- Erdocia, X., Prado, R., Corcuera, M.Á., Labidi, J. Effect of different organosolv treatments on the structure and properties of olive tree pruning lignin. *J. Ind. Eng. Chem.* 2014, 20, 1103-1108.
- Evtuguin, D.V., Neto, C.P., Silva, A.M.S., Domingues, P.M., Amado, F.M.L., Robert, D., Faix, O. Comprehensive study on the chemical structure of dioxane lignin from plantation *Eucalyptus globulus* wood. *J. Agric. Food. Chem.* 2001, 49, 4252-4261.
- Freire, C.S.R., Silvestre, A.J.D., Neto, C.P., Cavaleiro, J.A.S. Lipophilic extractives of the inner and outer barks of *Eucalyptus globulus*. *Holzforschung* 2002, 56, 372-379.
- Froass, P.M., Ragauskas, A.J., Jiang, J. Nuclear magnetic resonance studies. 4. Analysis of residual lignin after kraft pulping. *Ind. Eng. Chem. Res.* 1998, 37, 3388-3394.
- Fukagawa, N., Meshitsuka, G., Ishizu, A. A two-dimensional NMR study of birch milled wood lignin. *J. Wood Chem. Technol.* 1991, 11, 373-396.
- Gierer, J. Chemistry of Delignification. Part 1: General Concept and Reactions during Pulping. *Wood Sci. Technol.* 1985, 19, 289-312.
- Gierer, J., Imsgard, F., Norén, I. Studies on the degradation of phenolic lignin units of the β -aryl ether type with oxygen in alkaline media. *Acta Chem. Scand.* 1977, B 31, 561-572.
- Gosselink, R.J.A., de Jong, E., Guran, B., Abächerli, A. Co-ordination network for lignin-standardisation, production and applications adapted to market requirements (EUROLIGNIN). *Ind. Crop. Prod.* 2004, 20, 121-129.
- Granata, A., Argyropoulos, D.S. 2-Chloro-4,4,5,5-tetramethyl-1,3,2-dioxaphospholane, a reagent for the accurate determination of the uncondensed and condensed phenolic moieties in lignins. *J. Agric. Food. Chem.* 1995, 43, 1538-1544.
- Hallac, B.B., Pu, Y., Ragauskas, A.J. Chemical transformations of *Buddleja davidii* lignin during ethanol organosolv pretreatment. *Energ. Fuel* 2010, 24, 2723-2732.

- Heitner, C., Dimmel, D., Schmidt, J. Lignin and Lignans: Advances in Chemistry; Taylor & Francis, 2010.
- Holladay, J.E., Bozell, J.J., White, J.F., Johnson, D. 2007. Results of screening for potential candidates from biorefinery lignin. Pacific Northwest National Laboratory and National Renewable Energy Laboratory.
- Huang, F., Singh, P.M., Ragauskas, A.J. Characterization of milled wood lignin (MWL) in *Loblolly Pine* stem wood, residue, and bark. *J. Agric. Food. Chem.* 2011, 59, 12910-12916.
- Hugo, E.G., Vadim, K., Abraham, N. NMR chemical shifts of common laboratory solvents as trace impurities. *J. Org. Chem.* 1997, 62, 7512-7515.
- Ibarra, D., Chávez, M.I., Rencoret, J., Del Río, J.C., Gutiérrez, A., Romero, J., Camarero, S., Martínez, M.J., Jiménez-Barbero, J., Martínez, A.T. Lignin modification during *Eucalyptus globulus* kraft pulping followed by totally chlorine-free bleaching: A two-dimensional nuclear magnetic resonance, fourier transform infrared, and pyrolysis-gas chromatography/mass spectrometry study. *J. Agric. Food. Chem.* 2007, 55, 3477-3490.
- Lai, Y.Z., Guo, X.P. Variation of the phenolic hydroxyl group content in wood lignins. *Wood Sci. Technol.* 1991, 25, 467-472.
- Landucci, L.L. Quantitative ^{13}C NMR characterization of lignin 1. A methodology for high precision. *Holzforschung* 1985, 39, 355-360.
- Liitiä, T., Maunu, S.L., Sipilä, J., Hortling, B. Application of solid-state ^{13}C NMR spectroscopy and dipolar dephasing technique to determine the extent of condensation in technical lignins. *Solid State Nucl. Magn. Reson.* 2002, 21, 171-186.
- Lin, S.Y., Dence, C.W. Methods in lignin chemistry; Springer-Verlag, 1992.
- Lundquist, K. ^1H NMR spectral studies of lignins. Results regarding the occurrence of β -5 structures, β - β structures, non-cyclic benzyl aryl ethers, carbonyl groups and phenolic groups. *Nordic Pulp Paper Res. J.* 1992, 7, 4-8.
- Miranda, I., Gominho, J., Mirra, I., Pereira, H. Fractioning and chemical characterization of barks of *Betula pendula* and *Eucalyptus globulus*. *Ind. Crop. Prod.* 2013, 41, 299-305.
- Mota, I., Rodrigues Pinto, P.C., Novo, C., Sousa, G., Guerreiro, O., Guerra, Â.R., Duarte, M.F., Rodrigues, A.E. Extraction of polyphenolic compounds from *Eucalyptus globulus* bark:

- Process optimization and screening for biological activity. *Ind. Eng. Chem. Res.* 2012, 51, 6991-7000.
- Nanayakkara, B., Manley-Harris, M., Suckling, I.D. Understanding the degree of condensation of phenolic and etherified C-9 units of in situ lignins. *J. Agric. Food. Chem.* 2011, 59, 12514-12519.
- Nose, M., Mark, B.A., Furlan, M., Zajicek, J., Eberhardt, T.L., Lewis, N.G. Towards the specification of consecutive steps in macromolecular lignin assembly. *Phytochemistry* 1995, 39, 71-79.
- Ohra-aho, T., Gomes, F.J.B., Colodette, J.L., Tamminen, T. S/G ratio and lignin structure among *Eucalyptus* hybrids determined by Py-GC/MS and nitrobenzene oxidation. *J. Anal. Appl. Pyrolysis* 2013, 101, 166-171.
- Pinto, P.C., Borges da Silva, E.A., Rodrigues, A.E. Insights into oxidative conversion of lignin to high-added-value phenolic aldehydes. *Ind. Eng. Chem. Res.* 2011, 50, 741-748.
- Pinto, P.C., Evtuguin, D.V., Neto, C.P. Effect of structural features of wood biopolymers on hardwood pulping and bleaching performance. *Ind. Eng. Chem. Res.* 2005, 44, 9777-9784.
- Pinto, P.C., Evtuguin, D.V., Neto, C.P., Silvestre, A.J.D. Behavior of *Eucalyptus globulus* lignin during kraft pulping I. Analysis by chemical degradation methods *J. Wood Chem. Technol.* 2002a, 22, 93-108.
- Pinto, P.C., Evtuguin, D.V., Neto, C.P., Silvestre, A.J.D., Amado, F.M.L. Behavior of *Eucalyptus globulus* lignin during kraft pulping II. Analysis by NMR, ESI/MS and GPC. *J. Wood Chem. Technol.* 2002b, 22, 109 - 125.
- Pinto, P.C.R., Borges da Silva, E.A., Rodrigues, A.E. 2012. Lignin as source of fine chemicals: Vanillin and syringaldehyde. in: *Biomass Conversion*, (Eds.) C. Baskar, S. Baskar, R.S. Dhillon, Springer Berlin Heidelberg, pp. 381-420.
- Pu, Y., Cao, S., Ragauskas, A.J. Application of quantitative ³¹P NMR in biomass lignin and biofuel precursors characterization. *Energy Environ. Sci.* 2011, 4, 3154-3166.
- Saito, T., Perkins, J.H., Vautard, F., Meyer, H.M., Messman, J.M., Tolnai, B., Naskar, A.K. Methanol fractionation of softwood kraft lignin: Impact on the lignin properties. *ChemSusChem* 2014, 7, 221-228.

- Sannigrahi, P., Ragauskas, A.J., Miller, S.J. Lignin structural modifications resulting from ethanol organosolv treatment of *Loblolly Pine*. *Energ. Fuel* 2009, 24, 683-689.
- Santos R.B., Capanema, E.A., Balakshin, M.Y., Chang, H.-m., Jameel, H. Lignin structural variation in hardwood species. *J. Agric. Food. Chem.* 2012, 60, 4923-4930.
- Sjöström, E. Wood chemistry: Fundamentals and applications; Academic Press: London, 1993.
- Solár, R., Melcer, I., Kacik, F. Comparative study of pine wood and pine bark (*Pinus silvestris L.*) dioxan lignins. *Cellul. Chem. Technol.* 1988, 22, 39-52.
- Tarabanko, V., Petukhov, D. Study of mechanism and improvement of the process of oxidative cleavage of lignins into the aromatic aldehydes. *Chemistry for Sustainable Development* 2003, 11, 655-667.
- Tarabanko, V.E., Fomova, N.A., Kuznetsov, B.N., Ivanchenko, N.M., Kudryashev, A.V. On the mechanism of vanillin formation in the catalytic oxidation of lignin with oxygen. *React. Kinet. Catal. Lett.* 1995, 55, 161-170.
- Wen, J.-L., Xue, B.-L., Sun, S.-L., Sun, R.-C. Quantitative structural characterization and thermal properties of birch lignins after auto-catalyzed organosolv pretreatment and enzymatic hydrolysis. *J. Chem. Technol. Biotechnol.* 2013a, 88, 1663-1671.
- Wen, J.L., Sun, S.L., Yuan, T.Q., Xu, F., Sun, R.C. Structural elucidation of lignin polymers of *Eucalyptus* chips during organosolv pretreatment and extended delignification. *J. Agric. Food. Chem.* 2013b, 61, 11067-11075.
- Xia, Z., Akim, L.G., Argyropoulos, D.S. Quantitative ¹³C NMR analysis of lignins with internal standards. *J. Agric. Food. Chem.* 2001, 49, 3573-3578.
- Xie, Y., Yasuda, S. Difference of condensed lignin structures in *Eucalyptus* species. *Nordic Pulp and Paper Res. J.* 2004, 19, 18-21.

4

Characterization and comparative evaluation of industrial crops lignins

Lignins from industrial crops could be converted into valuable chemicals in the context of a second generation biorefinery, but prior understanding of their structure is required. This chapter is focused on the characterization of *in situ* and mild acidolysis lignins from stalks and roots of corn, cotton, sugarcane and tobacco. All the materials and the isolated lignins were subjected to alkaline NO. The isolated lignins were also analyzed by ^{13}C , ^{31}P , and HSQC NMR and FTIR spectroscopy. With the obtained data, the structural differences between the residues, stalks and roots, and isolated lignins are discussed in a comparative approach, highlighting for each material the characteristic features of its lignin. The knowledge of the composition and structure of corn, cotton, sugarcane, and tobacco lignins would help to maximize the exploitation of these important crops as a feedstock for the production of added-value products, such as V and Sy, in the perspective of a second generation biorefinery.

This chapter is based on the following publications:

- Costa, C.A.E., Coleman, W., Dube, M., Rodrigues, A.E., Pinto, P.C.R. Assessment of key features of lignin from lignocellulosic crops: Stalks and roots of corn, cotton, sugarcane, and tobacco. *Ind. Crop. Prod.* 2016, 92, 136-148.
- Costa, C.A.E.; Pinto, P.C.R.; Rodrigues, A.E. Radar tool for lignin classification on the perspective of its valorization. *Ind. Eng. Chem. Res.* 2015, 54, 7580–7590.

4.1 INTRODUCTION

Lignocellulosic materials resulting from the exploitation of agro-forest resources offer many advantages as feedstock to produce new value-added products in the context of a second generation biorefinery (Kleinert and Barth, 2008; Ragauskas et al., 2014). Besides the wide availability and associated low cost, some agricultural residues, such as cereal straws, contain comparable amounts of the major constituents common to wood species. Some of the major residues resulting from the production of corn (Kaparaju and Felby, 2010; Saliba et al., 2002), sugarcane (Guimarães et al., 2009; Maziero et al., 2012), wheat (del Río et al., 2012; Zikeli et al., 2014), rice (Salanti et al., 2010; Xiao et al., 2001), and flax (Buranov et al., 2010; Ross and Mazza, 2010) have been reported in the literature. Works focused in these agricultural residues have as a first challenge to accomplish specific structural information about their main components (cellulose, hemicellulose and lignin) followed by the study of their fractionation and afterwards, conversion into added-value products.

The amounts of the chemical components (cellulose, hemicellulose and lignin) of lignocellulosic biomass would be expected to vary depending on the morphological part of plant. For a profitable utilization and conversion of the agricultural crops into valuable products, an efficient extraction and detailed chemical characterization of their constituents is required. Lignin, making up to 5-30% of herbaceous crop's weight (Buranov and Mazza, 2008), plays an important role as raw material for the production of byproducts and biofuels (Azadi et al., 2013; Ragauskas et al., 2014). Due to its heterogeneity, prior characterization of the agricultural materials is essential and might allow an estimation of the feasibility for a specific application as well as selection of the better lignin source for a particular product.

4.2 EXPERIMENTAL SECTION: MATERIALS AND METHODS

4.2.1 Industrial crops and lignins: samples description

Stalks and roots of tobacco and corn were obtained from farms in North Carolina, sugarcane stalks and roots in Georgia, and cotton stalks and roots in South Carolina. Stalks and roots were harvested from the field and washed to remove debris and sand. Then, all samples were dried in a Sargent tray dryer at 333 K, 6 hours for the roots (9.6 %wt moisture) and 2.5 hours for the stalks (10.6 %wt moisture), chipped, milled and sieved to obtain a 40-60 mesh fraction.

Lignins were isolated from stalks and roots of corn, cotton, sugarcane, and tobacco by mild acidolysis, following the method described in section 3.2.2 (Chapter 3).

The designation of each material referenced in this work is summarized in Table 14.

Table 14 - Residues, morphological part, and designation of each material.

		Residue	Isolated lignin
Corn	stalks	Corn _{stalk}	LCorn _{stalk}
	roots	Corn _{root}	LCorn _{root}
Cotton	stalks	Cotton _{stalk}	LCotton _{stalk}
	roots	Cotton _{root}	LCotton _{root}
Sugarcane	stalks	SCane _{stalk}	LSCane _{stalk}
	roots	SCane _{root}	LSCane _{root}
Tobacco	stalks	Tob _{stalk}	LTob _{stalk}
	roots	Tob _{root}	LTob _{root}

4.2.2 Lignin content

Klason lignin was estimated as the solid material obtained after H₂SO₄ hydrolysis of the residue, corrected for moisture content, based on the method described in the literature (Lin and Dence, 1992).

A solution of 72% (w/w) H₂SO₄ was added to 1.0 g of residue and the mixture was left at room temperature for 2.5 hours. The mixture was diluted with water and hydrolyzed for 2 h under reflux. The resulting material was then submitted to vacuum filtration and washed with water until neutral pH, dried and weighted. For acid-soluble lignin quantification, a sample of 20.0 mL was taken from the resultant filtrate, pH was adjusted to 9.0 with NaOH 9M and then 50 mg of sodium borohydride (NaBH₄) were added and left stirring for 20 minutes. After that, the solution was acidified to pH 2 with H₂SO₄ 9M and diluted, and the absorbance was measured at 280 nm, using as a reference a solution of 1.8 % (w/w) H₂SO₄.

4.2.3 Inorganic and carbohydrates content

The inorganic and carbohydrates content in the residues of corn, cotton, sugarcane and tobacco and the respective isolated lignins was determined using the methods and techniques already described in section 3.2.4.1 and 3.2.4.2 (Chapter 3).

4.2.4 Nitrobenzene oxidation

All the isolated lignins and the stalks and roots of corn, cotton, sugarcane, and tobacco were submitted to alkaline NO as described in section 3.2.5.1 (Chapter 3)

4.2.5 2D-NMR spectral analysis: HSQC spectra

2D-NMR spectra of the isolated lignins were recorded at 298 K on a Bruker AVANCE III 600 HD spectrometer operating at 600.13 MHz for ^1H , equipped with 5 mm CryoProbe Prodigy and pulse gradient units, capable of producing magnetic field pulsed gradients in the z-direction of 50 G/cm.

About 50 mg of lignin was dissolved in 0.75 mL of DMSO- d_6 , and 2D-NMR spectra were recorded for HSQC. The central solvent peak was used as the internal reference (DMSO- d_6 , $\delta\text{C}/\delta\text{H}$ 40.0/2.5). The spectral widths were 5000 and 25000 Hz for the ^1H and ^{13}C dimensions, respectively. The number of collected complex points was 2048 for the ^1H dimension with a recycle delay of 5 s. The number of transients was 64, and 256 time increments were always recorded in the ^{13}C dimension. The $^1J_{\text{C-H}}$ used was 145 Hz. The J -coupling evolution delay was set to 3.2 ms. Squared cosine-bell apodization function was applied in both dimensions. Prior to Fourier transform the data matrices were zero filled to 1024 points in the ^{13}C dimension.

4.2.6 FTIR

FTIR spectra were recorded using a Bomem MB-Series spectrometer. The isolated lignins were analyzed in the form of potassium bromide (KBr) discs, which were prepared with about 1 mg of lignin plus 100 mg of KBr and pressed under vacuum.

The spectra were recorded in the range of 4000-600 cm^{-1} .

4.3 STRUCTURAL CHARACTERIZATION OF STALKS, ROOTS AND ISOLATED LIGNINS

4.3.1 Composition of stalks, roots and isolated lignins

The chemical composition of corn, cotton, sugarcane, and tobacco stalks and roots is depicted in Table 15. For isolated lignins this information is depicted in Table 16, as component weight per 100 g of dried material.

Non-cellulosic carbohydrates represent about 12.5-28.2% of the materials weight. The main sugar residues found are xylose and glucose; minor quantities of rhamnose, arabinose, and mannose were also detected. Inorganic content is quite low, between 1.9 and 7.1%, with exception of SCane_{root}, which contains 31.8%. The data analysis also reveals that SCane_{stalk} presents the lowest content of lignin (9.2%), while non-cellulosic polysaccharides content (28.2%) is the highest. In contrast, Cotton_{stalk} has the lowest content of non-cellulosic polysaccharides (12.5%, detailed composition is depicted in Table 17) and the highest content of lignin (24.6%).

Table 15 - Composition (ash, carbohydrates, and lignin, dry weight) of stalks and roots.

Residue		Inorganic compounds	Carbohydrates	Lignin content
		(%w/w)	(%w/w)	(%w/w)
Corn	stalk	4.7 ± 0.1	21.3 ± 1.0	15.3
	root	5.3 ± 0.1	16.8 ± 0.8	19.8
Cotton	stalk	2.8 ± 0.2	12.5 ± 0.6	24.6
	root	3.1 ± 0.2	15.7 ± 0.8	18.9
Sugarcane	stalk	1.9 ± 0.01	28.2 ± 1.4	9.2
	root	31.8 ± 1.8	16.9 ± 0.8	17.6
Tobacco	stalk	7.1 ± 0.3	16.8 ± 0.7	17.7
	root	2.1 ± 0.1	17.4 ± 0.8	15.0

Table 16 - Ash and carbohydrates contents as contaminants in isolated lignins (dry weight).

Lignins		Inorganic compounds	Carbohydrates
		(%w/W _{lignin})	(%w/W _{lignin})
LCorn	stalk	< 0.01	6.2 ± 0.3
	root	1.1 ± 0.04	6.7 ± 0.3
LCotton	stalk	0.46 ± 0.03	5.1 ± 0.2
	root	2.6 ± 0.2	7.2 ± 0.3
LSCane	stalk	1.5 ± 0.1	5.4 ± 0.2
	root	0.65 ± 0.1	3.2 ± 0.1
LTob	stalk	0.43 ± 0.02	6.9 ± 0.3
	root	0.91 ± 0.02	7.5 ± 0.3

The lignin content in residues (between 9.2 and 24.6 %) is in agreement with the data reported in the literature. Some authors studied the structural characterization of different residues of herbaceous plants (wheat straw, corn residue, triticale straw, and flax shives) and found lignin contents (Klason plus acid-soluble lignin) in the range 5 to 25% (del Río et al., 2012; Guimarães et al., 2009; Monteil-Rivera et al., 2013).

For isolated lignins (Table 16) a maximum of 2.6% of ash was found, while the content of co-extracted carbohydrates was between 3.2 and 7.5% accounting for a maximum of 10% of identified contaminants. The degree of contamination found for the studied lignins is in agreement with the values reported for other herbaceous lignins (Monteil-Rivera et al., 2013), but it is higher than the level of contamination found in acidolysis lignin from woody materials (Costa et al., 2014; Jääskeläinen et al., 2003). Moreover, other contaminants could be present, such as protein. Further analysis of lignins will clarify this assumption.

Table 17 - Composition of carbohydrate fraction (%w/w) of lignocellulosic materials and respective isolated lignins.

	Glc	Xyl	Ara	Gal	Rha	Man
Corn _{stalk}	6.68	10.52	1.19	0.54	0.14	0.56
LCorn _{stalk}	1.07	1.92	1.22	0.04	0.12	0.24
Corn _{root}	2.05	9.97	1.33	0.98	0.18	0.48
LCorn _{root}	0.81	1.97	1.31	0.12	0.10	0.09
Cotton _{stalk}	4.82	4.22	0.55	0.67	0.53	0.48
LCotton _{stalk}	1.35	1.63	0.71	0.13	0.24	0.12
Cotton _{root}	3.10	3.78	0.47	0.57	0.45	0.51
LCotton _{root}	1.18	1.22	0.72	0.12	0.18	0.11
SCane _{stalk}	19.67	5.58	0.43	0.26	0.03	0.46
LSCane _{stalk}	1.42	0.94	0.99	0.02	0.08	0.11
SCane _{root}	3.28	8.41	1.68	1.02	0.21	0.48
LSCane _{root}	0.62	1.08	0.68	0.10	0.11	0.07
Tob _{stalk}	1.10	10.49	0.55	0.58	0.61	0.75
LTob _{stalk}	0.43	3.77	0.19	0.20	0.40	0.26
Tob _{root}	0.97	9.23	0.48	0.51	0.54	0.66
LTob _{root}	2.49	2.78	0.06	0.18	0.25	0.02

*Glc – glucose; Xyl – xylose; Ara – arabinose; Gal – galactose; Rha – rhamnose; Man - mannose.

4.3.2 Analysis by NO

NO was applied directly to stalks and roots and to the respective acidolysis lignins. NO results are reported on lignin content (data from Table 15 and Table 16) for stalks/roots and lignins. The yields of NO products are depicted in Figure 16 (detailed information is depicted in Table 18).

For *in situ* lignins, NO total yields are in the range 32-46%, in accordance with other raw materials analyzed by this method (Agrupis et al., 2000; Nishimura et al., 2002; Pinto et al., 2015). Since *in situ* lignins are not subjected to delignification and/or isolation, they do not suffer structural changes induced by these processes, in particular in the non-condensed fraction (Costa et al., 2014; Costa et al., 2015). As such, these values present a real perspective of the unmodified structure of lignin. NO yields are lower for SCane_{root} and Cotton_{root}, indicating that these two materials contain the highest proportion of condensed structures.

All the lignins have V and Sy as main products that together with relatively fewer Hy content revealed that all the lignins can be denoted as S:G:H lignins. V and Sy contents vary between 15.2-21.1% and 6.4-18.8%, respectively. For Hy, lower contents were obtained (Figure 16); however, also in considerable amounts for Corn_{stalk} (6.6%), Corn_{root} (7.2%), and SCane_{stalk} (7.8%).

There are no major differences between the product profiles of stalks and roots for corn, cotton, and tobacco (direct analysis on materials). However, for sugarcane the two morphological parts present a difference of 27% between their total yields. This difference is mainly observed for Hy and Sy.

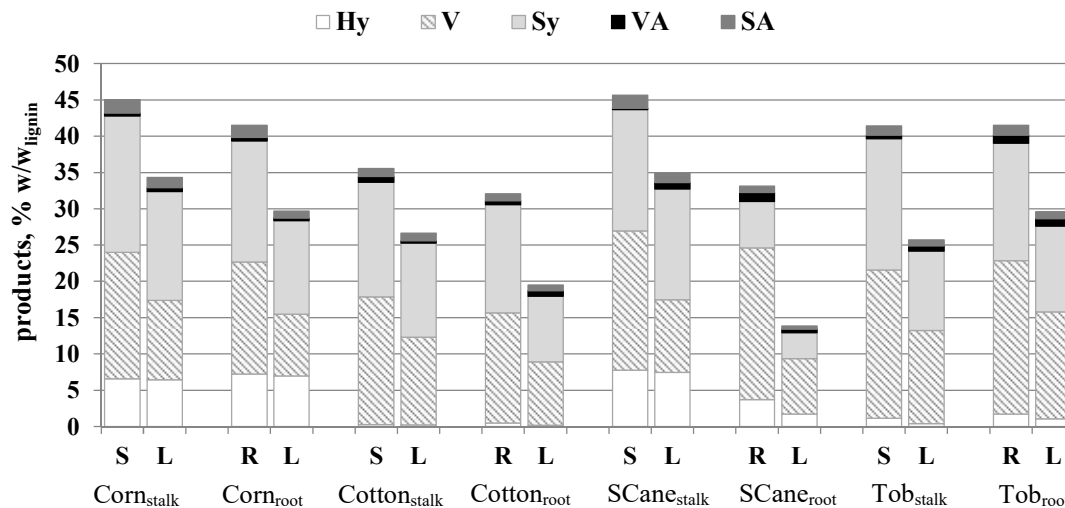


Figure 16 - Yields of monomeric phenolic products obtained by NO of stalks (S) and roots (R) and the respective isolated lignins (L) from corn, cotton, sugarcane, and tobacco, reported on lignin basis.

Table 18 - Yields of monomeric phenolic products obtained by NO of stalks, roots and isolated lignins.

lignin	products, % w/w _{lignin} *					total yield
	Hy	VA	SA	V	Sy	
Corn _{stalk}	6.57	0.42	1.83	17.4	18.8	45.0
LCorn _{stalk}	6.41	0.51	1.44	11.0	15.0	34.3
Corn _{root}	7.24	0.50	1.67	15.4	16.7	41.5
LCorn _{root}	6.95	0.36	0.98	8.54	12.8	29.7
Cotton _{stalk}	0.25	0.79	1.11	17.6	15.8	35.6
LCotton _{stalk}	0.21	0.35	1.02	12.1	12.9	26.6
Cotton _{root}	0.48	0.51	0.98	15.2	14.9	32.1
LCotton _{root}	0.15	0.75	0.78	8.75	9.06	19.5
SCane _{stalk}	7.76	0.17	1.81	19.2	16.7	45.6
LSCane _{stalk}	7.47	0.91	1.24	9.98	15.3	34.9
SCane _{root}	3.71	1.26	0.86	20.9	6.38	33.1
LSCane _{root}	1.70	0.47	0.44	7.64	3.58	13.8
Tob _{stalk}	1.15	0.51	1.26	20.4	18.1	41.4
LTob _{stalk}	0.39	0.71	0.84	12.8	11.0	25.7
Tob _{root}	1.72	1.13	1.33	21.1	16.2	41.5
LTob _{root}	1.07	1.04	0.96	14.7	11.8	29.6

* reported to nonvolatile solids weight after deducting ashes and carbohydrates.

The NO yields of isolated lignins present a decrease of 25-40% of the total yields found for *in situ* lignins, a consequence of some structural modifications induced by mild acidolysis process, namely condensation reactions. LSCane_{root} shows a relative decrease of 60% of the NO yield comparatively to the respective initial material, indicating that the structural changes for this lignin were more severe. Isolated lignins also have V and Sy as major products with significant amounts of Hy for LCCorn_{stalk}, LCCorn_{root} and LSCane_{stalk}, which is in accordance with the analysis of *in situ* lignins. The S/G ratio, obtained from NO, is higher for isolated lignins, between 0.50 and 1.55, than for the corresponding *in situ* lignins, in the range 0.33-1.16. This suggests that G units were more involved in condensed structures, which is plausible due to its additional free position in aromatic C₅ as compared with S units. The profile of products presents higher differences between species than between morphological parts. Roots lignins are more affected by the isolation process than stalks, except for tobacco. The observed variations in NO yields demonstrate that existing structural differences between lignins are important to explore.

4.3.3 ¹³C NMR

Isolated lignins were analyzed by quantitative ¹³C NMR and the spectra with the main assignments identified are shown in Figure 17 and Figure 18 for stalks and roots lignins, respectively. The assignments and the quantification of the structures/linkages and functional groups of lignin structure was made based on reference spectra and data available in the literature (Balakshin et al., 2015; Capanema et al., 2004; Pinto et al., 2002; Robert, 1992). The ¹³C NMR results are depicted in Table 19 and Table 20 for isolated lignin from stalks and roots, respectively.

The ¹³C NMR spectra of isolated lignins shown typical tertiary carbon resonances from S units (aromatic carbon C₂ and C₆) between 102.0 and 110.0 ppm, G units (aromatic carbon C₂, C₅ and C₆) between 110.0 and 123.0 ppm, and relatively fewer quaternary carbon resonances from H units (aromatic carbon C₄) at 157.0-163.0 ppm. Moreover, due to the higher complexity of non-wood lignins structure comparatively to wood ones, it is also important to consider the contribution of conjugated acid derivatives, such as ferrulates (FA), coumarates (CA) and *p*-hydroxy benzoic acids (PHBA), into the resonances of G-(FA) and H-units (CA and PHBA) (Balakshin and Capanema, 2015). For this reason, the quantification of G- and H-units should be corrected for the contribution of the characteristic signals of FA and CA types. The presence of FA and CA moieties was identified in the mild acidolysis lignins spectra by the assignment of the carbons in their carboxyl and ester groups, by the resonances centered at 166 and 168 ppm, respectively (Balakshin and Capanema, 2015; Oliveira et al., 2006). From the quantification of the conjugated acid derivatives, FA and CA, values between 0.1-0.4 /Ar were obtained.

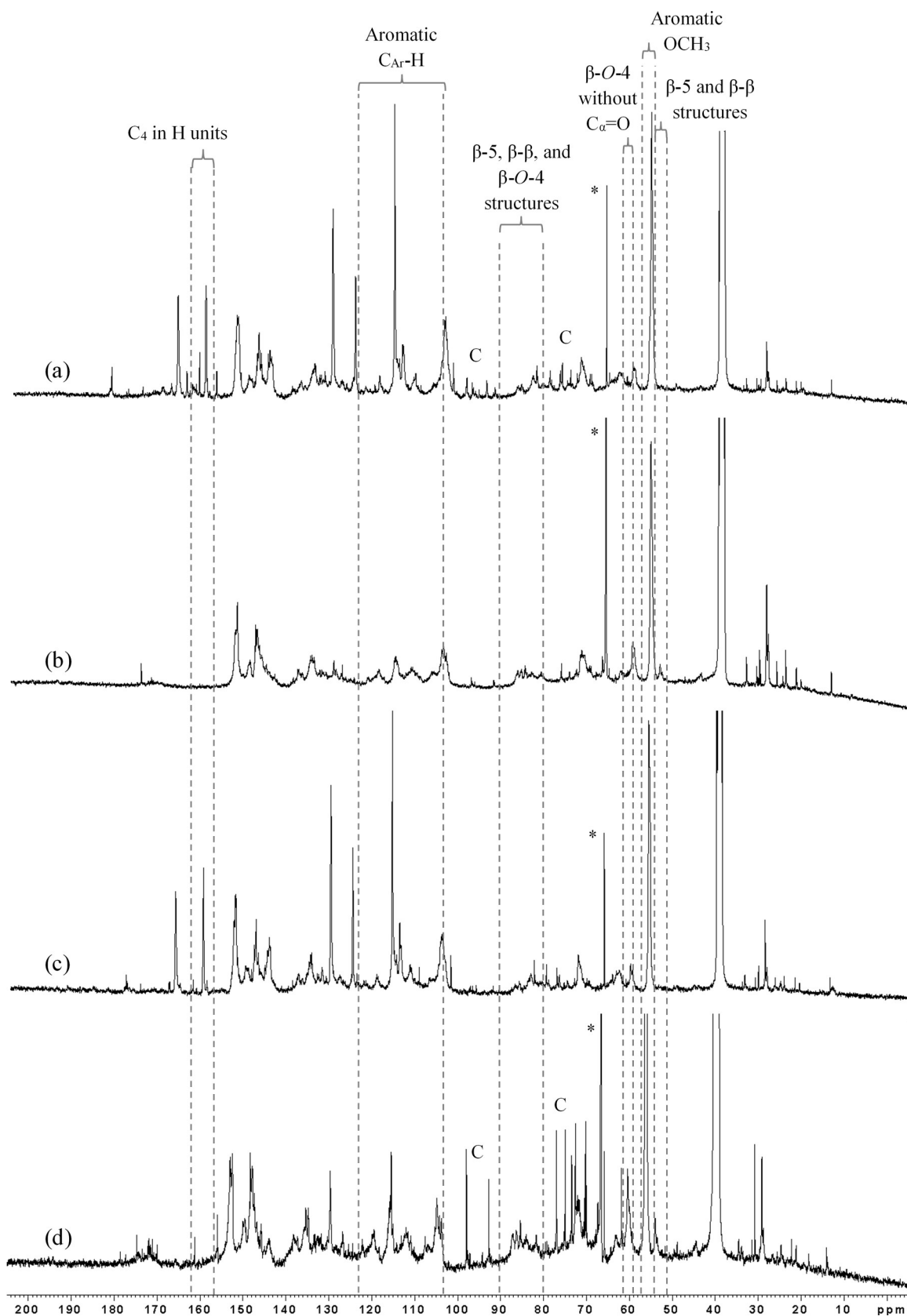


Figure 17 - Quantitative ^{13}C NMR spectra of (a) LCorn_{stalk}, (b) LCotton_{stalk}, (c) LSCane_{stalk}, and (d) LTob_{stalk} (in DMSO- d_6 ; * solvent peak (Hugo et al., 1997); C - carbohydrates contamination).

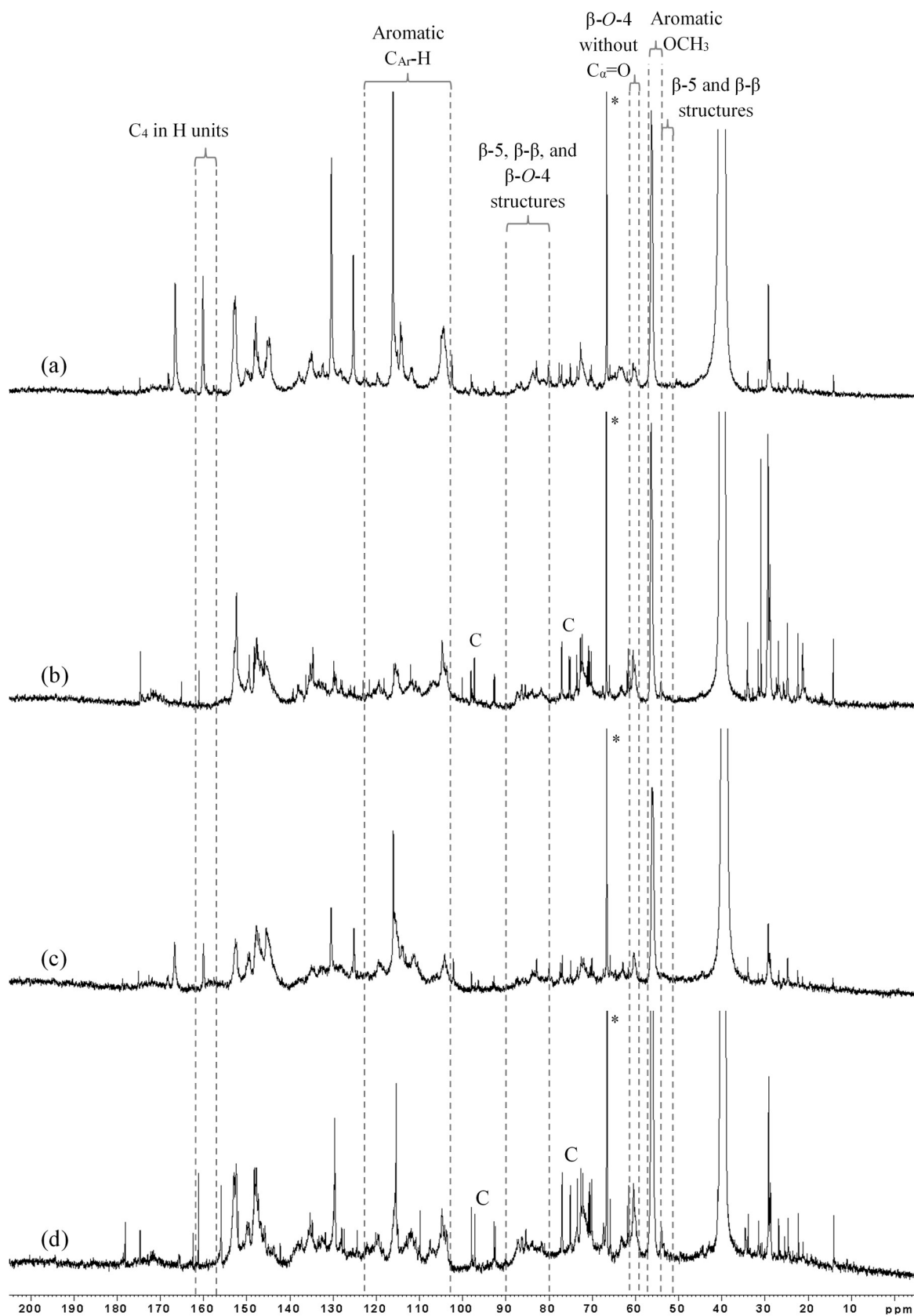


Figure 18 - Quantitative ^{13}C NMR spectra (a) L $\text{Corn}_{\text{root}}$, (b) L $\text{Cotton}_{\text{root}}$, (c) L $\text{SCane}_{\text{root}}$, and (d) L Tob_{root} (in DMSO-d_6 ; * solvent peak (Hugo et al., 1997); C - carbohydrates contamination).

Table 19 - Assignments and quantification (number per aromatic ring) of the structures/linkages and functional groups identified by ^{13}C NMR in lignins from stalks of corn, cotton, sugarcane, and tobacco.

Assignments	amount (number/Ar)			
	LCorn _{stalk}	LCotton _{stalk}	LSCane _{stalk}	LTob _{stalk}
C β in β -5 and β - β structures (δ 51.0-53.8 ppm)	0.15	0.20	0.07	0.21
Aromatic OCH $_3$ (δ 54.3-57.3 ppm)	1.20	1.47	0.99	1.37
C γ in β -O-4 structures without C α =O (δ 59.3-60.8 ppm)	0.21	0.37	0.16	0.36
C γ in β -5 and β -O-4 structures with C α =O; C γ in β -1 structures (δ 62.5-63.8 ppm)	0.19	0.15	0.16	0.15
C α in β -O-4 structures; C γ in pinorensinol/syringaresinol and β - β structures (δ 70.0-76.0 ppm)	0.68	0.87	0.47	1.09
C β in β -O-4 structures; C α in β -5 and β - β structures (δ 80.0-90.0 ppm)	0.45	0.64	0.36	0.74
Aromatic C $_{Ar}$ -H (δ 103.0-123.0 ppm)	2.37	2.37	2.37	2.19
C $_4$ in H units (δ 157.0–162.0 ppm)	0.15	0.06	0.08	0.18
CHO in benzaldehyde structures (δ 191.0-192.0 ppm)	0.02	0.05	0.04	0.03

^a Carbohydrates also contribute to these regions, especially to the region of 70–76 ppm by C $_3$ and C $_4$ of aromatic ring.

^b The region of aromatic C $_{Ar}$ -H was corrected for the contribution of C β conjugated present in CA and FA.

Table 20 - Assignments and quantification (number per aromatic ring) of the structures/linkages and functional groups identified by ^{13}C NMR in lignins from stalks of corn, cotton, sugarcane, and tobacco.

Assignments	amount (number/Ar)			
	LCorn _{root}	LCotton _{root}	LSCane _{root}	LTob _{root}
C β in β -5 and β - β structures (δ 51.0-53.8 ppm)	0.13	0.14	0.19	0.20
Aromatic OCH $_3$ (δ 54.3-57.3 ppm)	1.04	0.99	0.86	1.35
C γ in β -O-4 structures without C α =O (δ 59.3-60.8 ppm)	0.17	0.26	0.18	0.34
C γ in β -5 and β -O-4 structures with C α =O; C γ in β -1 structures (δ 62.5-63.8 ppm)	0.17	0.11	0.12	0.15
C α in β -O-4 structures; C γ in pinorensinol/syringaresinol and β - β structures (δ 70.0-76.0 ppm)	0.55	0.76	0.49	1.08
C β in β -O-4 structures; C α in β -5 and β - β structures (δ 80.0-90.0 ppm)	0.35	0.37	0.38	0.64
Aromatic C $_{Ar}$ -H (δ 103.0-123.0 ppm)	2.35	2.31	2.44	2.26
C $_4$ in H units (δ 157.0–162.0 ppm)	0.08	0.06	0.14	0.17
CHO in benzaldehyde structures (δ 191.0-192.0 ppm)	0.03	0.05	0.04	0.03

^a Carbohydrates also contribute to these regions, especially to the region of 70–76 ppm by C $_3$ and C $_4$ of aromatic ring.

^b The region of aromatic C $_{Ar}$ -H was corrected for the contribution of C β conjugated present in CA and FA.

The ^{13}C NMR data also indicate that the isolated lignins are mainly composed by β -O-4 structures, identified through their side chain carbons (C_α , C_β and C_γ) and quantified by the subtraction of the amount of β -5 and β - β structures (δ 51.0-53.8 ppm) from the integral of δ 82.5-90.0 ppm (Capanema et al., 2005; Costa et al., 2014). Moreover, small amounts of β - β , β -5 and β -1 linkages were also found in the NMR spectra.

The mild acidolysis lignins exhibit characteristic signals in the aliphatic region of the ^{13}C NMR spectra (10-35 ppm); these signals are usually considered as impurities from extractives like fatty acids (Abdelkafi et al., 2011; Oliveira et al., 2006). In previous works, it was suggested that these aliphatic moieties could belong to suberin-like substances, that are chemically linked to the lignin of the primary cell wall in certain tissues of annual plants by ester linkages via FA (Bernards, 2002; Clemente et al., 2013; Oliveira et al., 2009). The same feature may be suggested for the lignins of stalks and roots studied in this work. In the literature, it is assumed that FA moieties are responsible for cell wall cross-linking in several annual plants, like grasses (Hatfield et al., 1999).

LCorn_{stalk}, LTob_{stalk}, LCotton_{root}, and LTob_{root} show the typical signals assigned to carbons of carbohydrates (labelled as C, Figure 17 and Figure 18) that resonate between 70-80 ppm and 90-103 ppm, suggesting the presence of LCC (Buranov and Mazza, 2008; Ghaffar and Fan, 2013).

4.3.3.1.1 Lignin purification with dioxane

In order to study the effect of purification process on lignin structure two isolated lignins were selected and submitted to a nondegradative method of purification with dioxane. The selected lignins, LCotton_{stalk} and LSCane_{root}, were dissolved in dioxane and precipitated in cold water. The purified lignin was separated by centrifugation and freeze-dried.

The co-precipitated water soluble contaminants are easily eliminated by dissolution of lignin in dioxane and reprecipitation in water. However, if the contaminants are chemical linked to lignin, more severe conditions should be used but the core of lignin will be modified.

LCotton_{stalk} lignin was used as reference lignin to verify the impact of purification process. This lignin does not show carbohydrates contamination and, as such, any structural change is caused by the purification itself. LSCane_{root} was the sample with contamination that was subjected to the same process. Figure 19 and Figure 20 show the ^{13}C NMR spectra of the lignins before and after the purification; the results are depicted in Table 21 and Table 22.

For both lignins it is possible to observe that the purification with dioxane led to a lignin with different content of β -O-4 structures and H units. For LSCane_{root} (the contaminated one) there is a slight decrease of the signals attributed to carbohydrates. It can be concluded that the purification process leads to modifications in the representativeness of lignins, invalidating the comparison between them.

For lignins characterization it is important to reach a compromise between the presence and the identification of the contaminants and the decision about a purification process. Considering these samples, it could be concluded that the changes induced in lignin by the purification process are more unfavorable than the presence of the contaminants.

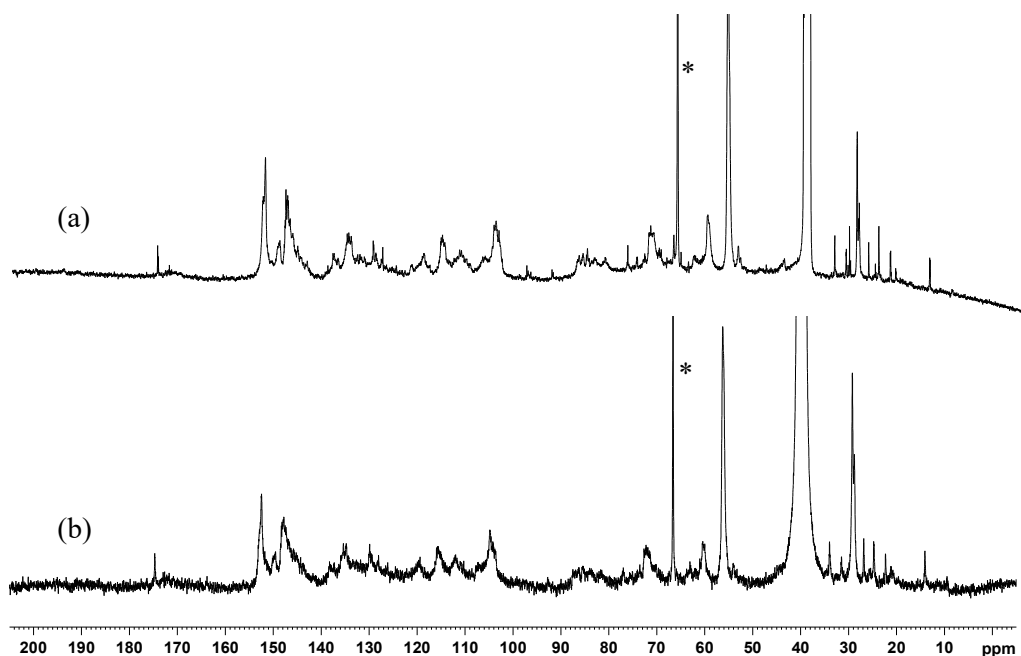


Figure 19 - Quantitative ^{13}C NMR spectra of LCotton_{stalk} before (a) and after (b) purification (in DMSO- d_6 ; * solvent peak (Hugo et al., 1997)).

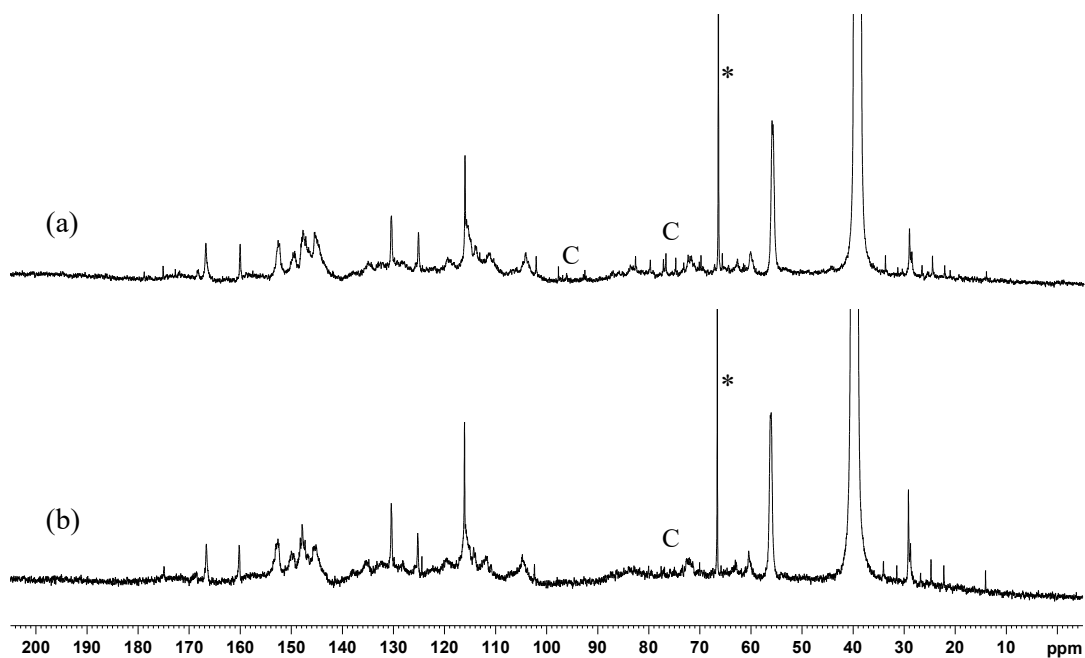


Figure 20 - Quantitative ^{13}C NMR spectra of LSCane_{root} before (a) and after (b) purification (in DMSO- d_6 ; * solvent peak (Hugo et al., 1997); C - carbohydrates contamination).

Table 21 - ^{13}C NMR assignments and quantification (number per aromatic ring) of the structures/linkages and functional groups identified in mild acidolysis lignins of cotton stalks and sugarcane roots before and after the dioxane purification.

assignments (spectroscopic range)	amount (number/Ar)			
	LCotton _{stalk}	LCotton _{stalk} purified	LSCane _{root}	LSCane _{root} purified
C _β in β-5 and β-β structures (δ 51.0-53.8 ppm)	0.19	0.14	0.19	0.12
Aromatic OCH ₃ (δ 54.3-57.3 ppm)	1.41	1.07	0.85	0.82
C _γ in β-O-4 structures without Cα=O (δ 59.3-60.8 ppm)	0.35	0.23	0.18	0.16
C _γ in β-5 and β-O-4 structures with Cα=O; C _γ in β-1 (δ 62.5-63.8 ppm)	0.14	0.11	0.12	0.12
Cα in β-O-4 structures; C _γ in pinoresinol/syringaresinol and β-β structures (δ 70.0-76.0 ppm)	0.84	0.60	0.49	0.52
C _β in β-O-4 structures; Cα in β-5 and β-β structures (δ 80.0-90.0 ppm)	0.82	0.58	0.52	0.60
Aromatic C _{Ar} -H (δ 103.0-123.0 ppm)	2.20	2.20	2.40	2.29
Aromatic C _{Ar} -C (δ 123.0-137.0 ppm)	1.36	1.53	1.44	1.48
C ₄ in H units (δ 157.0-162.0 ppm)	0.06	0.05	0.20	0.26
CHO in benzaldehyde structures (δ 191.0-192.0 ppm)	0.04	0.02	0.04	0.03
CHO in cinnamaldehyde structures (δ 193.5-194.5 ppm)	0.05	0.02	0.04	0.03

Table 22 - β-O-4 structures content (number per 100 aromatic rings), S:G:H ratio, and DC calculated for mild acidolysis lignins of cotton stalks and sugarcane roots before and after the dioxane purification.

lignin	β-O-4 structures (number/100Ar)	DC (%)	S:G:H
LCotton _{stalk}	63	26	48:45:07
LCotton _{stalk} purified	45	29	46:49:05
LSCane _{root}	33	22	28:62:10
LSCane _{root} purified	48	25	22:54:24

4.3.4 HSQC spectra of corn stalks lignin

The isolated lignin from corn stalks was analyzed by 2D-NMR. In the HSQC NMR spectrum, displayed in Figure 21, two important regions could be considered that corresponding to side-chain ($\partial\text{C}/\partial\text{H}$ 50-90/2.5-5.5 ppm) and the aromatic/unsaturated ($\partial\text{C}/\partial\text{H}$ 90-160/6.0-8.0 ppm) ^{13}C - ^1H correlations in several lignin moieties.

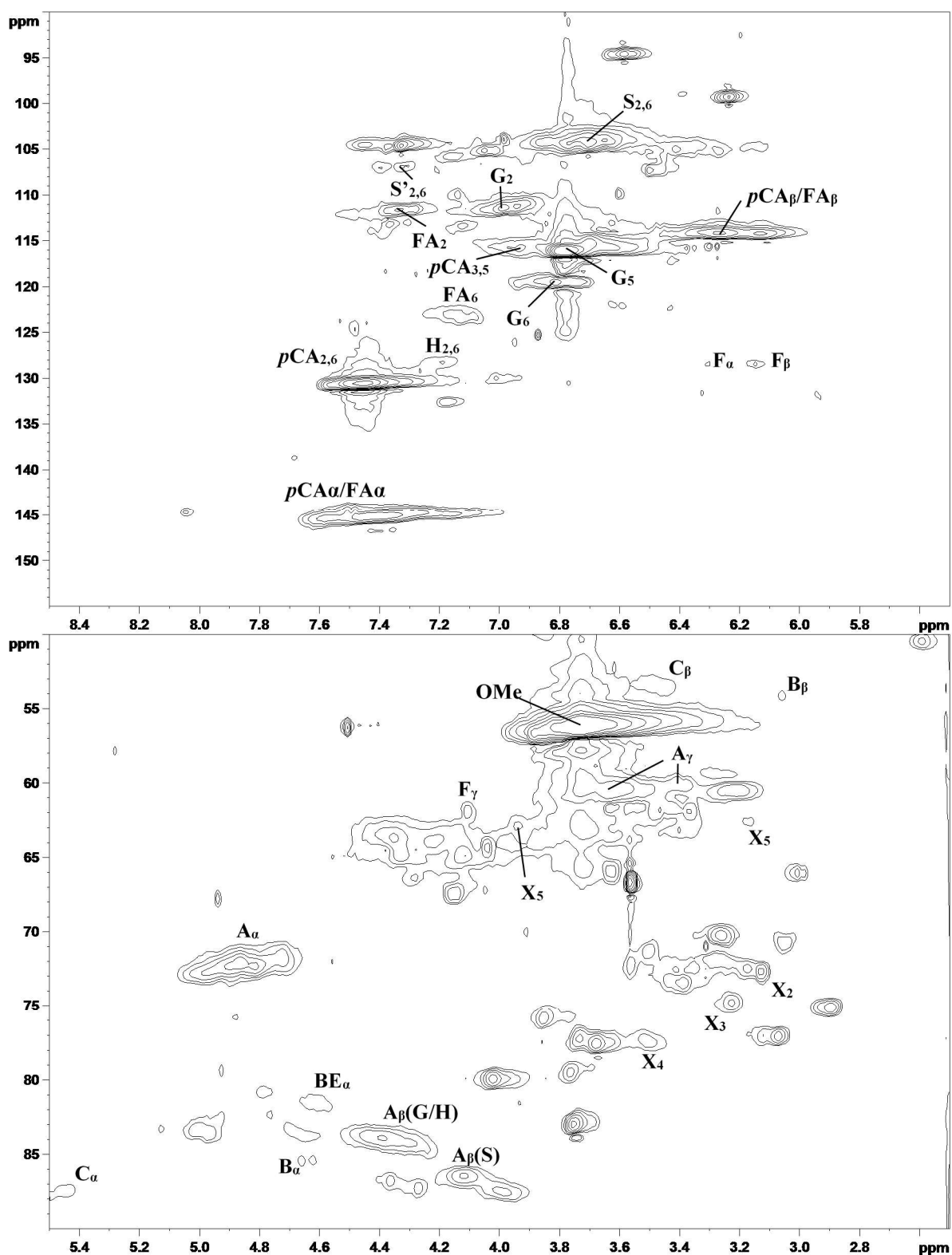


Figure 21 - Side-chain (∂_C/∂_H 50-90/2.5-5.5) and aromatic/unsaturated (∂_C/∂_H 90-160/6.0-8.0) regions in the HSQC NMR spectrum of corn stalks lignin (see Table 23 for signal assignments).

The assignments of the main lignin cross-signals assigned in the HSQC spectrum, depicted in Table 23, were identified by comparison with the correlations signals reported in the literature (Balakshin et al., 2011; del Río et al., 2012; Fernández-Costas et al., 2014; Rencoret et al., 2015).

Table 23 - The NMR assignments of major components in the HSQC spectrum of the corn stalks lignin.

	Label	Chemical shift (ppm)		Assignments
		¹³ C	¹ H	
Side-chain region	C _β	53.1	3.46	C _β -H _β in phenylcoumaran substructures
	B _β	54.0	3.05	C _β -H _β in β-β (resinol) substructures
	OCH ₃	56.0	3.70	C-H in methoxyls
	A _γ	59.9	3.40 and 3.70	C _γ -H _γ in β-O-4 substructures
	F _γ	62.0	4.10	C _γ -H _γ in p-hydroxycinnamyl alcohol
	A _α	72.0	4.85	C _α -H _α in β-O-4 unit
	BE _α	81.3	4.62	C _α -H _α in benzyl ether LCC
	A _β (G/H)	83.9	4.40	C _β -H _β in β-O-4 linked to G/H units
	B _α	85.5	4.66	C _α -H _α in β-β (resinol) substructures
	A _β (S)	86.4	4.10	C _β -H _β in β-O-4 linked to S units
	C _α	87.6	5.45	C _α -H _α in phenylcoumaran substructures
Aromatic region	S _{2,6}	103.9	6.69	C _{2,6} -H _{2,6} in syringyl units
	S' _{2,6}	106.5	7.28	C _{2,6} -H _{2,6} in oxidized (C _α =O) S units
	FA ₂	111.0	7.35	C ₂ -H ₂ in ferulate
	G ₂	111.5	6.99	C ₂ -H ₂ in guaiacyl units
	pCA _β /FA _β	113.9	6.27	C _β -H _β in p-coumarate and ferulate
	G ₅	115.5	6.75	C ₅ -H ₅ in guaiacyl units
	pCA _{3,5}	115.8	6.93	C _{3,5} -H _{3,5} in p-coumarate
	G ₆	118.8	6.81	C ₆ -H ₆ in guaiacyl units
	FA ₆	123.1	7.17	C ₆ -H ₆ in ferulate
	F _β	128.2	6.15	C _β -H _β in p-hydroxycinnamyl alcohol
	F _α	128.2	6.30	C _α -H _α in p-hydroxycinnamyl alcohol
	H _{2,6}	128.5	7.19	C _{2,6} -H _{2,6} in H units
	pCA _{2,6}	130.5	7.48	C _{2,6} -H _{2,6} in p-coumarate
	pCA _α /FA _α	144.8	7.45	C _α -H _α in p-coumarate and ferulate

The correlation δ_C/δ_H 50-90/2.5-5.5 ppm refers to inter-unit linkages and terminal structures in lignin, and also LCC. Important correlations such as those from substructures of β-aryl structures (β-O-4, A), resinol (β-β, B), and phenylcoumaran (β-5, C) can be assigned in this region. The most prominent cross-signals represent OCH₃ groups and side-chains in β-O-4 substructures. C_γ-H_γ correlations in β-O-4 substructures were clearly observed at 59.9/3.4 and 59.9/3.7 ppm, while at 72.0/4.85 ppm it is possible to identify weaker signals that correspond to C_α-H_α correlations. Similarly, C_β-H_β correlations corresponding to β-O-4 structures linked to G, S, and H units were also identified in the spectrum, as well the signals corresponding to C_α-H_α and C_β-H_β correlations of phenylcoumaran (C_α and C_β) and resinol (B_α and B_β) substructures.

In the side-chain region of HSQC spectrum important information about the presence of LCC linkages can also be found. According to the literature (Balakshin et al., 2011; Wen et al., 2012) the corresponding signals of phenyl glycoside and esters linkages can be detected in the 2D NMR spectra of lignins; in the case of benzyl ether LCC structures signals are clearly attributed to: (a) C₁-linkages between the α -position of lignin and primary OH groups of carbohydrates and (b) C₂-linkages between the α -position of lignin and secondary OH groups of carbohydrates. For corn stalks lignin only the signals of C₁-linkages between the α -position of lignin and primary OH groups of carbohydrates (BE α) were identified by a cross-peak at 81.2/4.62 ppm. Moreover, in the side-chain region strong signals from C₂-H₂, C₃-H₃, C₄-H₄, and C₅-H₅ correlations assigned to carbohydrate moieties (X₂, X₃, X₄, and X₅) were also clearly identified at δ_C/δ_H 73.0/3.10, 74.0/3.36, 77.2/3.52, and 63.5/3.15 and 3.90 ppm, respectively (Fernández-Costas et al., 2014; Wen et al., 2012). The referred signals associated to LCC are frequently identified by 2D NMR analysis of lignins, and were already found in annual, hardwood and softwood lignins (Balakshin et al., 2011; del Río et al., 2012; Fernández-Costas et al., 2014; Wen et al., 2012).

The ¹³C-¹H correlations δ_C/δ_H 90-160/6.0-8.0 ppm correspond to the aromatic rings and unsaturated side chains of the H, G, and S lignin units and *p*CA and FA moieties that are associated with the lignin. The S units present a strong signal that corresponds to C_{2,6}-H_{2,6} correlation (S_{2,6}), while G units were identified by different correlation signals for C₂-H₂, C₅-H₅, and C₆-H₆ (G₂, G₅ and G₆, respectively). For H units cross-signals corresponding to C_{2,6}-H_{2,6} were observed (H_{2,6}). In literature it is stated that the signal of H units could be partially overlapped in the spectra by a cross signal at δ_C/δ_H 128.5/7.24 ppm from protein (as lignin contaminant), hindering H assessment (Rencoret et al., 2015; Santos J.I. et al., 2015), which was not the case. Cross-signals corresponding to C_{2,6}-H_{2,6} and C_{3,5}-H_{3,5} correlations of *p*CA aromatic ring were also identified, the later overlapping with G₅ signals from guaiacyl units in corn stalks lignin. The unsaturated C α -H α and C β -H β correlations of *p*CA were also noted in this region and are highly consistent with the reported NMR data for *p*CA units (del Río et al., 2012; Wen et al., 2012). In addition to the signals of *p*CA units, minor signals of FA were also identified. The signals of C₂-H₂ (FA₂) and C₆-H₆ (FA₆) confirm the presence of these moieties, while their signals of unsaturated C α -H α and C β -H β correlations are overlapped with those of *p*CA units.

The overall results from HSQC analysis provided additional information on the interunit linkages as well as about the composition of the isolated lignin from corn stalks lignin, clarifying the presence of contaminants.

4.3.5 ^{31}P NMR

Quantitative ^{31}P NMR analysis of the isolated lignins from stalks of corn, cotton, sugarcane, and tobacco was performed. The ^{31}P NMR spectra of the phosphitylated lignins are shown in Figure 22. Quantification of the different hydroxyl groups is presented in Table 24.

Table 24 - Assignments and quantification of phenolic and aliphatic hydroxyl groups and carboxylic acids in lignins by ^{31}P NMR.

Assignments	amount (mmol/g lignin)			
	LCorn _{stalk}	LCotton _{stalk}	LScane _{stalk}	LTob _{stalk}
Aliphatic OH	3.33	3.40	2.56	4.02
Carboxylic acids	0.06	0.25	0.22	0.19
Total phenolic units	2.73	1.82	2.48	1.60
5-substituted phenolic units	0.72	1.10	0.94	0.93
Non-condensed phenolic units				
G phenolic units	1.93	0.71	1.51	0.67
H phenolic units	0.08	0.01	0.02	0.00

The overall content of phenolic OH in lignins varies between 1.6 and 2.7 mmol/g_{lignin}. Lignins from stalks of corn and sugarcane (LCorn_{stalk} and LScane_{stalk}) showed the highest content of total phenolic OH groups (2.7 and 2.5 mmol/g_{lignin}, respectively) comparatively to cotton and tobacco stalks (1.8 and 1.6 mmol/g_{lignin}, respectively).

The set of signals in the region between 146.0 and 145.5 ppm are associated to carbohydrates (Jääskeläinen et al., 2003). The presence of these signals may explain some of the differences found in the aliphatic hydroxyl group content for the stalks lignins. LTob_{stalk} was found to have the highest content of free aliphatic hydroxyls groups (4 mmol/g_{lignin}) and also of carbohydrates (7 %w/w_{lignin}); this is related with the phosphorylation of hydroxyls of carbohydrates that are quantified by ^{31}P NMR as aliphatic OH groups, as also verified in the literature (Zikeli et al., 2014). Consequently, the aliphatic hydroxyl content is strongly dependent on carbohydrates and for this reason it was not accounted for in the total phenolic OH.

The overall of ^{31}P NMR data reveals that the content of phenolic hydroxyl groups is dependent on the species since significant differences between the OH groups distribution were found in the isolated lignins. The content of OH groups is an important structural parameter in lignins characterization since it affects some lignin applications.

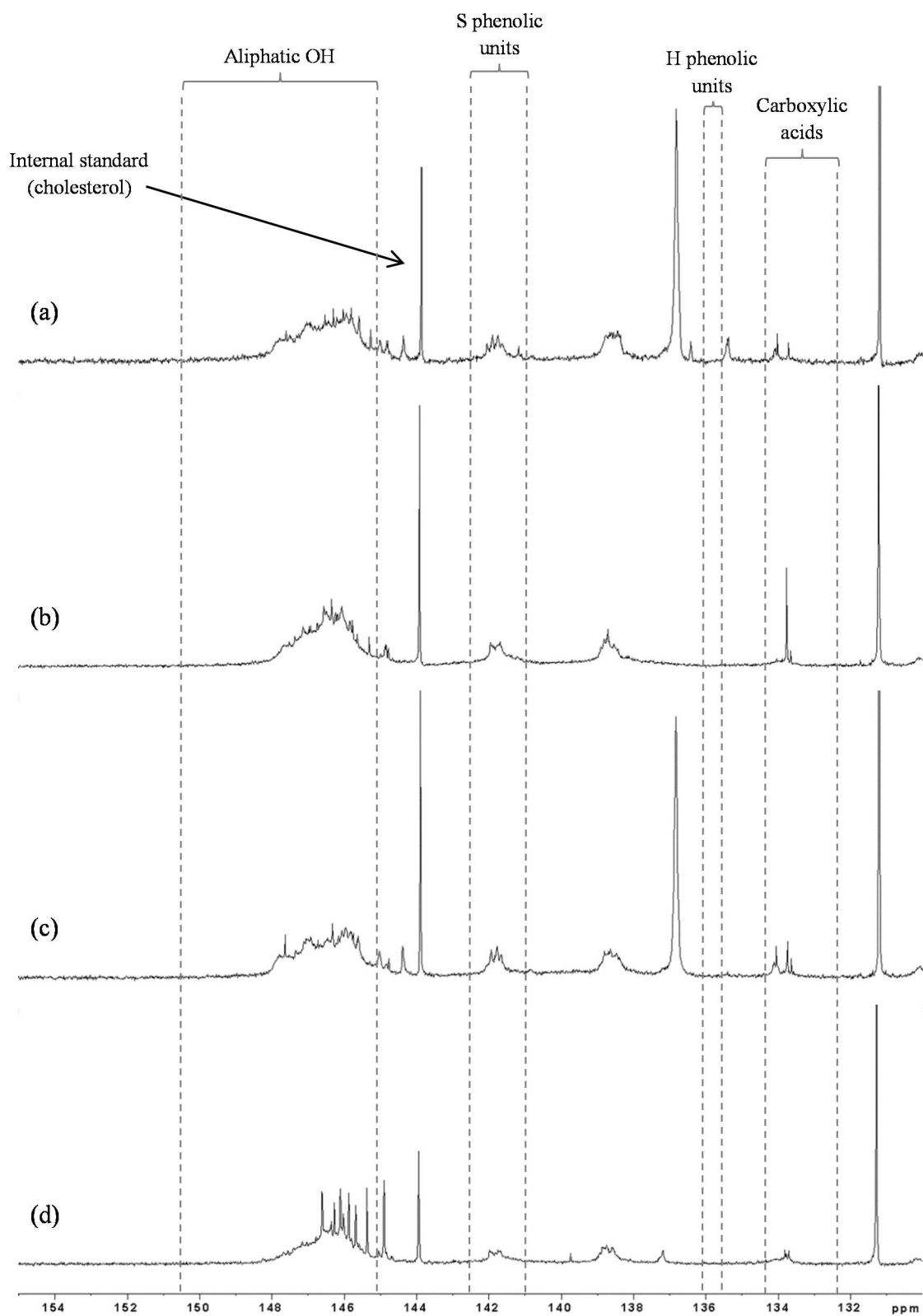


Figure 22 - Quantitative ^{31}P NMR spectra (δ 155-130 ppm) of phosphitylated lignins: (a) LCorn_{stalk}, (b) LCotton_{stalk}, (c) LSCane_{stalk}, and (d) LTob_{stalk} (in CDCl_3).

4.3.6 FTIR

The FTIR spectra of mild acidolysis lignins are presented in Figure 23 for stalks and roots lignins. In FTIR spectra the peak positions of the major absorption bands assigned to the corresponding functional groups were identified according to the literature (Faix, 1991; Hoareau et al., 2004; Monteil-Rivera et al., 2013; Singh et al., 2005).

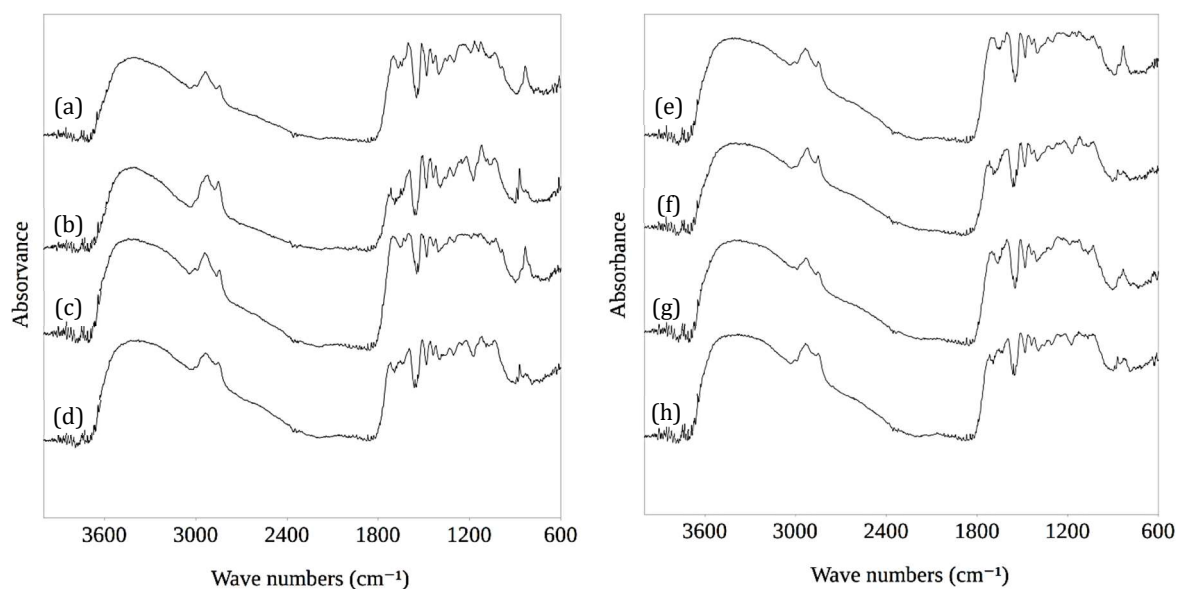


Figure 23 - FTIR absorption spectra of (a) L_{Corn}_{stalk}, (b) L_{Cotton}_{stalk}, (c) L_{SCane}_{stalk}, (d) L_{Tob}_{stalk}, (e) L_{Corn}_{root}, (f) L_{Cotton}_{root}, (g) L_{SCane}_{root}, and (h) L_{Tob}_{root}.

The fingerprint region of lignins is from 700 cm^{-1} to 1600 cm^{-1} while typical stretching of chemical groups was observed at 2800 cm^{-1} to 3500 cm^{-1} . In general, the positions of the absorption bands in all the spectra are rather similar, except for a minor shifting of some peaks. All the spectra present important bands at 1600, 1510 and 1425 cm^{-1} assigned to the aromatic skeletal vibration, which is a fundamental structure of lignin. A dominating peak near to 1125 cm^{-1} is attributed to guaiacyl-syringyl (G-S) lignins (Faix, 1991). S ring absorption is observed at 1330 cm^{-1} , while G ring appears only as a small shoulder at 1260 cm^{-1} . For H units an absorption band is observed at 834 cm^{-1} . The presence of both absorption bands at 1260 and 834 cm^{-1} is typical of S:G:H lignins (Faix, 1991). The bands at 1717 cm^{-1} is attributed to unconjugated C=O stretching (vibration of unconjugated ketones, ester or carboxylic groups), and the band near 1660 cm^{-1} can be assigned to conjugated carbonyl present in typical lignin groups. This latter one is frequently overlapped by a large band at 1657 cm^{-1} attributed to proteins (Duarte et al., 2000; Singh et al., 2005).

In FTIR spectra of L_{Corn}_{stalk}, L_{Corn}_{root}, L_{SCane}_{stalk}, and L_{SCane}_{root} a noticeable interference of proteins was observed in the region near to 1650 cm^{-1} . On the other hand, the residual content of sugars in lignins was also visible in the spectra, revealed by different bands between 1030 and 1150

cm^{-1} (at 1115 and 1030 cm^{-1}), that are assigned to: (1) C–O stretching vibration characteristic of cellulose, hemicellulose, and lignin, and (2) C–O–C ether linkage of the skeletal vibration of both pentose and hexose unit (Santos J.I. et al., 2015; Wen et al., 2012). Furthermore, the band at 900 cm^{-1} originating from the β -glycosidic linkages between the monosaccharide units (Wen et al., 2012) denotes the presence of, at least, oligosaccharides.

Contaminants, such as carbohydrates, could be removed from lignins through a purification process, depending on the conditions; however, as already confirmed in section 4.3.3.1.1, the purification leads to modifications in the representativeness of lignins, invalidating the comparison between them. However, contaminants comprising long-chain aliphatic compounds found in cuticular waxes, cutin, and suberin are more difficult to remove due to its higher resistance, probably due to their strong linkages with lignin (Clemente et al., 2013). This type of associations were already studied by Oliveira and co-workers (Oliveira et al., 2006); the authors have proved that the purification of dioxane lignins from leaf and stalk fractions of a banana plant did not remove all the aliphatic impurities, indicating that they are strongly bonded or even chemically linked to lignin. Considering this, the FTIR spectra of all the lignins contain high amounts of aliphatic moieties of non-lignin origin. These contaminations belong to fatty substances identified from the absorptions at 2940–2830 cm^{-1} , assigned to C–H stretching in aliphatic moieties, and 1700–1710 cm^{-1} , corresponding to C=O stretching of carboxylic acids (Oliveira et al., 2009). This statement was corroborated with the ^{13}C NMR spectra (Figure 17 and Figure 18), which revealed the characteristic resonances between 10 and 35 ppm, assigned to –CH– and –CH₂– moieties in aliphatic chains, as already stated before in section 4.3.4.

4.4 STRUCTURAL CHARACTERIZATION OF TOBACCO LIGNINS

In this section, lignins from stalks of *Nicotiana tabacum* produced by butanol and ethanol organosolv, steam explosion, and mild acidolysis were characterized. Data from ^{13}C NMR and NO led to the main structural features of these lignins for the impact evaluation of each process on lignin structure. This comparative study was performed for the first time.

4.4.1 *N. tabacum* lignins: description and composition

From tobacco stalks, four lignins were considered: lignin produced by organosolv process using butanol (LTobO_{but}) and ethanol (LTobO_{ethan}), lignin produced by a steam explosion process (LTobSE), and another one isolated by mild acidolysis (LTob_{stalk}).

LTobO_{but} was produced by pulping with butanol-water 50/50 v/v, at 451 K, 30-60 min (with H₂SO₄); LTobO_{ethan} was produced in standard autocatalyzed conditions at 468 K for 90 min, and LTobSE was produced at 478 K, 10 min residence time, with 15% caustic loading.

The content of inorganics and carbohydrates of tobacco lignins is depicted in Table 25 as component weight per 100 g of lignin.

Table 25 - Inorganic compounds and carbohydrate contents of lignins.

	lignins			
	LTobO_{but}	LTobO_{ethan}	LTobSE	LTob_{stalk}
Inorganic compounds (%w/w _{lignin})	3.1 ± 0.2	0.38 ± 0.01	1.2 ± 0.06	0.43 ± 0.02
Carbohydrates (%w/w _{lignin})	2.3 ± 0.1	1.1 ± 0.05	0.66 ± 0.02	6.9 ± 0.29

The maximum amount of contaminants measured (inorganics and carbohydrates) in lignins from tobacco stalks is 7.2% for LTobO_{stalk}, which is in agreement with the degree of contamination found for other lignins from herbaceous plants (Buranov and Mazza, 2008; Ghaffar and Fan, 2013).

The content of the main sugar residues found in the carbohydrate fraction of tobacco lignins is detailed in Table 26.

Table 26 - Detailed composition of carbohydrate fraction (%w/w_{lignin}) of tobacco lignins.

	Glc	Xyl	Ara	Gal	Rha	Man
LTobO _{but}	0.79	0.54	0.17	0.12	0.11	0.17
LTobO _{ethan}	0.30	0.40	0.12	0.01	0.09	0.01
LTobSE	0.15	0.25	0.05	0.05	0.06	0.01
LTob _{stalk}	0.43	3.77	0.19	0.20	0.40	0.26

*Glc – glucose; Xyl – xylose; Ara – arabinose; Gal – galactose; Rha – rhamnose; Man - mannose.

The main sugar residue obtained for all the tobacco lignins was xylose, except for LTobO_{but}, followed by glucose. Compared to wood species (softwood and hardwood), lignins from herbaceous plants usually contain higher levels of carbohydrates, due to the presence of LCC (Buranov and Mazza, 2008). Additionally, compared to values found for acidolysis lignins and pulping liquor lignins from hardwoods, presented in this thesis, the overall results are similar.

4.4.2 Analysis by NO

V, Sy, Hy, VA, and SA are the main monomeric phenolics that result from the oxidation of the noncondensed fraction of lignin by NO. The quantification is reported in Table 27.

Table 27 - Yields of monomeric phenolic products obtained by NO of lignins from tobacco stalks.

lignin	products, % w/w _{lignin} *					
	Hy	VA	SA	V	Sy	total yield
LTobO _{but}	0.42	0.88	0.79	2.8	2.5	7.4
LTobO _{ethan}	0.33	0.63	0.47	7.2	4.8	13.5
LTobSE	0.37	0.77	0.26	5.2	3.2	9.8
LTob _{stalk}	0.39	0.71	0.84	12.8	10.9	25.7

* reported to nonvolatile solids weight after deducting ashes and carbohydrates.

V and Sy are the main products, accounting for 72–93% of the total phenolic monomers identified. Minor contents of their corresponding aromatic acids (SA and VA) and Hy were also obtained. The NO yield of lignins follows the sequence LTob_{stalk} > LTobO_{ethan} > LTobSE > LTobO_{but}, indicating that the delignification process, organosolv (in particular with butanol) and steam explosion, have induced an increase in the number of condensed linkages. NO has been one of the approaches for the evaluation of the potential for lignin to produce V and Sy by oxidative depolymerization. In the literature it is suggested that the yield from oxidation with O₂ can reach 50% of the NO yield (Tarabanko et al., 1995), while in other studies with diverse lignins lower relative yields (19–36%) were obtained (Pinto et al., 2011).

4.4.3 ¹³C NMR

The structures, linkages and functional groups of tobacco lignins were assessed by ¹³C NMR based on acquisition conditions and assignments referred in the literature (Capanema et al., 2004; Capanema et al., 2005; Costa et al., 2014). The assignments and the corresponding chemical shifts, as well as the resulting content (number/Ar) are presented in Table 28. The spectra of tobacco lignins with the main assignments identified are shown in Figure 24.

In addition to H units, *p*-coumaric and ferulic esters can be found in lignins of annual plants. However, these phenolic moieties should not represent a noteworthy interference on ¹³C NMR spectra (Heitner et al., 2010) due to the usually low percentage in lignins (Rencoret et al., 2015), in particular, in those resulting from extensive delignification processes due to the cleavage of the ester linkages. For tobacco stalks lignins, no information about the content of this structure has been reported in the literature. In the delignification process resulting from organosolv and steam

explosion, this ether linkage is cleaved, liberating phenolic and aliphatic OH groups, improving the lignin solubility in the medium. The extent of the cleavage depends on the process and conditions.

Table 28 - Assignments and quantification (number per aromatic ring) of the structures/linkages and functional groups identified by ^{13}C NMR for tobacco lignins.

assignments (spectroscopic range)	amount (number/Ar)			
	LTobO _{but}	LTobO _{ethan}	LTobSE	LTob _{stalk}
C _β in β-5 and β-β structures (δ 51.0-53.8 ppm)	0.29	0.19	0.23	0.20
Aromatic OCH ₃ (δ 54.3-57.3 ppm)	0.91	0.97	0.84	1.31
C _γ in β-O-4 structures without C _α =O (δ 59.3-60.8 ppm)	0.31	0.26	0.19	0.34
C _γ in β-5 and β-O-4 structures with C _α =O; C _γ in β-1 (δ 62.5-63.8 ppm)	0.20	0.11	0.11	0.15
C _α in β-O-4 structures; C _γ in pinoresinol/syringaresinol and β-β structures (δ 70.0-76.0 ppm)	0.53	0.44	0.53	1.04
C _β in β-O-4 structures; C _α in β-5 and β-β structures (δ 80.0-90.0 ppm)	0.45	0.51	0.65	0.91
Aromatic C _{Ar} -H (δ 103.0-123.0 ppm)	1.93	2.07	1.99	2.04
Aromatic C _{Ar} -C (δ 123.0-137.0 ppm)	1.67	1.74	1.82	1.44
C ₄ in H units (δ 157.0-162.0 ppm)	0.16	0.13	0.18	0.15
CHO in benzaldehyde structures (δ 191.0-192.0 ppm)	0.05	0.06	0.06	0.03
CHO in cinnamaldehyde structures (δ 193.5-194.5 ppm)	0.05	0.07	0.07	0.03

The values for β-O-4 structures are 0.16, 0.32, 0.42, and 0.71 for LTobO_{but}, LTobO_{ethan}, LTobSE, and LTob_{stalk}, respectively (results summarized in Table 28). The considerably lower amount of β-O-4 structures in lignins resulting from organosolv and steam explosion processes compared to lignin from mild acidolysis is the result of the extensive depolymerization in the formers. The β-O-4 cleavage was also reported in the literature (Agrupis et al., 2000; Xu et al., 2008) as result of other processes, such as kraft delignification of perennial grasses (Pinto et al., 2015). Organosolv process with butanol of tobacco stalks has led to a lignin with the lowest content of β-O-4 structures. Other frequent carbon-carbon linkages, such as β-5, found in phenylcoumarans, and β-β, found in resins, depicted in Table 28, were also found in high amounts in tobacco lignins, compared to lignins from other species (Pinto et al., 2015).

Another observation can be drawn from the NMR data: processing induces changes in methoxyl content (decrease from LTob_{stalk} to LTobO_{but}, being more accentuated for LTobSE) mainly due to demethoxylation reactions but also due to degradation of S units and/or topochemical effects of delignification. The lower methoxyl content found in processed lignins (organosolv and steam explosion) due to the demethoxylation reactions was already noticed by other authors (Li et al., 2009; Sun et al., 2004; Wen et al., 2013). This could be pointed out as one of the reasons for the

lower value of methoxyl found by ^{13}C NMR (δ 54.3-57.3 ppm) than the methoxyl content calculated from the S:G:H ratio.

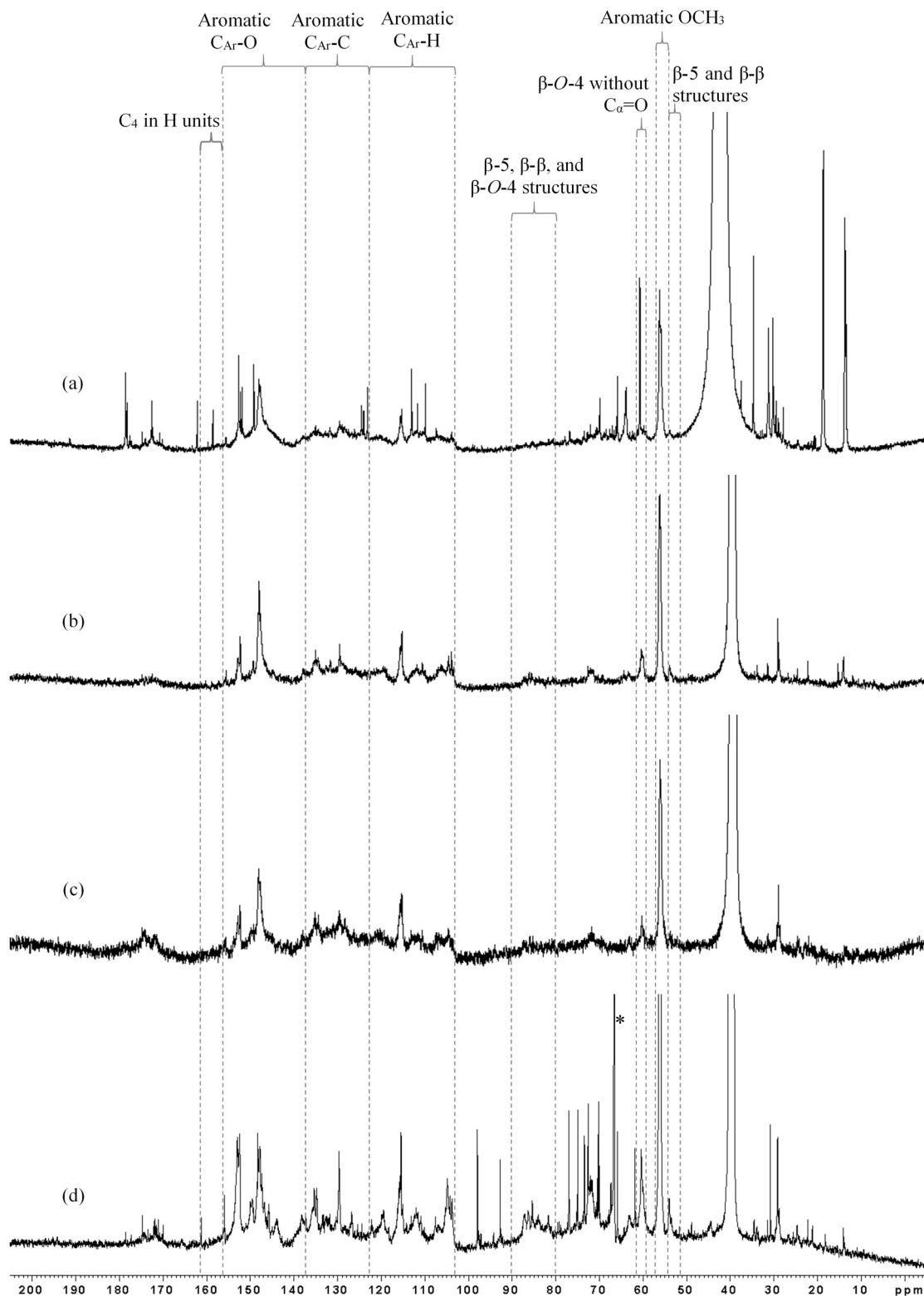


Figure 24 - Quantitative ^{13}C NMR spectra of (a) LTobO_{but}, (b) LTobO_{ethan}, (c) LTobSE, and (d) LTob_{stalk} (DMSO- d_6 ; * solvent peak (Hugo et al., 1997)).

4.5 RADAR CLASSIFICATION OF INDUSTRIAL CROPS LIGNINS

The proposed methodology for radar classification was applied to industrial crops lignins. Radar representation allows a direct classification of the different stalks and roots lignins by comparison of their key descriptors.

The selected parameters as descriptors for radar classification of corn, cotton, sugarcane, and tobacco lignins are depicted in Table 29 and presented as radar plots in Figure 25 and Figure 26 for stalks and roots, respectively. The selected parameters were β -O-4 linkages content, the number of NCS, the content of S, G, and H units, and the yield of V and Sy (obtained by NO).

Table 29 - Main structural characteristics of lignins from stalks and roots of tobacco, corn, cotton, and sugarcane.

Lignin		β -O-4 structures (n/100Ar)	NCS (n/100ppu)	S:G:H	S/G
LCorn	stalk	30	92	43:44:13	0.96
	root	22	84	41:51:08	0.79
LCotton	stalk	44	92	49:45:06	1.09
	root	23	87	50:43:07	1.17
LSCane	stalk	29	86	41:51:08	0.81
	root	19	85	27:59:14	0.46
LTob	stalk	53	73	37:46:17	0.80
	root	45	77	34:49:17	0.69

Herbaceous plants usually present higher contents of H units than woody materials (Pinto et al., 2015), which is in accordance with the S:G:H ratio found for isolated lignins from corn, cotton, sugarcane, and tobacco (Table 29). However, the content of V and Sy precursors in herbaceous lignins are naturally lower in comparison to woody biomasses.

α - and β -ether linkages are one of the most important linkages type in lignin structure, which are mostly preserved in the isolation by acidolysis lignins. LCotton_{stalk}, LTob_{stalk} and LTob_{root} have the highest content of β -O-4 linkages; at the same time, LTob_{stalk} and LTob_{root} have the highest values of DC (lowest NCS). These two characteristics together, point out LTob_{stalk} and LTob_{root} as lignins having high frequency of inter-linkages between ppu thus revealing a complex tridimensional structure.

The S:G:H ratios calculated for the different lignins indicated a predominance of G over S units for roots and stalks of corn, sugarcane and tobacco, with a S/G ratio in the range of 0.44-0.90 (Table 29). For cotton lignins higher values of S than G units were found. Among all, LTob_{root} and LSCane_{root} have the most favorable S/G considering vanillin production in a possible valorization route, i.e. for these lignins a higher content of G units than S units was found (Figure 26).

The main differences between lignins isolated from stalks and roots of each species are the lower content of β -aryl structures (β -O-4) and, in general, the lower S/G ratio in the later. For LSCane and LToB the DC is similar for roots and for stalks but in the case of LCorn and LCotton there a change on the frequency of condensed linkages. The differences found between species exceeded the differences between lignins from the two morphologic parts of the same plant, confirming the lignin specificity of each species, but there is high similarity between corn and sugarcane lignins.

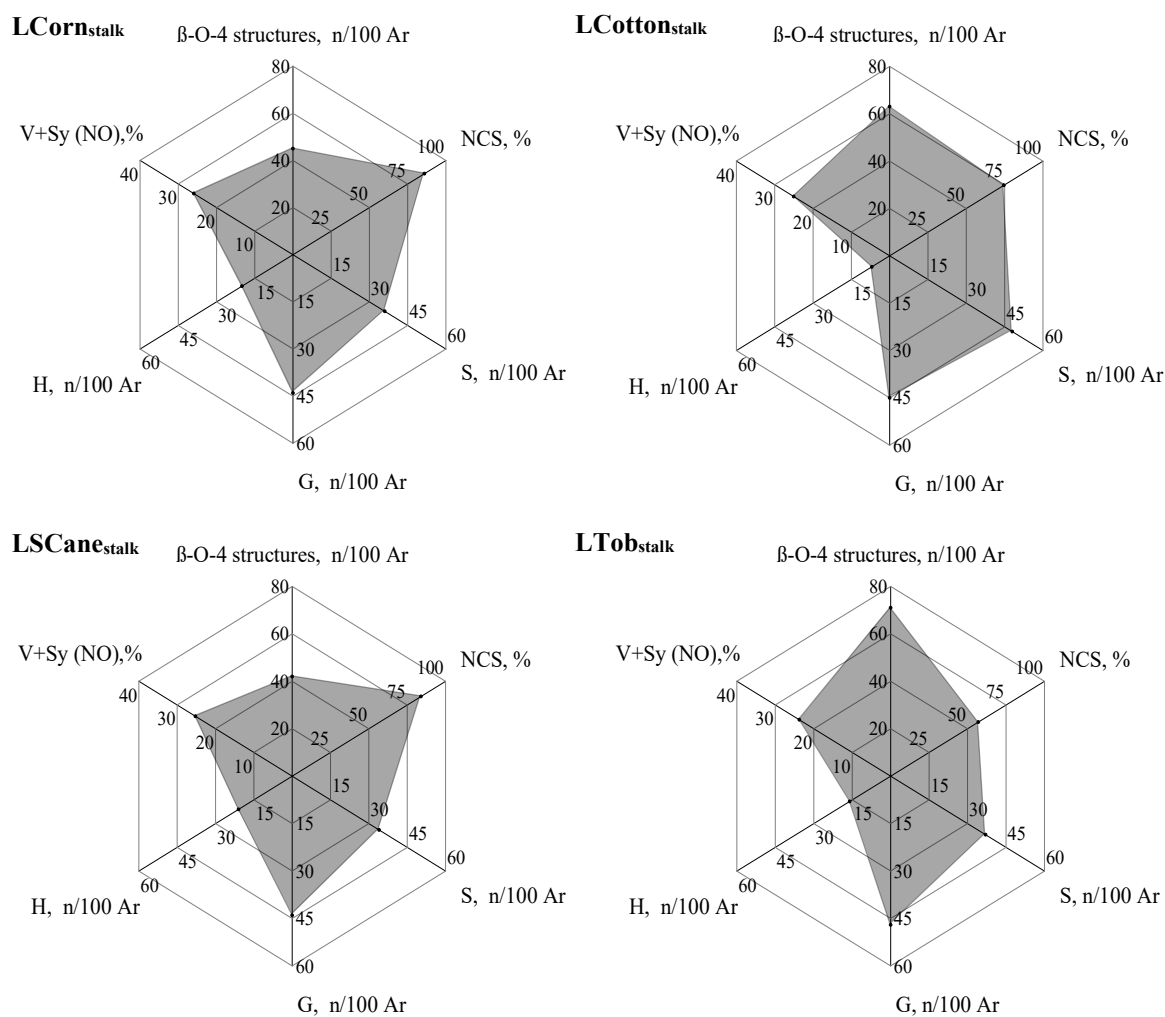


Figure 25 - Radar classification for stalks lignins from corn, cotton, sugarcane, and tobacco.

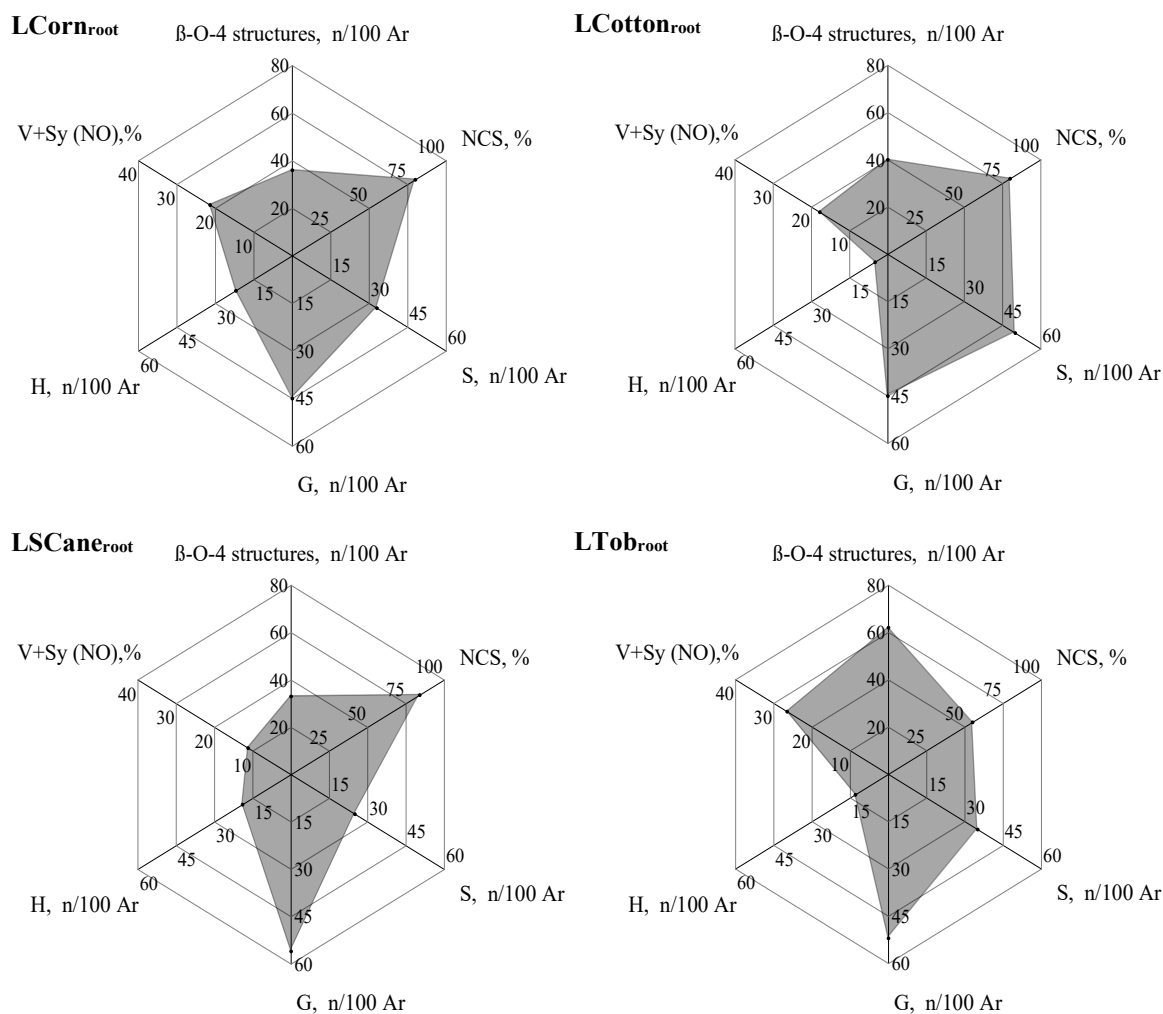


Figure 26 - Radar classification for roots lignins from corn, cotton, sugarcane, and tobacco.

4.6 RADAR CLASSIFICATION OF TOBACCO LIGNINS

The values of all the parameters for tobacco lignins are depicted in Table 30 and presented as radar plots in Figure 27. This representation allows a direct classification of tobacco lignins by comparison of the key descriptors.

Table 30 - Main structural characteristics of tobacco lignins.

Lignin	β -O-4 structures (n/100Ar)	NCS (n/100ppu)	S:G:H	S/G
LTobO _{but}	16	45	38:48:18	0.79
LTob _{ethan}	32	58	38:49:13	0.77
LTobSE	42	49	31:50:19	0.62

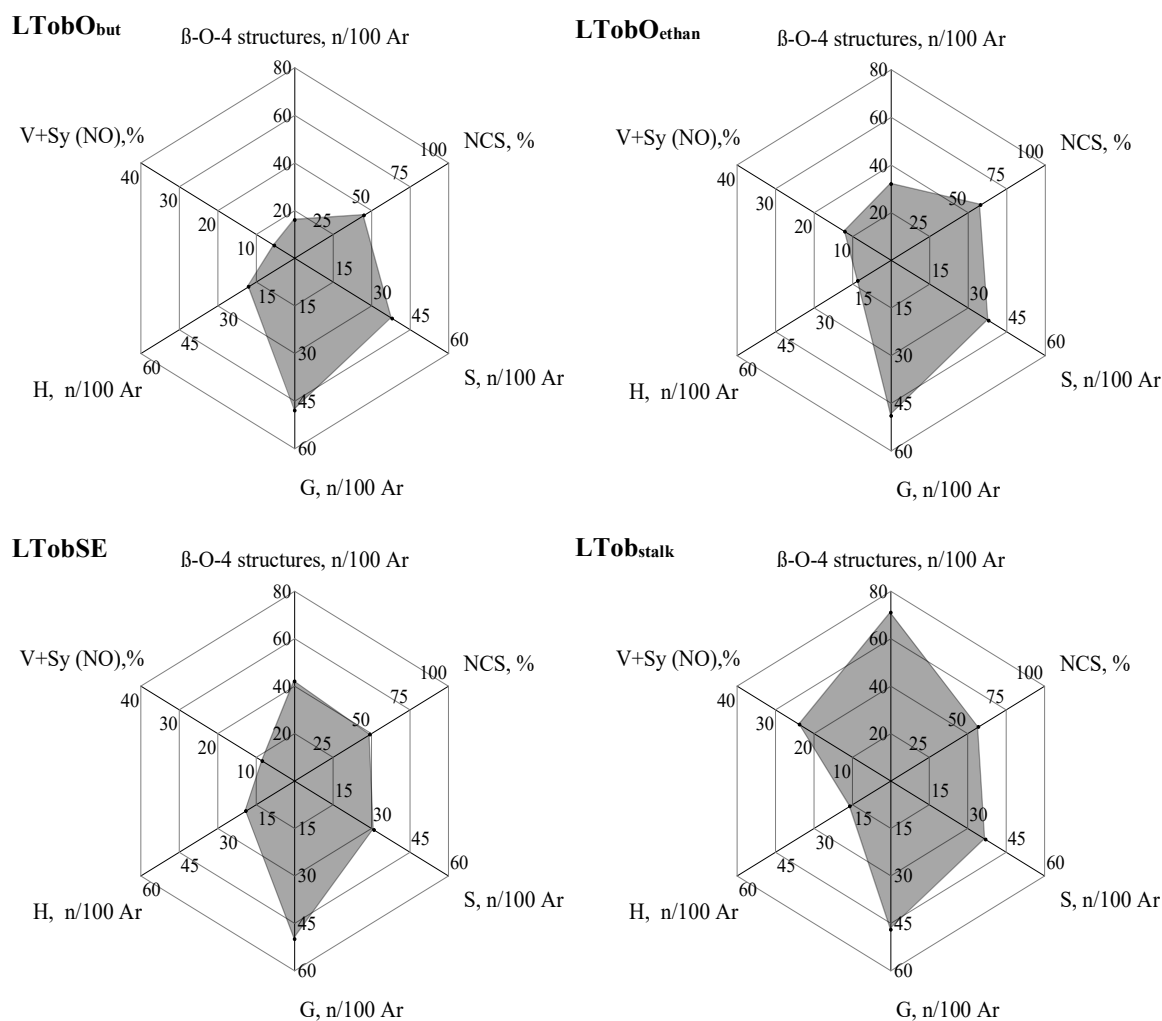


Figure 27 - Radar classification for tobacco lignins produced by different processes.

The area defined by β -O-4 and NCS in each radar plot provides the first illustration of the amount of lignin degradation effected by processing as compared with lignin isolated by mild acidolysis. The radar plots demonstrate that **LTobO_{but}** is the lignin with the lowest area of the triangle defined by triangle Δ and, as such, is the most transformed lignin. These observations and the low values of Sy and V (produced by NO) suggest that this lignin is the one with the lowest potential as a source of V and Sy by alkaline oxidation by O_2 . The representation of G and S as axes of radar plots is particularly relevant when comparing lignins from different origins due to natural variation among species (higher variation than for the same lignin produced by different processes). In these cases, it is more difficult to classify and evaluate the lignins. The descriptors G and S reveal two levels of impact on lignin: (1) different reactivity of S and G could impart different ability for Sy and V production for the same triangle Δ , (2) β -O-4 and NCS could be unevenly distributed between G and S units. This is the particular case of G units which are more prone to condensation, and therefore, V production is unfavorable in comparison to Sy. As a result, the information imparted by triangle Δ should be complemented by the S and G content and the Sy

and V data resulting from NO. Among the tobacco lignins, S and G did not show noteworthy differences. However, Sy and V descriptors showed that LTobO_{but} is the least reactive lignin, followed by LTobSE.

Among all the tobacco stalks lignins, the lowest value of NCS was found for LTobO_{but} (Table 30), followed by LTobSE, and finally LTobO_{ethan}, which presented a similar value to that of mild acidolysis lignin. This observation has led to the conclusion that organosolv process with ethanol was the industrial process imparting fewer modifications to tobacco stalks lignin.

In this study, the ranking of lignins was performed using constant weighting factors for each descriptor. As such, and based on the classification, the ascending order of lignins according to the prospective yield for V and Sy by oxidation with O₂ in alkaline medium under the same conditions (pH, temperature, O₂ partial pressure) is LTobO_{but} < LTobSE < LTobO_{ethan} < LTob_{stalk}.

4.7 CONCLUSIONS

The characterization of *in situ* and mild acidolysis lignins from two morphological parts (stalks and roots) of corn, cotton, sugarcane, and tobacco shows that the differences found between species exceeded the differences between morphological parts confirming the lignin specificity of each species.

LCorn_{stalk} and LSCane_{stalk} are the closest lignins, having similar frequency of β-aryl inter linkages (the lowest among all stalks lignin, 30/100Ar, 29/100Ar). These two lignins also present the highest content of phenolic hydroxyl groups, in particular in non-condensed G units (2.7 and 2.5 mmol/g_{lignin}, respectively) comparatively to cotton and tobacco stalks (1.8 and 1.6 mmol/g_{lignin}, respectively). Among all the lignins, LTob_{root} and LSCane_{root} have the most favorable S/G considering vanillin production in a possible valorization route.

The structural data obtained for tobacco lignins demonstrated once again the effect of processing evidenced by the drastic changes induced in the lignin structure by organosolv pulping with butanol, ranking this lignins as the less promising for the production of V and Sy by oxidation with O₂ in alkaline medium.

Data generated in this study is an important tool for the design of processes to convert these agro-industrial waste materials into lignin-based high added-value products. Moreover, the understanding of agricultural crops will contribute to the diversification of the biomass feedstock supply for bio-based products and for the design of effective deconstruction strategies for biorefinery purposes.

4.8 REFERENCES

- Abdelkafi, F., Ammar, H., Rousseau, B., Tessier, M., El Gharbi, R., Fradet, A. Structural analysis of Alfa grass (*Stipa tenacissima* L.) lignin obtained by acetic acid/formic acid delignification. *Biomacromolecules* 2011, 12, 3895-3902.
- Agrupis, S., Maekawa, E., Suzuki, K. Industrial utilization of tobacco stalks II: Preparation and characterization of tobacco pulp by steam explosion pulping. *J. Wood Sci.* 2000, 46, 222-229.
- Azadi, P., Inderwildi, O.R., Farnood, R., King, D.A. Liquid fuels, hydrogen and chemicals from lignin: A critical review. *Renew. Sust. Energ. Rev.* 2013, 21, 506-523.
- Balakshin, M., Capanema, E., Gracz, H., Chang, H.m., Jameel, H. Quantification of lignin-carbohydrate linkages with high-resolution NMR spectroscopy. *Planta* 2011, 233, 1097-1110.
- Balakshin, M.Y., Capanema, E.A. Comprehensive structural analysis of biorefinery lignins with a quantitative ^{13}C NMR approach. *RSC Advances* 2015, 5, 87187-87199.
- Balakshin, M.Y., Capanema, E.A., Santos, R.B., Chang, H., Jameel, H. Structural analysis of hardwood native lignins by quantitative ^{13}C NMR spectroscopy. *Holzforschung* 2015, 70, 95-108.
- Bernards, M.A. Demystifying suberin. *Canadian Journal of Botany* 2002, 80, 227-240.
- Buranov, A.U., Mazza, G. Lignin in straw of herbaceous crops. *Ind. Crop. Prod.* 2008, 28, 237-259.
- Buranov, A.U., Ross, K.A., Mazza, G. Isolation and characterization of lignins extracted from flax shives using pressurized aqueous ethanol. *Bioresour. Technol.* 2010, 101, 7446-7455.
- Capanema, E.A., Balakshin, M.Y., Kadla, J.F. A comprehensive approach for quantitative lignin characterization by NMR spectroscopy. *J. Agric. Food. Chem.* 2004, 52, 1850-1860.
- Capanema, E.A., Balakshin, M.Y., Kadla, J.F. Quantitative characterization of a hardwood milled wood lignin by nuclear magnetic resonance spectroscopy. *J. Agric. Food. Chem.* 2005, 53, 9639-9649.
- Clemente, J.S., Simpson, M.J., Simpson, A.J., Yanni, S.F., Whalen, J.K. Comparison of soil organic matter composition after incubation with maize leaves, roots, and stems. *Geoderma* 2013, 192, 86-96.

- Costa, C.A.E., Pinto, P.C.R., Rodrigues, A.E. Evaluation of chemical processing impact on *E. globulus* wood lignin and comparison with bark lignin. *Ind. Crop. Prod.* 2014, 61, 479-491.
- Costa, C.A.E., Pinto, P.C.R., Rodrigues, A.E. Radar tool for lignin classification on the perspective of its valorization. *Ind. Eng. Chem. Res.* 2015, 54, 7580-7590.
- del Río, J.C., Rencoret, J., Prinsen, P., Martínez, Á.T., Ralph, J., Gutiérrez, A. Structural characterization of wheat straw lignin as revealed by analytical pyrolysis, 2D-NMR, and reductive cleavage methods. *J. Agric. Food. Chem.* 2012, 60, 5922-5935.
- Duarte, A.P., Robert, D., Lachenal, D. *Eucalyptus globulus* kraft pulp residual lignins. Part 1. Effects of extraction methods upon lignin structure. *Holzforschung* 2000, 54, 365-372.
- Faix, O. Classification of lignins from different botanical origins by FT-IR spectroscopy. *Holzforschung* 1991, 45, 21-27.
- Fernández-Costas, C., Gouveia, S., Sanromán, M.A., Moldes, D. Structural characterization of Kraft lignins from different spent cooking liquors by 1D and 2D Nuclear Magnetic Resonance spectroscopy. *Biomass Bioenergy* 2014, 63, 156-166.
- Ghaffar, S.H., Fan, M. Structural analysis for lignin characteristics in biomass straw. *Biomass Bioenergy* 2013, 57, 264-279.
- Guimarães, J.L., Frollini, E., Silva, C.G., Wypych, F., Satyanarayana, K.G. Characterization of banana, sugarcane bagasse and sponge gourd fibers of Brazil. *Ind. Crop. Prod.* 2009, 30, 407-415.
- Hatfield, R.D., Ralph, J., Grabber, J.H. Cell wall cross-linking by ferulates and diferulates in grasses. *J. Sci. Food Agric.* 1999, 79, 403-407.
- Heitner, C., Dimmel, D., Schmidt, J. *Lignin and Lignans: Advances in Chemistry*; Taylor & Francis, 2010.
- Hoareau, W., Trindade, W.G., Siegmund, B., Castellan, A., Frollini, E. Sugar cane bagasse and curaua lignins oxidized by chlorine dioxide and reacted with furfuryl alcohol: characterization and stability. *Polym. Degrad. Stab.* 2004, 86, 567-576.
- Hugo, E.G., Vadim, K., Abraham, N. NMR chemical shifts of common laboratory solvents as trace impurities. *J. Org. Chem.* 1997, 62, 7512-7515.

- Jääskeläinen, A.S., Sun, Y., Argyropoulos, D.S., Tamminen, T., Hortling, B. The effect of isolation method on the chemical structure of residual lignin. *Wood Sci. Technol.* 2003, 37, 91-102.
- Kaparaju, P., Felby, C. Characterization of lignin during oxidative and hydrothermal pre-treatment processes of wheat straw and corn stover. *Bioresour. Technol.* 2010, 101, 3175-3181.
- Kleinert, M., Barth, T. Towards a lignin-cellulosic biorefinery: Direct one-step conversion of lignin to hydrogen-enriched biofuel. *Energ. Fuel* 2008, 22, 1371-1379.
- Li, J., Gellerstedt, G., Toven, K. Steam explosion lignins; their extraction, structure and potential as feedstock for biodiesel and chemicals. *Bioresour. Technol.* 2009, 100, 2556-2561.
- Lin, S.Y., Dence, C.W. *Methods in lignin chemistry*; Springer-Verlag, 1992.
- Maziero, P., Neto, M.d.O., Machado, D., Batista, T., Cavalheiro, C.C.S., Neumann, M.G., Craievich, A.F., Rocha, G.J.d.M., Polikarpov, I., Gonçalves, A.R. Structural features of lignin obtained at different alkaline oxidation conditions from sugarcane bagasse. *Ind. Crop. Prod.* 2012, 35, 61-69.
- Monteil-Rivera, F., Phuong, M., Ye, M., Halasz, A., Hawari, J. Isolation and characterization of herbaceous lignins for applications in biomaterials. *Ind. Crop. Prod.* 2013, 41, 356-364.
- Nishimura, N., Izumi, A., Kuroda, K. Structural characterization of kenaf lignin: Differences among kenaf varieties. *Ind. Crop. Prod.* 2002, 15, 115-122.
- Oliveira, L., Evtuguin, D., Cordeiro, N., Silvestre, A.J.D. Structural characterization of stalk lignin from banana plant. *Ind. Crop. Prod.* 2009, 29, 86-95.
- Oliveira, L., Evtuguin, D.V., Cordeiro, N., Silvestre, A.J.D., Silva, A.M.S., Torres, I.C. Structural characterization of lignin from leaf sheaths of “dwarf cavendish” banana plant. *J. Agric. Food. Chem.* 2006, 54, 2598-2605.
- Pinto, P.C., Borges da Silva, E.A., Rodrigues, A.E. Insights into oxidative conversion of lignin to high-added-value phenolic aldehydes. *Ind. Eng. Chem. Res.* 2011, 50, 741-748.
- Pinto, P.C., Evtuguin, D.V., Neto, C.P., Silvestre, A.J.D., Amado, F.M.L. Behavior of *Eucalyptus globulus* lignin during kraft pulping II. Analysis by NMR, ESI/MS and GPC. *J. Wood Chem. Technol.* 2002, 22, 109 - 125.

- Pinto, P.C.R., Oliveira, C., Costa, C.A., Gaspar, A., Faria, T., Ataíde, J., Rodrigues, A.E. Kraft delignification of energy crops in view of pulp production and lignin valorization. *Ind. Crop. Prod.* 2015, 71, 153-162.
- Ragauskas, A.J., Beckham, G.T., Biddy, M.J., Chandra, R., Chen, F., Davis, M.F., Davison, B.H., Dixon, R.A., Gilna, P., Keller, M., Langan, P., Naskar, A.K., Saddler, J.N., Tschaplinski, T.J., Tuskan, G.A., Wyman, C.E. Lignin valorization: Improving lignin processing in the biorefinery. *Science* 2014, 344, 1246843.
- Rencoret, J., Prinsen, P., Gutiérrez, A., Martínez, Á.T., del Río, J.C. Isolation and structural characterization of the milled wood lignin, dioxane lignin, and cellulolytic lignin preparations from brewer's spent grain. *J. Agric. Food. Chem.* 2015, 63, 603-613.
- Robert, D. 1992. Carbon-13 Nuclear Magnetic Resonance Spectrometry. in: *Methods in Lignin Chemistry*, (Eds.) S.Y. Lin, C.W. Dence, Springer Berlin Heidelberg. Berlin, Heidelberg, pp. 250-273.
- Ross, K., Mazza, G. Characteristics of lignin from flax shives as affected by extraction conditions. *International Journal of Molecular Sciences* 2010, 11, 4035-4050.
- Salanti, A., Zoia, L., Orlandi, M., Zanini, F., Elegir, G. Structural characterization and antioxidant activity evaluation of lignins from rice husk. *J. Agric. Food. Chem.* 2010, 58, 10049-10055.
- Saliba, E.O.S., Rodriguez, N.M., Pilo-Veloso, D., Morais, S.A.L. Chemical characterization of the lignins of corn and soybean agricultural residues. *Arq. Bras. Med. Vet. Zootec.* 2002, 54, 42-51.
- Santos J.I., Martín-Sampedro, R., Fillat, Ú., Oliva, J.M., Negro, M.J., Ballesteros, M., Eugenio, M.E., Ibarra, D. Evaluating lignin-rich residues from biochemical ethanol production of wheat straw and olive tree pruning by FTIR and 2D-NMR. *Int. J. Polym. Sci.* 2015, 2015, 1-11.
- Singh, R., Singh, S., Trimukhe, K.D., Pandare, K.V., Bastawade, K.B., Gokhale, D.V., Varma, A.J. Lignin-carbohydrate complexes from sugarcane bagasse: Preparation, purification, and characterization. *Carbohydr. Polym.* 2005, 62, 57-66.
- Sun, X.F., Xu, F., Sun, R.C., Wang, Y.X., Fowler, P., Baird, M.S. Characteristics of degraded lignins obtained from steam exploded wheat straw. *Polym. Degrad. Stab.* 2004, 86, 245-256.

- Tarabanko, V.E., Fomova, N.A., Kuznetsov, B.N., Ivanchenko, N.M., Kudryashev, A.V. On the mechanism of vanillin formation in the catalytic oxidation of lignin with oxygen. *React. Kinet. Catal. Lett.* 1995, 55, 161-170.
- Wen, J.L., Sun, S.L., Yuan, T.Q., Xu, F., Sun, R.C. Structural elucidation of lignin polymers of *Eucalyptus* chips during organosolv pretreatment and extended delignification. *J. Agric. Food. Chem.* 2013, 61, 11067-11075.
- Wen, J.L., Xue, B.L., Xu, F., Sun, R.C. Unveiling the structural heterogeneity of bamboo lignin by in situ HSQC NMR technique. *Bioenerg. Res.* 2012, 5, 886-903.
- Xiao, B., Sun, X.F., Sun, R. Chemical, structural, and thermal characterizations of alkali-soluble lignins and hemicelluloses, and cellulose from maize stems, rye straw, and rice straw. *Polym. Degrad. Stab.* 2001, 74, 307-319.
- Xu, F., Sun, R.C., Zhai, M.Z., Sun, J.X., Jiang, J.X., Zhao, G.J. Comparative study of three lignin fractions isolated from mild ball-milled *Tamarix austromogoliac* and *Caragana sepium*. *J. Appl. Polym. Sci.* 2008, 108, 1158-1168.
- Zikeli, F., Ters, T., Fackler, K., Srebotnik, E., Li, J. Successive and quantitative fractionation and extensive structural characterization of lignin from wheat straw. *Ind. Crop. Prod.* 2014, 61, 249-257.

5 Lignins oxidation in alkaline medium

Lignin is one of the main components of pulping liquors and a potential source of high-added value chemicals. One of the aims of this chapter is to evaluate the potential of industrial *Eucalyptus globulus* sulfite liquor and kraft liquors (collected at different stages of processing before the recovery boiler) for the production of V and Sy by oxidation with O₂ in alkaline medium. Oxidations were performed in a jacketed reactor with controlled temperature and pressure by direct reaction of pulping liquors and reaction of kraft lignins isolated from liquors.

An ethanol organosolv lignin from tobacco stalks was also submitted to oxidation and the effect of the reaction conditions (initial lignin concentration, temperature and partial pressure of O₂) was studied in order to achieve the best conditions to reach the maximum yields of phenolic monomers. The kinetic study of products formation from this lignin was also performed and the results led to the evaluation of its potential as source of V and Sy.

The experimental validation of the radar classification developed previously is also an objective of this chapter. Butanol and ethanol organosolv lignins from tobacco stalks were depolymerized by oxidation with O₂ in alkaline medium and the results allow validating the assumptions from radar classification.

This chapter is based on the following publication:

- Pinto, P.C.R.; Costa, C.E.; Rodrigues, A.E. Oxidation of lignin from *Eucalyptus globulus* pulping liquors to produce syringaldehyde and vanillin. Ind. Eng. Chem. Res. 2013, 52, 4421-4428.

5.1 INTRODUCTION

The aim of the pulping processes is to delignify the wood matrix by promoting the lignin dissolution in pulping liquor, liberating the cellulose and a fraction of the original hemicelluloses. The world dominant process to produce pulp for papermaking is kraft pulping, whereas the sulfite process accounts for about 5% of the world chemical pulp production (Sixta et al., 2008). Acid sulfite pulping of *Eucalyptus globulus* wood has significance in South Africa, Portugal, and Spain for production of total chlorine free bleached dissolving pulps and pulps for papermaking.

Pulping operations are highly integrated and dependent on pulping liquor, which is concentrated and burned in the recovery boiler, supplying energy to the pulp mill operations with simultaneously recovery of pulping chemicals (Krotschek and Sixta, 2008). In some mills, part of liquor/lignin produced is diverted to increase the pulp production capacity (situations where recovery furnace is limited) or to upgrade its organic components, mainly lignin. The largest volume of lignin produced worldwide comes from wood pulping; the lignin generated is known as lignosulfonates or as kraft lignin depending on the process used, sulfite or kraft pulping, respectively. Moreover, the emerging biorefining activity is also producing side streams containing lignin that claims for valorization due to environmental and economic issues.

The aim of the work presented in this section is to contribute to the evaluation of the potential of *E. globulus* lignin as source of Sy and V. Lignins from two pulping processes (kraft and sulfite), three kraft liquor processing stages (at the outlet of digester, after evaporation and after heat treatment), and isolated kraft lignins are studied by oxidation with O₂ in alkaline medium. For each, the profiles of Sy, V, and other minor products are established, as well as the yields, selectivity, time to maximum, temperature profile, and oxygen uptake during the reaction.

5.2 EXPERIMENTAL SECTION: MATERIALS AND METHODS

5.2.1 Sulfite and kraft liquors and lignins: description

Liquors from two pulping processes (kraft and sulfite), three kraft liquor processing stages (at the outlet of digester, after evaporation and after heat treatment) and the isolated lignins from kraft liquors are studied by oxidation with O₂ in alkaline medium

Eucalyptus globulus kraft liquors were collected at different stages of a Portuguese bleached kraft pulp plant: at the outlet of kraft digester (thin kraft liquor, hereby referred as KL, dry solids, 21.6% w/w_{liquor}), after the evaporation stage (EKL, dry solids, 79.4% w/w_{liquor}), and after heat treatment (HTKL, dry solids, 83.9% w/w_{liquor}), just before the recovery furnace. Industrial spent liquor from magnesium-based acidic sulfite pulping of *E. globulus* was collected after the

evaporation step in a Portuguese sulfite pulp mill and it is hereby referred as sulfite liquor (SL, dry solids, 68.0% w/w_{liquor}).

5.2.2 Lignins isolation

Kraft lignins were isolated from respective liquors by slow acidification with 5 M H₂SO₄ (95-97%), until pH 5. The mixture was maintained under agitation at low temperature (283 K) during acidification. The precipitated lignin was recovered by centrifugation, washed two times with distilled water, and freeze-dried.

Lignins isolated from kraft liquors were designated as KLLig, EKLLig, and HTKLLig. The yields on lignin recovered from this isolation procedure were 45% for KLLig, 24% for EKLLig, and 16% for HTKLLig, calculated with reference to the total dissolved solids on the respective liquors.

5.2.3 Characterization of pulping liquors and lignins

5.2.3.1 Total dissolved solids and ash content

For the determination of total dissolved solids (TDS) 20.0 mL of KL was added to prior dried crucibles containing calcinated and sieved sand. For the other pulping liquors, a weighted portion of liquor was diluted with water to 20.00 mL. The solution was added to crucibles with sand as described for KL. The dilution with water was performed for the high viscous liquors (EKL, HTEKL, and SL) to ensure the wetting of the sand by the liquid avoiding projection of the material during the heating period and consequent losses. The crucibles with liquors were dried at 105 °C to constant weight. After that, the crucibles were submitted to incineration at 550 °C for 8 h for ash quantification.

Ashes of isolated lignins were also gravimetrically quantified as already described in section 3.2.4.1 (Chapter 3).

5.2.3.2 Carbohydrate content

For carbohydrate content analysis, freeze-dried sulfite and kraft liquors, and isolated lignins were submitted to acid methanolysis as previously described in section 3.2.4.2 (experimental section of Chapter 3).

5.2.3.3 Nitrobenzene oxidation

Freeze-dried pulping liquors and isolated lignins were submitted to alkaline NO as already described in section 3.2.5.1 (Chapter 3) concerning reaction conditions and products analysis.

5.2.4 Oxidation experiments

Oxidations with O₂ in alkaline medium were performed in a Büchi AG laboratory autoclave with a capacity of 1 L (model BEP280 type II, Switzerland). The heating and control of the reactor temperature was assured by a Haake thermostatic bath (model N2-B, Karlsruhe, Germany). The temperature inside the reactor was measured using thermocouples type K, and a pressure transducer (Kulite model XYME-190 M G, Leonia, USA) was used to assess total pressure. The flow rate of O₂ was measured by means a mass flow meter EL FLOW (Bronkhorst High-Tech B.V.) model F-201C-FAC-11-V and expressed as a standard cubic centimeter per minute (sccpm). Reaction mixture samples were collected at preset time intervals by means an electro valve (Asco Netherlands) and a universal fractions collector Eldex. The signals of the thermocouple, flowmeter, and pressure transducer were recorded by means an acquisition board and a LabView program. The experimental setup for batch oxidation of lignin is presented in Figure 28.

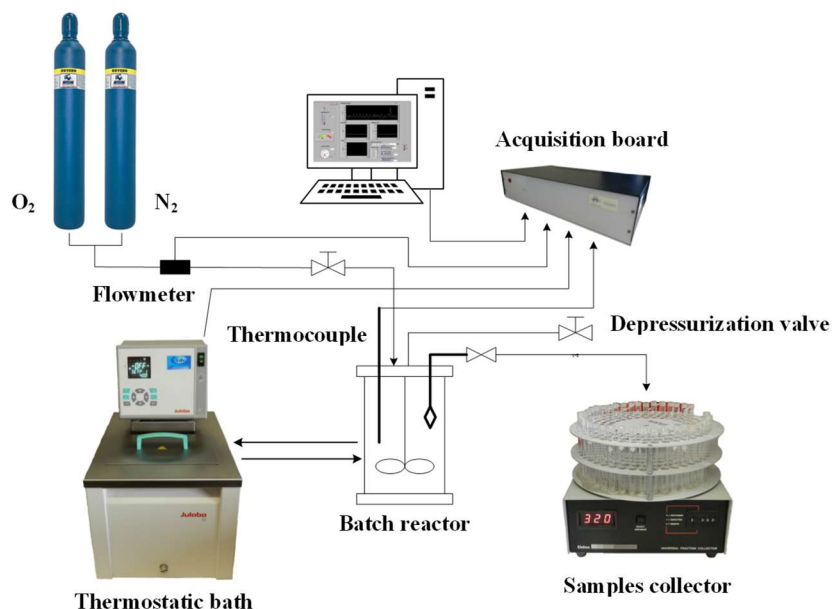


Figure 28 - Experimental setup for batch oxidation of lignins and pulping liquors.

For each oxidation essay, about 30 g of lignin or the corresponding weight of total dissolved solids for sulfite liquor were dissolved in 300 mL of an alkaline solution containing 40 g of NaOH. For kraft liquors (which are already alkaline), the weight corresponding to a total 30 g of nonvolatile solids was diluted to 300 mL with water, and the pH was measured. Since the values

found were in the range of 11-13, NaOH was added (between 10 and 20 g) to reach pH values higher than 13.8. The resulting mixture was diluted to 500 mL and introduced into the preheated reactor. Pressurization of the reactor was done with nitrogen until 6.8 bar. The reaction time started when the initial temperature reached 393 K. At this time, O₂ was introduced starting the data acquisition. The total pressure in the reactor was kept at 9.8 bar with a partial pressure of O₂ of 3.0 bar by continuous supply of O₂ along the time. At each sampling time, the electro valve was first opened to clean the sampling line and immediately after that 2 mL of the reaction mixture was collected in a clean tube. This operation was repeated until the end of the reaction.

The extraction and analysis of the oxidation products was performed by the procedure and the equipment and conditions as described in the following section.

5.2.5 Extraction and analysis of the oxidation products

The low molecular weight phenolic compounds produced by lignin oxidation were extracted by solid phase extraction (SPE) and analyzed by HPLC.

For the SPE procedure, LiChrolut EN (40-120 µm) 500 mg, 6 mL (Merck) SPE cartridges were used. First, 7 mL of methanol was applied on the column for the sorbent bed solvation; prior to sample loading, 12 mL of 95:5 (v/v) water:methanol with 0.1% (v/v) formic acid was used for SPE column equilibration. The samples were diluted with distilled water (1:1), acidified to pH 2 with H₂SO₄ solution (6 M), and loaded on the prepared cartridge. The cartridge was then washed with 12 mL of solution 95:5 (v/v) water:methanol with 0.1% (v/v) formic acid for interference elution. Finally, the phenolic compounds were eluted using 7 mL of 5:95 (v/v) water:methanol with 0.1% (v/v) formic acid. The volume was collected to a volumetric flask and brought up to 10.00 mL in volume with the same solution. The analysis of the extracted products was performed using the equipment and the conditions as previously described in section 3.2.5.1 (Chapter 3).

5.3 OXIDATION OF LIGNIN FROM EUCALYPTUS PULPING LIQUORS

5.3.1 Composition of pulping liquors and lignins

Pulping liquor contains dissolved organic material (removed from the wood during pulping), namely degradation products of lignin, carbohydrates, and extractives and the residual inorganic pulping chemicals. In kraft liquor, colloidal fragments of lignin are stabilized by ionized phenolic and carboxylic acid groups (stability is pH dependent), whereas carbohydrates (mainly from hemicelluloses) are present as oligosaccharides (Lisboa et al., 2005) and as saccharinic acids. In general, lignin from sulfite liquor has high molecular weight than kraft lignin, and it is present as

sulfonation products (Sixta et al., 2008). Table 31 presents inorganic and carbohydrate contents in the pulping liquors and in the isolated lignins.

Table 31 - Inorganic and carbohydrate contents of *E. globulus* sulfite and kraft liquors and isolated lignins.

	sample	Inorganic compounds	Carbohydrates
		(%w/wTDS)	(%w/wTDS)
liquors	KL	45.7±1.5	6.44±0.2
	EKL	49.8±1.9	4.35±0.2
	HTKL	49.7±1.8	4.26±0.1
	SL	8.49±0.3	9.84±0.4
lignins	KLlig	12.6±0.5	5.63±0.2
	EKLlig	8.51±0.3	6.84±0.3
	HTKLlig	1.72±0.06	12.2±0.5

Inorganic content is significantly lower in sulfite liquor comparatively to kraft ones. From the technological point of view this could be an advantage if the utilization of liquor as raw material for oxidation is envisaged, due the lower probability of formation of incrustations in the reactor and tubing. However, for this liquor (as for isolated lignins) 40 g of NaOH must be added per 60 g of solids to achieve the pH for enolization of phenolic groups (necessary for the oxidation to occur).

Besides inorganics, sugar and lignosulfonates, other components such as pyrogallol, gallic acid, and β -sitosterol were previous reported in SL in very low percentage (Marques et al., 2009). In black liquors (Krotschek and Sixta, 2008), and particularly in kraft liquor from *E. globulus* (Pascoal et al., 1999), the solids are also composed by aliphatic carboxylic acids, some of those volatile (acetic acid, for example) and, therefore, not accounting for solids as quantified in this work. Comparatively to original kraft liquors, the isolated lignins reveal a lower content of inorganic material, in particular HTKLlig. However, for carbohydrate content the same trend is not observed.

Two remarks can be drawn from the results on carbohydrate content: first, a considerable carbohydrates fraction of kraft liquor remains with isolated lignins, which could be attributed to a coprecipitation of the liquor polysaccharides, already reported in the literature (Lisboa et al., 2005). Second, the carbohydrate contribution for precipitated material (isolated lignins) increases about twice with liquor heat treatment (Table 31, HTKLlig). The aim of the heat treatment is the viscosity reduction of the evaporated liquor (around 80% dry solids) by partially disrupting the lignin structure, enhancing the rheological proprieties of the liquor at the recovery furnace (Ryham, 1990). Therefore, smaller fragments of lignin are certainly generated, increasing its solubility in water and promoting its removal during the precipitated lignin washing (at the isolation procedure). In accordance, the yield of HTKLlig was the lowest of the three (about 16%). However, the

carbohydrate content of this material is about twice that of KLlig and EKLLig, suggesting that a resistant fraction of carbohydrates remains coprecipitated or even linked with lignin. In accordance, carbon-carbon linkage between sugars and lignin promoted by alkali was previously reported in literature (Gierer and Wännström, 1984).

5.3.2 Characterization of liquors and lignins by NO

The results of analytical NO of pulping liquors and isolated lignins are depicted in Figure 29. NO analysis is based on the yields and types of simple phenolic aldehydes and acids produced. Results for Hy, V, VA, Sy, and SA are reported to total dissolved solids weight after deducting ashes and carbohydrates, hereafter designated as “lignin”.

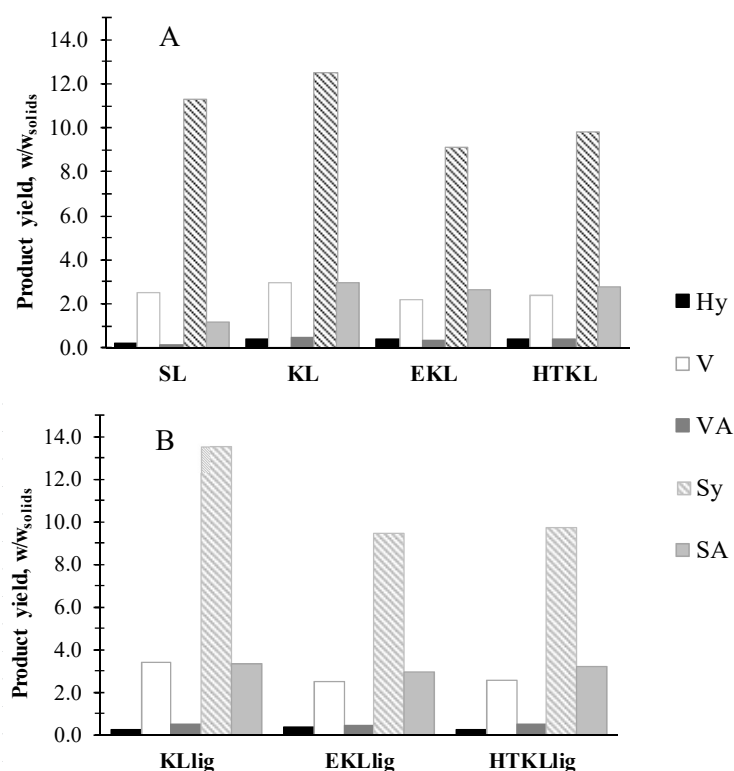


Figure 29 – Yields of monomeric phenolic products obtained by NO of pulping liquors (A) and lignins (B).

Among pulping liquors, KL presents the highest Sy yield followed by SL. However, KL also gives a higher relative content of SA. This result is probably related with a higher content of carbonyl group at C α (benzyl carbon) of lignin which leads to the corresponding carboxylic acid (Gierer et al., 1977). It may be suggested that, in the case of SL, there is a lower probability of this occurrence due to the sulfonation of C α of ppu of lignins during pulping (one of the main reactions of sulfite pulping) (Sixta et al., 2008). The ratio Sy/SA is near 9 for SL, whereas for all other liquors and lignins the value is between 3.1 and 4.2. High yield and high aldehyde/acid ratio are

advantages in the perspective of this route of lignin valorization. As far as NO could anticipate the results on oxidation with O₂ in alkaline medium, from the point of view of selectivity for aldehydes, the SL is advantageous over kraft liquors and isolated lignins.

After the evaporation process of KL, the content of aldehydes markedly decreases, while acids remain nearly constant for liquors and respective lignins (Figure 29). The highest decrease on NO yield occurs from KL to EKL and KLlig to EKLLig confirming that lignin condensation was promoted during evaporation process, whereas no change was noticed with the heat treatment (HTKL and HTKLLig). This observation suggests that the resulting splitting of lignin occurring during liquor heat treatment would balance any eventual heat-promoted increase on condensation. Small differences on total yields were noticed between each kraft liquor and its respective isolated lignin. From the overall results, carbohydrate and ashes fraction in pulping liquors and isolated lignins does not seem to affect the conversion by NO.

5.3.3 Oxidation of liquors and isolated lignins with O₂ in alkaline medium

As referred in the experimental section, the oxidation of pulping liquors and lignins were carried out in 2 M NaOH or the equivalent to pH ≥ 13.8 in the case of pulping liquors. All of the oxidation experiments began at 393 K and pO_2 of 3 bar (total pressure of 9.8 bar) with constant oxygen supply along the reaction time. The time evolution of products yields (weight of compound per 100 g of lignin after deducing ashes and carbohydrates) and pH for *E. globulus* liquors and lignins are presented in Figure 30 and Figure 31, respectively.

The main phenolic products identified in the oxidation mixture were Sy, V, and the respective carboxylic acids, SA and VA, all arisen from the splitting of C α -C β of lignin S and G units, respectively (Gierer et al., 1977). Moreover, the products from C β -C γ cleavage, VO and SO (Tarabanko et al., 2004) were also identified, as well as Hy, in minor quantity. The progress of the products yield with reaction time does not significantly differ among the liquors and lignins: during oxidation Sy reaches to a maximum yield at reaction time between 15 and 20 min followed by a decrease for longer reaction times. For V, the time to maximum is higher in general and, after the maximum, a smooth drop occurs when compared with Sy. These observations are in accordance with the different reactivity of syringyl and guaiacyl nuclei already stated in literature (Tsutsumi et al., 1995) and confirmed for other lignins (Pinto et al., 2011). The oxidation yield obtained for each product is the net result of its production and degradation.

Data depicted in Figure 32 show time evolution of temperature and O₂ input in the oxidation of liquors and lignins. As a general trend, the maximum temperature and O₂ uptake during oxidation is higher for isolated lignins than for the respective liquors, probably due to the higher extent of lignin reaction in the formers, revealed in the yield (as depicted in Figure 33). Concerning

the temperature profile, it is clear that the maximum is coincident with those of phenolics production rate in both liquors and lignins. However, a lower input of O_2 is observed in the direct oxidation of kraft liquors, which could be a consequence of its high content on inorganic compounds (Table 31).

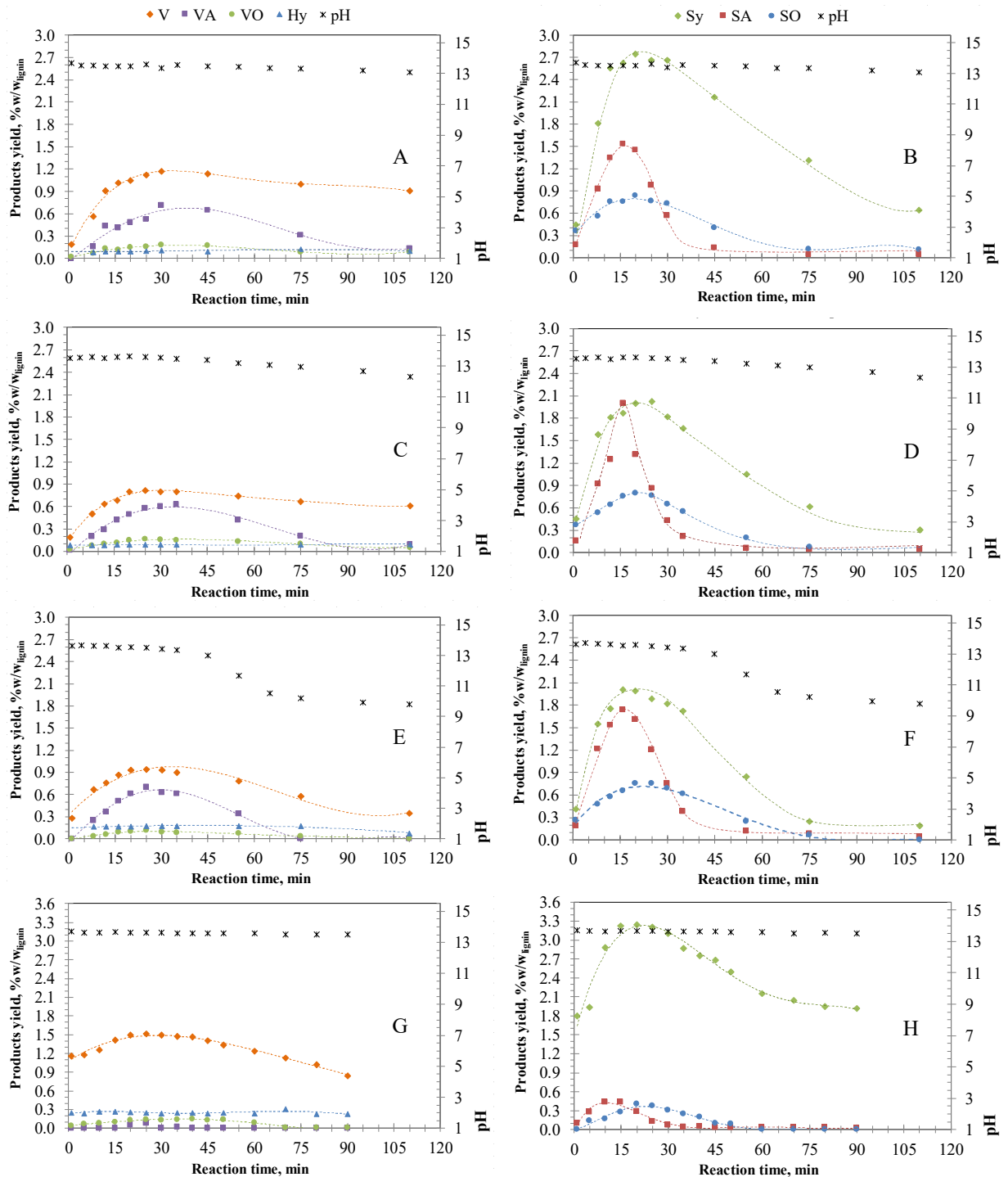


Figure 30 – Time evolution of monomeric products (V, VA, VO, Hy, Sy, SA, and SO) and pH of reaction medium during the oxidation of *E. globulus* pulping liquors KL (A and B), EKL (C and D), HTKL (E and F), and SL (G and H). General conditions: solids concentration 60 g/L, $pH \geq 13.8$, $pO_2 = 3$ bar, $P_{total} = 9.8$ bar, $T_i = 393$ K.

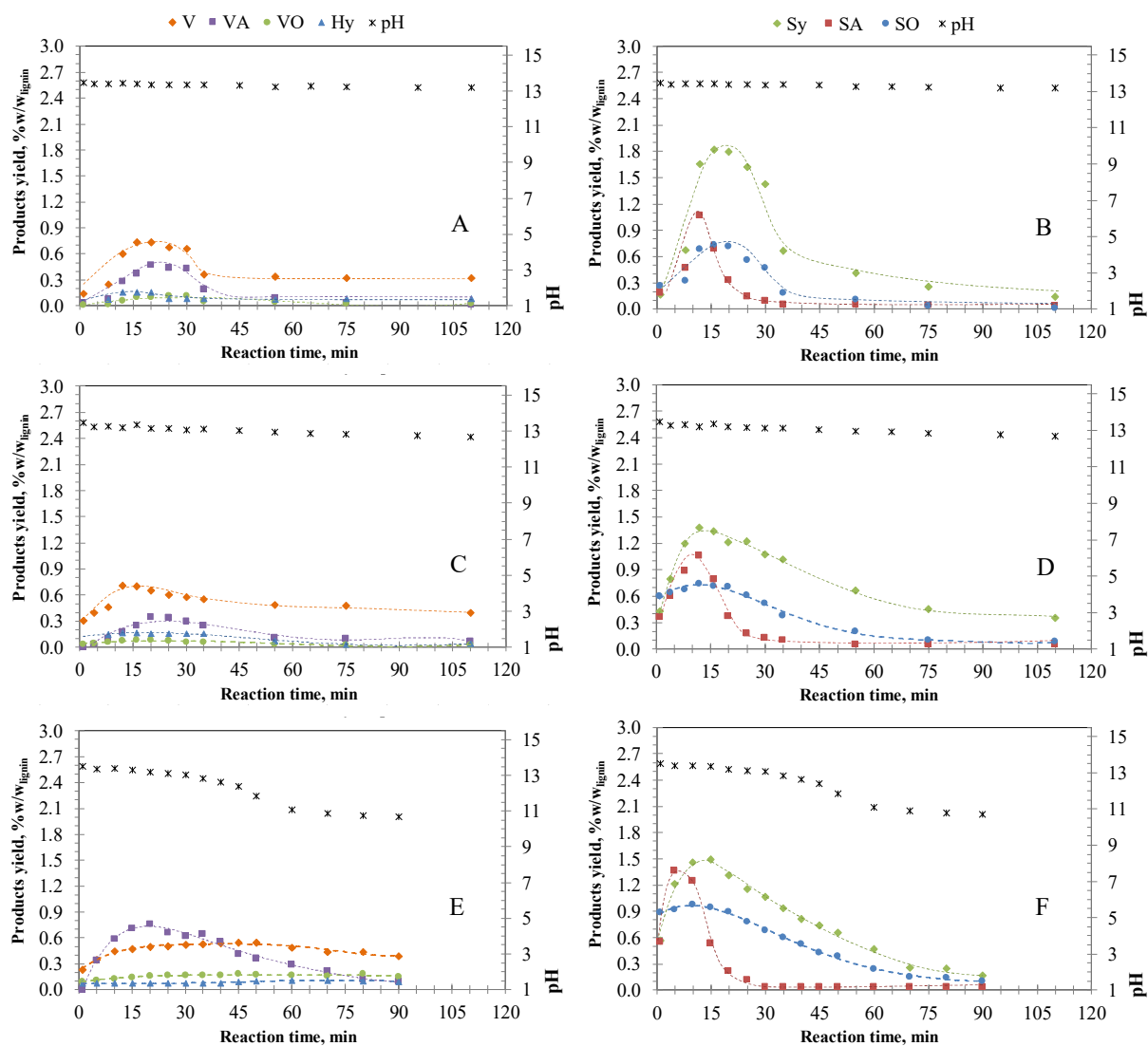


Figure 31 - Time evolution of monomeric products (V, VA, VO, Hy, Sy, SA, and SO) and pH of reaction medium during the oxidation of isolated lignins KLLig (A and B), EKLLig (C and D), HTKLLig (E and F) from *E. globulus* kraft liquors. General conditions: solids concentration 60 g/L, $\text{pH} \geq 13.8$, $p\text{O}_2 = 3$ bar, $P_{\text{total}} = 9.8$ bar, $T_{\text{initial}} = 393$ K.

Inorganic components of kraft liquors are mainly NaOH, NaHS, Na_2CO_3 , K_2CO_3 , and Na_2SO_4 , contributing to high ionic strength of the solution, thus decreasing the solubility of O_2 in the reaction medium (Millero and Huang, 2003; Tromans, 1998) and finally reducing the consumption during oxidation and limiting, by this way, the products formation. In the corresponding isolated lignins, ashes content is considerably lower: 4, 6, and 29 times for KLLig, EKLLig, and HTKLLig, respectively. Moreover, it is quite probable that low molecular weight organic compounds, including lignin derivatives (always present in pulping liquors, but certainly at very lower level in isolated lignins) quickly undergo degradation in alkaline media with the concomitant CO_2 production. This would contribute to the total pressure of the system, hindering the introduction of additional O_2 and, finally, lowering the O_2 uptake (Figure 32).

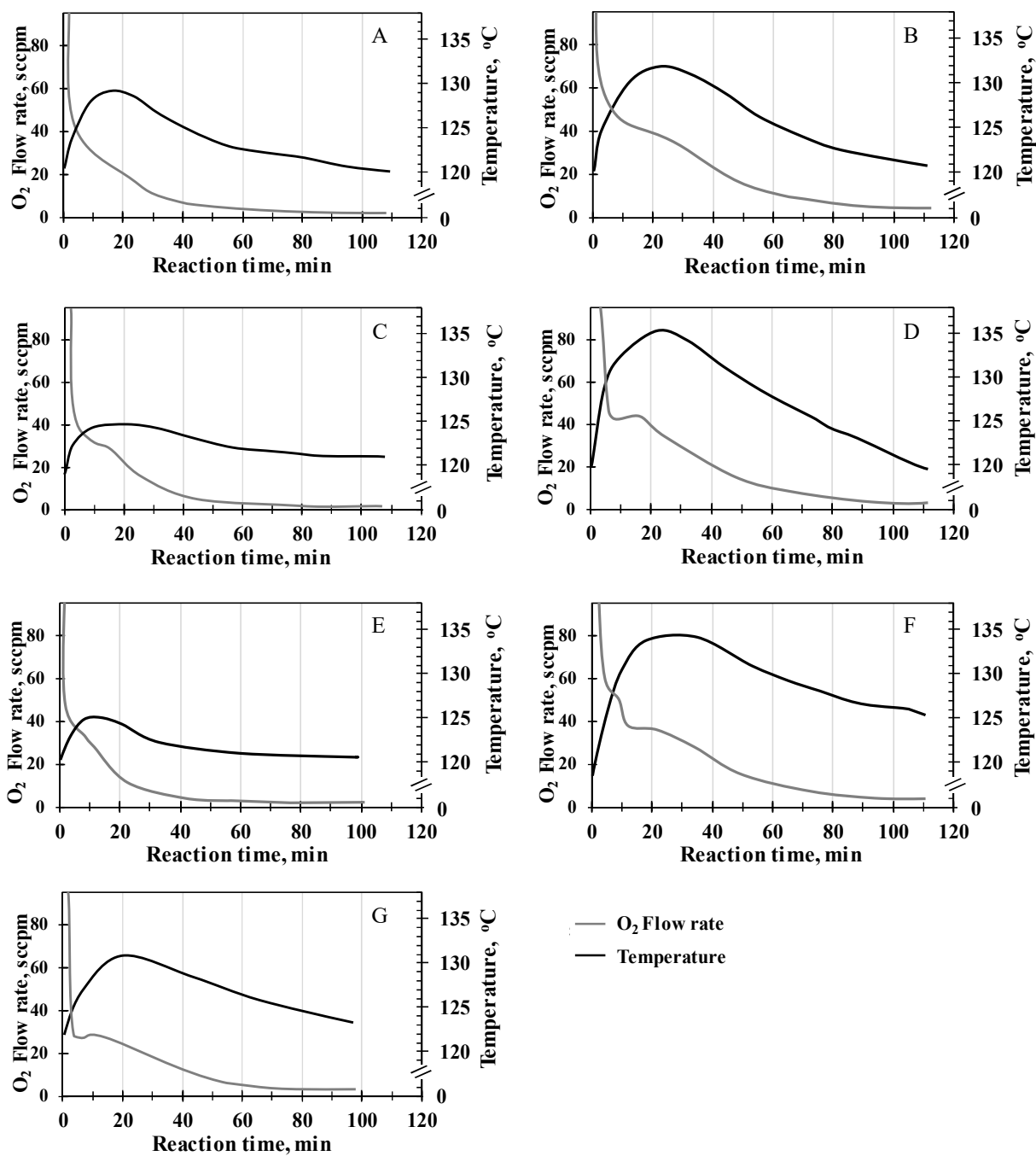


Figure 32 – Time evolution of temperature and O₂ uptake during the oxidation of liquors and lignins: KL (A), KLLig (B), EKL (C), EKLLig (D), HTKL (E), HTKLLig (F), and SL (G). General conditions: lignin concentration 60 g/L, pH \geq 13.8, $pO_2 = 3$ bar, $P_{total} = 9.8$ bar, $T_{initial} = 120$ °C.

During oxidation it is likely that carbohydrates undergo degradation reactions, consuming alkali and O₂ and thus leading to low molecular aliphatic compounds and CO₂ contributing to the total pressure. Additionally, carbohydrates can react with benzaldehyde structures via alkali-promoted reaction (Gierer and Wännström, 1984). These facts lead us to postulate that the carbohydrate presence is unfavorable to the process. However, the results suggest that other factors (such the already mentioned inorganic content and also lignin structure) seem to overcome the

eventual impairment of lignin oxidation to aldehydes caused by carbohydrates, since no effect of these compounds were noticed (as already stated for NO, section 5.3.2).

In the oxidation conditions of this work no visible effect was noticed due to alkali competing reactions (such as the abovementioned carbohydrate reactions) on pH along the reaction: the profiles were similar for liquors and respective lignins. However, for HTKL and the respective lignin, after 50 min of reaction an intense decline is observed reaching a final value of 10 (graphs E and F in Figure 30 and Figure 31), whereas final pH for the other materials is within 12 and 14.

More than the carbohydrate and inorganic contents, in conditions where alkali and O₂ are not limiting factors, the lignin structure is undoubtedly the main factor for the final yield. NO results have demonstrated that KL has lower content on condensed structures and more potential for aldehyde production. In spite of the different reaction mechanisms involved in NO and oxidation with O₂, NO is frequently considered as an “evaluator” of lignins, representing the maximum yields that could be achieved in oxidation. Usually, yield of O₂ oxidation is about 30-50% of NO. The amount of Sy and V produced from SL by oxidation with O₂ is considerable higher than for the other materials, reaching 29% and 60% of the NO value, respectively. The most probable reason for this is the structure of the noncondensed fraction of liginosulfonate: the most reactive structures toward oxidation with O₂ are those carrying conjugated double bonds (at lateral chain); under alkaline conditions, these structures are promptly produced by the elimination of the sulfonic group at C α in SL lignin. Kraft lignin also contains these unsaturated structures as well as the precursors; however, due to the more intensive lignin fragmentation in kraft pulping than in sulfite pulping, the availability of these reactive structures in the noncondensed fraction is probably lower in kraft lignins. In short, within all tested materials, SL was those with better overall performance considering yields, selectivity (ratio aldehydes/acids) and O₂ uptake, in spite of its contents in inorganic and carbohydrates.

Finally, minor compounds detected and quantified in the oxidation mixture for all of the pulping liquors and lignins were Hy (<0.2%), VO (0.1-0.2%), and SO (0.4-1%). As stated before, acetoderivatives are products of the C β -C γ cleavage competing with cleavage of C α -C β (leading to Sy, V, SA, and VA).

Figure 33 summarizes the results on the main products identified as oxidation products of pulping liquors and all isolated lignins. The yields, on lignin basis, are higher for isolated kraft lignins than for kraft liquors.

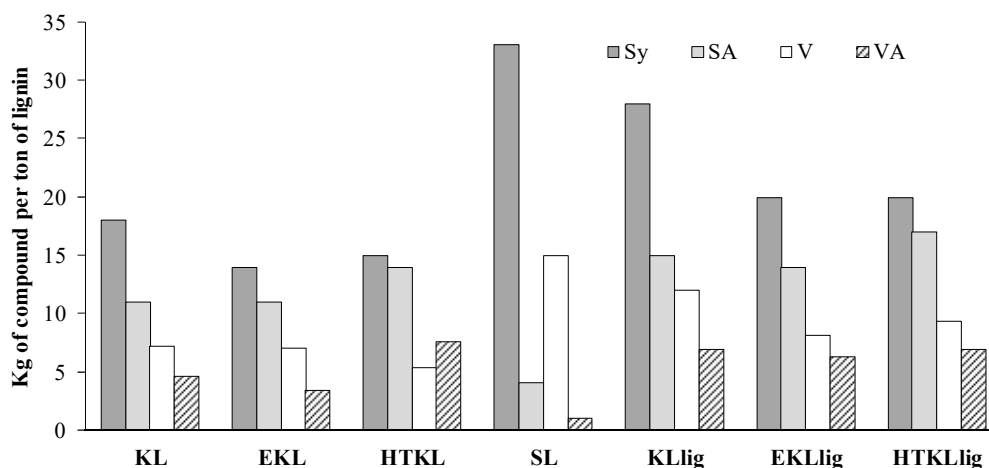


Figure 33 - Yields of Sy, SA, V, and VA produced in the oxidation of pulping liquors and lignins with O₂ in alkaline medium (lignin concentration 60 g/L, pH \geq 13.8, $pO_2 = 3$ bar, $P_{total} = 9.8$ bar, $T_{initial} = 120$ °C).

Data depicted in Figure 33 show that SA and VA content is higher for kraft liquors and respective lignins than for SL. The ratios Sy/SA and V/VA are a measure of process selectivity for aldehydes. Sy/SA ratio for SL is about 10 times higher than the average of the other materials. These ratios slightly decrease with liquor processing (from KL/KLLig to EKL/EKLLig, and to HTKL/HTKLLig) denoting a decrease on selectivity, but are higher in the isolated lignins than in the respective liquors. This last observation suggests that the lab isolation (with its washing process) remove a fraction of lignin that would contribute for the acids production. Rather than being a product of further oxidation of corresponding aldehydes, the acids are more likely a byproduct of oxidation related with the content of some particular lignin structures, namely those carrying a carbonyl group at C α (Gierer et al., 1977). Oxidation mechanisms in complex mixtures are difficult to rationalize, and therefore, the real source of VA and SA remains not clearly assigned. The knowledge about these mechanisms at high temperature and pressure would be important from the point of view of process control, aiming to improve selectivity and yield on aldehydes.

5.3.4 Conclusions

Among all of the studied materials, SL clearly stands out as the raw-material with highest potential for Sy and V production: in the conditions of this study, SL produces about 33 kg of Sy and 15 kg of V per ton of lignin by direct oxidation of the liquor. These values represent about 20% more than the yield obtained by oxidation of the KLLig.

The Sy and V values obtained for both liquor and lignins were converted for the basis of kraft liquor total dissolved solids, as presented in Table 32. From the technological point of view it

is important to understand the benefit of lignin isolation on product yields, considering that the pulping liquors could be directly oxidized.

Table 32 - Sy and V yields per ton of total dissolved solids.

sample	kg of product per ton of solids		
	Sy	V	
liquors	KL	8.6	3.5
	EKL	6.4	3.3
	HTKL	6.9	2.5
lignins	KLlig	10.3	4.4
	EKLlig	4.1	1.6
	HTKLlig	2.8	1.3

The results depicted in Table 32 show that the isolation of lignin is advantageous only in the case of the KL, leading to an increase of about 20% for Sy and 25% for V. Also, the selectivity is higher due to the lower proportion of SA and VA produced from isolated lignins (Figure 33). By comparing the yields for EKL with EKLlig and HTKL with HTKLlig (Table 32), it is possible to conclude that the additional yield accomplished by oxidizing the isolated lignins is not enough to overcome the low recovery yield of lignin in the preceding isolation process (yields of isolation 24% and 16% for EKL and HTKL, respectively; see section 5.2.2). Therefore, the productivity by ton of solids is rather lower than the values found for direct oxidation of kraft liquors. In the case of KL, the balance between the cost of isolation and the extra value obtained from the higher yields should be decisive if this route for lignin valorization is envisaged.

5.4 OXIDATION OF ETHANOL ORGANOSOLV LIGNIN FROM TOBACCO STALKS

Since the goal of alkaline oxidation is to achieve the maximum conversion into phenolic compounds, mainly V and Sy, several studies are focused in the discussion of the effect of reaction conditions in products yields obtained from lignin or spent liquors oxidation (Araújo, 2008; Araújo et al., 2010; Dardelet et al., 1985; Fargues et al., 1996; Mathias, 1993; Mathias and Rodrigues, 1995; Pácek et al., 2013; Sales et al., 2006; Santos S.G. et al., 2011).

In this section, an ethanol organosolv lignin from tobacco stalks (LTobO_{ethan}) was submitted to oxidation with O₂ in alkaline medium, using the equipment already described in section 5.2.4, and the effect of selected reaction conditions was studied. The starting operating parameters were defined based on previous works (typically p_{O_2} =3 bar, $T_{initial}$ =393 K, 60 g/l of lignin, and 2M of NaOH) (Fargues et al., 1996; Mathias and Rodrigues, 1995). However, lignins have different reactivity towards oxidation and the final yields and selectivity is the result of the reactions leading

to aldehydes production, degradation, and competing reactions. For these reasons, the oxidation conditions should be carefully studied to maximize the aldehydes production and minimize degradation reactions (Kim and Pan, 2010; Pinto et al., 2012).

Figure 34 to Figure 36 show the concentration profiles of the main phenolic products identified in the resulting mixture of LTobO_{ethan} oxidation in aqueous NaOH with molecular oxygen considering the variation of pO_2 , initial concentration of lignin, and initial temperature. The reaction conditions were selected in order to obtain the maximum yields of the phenolic products V, Sy, VA, SA, VO, SO, and Hy. Moderated partial pressures of oxygen and short reaction times must be employed in order to avoid the degradation of the oxidation products.

5.4.1 Influence of oxidation conditions on the phenolics products yield

5.4.1.1 Lignin initial concentration

To understand the effect of lignin concentration on the phenolics products yield obtained through oxidation in alkaline medium at constant initial temperature (393 K) and constant pO_2 (3 bar), the initial concentration of LTobO_{ethan} was changed between 15, 30, and 60 g/L. The Figure 34 shows the monomeric products profile obtained for each experiment.

The maximum yield of V and Sy was obtained for the oxidation with an initial lignin concentration of 30 and 15 g/L, respectively (Table 33). For the oxidation reaction with a lignin concentration of 30 g/L, the maximum yield of V reached 1.51 % w/w_{lignin}, after 27 minutes of reaction; after that time a decrease in its concentration is observed. For the oxidation reaction with an initial lignin concentration of 15 g/L, the maximum yield of Sy was 1.80 % w/w_{lignin}, after 18 minutes of reaction.

Table 33 - Comparison between the maximum yield (η_{\max}) and the respective reaction time to maximum ($t_{\eta_{\max}}$) obtained for V and Sy during the oxidation with different initial concentrations of LTobO_{ethan}.

[lignin], g/L	η_{\max} (% w/w _{lignin}) [*]		$t_{\eta_{\max}}$ (min.)		T_{\max} (K)
	V	Sy	V	Sy	
15	1.31	1.80	25	16	399
30	1.51	1.09	27	18	403
60	1.21	0.94	55	35	407

* reported to lignin weight after deducting ashes and carbohydrates.

The effect of lignin initial concentration on the V production was already studied by other authors. Fargues and co-workers studied the V production from the oxidation of a softwood lignin

in a batch reactor at 393 K and with pO_2 of about 3 bar. The author found that the maximum yield of V on lignin basis (% w/w_{lignin}) decreases with the lignin concentration: 10%, 8.3%, and 3.0% for an initial concentration of 30 g/L, 60 g/L and 120 g/L, respectively, concluding that a lignin concentration of 120 g/L does not lead to a higher production yield of V (Mathias, 1993). A similar decrease in the phenolics yields with the decrease of lignin concentration was also found by Fisher and Marshall (Fisher and Marshall, 1951); these authors compared the oxidation yields of a waste sulfite liquor before and after its dilution in an alkaline solution.

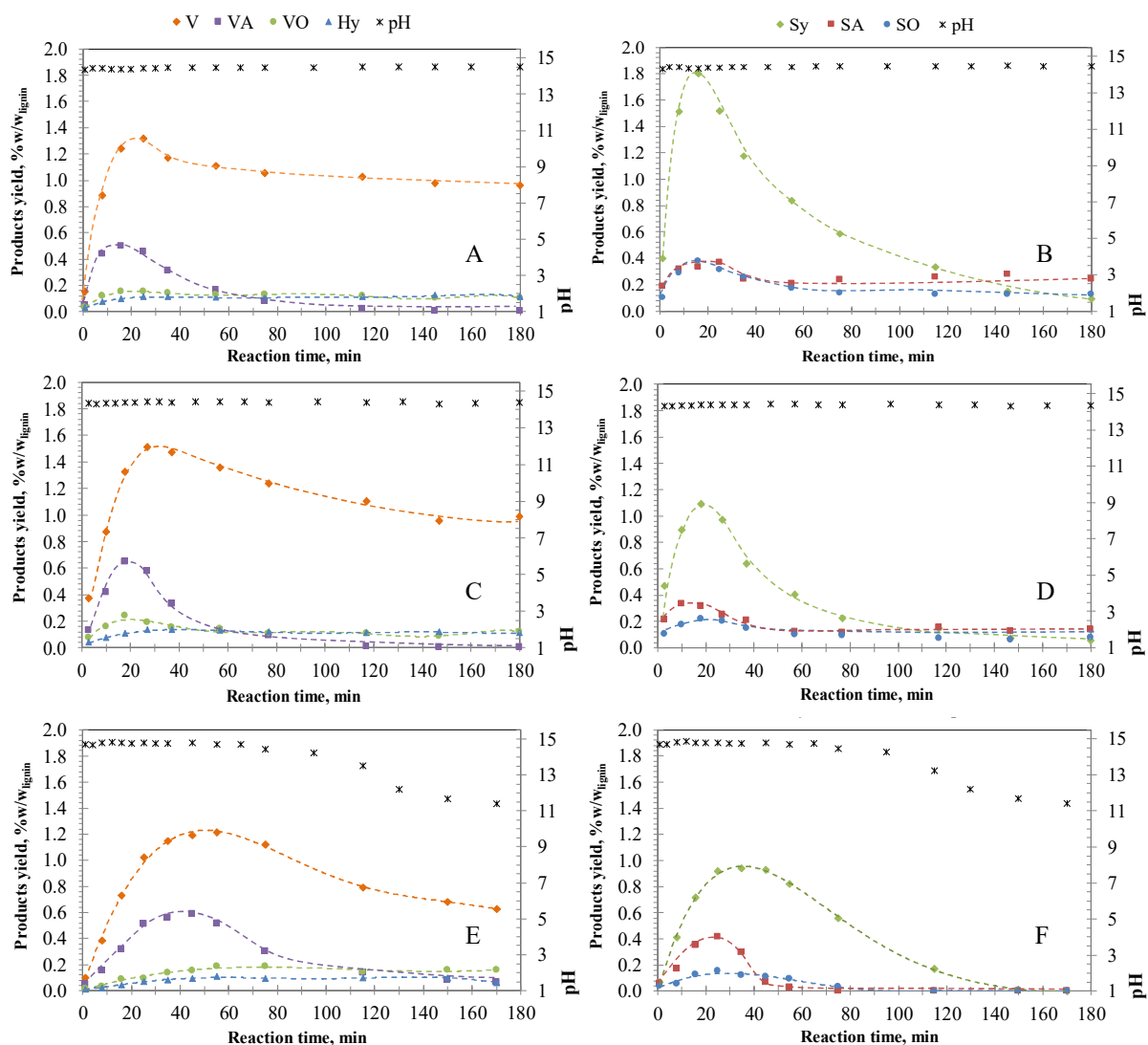


Figure 34 – Time evolution of monomeric products (V, VA, VO, Hy, Sy, SA, and SO) and pH of reaction medium during the oxidation reaction with different initial concentrations of LTOB_{ethan}: 15 g/L (A and B), 30 g/L (C and D), and 60 g/L (E and F). General conditions: $T_{initial} = 393$ K, $pH \geq 13.8$, $P_{total} = 9.8$ bar, and $pO_2 = 3$ bar.

For the experiments with and LTOB_{ethan} initial concentration of 15 and 30 g/L the pH value during the reaction does not show the same profile as compared with the reaction with 60 g/L. This change could be related with the low degradation rate of V found for these experiments. After 160

min of reaction only about 30% of V suffer degradation in the experiments with lower values of initial lignin concentration, comparatively to about 50% found for the reaction performed with 60 g/L.

The data from Table 33 also show that there is a difference of 14, 10, and 6 K between the initial temperature and the maximum value of temperature reached during the reaction with LTobO_{ethan} initial concentration of 60, 30, and 15 g/L, respectively. The concentration of the phenolic aldehydes and their respective acids increases continuously until a maximum value which is coincident with the maximum temperature. In fact, the oxidation with O₂ is an exothermic reaction, and after the maximum the temperature as well as the concentration of products decreases continuously, in the last case due to the dominance of degradation over the production reactions. In the literature, values of 13 and 9 K were reported for the difference between the initial temperature and the maximum value reached during the oxidation of a hardwood organosolv lignin and a softwood kraft lignin, respectively (Pinto et al., 2011). For a commercial ktaft lignin, Indulin AT, differences in the same order (10-15 K) were found (Araújo et al., 2010). However, the heat of an oxidation differs between lignins and reaction conditions.

5.4.1.2 Partial pressure of O₂

The effect of pO_2 in the range 2-4 bar was tested for LTobO_{ethan} oxidation with an initial concentration of 60g/L, an initial temperature of 393 K, and a total pressure (N₂ and O₂ plus water vapor) of about 9.8 bar. The time evolution of oxidation products is presented in Figure 35 for each experiment performed with a different pO_2 .

The results demonstrate that the main effect of pO_2 was on the rate of products formation, shortening the time to maximum (Table 34). Among the experiments with a pO_2 of 3 and 4 bar only a slight difference in the maximum yields of V and Sy is observed. However, the reaction time to reach the maximum is higher for the oxidation that starts with 2 bar of oxygen pressure. Mathias studied the oxidation of a softwood kraft lignin and also found similar V yields for reactions with different initial pO_2 , although obtained in different reaction times (Mathias, 1993).

Table 34 - Comparison between the maximum yield ($\eta_{max.}$) and the respective reaction time to maximum ($t_{\eta_{max.}}$) obtained for V and Sy during the oxidation of LTobO_{ethan} with different values of pO_2 .

pO_2 (bar)	$\eta_{max.}$ (% w/wlignin)*		$t_{\eta_{max.}}$ (min.)		$T_{max.}$ (K)
	V	Sy	V	Sy	
2	1.01	0.84	75	55	400
3	1.21	0.94	55	35	407
4	1.15	0.83	35	16	410

* reported to lignin weight after deducting ashes and carbohydrates.

In the oxidation reaction with a pO_2 of 2 bar an insufficient amount of oxygen could be the reason for the low yield of phenolic compounds found comparatively with the other experiments. In the literature, it was referred that a value of oxygen pressure below 2 bar was not enough to fulfil the condition of the pseudoconstant oxygen concentration during the oxidation of a sulfonated lignin, due to the insufficient amount of oxygen in the reactor (Santos S.G. et al., 2011).

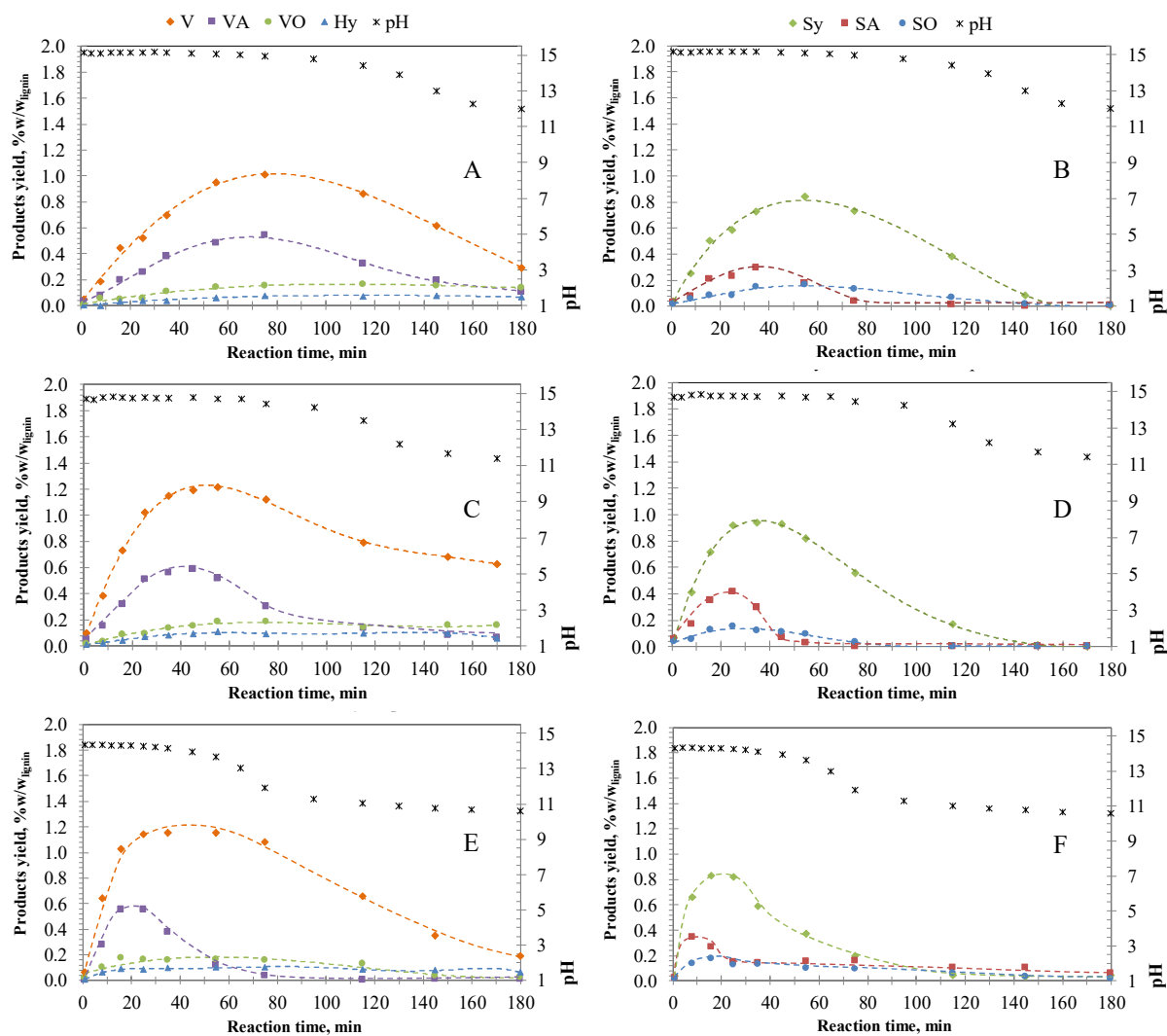


Figure 35 – Time evolution of monomeric products (V, VA, VO, Hy, Sy, SA, and SO) and pH of reaction medium during the oxidation of LTobO_{ethan} with different partial pressures of oxygen: 2 bar (A and B), 3 bar (C and D), and 4 bar (E and F). General conditions: lignin concentration 60 g/L, $T_{initial} = 393$ K, $pH \geq 13.8$, and $P_{total} = 9.8$ bar.

5.4.1.3 Initial temperature

The effect of the initial temperature in the products yield from oxidation of LTobO_{ethan} was also studied and is shown in Figure 36. The reaction was performed with 60 g/L of lignin, in 2 M NaOH solution, with 3 bar of pO_2 , a total pressure of about 9.8 bar, and at three different initial temperatures: 393 K, 413 K, and 433 K.

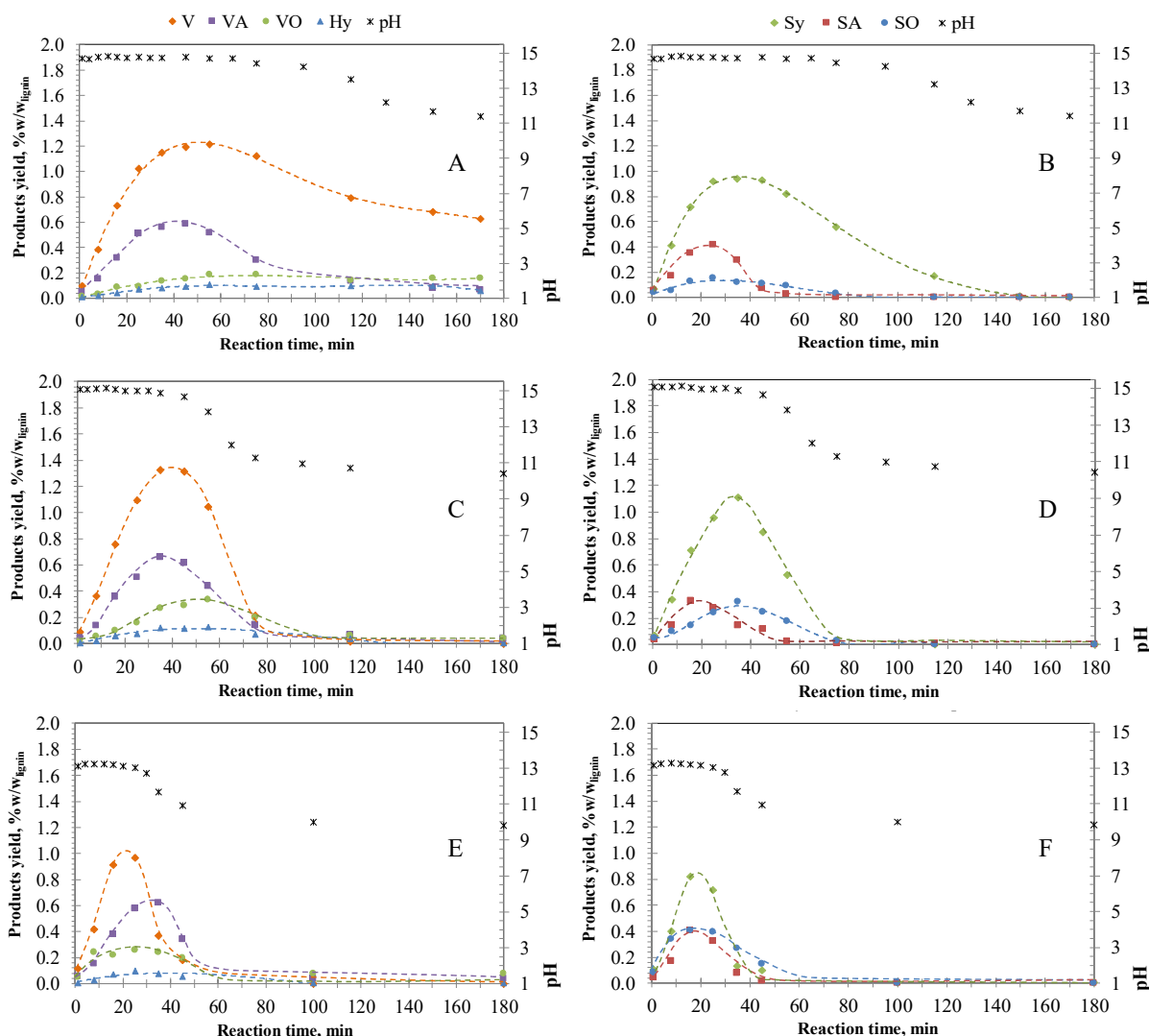


Figure 36 – Time evolution of monomeric products (V, VA, VO, Hy, Sy, SA, and SO) and pH of reaction medium during the oxidation of LTobO_{ethan} with different initial temperatures of reaction: 393 K (A and B), 413 K (C and D), and 433 K (E and F). General conditions: lignin concentration 60 g/L, pH \geq 13.8, $P_{\text{total}} = 9.8$ bar, $pO_2 = 3$ bar.

The overall results (Table 35) demonstrate that with an initial temperature of 413 K higher yields of phenolic products were obtained, 1.32 % w/w_{lignin} for V and 1.11 % w/w_{lignin} for Sy, after 35 minutes of reaction; after that time a decrease in products concentration, due to their degradation, is observed. A higher initial temperature (433 K) led to shorter reaction times, since the maximum yield of V and Sy were obtained after 25 and 16 minutes, respectively; however, its degradation is also higher. In fact, the temperature has an important effect on the rate of oxidation products degradation: at 433 K after 45 minutes of reaction about 69% of the maximum yield of products was consumed while at 413 K the decrease was only about 10%. This effect is even more clear for long reaction times. The faster degradation found for V is also related with the higher reduction of the pH in the experiment with an initial temperature of 433 K.

Table 35 - Comparison between the maximum yield ($\eta_{\max.}$) and the respective reaction time to maximum ($t_{\eta_{\max.}}$) obtained for V and Sy during the oxidation of LTobO_{ethan} with different initial temperatures of reaction.

T_{initial} (K)	$\eta_{\max.}$ (% w/wlignin)*		$t_{\eta_{\max.}}$ (min.)		$T_{\max.}$ (K)
	V	Sy	V	Sy	
393	1.21	0.94	55	35	407
413	1.32	1.11	35	35	427
433	0.97	0.82	25	16	440

* reported to lignin weight after deducting ashes and carbohydrates.

As already referred, the alkaline oxidation with O₂ is an exothermic reaction, and considering the experiment with an initial temperature of 433 K it is possible to observe that there is a difference of 7 K between the initial temperature and the maximum value reached during the reaction; while for the other experiments, this value reaches 14 K. The high initial temperature is probably the responsible for the low yield on phenolic compounds, due to the higher rate of degradation. It is well known that the oxidation yield of each aromatic product is the result of its formation and its consequent degradation in the reaction medium (Pinto et al., 2012).

The profiles of VA and SA are very close to the corresponding aldehydes, usually with a maximum at the same reaction time, followed by an equivalent decline. If the total content of oxidation products from S units is taken into account (Sy, SA and, SO) (Figure 36), it is possible to observe a higher relative percentage of SA and SO for the oxidation with an initial temperature of 433 K. The same behavior is obtained for G units, considering VA and VO. This ascertains that an initial temperature of 433 K leads to more co-products.

Moreover, it is important to highlight that the general trend of the oxidation profiles depends strongly on the lignin sources. According to Araujo et al. (2010) experiments using a high-molecular weight lignin showed a lower conversion to phenolic products when compared with oxidation reactions of a low-molecular weight lignin.

5.5 KINETICS OF PHENOLICS PRODUCTION FROM TOBACCO LIGNIN OXIDATION

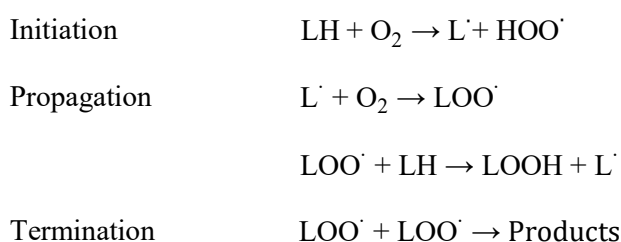
The kinetic study of LTobO_{ethan} oxidation has two main objectives: (1) to analyze the effect of process parameters (temperature, pO_2 and lignin initial concentration) on the yield of V and Sy and (2) to evaluate the kinetic parameters of the lignin oxidation process to produce V and Sy.

Under the selected reaction conditions of temperature, pO_2 , and initial lignin concentration the kinetics of the LTobO_{ethan} oxidation was studied. As referred in the previous section, all the oxidation experiments were performed in alkaline medium (2 M NaOH solution), with a total pressure of about 9.8 bar, and a constant oxygen supply along the reaction time. The effect of the initial lignin concentration was studied in the range 393-433 K, with a pO_2 of 3 bar, and with 60

g/L of lignin initial concentration. The effect of pO_2 (value at the beginning of the reaction) between 2 and 4 bar was also tested, with an initial lignin concentration of 60 g/L, and an initial temperature of 393 K. To study the effect of the initial concentration of LTobO_{ethan} experiments with 15, 30, and 60 g/L of lignin, an initial temperature of 393 K, and a pO_2 of 3 bar was used.

In this study it was assumed that the effect of the NaOH concentration on V and Sy yield would be negligible due to its very high concentration and the fact that the pH was higher than 12 during the oxidation experiments, as already assumed by other authors (Fargues et al., 1996; Pacek et al., 2013; Pinto et al., 2013). Moreover, Fargues and co-workers (Fargues et al., 1996) studied the kinetics of V oxidation and referred that at least 2M in NaOH is required to achieve the favourable conditions to preserve the produced vanillin.

An effective understanding of the reaction mechanisms is essential for the development of kinetic models. However, for this study it is sufficient to quantify the global reaction rate by identifying the major oxidation pathways. The oxidation comprises the depolymerization of lignin, in alkaline medium, which promotes the lignin solubilization by the hydroxyl anions (Fargues et al., 1996; Tarabanko et al., 2001). It is also well known that the reaction mechanism of the lignin oxidation leads to the production of a great variety of intermediate products. In a general way, it is considered that the oxidation proceeds in two or more steps, where lignin is depolymerized into fragments producing aromatic aldehydes, other products of lower molecular weight, and smaller molecules such as carbon dioxide and water (Fargues et al., 1996; Tarabanko and Petukhov, 2003). The reaction scheme for the global mechanism proposed for V and Sy production from lignin (L) oxidation with O_2 in alkaline medium can be represented as:



The radical LOO' will further suffer several types of reactions during oxidation, leading mainly to V and Sy (Fargues et al., 1996; Tarabanko et al., 2001).

In this work the experimental kinetic study was entirely based on the concentration of V and Sy as a function of reaction time, since it was not possible to measure the concentration of lignin or all the oxidation products during the reaction (Fargues et al., 1996; Mathias, 1993).

5.5.1 Kinetic study of LTobO_{ethan} oxidation

As already referred, for the kinetic study of phenolics production from LTobO_{ethan} oxidation three initial temperatures were tested: 393, 413, and 433 K, using a pO_2 of 3 bar and an initial lignin concentration of 60 g/L.

The effect of pO_2 in the range 2.0-4.0 bar was also tested; these experiments were performed with an initial lignin concentration of 60 g/L and an initial temperature 393 K.

For the study of the effect of the initial LTobO_{ethan} concentration three different concentrations were studied (15, 30, 60 g/L) all of these oxidations have been initiated with a temperature of 393 K and a pO_2 of 3 bar.

All the oxidation reactions were performed in alkaline medium, with 2M NaOH, and the total pressure in the reactor was kept at 9.8 bar (Table 36).

Table 36 - Experimental conditions for the kinetic study of LTobO_{ethan} oxidation.

Reaction conditions	
Temperature, K	393 / 413 / 433
[lignin], g/L	15 / 30 / 60
pO_2 , bar	2 / 3 / 4
Total pressure, bar	≈ 9.8
[NaOH], M	2
Mixture volume, L	0.5

5.5.2 Effect of initial lignin concentration

The kinetics of the LTobO_{ethan} oxidation can be studied using a simple equation that relates the initial reaction rate of products formation to the concentration of lignin and the pO_2 at the time that the reaction begins:

$$r_{oxid} = k_{oxid} [\text{lignin}]^n pO_2^m \quad (1)$$

where r_{oxid} is the initial reaction rate of phenolics production from LTobO_{ethan} oxidation, k_{oxid} is the oxidation rate constant, and n and m are the reaction orders with respect to [lignin] and pO_2 , respectively.

The order of the reaction considering V and Sy production with respect to the initial lignin concentration was studied. V and Sy profile for each oxidation with an initial lignin concentration of 15, 30, and 60 g/L are shown in Figure 37.

In this approach it will be considered that there is no degradation of the V and Sy in the beginning of the reaction. Considering temperature and pO_2 , as these parameters undergo some variations during the oxidation, only the initial values were considered.

The plot of V and Sy conversion (product concentration, g/L) against reaction time (considering t_{max} as the value where the maximum yield of products was obtained) enables the determination of the initial rate of production (r_{oxid}) for each experiment.

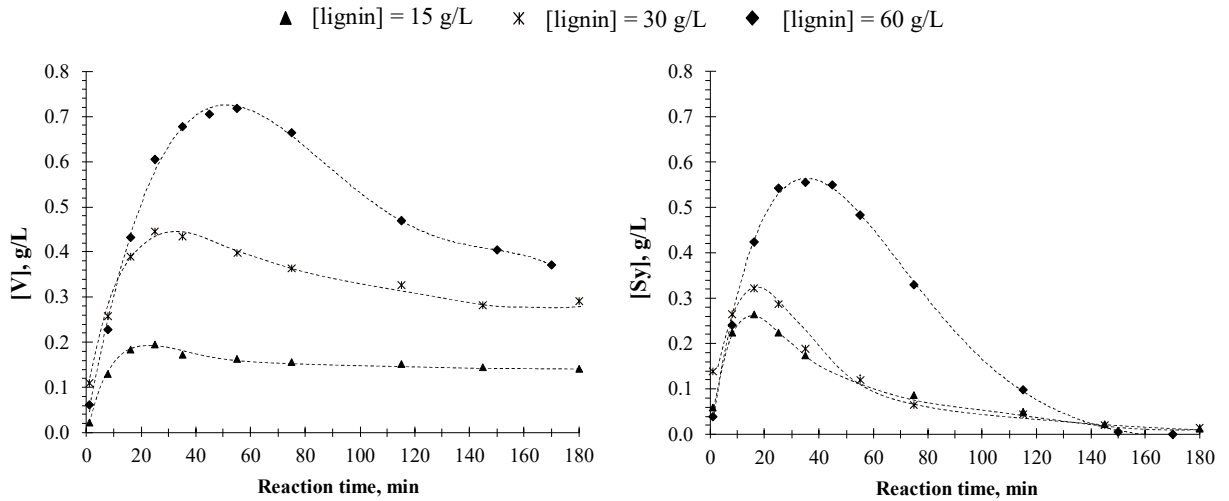


Figure 37 – Effect of initial LTobO_{ethan} concentration (15, 30, 60 g/L) on V and Sy concentration during oxidation. General conditions: $T_{initial} = 393$ K, $pH_{initial} \geq 13.8$, $P_{total} = 9.8$ bar, $pO_2 = 3$ bar.

The logarithmic representation of the r_{oxid} found for each reaction as a function of the lignin initial concentration for V and Sy (Figure 38) leads to the calculation of the reaction order n stated in the equation (1).

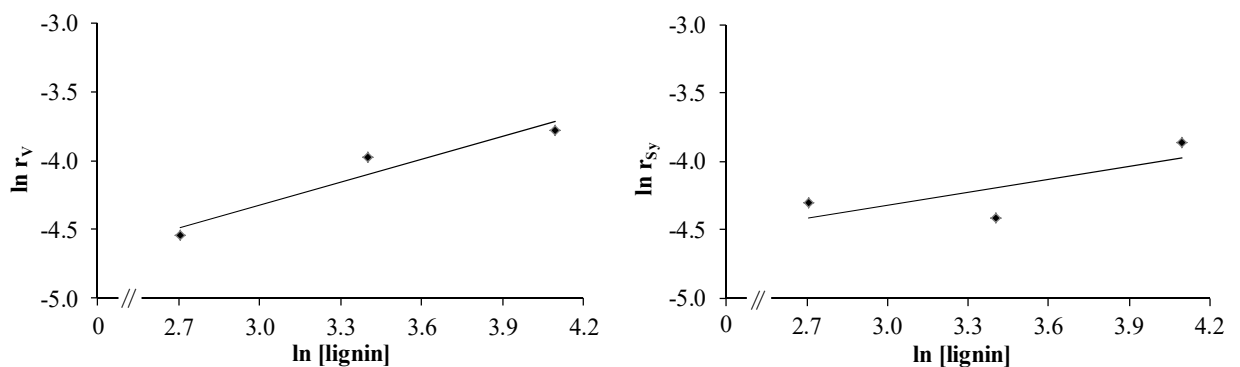


Figure 38 – Initial reaction rate of V and Sy production as a function of initial LTobO_{ethan} concentration.

A straight line with slope equal to 0.55 for V and 0.31 in the case of Sy was obtained. This value determines the reaction order of V and Sy production with respect to initial concentration of

lignin. According to Tarabanko and co-workers the half kinetic orders are characteristic for the radical chain oxidation (Tarabanko et al., 2001).

Considering LTobO_{ethan} oxidation in alkaline medium, under the reported conditions, the following kinetic laws were obtained for V (equation (2)) and Sy (equation (3)):

$$r_V = k_V [\text{lignin}]^{0.55} pO_2^m \quad (2)$$

$$r_{Sy} = k_{Sy} [\text{lignin}]^{0.31} pO_2^m \quad (3)$$

Fargues and co-workers studied the production of V from the oxidation of a *Pinus spp.* kraft lignin in alkaline medium and they also found that the maximum yield of V (wt%) decreases with the initial concentration of lignin (Fargues et al., 1996). Moreover, a reaction order of 1 with respect to lignin concentration was obtained by these authors.

5.5.1 Effect of oxygen partial pressure

For the study of the pO_2 effect on the reaction rate of V and Sy production three experiments with values between 2 and 4 bar were performed. The initial concentration of lignin (60 g/L), the initial temperature (393 K), and the total pressure (~9.8 bar) were kept constant. In a similar way as the determination of the reaction order with respect to initial lignin concentration, from the relationship between the initial reaction rate and the initial pO_2 it is possible to find the reaction order m in equation (1). The representation of V and Sy concentration (g/L) as function of reaction time (min) for the oxidation with different initial pO_2 is shown in Figure 39.

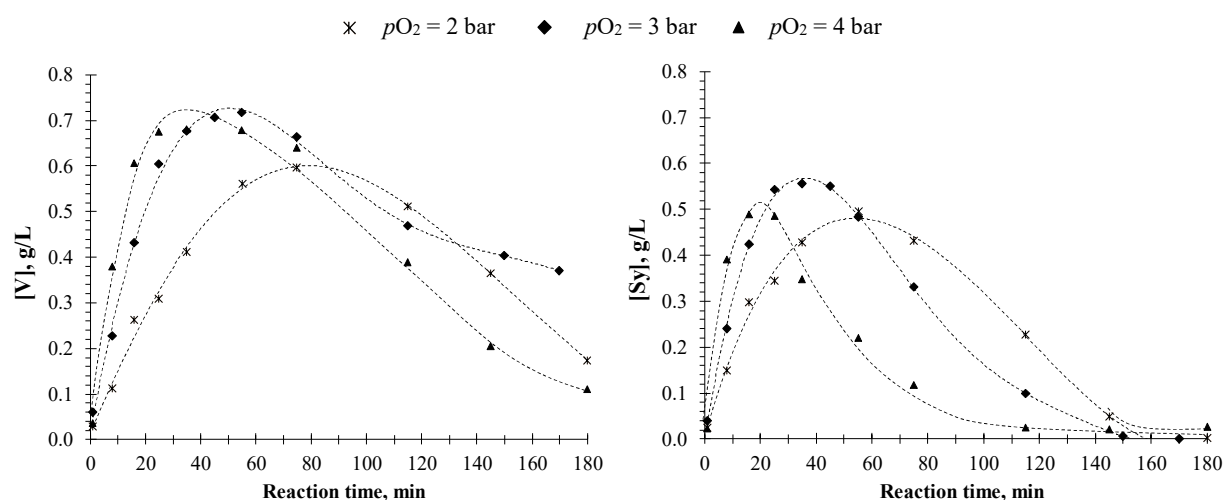


Figure 39 - Effect of partial pressure of O_2 (2, 3, 4 bar) on V and Sy concentration during LTobO_{ethan} oxidation. General conditions: lignin concentration 60 g/L, $T_{\text{initial}} = 393$ K, $pH_{\text{initial}} \geq 13.8$, $P_{\text{total}} = 9.8$ bar.

It is possible to observe that as the partial pressure increased, the oxidation rate of lignin increased, but the maximum of products yield does not follow the same trend. However, the increase in pO_2 also led to an increase in the products degradation after the maximum yield was reached. This increase means that, at higher partial pressures, the products yield becomes more sensitive to degradation. This trend was also noted by Pacek and co-workers in the kinetic study of a sodium lignosulfonate oxidation to produce V (Pacek et al., 2013). The authors referred that the maximum value of V concentration was independent of the pO_2 ; as the partial pressure increased, the oxidation rate of lignin to V also increased, but the maximum V yield remained constant. However, the increase in pO_2 also led to an increased V oxidation rate after the maximum V concentration was reached. This increase means that, at higher pO_2 , the V yield becomes more sensitive to the residence time and the control of the process might be more difficult.

From the log-log representation of the r_{oxid} as a function of the initial pO_2 , a straight line was obtained (Figure 40).

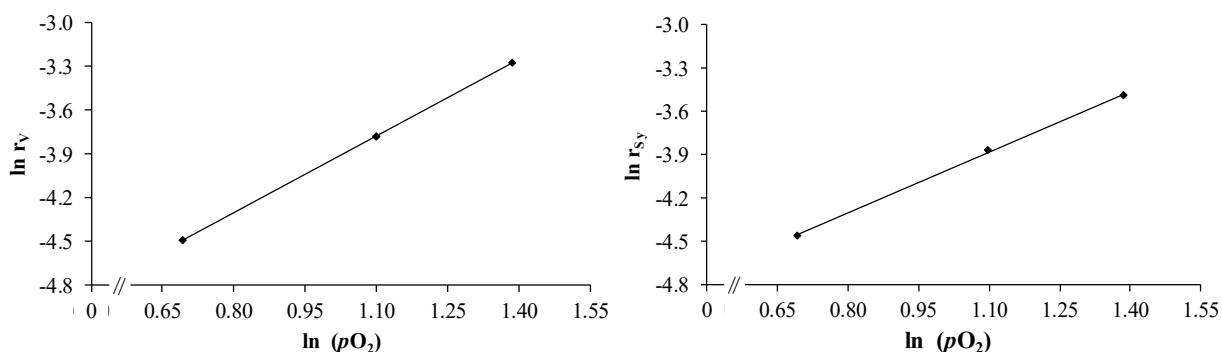


Figure 40 - Initial reaction rate of V and Sy production as a function of partial pressure of O_2 .

The slope value is 1.7 and 1.4 for V and Sy, respectively, and represents the reaction order m with respect to oxygen concentration (equation (4) and (6)).

$$r_V = k_V [\text{lignin}]^{0.55} pO_2^{1.7} \quad (4)$$

$$r_{Sy} = k_{Sy} [\text{lignin}]^{0.31} pO_2^{1.4} \quad (5)$$

The reaction order found for the pO_2 is in agreement with the literature, where values between 0.6 and 1.75 have been reported. Tarabanko and their co-authors reported a $m=0.56$ for the oxidation of a aspen wood with an oxygen working pressure between 2 and 13 bar, at pH 11.6., and with an initial temperature of 383 K (Tarabanko et al., 2001). Santos et al. found a $m=1$ for the oxidation of a eucalyptus lignosulfonate lignin in a pure oxygen atmosphere for pressures 2.0-10 bar, at a temperatures of 413 K, while Fargues et al. reports a $m=1.75$ for the oxidation of a *Pinus spp.* kraft lignin at $pH > 11.5$ (Fargues et al., 1996; Santos S.G. et al., 2011).

5.5.2 Effect of initial temperature

The effect of temperature in the reaction rate and yield of phenolic products from LTobO_{ethan} lignin oxidation was studied in the range 393–433 K, and the results are shown in Figure 41.

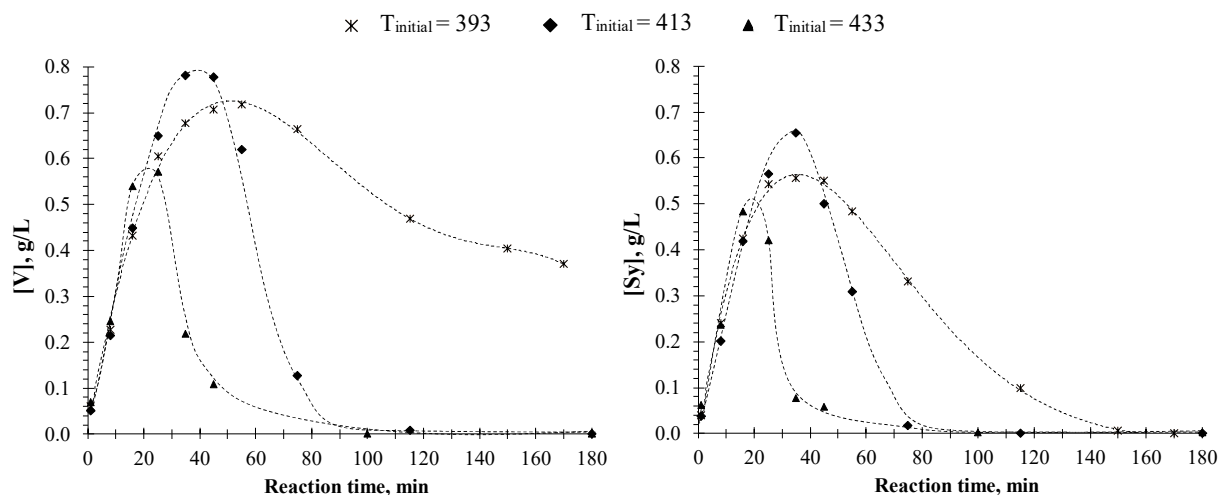


Figure 41 - Effect of initial temperature (393, 413, 433 K) on V and Sy concentration during LTobO_{ethan} oxidation. General conditions: lignin concentration 60 g/L, pH_{initial} ≥ 13.8, P_{total} = 9.8 bar, pO₂ = 3 bar.

Taking into account the equation (1), k_{oxid} can be related to temperature using Arrhenius equation to give the initial reaction rate as a function of the initial concentration of lignin, pO_2 , and temperature:

$$r_{oxid} = A \exp\left(-\frac{E_a}{RT}\right) [\text{lignin}]^n pO_2^m \quad (6)$$

In contrast to the effect of pO_2 , the reaction temperature not only increases the reaction rate but also affects the competitive reactions of lignin oxidation, resulting in the variation of phenolics products yield.

The energy of activation (E_a) and the constant, A, in the Arrhenius equation for V and Sy production were estimated from the slope and the intercept, respectively, of the linear regression of $\ln k$ versus $1/T$ (Figure 42). The E_a calculated from the experimental data was 18.3 and 10.2 kJ/mol for V and Sy, respectively. Thus, the kinetics of LTobO_{ethan} oxidation for the production of V and Sy can be related to the initial concentration, pO_2 , and temperature by:

$$r_V = 4.8579 \exp\left(-\frac{18272}{RT}\right) [\text{lignin}]^{0.55} pO_2^{1.7} \quad (7)$$

$$r_{Sy} = 0.4895 \exp\left(-\frac{10386}{RT}\right) [\text{lignin}]^{0.31} pO_2^{1.4} \quad (8)$$

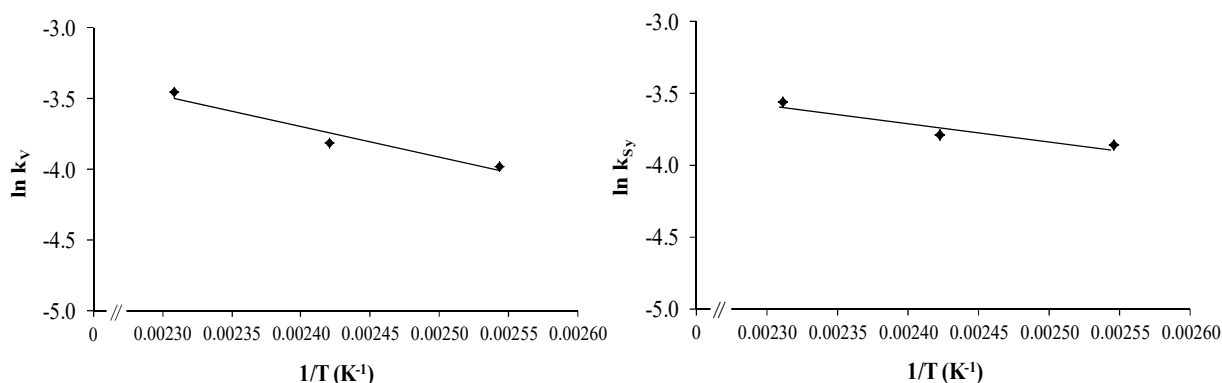


Figure 42 - Initial reaction rate of V and Sy production as a function initial temperature.

The value of E_a found for Sy is lower than for V; in fact, the S units have higher reactivity than G counterparts in alkaline medium and under O_2 oxidation conditions. Thus, the oxidation of S units is faster than G units for both production and degradation of aldehydes. Santos and co-workers (Santos S.G. et al., 2011) also found a lower value of E_a for Sy (62.6 kJ/mol) than for V (70.5 kJ/mol), in the oxidation kinetic of a lignosulfonate from acidic magnesium-based sulfite pulping of eucalyptus wood with O_2 under alkaline conditions.

The E_a found in this work is lower than the values reported for the oxidation of different lignins to aromatic aldehydes under similar conditions. Fargues and co-workers (Fargues et al., 1996) calculated the E_a for the V production from a softwood kraft lignin oxidation and they found a value of 29.1 kJ/mol. Other authors also reported the kinetics and the E_a of V and Sy production from hardwood lignins and values of E_a in the range 48.0-70.5 kJ/mol were obtained (Santos S.G. et al., 2011; Tarabanko et al., 2001). The larger the E_a , the more temperature-sensitive is the rate of reaction.

5.5.3 Conclusions

The kinetic study of V and Sy production from alkaline oxidation with O_2 of tobacco organosolv lignin was carried out in order to analyze the effect of process parameters (temperature, pO_2 and lignin initial concentration) on the yield of V and Sy as well as to evaluate the kinetic parameters of the lignin oxidation process to produce these phenolic monomers.

From the experiments under different oxygen partial pressures the reaction order found was 1.7 for V and 1.4 in the case of Sy. With respect to initial concentration of lignin the reaction order obtained for V and Sy production was 0.55 and 0.31, respectively. From the experiments with different values of initial temperature the E_a calculated was 18.3 kJ/mol for V and 10.2 kJ/mol for Sy, demonstrating that S units have higher reactivity than G counterparts in alkaline medium and under O_2 oxidation conditions.

5.6 EXPERIMENTAL VALIDATION OF THE RADAR CLASSIFICATION OF TOBACCO LIGNINS

Experimental validation of the radar classification of tobacco lignins was accomplished using the two organosolv lignins from tobacco stalks, L_{Tob}O_{but} and L_{Tob}O_{ethan}. The radar plots made with the key descriptors of these lignins are presented in Figure 43.

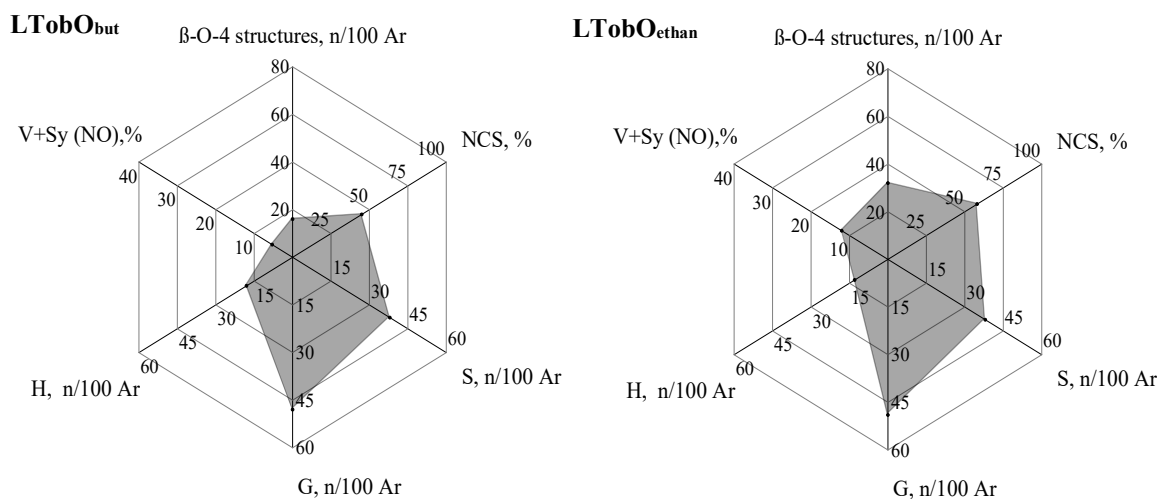


Figure 43 - Radar classification for L_{Tob}O_{but} and L_{Tob}O_{ethan} lignins.

Batch oxidation in alkaline medium with O₂ of L_{Tob}O_{but} and L_{Tob}O_{ethan} lignins was performed under the conditions described in section 5.2.4. The products profile for each lignin is presented in Figure 44, disclosing the maximum yields obtained for V and Sy.

L_{Tob}O_{ethan} lignin produces 1.2% of V and 0.94% of Sy, while for L_{Tob}O_{but} lower maximum values were obtained (0.74% of V and 0.34% of Sy), which is in accordance with the prediction provided by the radar classification using the selected descriptors (see section 4.6). Based on the radar classification, the ascending order of lignins according to the prospective yield for V and Sy by oxidation with O₂ in alkaline medium under the same conditions (pH, temperature, pO₂) were L_{Tob}O_{but} < L_{Tob}O_{ethan}.

Other phenolic compounds were also identified in the oxidation mixture in lower percentages: Hy, SA, VA, SO, and VO. Considering G-derivatives, the yield of VA and VO represent 49% to 55% and 16% to 20% of the maximum yield obtained for V, respectively. The proportion of SA and SO relative to the maximum yield of Sy was between 43% and 45% for SA and 16% and 20% for SO. The different reactivity of S and G units influences the time to maximum yield of Sy and V, and is lower for S-derivatives. These observations are in accordance with product profiles obtained by alkaline oxidation with O₂ of other lignins from different species and delignification processes (Pinto et al., 2011).

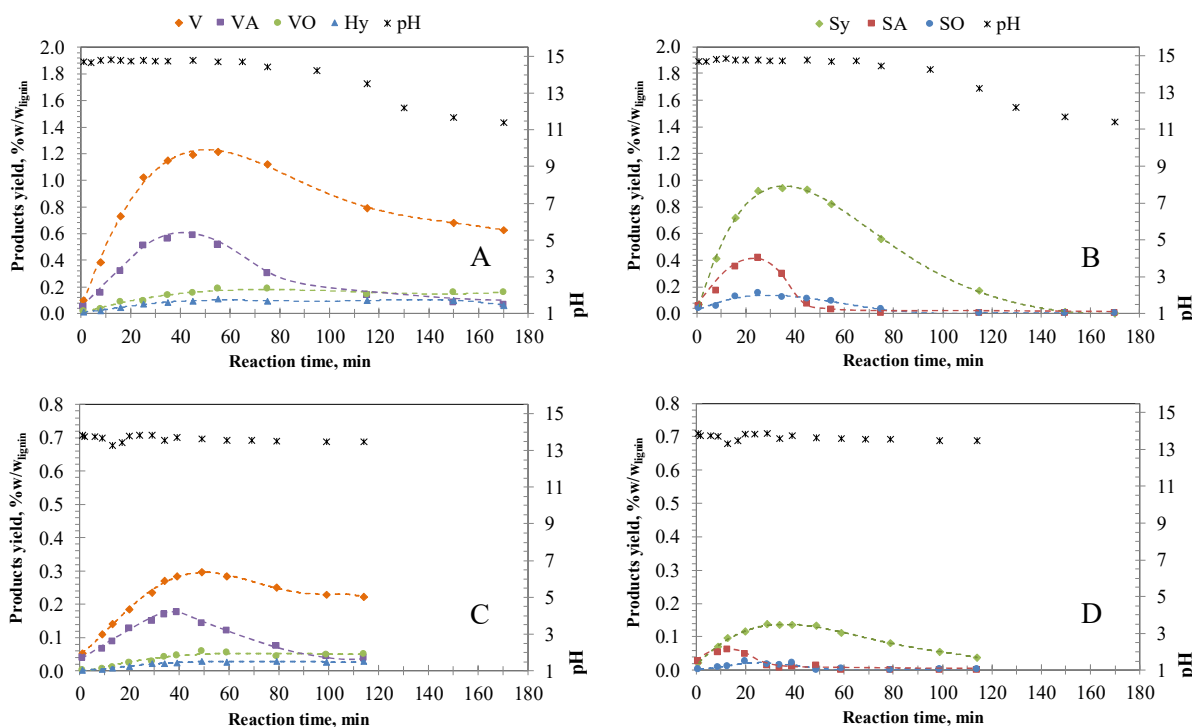


Figure 44 – Time evolution of monomeric products (V, VA, VO, Hy, Sy, SA, and SO) during the oxidation of LTobO_{ethan} (C and D) and LTobO_{but} (A and B). General conditions: 60 g/L of lignin, 2 M NaOH, $p_{O_2} = 3$ bar, $P_{total} = 9.8$ bar, $T_{initial} = 393$ K.

Oxidation with O₂ in alkaline medium of LTobO_{but} and LTobO_{ethan} under the same conditions has confirmed the qualitative differences of yields predicted by the radar classification. The radar classification of lignins can be adapted to include different or additional descriptors according to the application planned for the lignin being a useful predictive tool for product and process design.

5.7 REFERENCES

- Araújo, J.D. 2008. Production of vanillin from lignin present in the Kraft black liquor of the pulp and paper industry, in: *LSRE, Department of Chemical Engineering, Faculty of Engineering University of Porto*. Porto.
- Araújo, J.D.P., Grande, C.A., Rodrigues, A.E. Vanillin production from lignin oxidation in a batch reactor. *Chem. Eng. Res. Des.* 2010, 88, 1024-1032.
- Dardelet, S., Froment, P., Lacoste, N., Robert, A. Aldéhyde syringique: Possibilités de production à partir de bois feuillus. *Revue - A.T.I.P.* 1985, 39, 267-274.
- Fargues, C., Mathias, A., Rodrigues, A. Kinetics of vanillin production from kraft lignin oxidation. *Ind. Eng. Chem. Res.* 1996, 35, 28-36.

- Fisher, J.H., Marshall, B.H. 1951. Method of producing vanillin, Ontario Paper Company LTD United States.
- Gierer, J., Imsgard, F., Norén, I. Studies on the degradation of phenolic lignin units of the β -aryl ether type with oxygen in alkaline media. *Acta Chem. Scand.* 1977, B 31, 561-572.
- Gierer, J., Wännström, S. Formation of alkali-stable C-C-bonds between lignin and carbohydrate fragments during kraft pulping. *Holzforschung* 1984, 38, 181-184.
- Kim, D.-E., Pan, X. Preliminary study on converting hybrid poplar to high-value chemicals and lignin using organosolv ethanol process. *Ind. Eng. Chem. Res.* 2010, 49, 12156-12163.
- Krotschek, A.W., Sixta, H. 2008. Recovery. in: *Handbook of Pulp*, (Ed.) H. Sixta, Vol. 2, Wiley-VCH Verlag GmbH&Co. KGaA. Weinheim, Germany, pp. 967-994.
- Lisboa, S.A., Evtuguin, D.V., Neto, C.P., Goodfellow, B.J. Isolation and structural characterization of polysaccharides dissolved in *Eucalyptus globulus* kraft black liquors. *Carbohydr. Polym.* 2005, 60, 77-85.
- Marques, A.P., Evtuguin, D.V., Magina, S., Amado, F.M.L., Prates, A. Chemical composition of spent liquors from acidic magnesium-based sulphite pulping of *Eucalyptus globulus*. *J. Wood Chem. Technol.* 2009, 29, 322 - 336.
- Mathias, A.L. 1993. Produção de vanilina a partir da lenhina: Estudo cinético e do processo (in Portuguese language), in: *LSRE, Department of Chemical Engineering*, Faculty of Engineering University of Porto. Porto.
- Mathias, A.L., Rodrigues, A.E. Production of vanillin by oxidation of *Pine* kraft lignins with oxygen. *Holzforschung* 1995, 49, 273-278.
- Millero, F.J., Huang, F. Solubility of oxygen in aqueous solutions of KCl, K₂SO₄, and CaCl₂ as a function of concentration and temperature. *Journal of Chemical & Engineering Data* 2003, 48, 1050-1054.
- Pacek, A.W., Ding, P., Garrett, M., Sheldrake, G., Nienow, A.W. Catalytic conversion of sodium lignosulfonate to vanillin: Engineering aspects. Part 1. Effects of processing conditions on vanillin yield and selectivity. *Ind. Eng. Chem. Res.* 2013, 52, 8361-8372.
- Pascoal, N.C., E., B., D.V., E., A.J.D., S. Total fractionation and analysis of the organic components of industrial *Eucalyptus globulus* kraft black liquor. *Appita J.* 1999, 52, 213-217.

- Pinto, P.C., Borges da Silva, E.A., Rodrigues, A.E. Insights into oxidative conversion of lignin to high-added-value phenolic aldehydes. *Ind. Eng. Chem. Res.* 2011, 50, 741-748.
- Pinto, P.C.R., Borges da Silva, E.A., Rodrigues, A.E. 2012. Lignin as source of fine chemicals: Vanillin and syringaldehyde. in: *Biomass Conversion*, (Eds.) C. Baskar, S. Baskar, R.S. Dhillon, Springer Berlin Heidelberg, pp. 381-420.
- Pinto, P.C.R., Costa, C.E., Rodrigues, A.E. Oxidation of lignin from *Eucalyptus globulus* pulping liquors to produce syringaldehyde and vanillin. *Ind. Eng. Chem. Res.* 2013, 52, 4421-4428.
- Ryham, R. 1990. High solids evaporation of kraft black liquor using heat treatment. *TAPPI Engineering Conference*, Seattle Washington. pp. 677-681.
- Sales, F.G., Maranhão, L.C.A., Lima Filho, N.M., Abreu, C.A.M. Kinetic evaluation and modeling of lignin catalytic wet oxidation to selective production of aromatic aldehydes. *Ind. Eng. Chem. Res.* 2006, 45, 6627-6631.
- Santos S.G., Marques, A.P., Lima, D.L.D., Evtuguin, D.V., Esteves, V.I. Kinetics of eucalypt lignosulfonate oxidation to aromatic aldehydes by oxygen in alkaline medium. *Ind. Eng. Chem. Res.* 2011, 50, 291-298.
- Sixta, H., Potthast, A., Krottschek, A.W. 2008. Chemical pulping processes. in: *Handbook of Pulp*, (Ed.) H. Sixta, Vol. 1, Wiley-VCH Verlag GmbH&Co. KGaA. Weinheim, Germany, pp. 109-475.
- Tarabanko, V., Petukhov, D. Study of mechanism and improvement of the process of oxidative cleavage of lignins into the aromatic aldehydes. *Chemistry for Sustainable Development* 2003, 11, 655-667.
- Tarabanko, V.E., Pervishina, E.P., Hendogina, Y.V. Kinetics of aspen wood oxidation by oxygen in alkaline media. *React. Kinet. Catal. Lett.* 2001, 72, 153-162.
- Tarabanko, V.E., Petukhov, D.V., Selyutin, G.E. New mechanism for the catalytic oxidation of lignin to vanillin. *Kinet. Catal.* 2004, 45, 569-577.
- Tromans, D. Oxygen solubility modeling in inorganic solutions: concentration, temperature and pressure effects. *Hydrometallurgy* 1998, 50, 279-296.
- Tsutsumi, Y., Kondo, R., Sakai, K., Imamura, H. The difference of reactivity between syringyl lignin and guaiacyl lignin in alkaline systems. *Holzforschung* 1995, 49, 423-428.

6 Lignin fractionation by ultrafiltration

The aim of this chapter was to study the fractionation of *E. globulus* industrial kraft liquor by ultrafiltration. Ultrafiltration allows the separation of different lignin fractions with a specific molecular weight from the kraft liquor. Tubular membranes with nominal cut-offs of 50, 15 and 5 kDa were used. In the first step, the black liquor was filtered with the 50 kDa membrane. Permeate of this filtration was additionally fractionated with the 15 kDa membrane. In the last step, the permeate of the 15 kDa membrane was fractionated with the 5 kDa membrane. The differences between the composition of each resulting fraction were assessed by nitrobenzene oxidation and ^{13}C and ^{31}P NMR. In addition, the lignins in ultrafiltration fractions have been isolated by acid precipitation and studied by means of the same analytical techniques, being able to establish the differences in their composition and structural characteristics and subsequently their more adequate commercial application as high added-value products (chemical reactants, resins and biocomposites, antioxidants agents, etc.).

6.1 INTRODUCTION

Lignin is actually considered a product with potentially attractive applications from an economic and ecological point of view. However, its high structural diversity and also broad molecular weight distribution makes its commercial use a difficult task. Molecular mass is a key parameter affecting the reactivity and thermo-mechanical behavior of lignin; the molecular weight of lignin molecules can vary between 1,000 Da and 300,000 Da within a same sample (Tolbert et al., 2014; Toledano et al., 2010a). Fractionation has become one of the most effective methods to obtain relatively homogeneous lignin fractions, which makes possible to understand more easily its composition, structure, and its use as source of phenolic compounds (Cui et al., 2014).

In the literature, there are three main methods applied for lignin fractionation, which include sequential organic solvent extraction, selective precipitation, and membrane ultrafiltration (Cui et al., 2014; Toledano et al., 2010a). The membrane separation processes have been widely studied in the last years because its implementation is of great interest in several fields such as food, chemical, biological and pharmaceutical industries. These processes have all the necessary qualities to be key separation units in biorefineries because of their excellent fractionation capability, low chemical consumption and low energy requirement (Jönsson et al., 2008). Membrane technology can be used to extract diverse components from black liquor (Arkell et al., 2014). However, the extent or effectiveness of membrane technology depends on several operation conditions as the type of membrane used and the cut-off or particle size that it can retain as also the feed concentration and the flux (Humpert et al., 2016; Jönsson et al., 2008; Satyanarayana et al., 2000). Ultrafiltration allows obtaining lignin fractions with defined molecular weight distributions that vary in composition, chemical structure, and properties. In literature, it is demonstrated that lignin fractions obtained from membranes are less contaminated, since ultrafiltration allow removing carbohydrates and inorganic material, and show different amounts of phenolic hydroxyl groups, α -oxidized aromatics and carboxylic groups (Keyoumu et al., 2004; Sevastyanova et al., 2014). The obtained ultrafiltration lignin fractions with different molecular weight, composition and structural characteristics could be used for specific industrial applications as value-added products.

6.2 EXPERIMENTAL SECTION: MATERIALS AND METHODS

6.2.1 Kraft liquor

The industrial *Eucalyptus globulus* kraft liquor (KL) used in the ultrafiltration process was collected in a Portuguese pulp mill. The weak black liquor was taken before the evaporation unit and there was no liquor prefiltration before the ultrafiltration experiments.

6.2.2 Ultrafiltration equipment and experimental set-up

The experimental set-up used for the ultrafiltration experiments is shown in Figure 45. The cross flow ultrafiltration was carried out in a tubular membrane unit from Orelis, France, with a direct drive rotary vane pump (model PA1011, Fluid-O-Tech, Italy), a frequency inverter (MC07, Movitrac®B, Sew Eurodrive, Germany), an inlet and outlet pressure gauges filled with glycerin (Genebre, Spain), a feed tank, and a rotameter (Flowtech, China). The pump used is of positive displacement that operates maintaining the flowrate constant throughout the process.

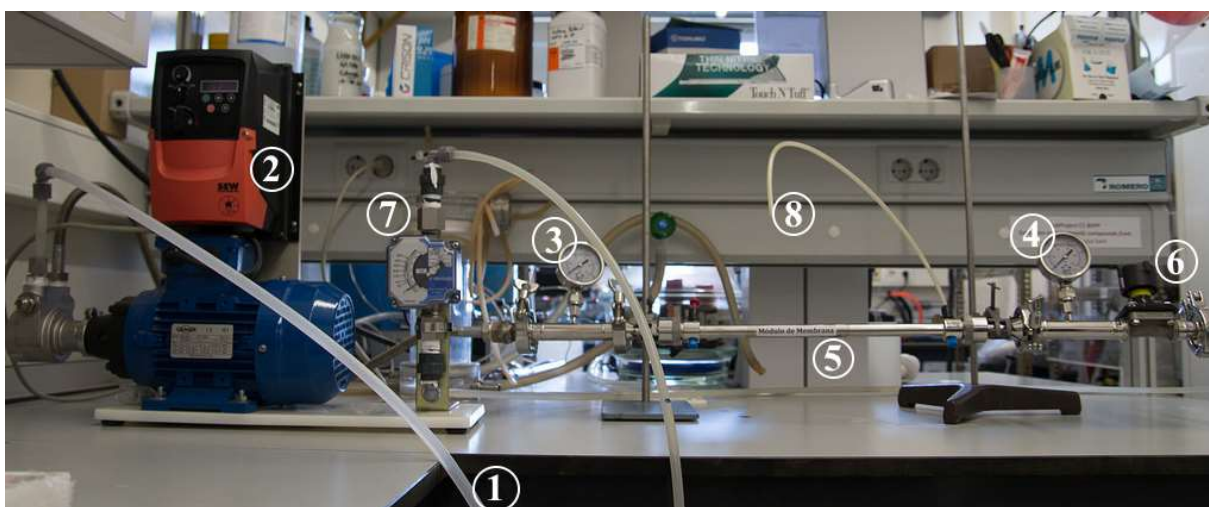


Figure 45 - Experimental set-up for cross-flow ultrafiltration in concentration mode: 1) feed tube, 2) direct drive rotary vane pump, 3) inlet pressure gauge, 4) outlet pressure gauge, 5) tubular membrane, 6) circulating valve; 7) rotameter, and 8) permeate collector tube.

The ultrafiltration unit withstands maximum operating pressure and temperature of 7 bar and 80 °C, respectively, and a maximum differential pressure of 4 bar. The permeate chamber holds a volume of 17 mL and the collector tube of permeate about 4 mL. Since the permeate side is open to the atmosphere there is no back pressure.

Three tubular ceramic membranes with molecular weight cut-off (molecular weight at which the membrane rejects 90% of solute molecules (Zabkova et al., 2007)) of 5, 15 and 50 kDa were used for the ultrafiltration experiments. All the membranes have 1 channel, 400 mm length, inside and external diameters of 6 and 10 mm, respectively, and a total effective area of 0.008 m². Membranes with a cut-off of 50 and 15 kDa have a zirconium dioxide (ZrO₂) active layer on a ceramic support composed with titanium dioxide-aluminium oxide (TiO₂-Al₂O₃) and were manufactured by CTI, Céramiques Techniques Industrielles (France) while the 5 kDa membrane (Filtanium™) has an active layer in TiO₂ on a patented ATZ (alumina-titania-zirconia) support composed with TiO₂-Al₂O₃-ZrO₂ and was manufactured by TAMI Industries (France). These membranes are suitable for the filtration of strong alkaline solutions with pH values until 14 at high pressures (maximum of 10 bar) and high temperatures.

All the experiments were carried out with a total recirculation of the feed solution. The feed solutions had a temperature in the range 18-30 °C during the ultrafiltration and the transmembrane pressure (TMP) was in the range 1.4-4.0 bar. The performance of each membrane before and after the experiments was evaluated in this study. All the generated lignin fractions were stored in the fridge prior to analyses and lignin isolation.

6.2.3 Composition of fractions and isolated lignins

The four fractions generated, retentates from 50, 15 and 5 kDa membranes ($R_{50\text{kDa}}$, $R_{15\text{kDa}}$ and $R_{5\text{kDa}}$) and permeate of 5 kDa membrane ($P_{5\text{kDa}}$), in addition to the rough black liquor were characterized concerning density, TDS, inorganic matter, carbohydrates and lignin content.

Each fraction was submitted to acidification with 5 M H_2SO_4 until pH 5 (see experimental procedure already described in section 5.2.2, Chapter 5) in order to isolate the corresponding lignin. The isolation process resulted in four hardwood kraft lignins ($LR_{50\text{kDa}}$, $LR_{15\text{kDa}}$, $LR_{5\text{kDa}}$, and $LP_{5\text{kDa}}$) in addition to the unfractionated lignin isolated directly from the kraft liquor (LKL).

The analyses of TDS, inorganic matter (ashes) and carbohydrates content were performed using the methods and conditions already described in section 5.2.3 (Chapter 5).

6.2.4 Nitrobenzene oxidation

Freeze-dried liquor and fractions and isolated lignins were submitted to alkaline NO as already described in section 3.2.5.1 (Chapter 3) concerning reaction conditions and products analysis.

6.2.5 NMR analysis

Sample preparation, conditions and equipment parameters used in ^{13}C and ^{31}P NMR analyses were the same as already described in a previous section of this thesis - section 3.2.5 (Chapter 3).

6.2.6 Gel permeation chromatography (GPC)

Molar mass analyses have been performed on a HPLC system, previously described in section 3.2.5.1 (Chapter 3), using UV detection set to 268 nm. Two Agilent gel columns placed in series were used: an OligoPore column 300x7.5 mm with nominal particle size of 6 μm that measures molecular weights up to 4,500 $\text{g}\cdot\text{mol}^{-1}$ and a MesoPore column 300x7.5 mm with nominal particle size of 3 μm that measures molecular weights up to 25,000 $\text{g}\cdot\text{mol}^{-1}$. A guard

column Oligopore 50x7.5 mm was assembled prior to the columns. GPC analyses were performed at 70 °C with a flowrate of 0.8 mL.min⁻¹ and employing an isocratic mobile phase of dimethylformamide (DMF) with 0.5% w/v of lithium chloride (LiCl). The system was calibrated with 10 polystyrene molecular weight standards ranging from 162 to 4910 g.mol⁻¹. For GPC analyses about 5 mg.mL⁻¹ of each polystyrene standard and isolated lignin were dissolved in the mobile phase solvent; lignins were stirred and filtered through a 0.2 µm syringe filter before injection.

6.3 ULTRAFILTRATION PROCESS

6.3.1 Water membrane permeability

Water permeability of each membrane was obtained by measuring deionized water permeate flowrate for different values of TMP (Pa). The TMP was adjusted by the circulating valve of the system (Figure 45) and corresponds to the average of membrane inlet and outlet pressure.

The permeate flux, J (m³.s⁻¹.m⁻²), for each TMP is calculated as following:

$$J = \frac{Q_p}{A_m} \quad (9)$$

where Q_p (m³.s⁻¹) is the permeate flowrate measured for a certain TMP and A_m is the effective membrane surface area (0.008 m²). Temperature was monitored and the permeate flowrate corrected for 25 °C. Assays were performed with a feed flowrate of 210 L.h⁻¹.

Water permeate flux (J_w) was determined using new membranes allowing to obtain the membrane hydraulic resistance coefficient (R_m , m⁻¹) by applying the Darcy's law:

$$J_w = \frac{\text{TMP}}{\mu_0 R_m} \quad (10)$$

where μ_0 (Pa.s) is the viscosity of water at 25 °C.

Membrane permeability coefficient (L_p , m³.s⁻¹.m².Pa⁻¹) to water is obtained from the slope of the graphical representation of J_w vs. TMP. It represents the amount of feed crossing the membrane per time unit, per membrane area unit and TMP unit. This coefficient will be used to determine the initial membrane permeability recovery through each cleaning cycle.

The variation of the water permeate flux, calculated from equation (10), for each TMP is represented in Figure 46 considering 5, 15 and 50 kDa membranes before the ultrafiltration process.

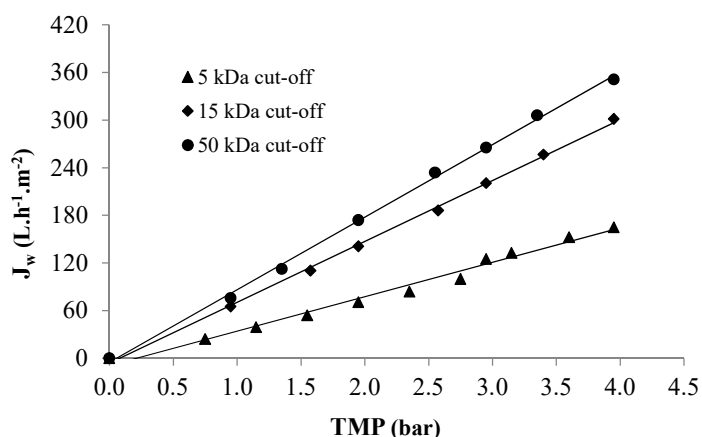


Figure 46 - Water permeate fluxes through the ceramic membranes for different TMP at 25 °C, flowrate set to 210 L.h⁻¹ and a membrane surface area of 0.008 m².

It is possible to observe that the water permeate flux increased with the increase of TMP for all the membranes. The membranes with higher cut-off show higher values of water permeability than lower cut-off membranes.

6.3.2 Permeate flux

Kraft liquor was submitted to ultrafiltration sequence with three different tubular ceramic membranes with cut-offs of 50, 15 and 5 kDa, as shown in Figure 47.

During the fractionation sequence in concentration mode the kraft liquor was filtered successively increasing the membrane cut-off. A starting volume of 9.5 L of hardwood (*E.globulus*) weak black liquor was processed. At the end, four different lignin fractions were obtained in addition to the original weak black liquor: R_{50kDa}, R_{15kDa}, R_{5kDa}, and P_{5kDa}.

For all the experiments the retentate flowrate was initially fixed between 210 and 280 L.h⁻¹, the TMP was in the range 1.4-4.0 bar and the operating temperature were 26 ± 4 °C except for 15 kDa membrane that have an initial processing temperature lower than 20 °C.

In the first step, KL was processed with the highest membrane cut-off, 50 kDa, which resulted in a volume reduction (VR, permeate volume divided by initial feed volume) of 0.63, which means that the kraft liquor volume was reduced so that about 37% remained as retentate, and a volume concentration factor (VCF) of 2.7 (initial feed volume divided by the retentate volume). In the second stage, the resulting permeate stream from the first step (P_{50kDa}) was further fractionated using the 15 kDa cut-off membrane, which resulted in a VR of 0.72 corresponding to a VCF of 3.6. Finally, the permeate from the second step (P_{15kDa}) was further fractionated with a membrane having a 5 kDa cut-off, which resulted in a VR of about 0.44 and a VRF of 1.8.

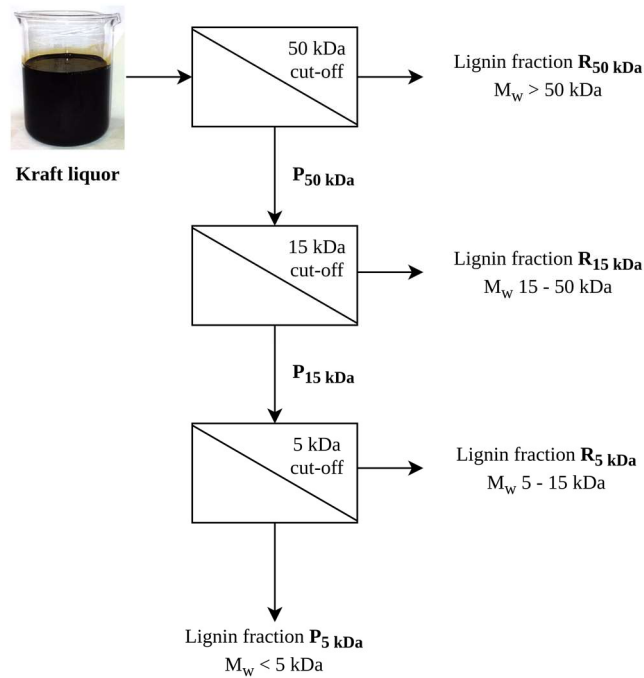


Figure 47 – Schematic representation of the sequential fractionation of the kraft liquor performed with 5, 15 and 50 kDa membranes.

The permeate flux behavior with time observed during the ultrafiltration sequence for each membrane was graphically represented in Figure 48. For 50 and 5 kDa membrane stages the flux decreased during processing time. Moreover, the performance of the 5 kDa membrane presents a sharp decrease of the initial flux during the first 2 hours of operation reaching a final permeate flux of $6.46 \text{ L}\cdot\text{m}^{-2}\cdot\text{h}^{-1}$ after 36 hours of processing. This rapid initial decline of flux was caused by the fast membrane pore blocking followed by the formation and growth of a cake layer, adsorption and concentration polarization (Humpert et al., 2016). In the case of 50 kDa membrane, through Figure 48C, it was observed a slight decrease of the initial permeate flux that could be related with the high molecular weight fraction present in black liquor that also form a cake layer at the membrane surface, causing a flux reduction. Dafinov et al. studied the filterability of rough black liquor via ceramic ultrafiltration membranes with molecular weight cut-off of 1, 5 and 15kDa; they also observed a strong flux decrease due to the formation of a gel layer on the membrane surface (Dafinov et al., 2005).

In processing with 15 kDa membrane it was observed a slight increase in their flux in the first hour of processing that represents a different performance to that observed for the other two membranes. This is a consequence of the feed solution ($P_{5\text{kDa}}$) temperature in the beginning of the processing that was lower than $20 \text{ }^\circ\text{C}$; the consequent increase of the temperature with the processing time caused a slight increase in the flux. The relation between the operating temperature and the flux was already stated in the literature. Arkell et al. studied lignin separation process from softwood black liquor by membrane filtration and found that ceramic membranes exhibited lower

retention when the ultrafiltration proceed at high temperatures since it leads to a better diffusion of the feed solution through the membrane and consequently higher fluxes (Arkell et al., 2014).

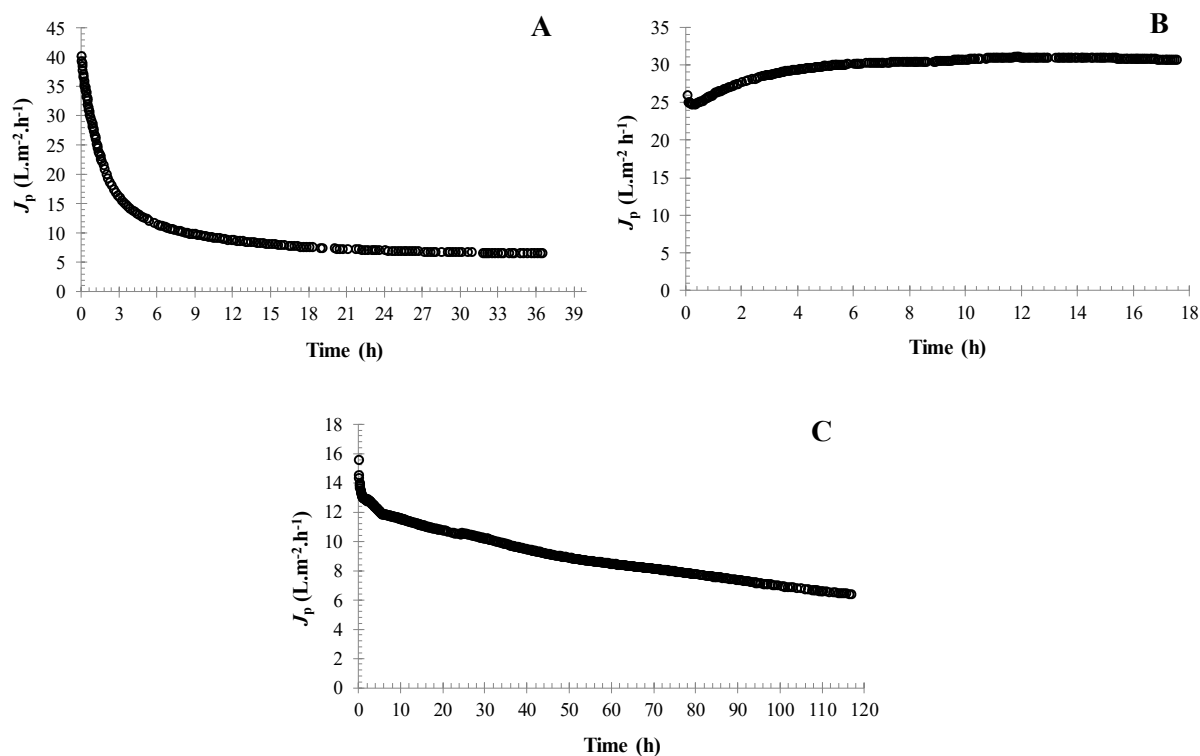


Figure 48 - Permeate flux behavior with operating time obtained for the processing with the 5 kDa (A), 15 kDa (B) and 50 kDa (C) membranes.

The permeate flux, calculated from equation (9), in the beginning and at the end of the processing with each membrane is presented in Table 37.

Table 37 - Initial and final fluxes of 50, 15 and 5 kDa membranes.

Membrane cut-off	Initial flux ($L \cdot m^{-2} \cdot h^{-1}$)	Final flux ($L \cdot m^{-2} \cdot h^{-1}$)
50 kDa	15.5	6.36
15 kDa	26.0	30.7
5 kDa	40.2	6.46

The initial flux was higher when concentrating ultrafiltration permeates from 50 kDa and 15 kDa membranes than when concentrating the untreated black liquor. The initial flux was $15.5 L \cdot m^{-2} \cdot h^{-1}$ when using 50 kDa membrane for the concentrating of rough black liquor. For the lower cut-offs membranes, 15 and 5 kDa, the initial flux was about 26 and 40 $L \cdot m^{-2} \cdot h^{-1}$, respectively.

The higher initial flux obtained when processing with the 5 kDa membrane ($40.2 L \cdot m^{-2} \cdot h^{-1}$) could be related to the fact that higher molecules had already been removed from the black liquor

by the ultrafiltration with 50 and 15 kDa membranes, showing the importance of a membrane sequence in the process productivity. Jönsson and their co-workers also found, in a work about concentration and purification of lignin in hardwood kraft liquor by ultrafiltration and nanofiltration, that a high dry solids content of the feed solution resulted in low flux (Jönsson et al., 2008).

6.3.3 Membrane fouling and cleaning

Membrane fouling is defined as an irreversible formation of deposits on the active surface of a membrane, causing a decline flux and a loss of performance (Satyanarayana et al., 2000). The filtration of black liquor is prone to fouling and this becomes a significant factor in the context of industrial processes. Therefore, effective cleaning strategies are necessary to reduce the rate of fouling and prolong the life of membranes. In this work the cleaning of ceramic membranes after filtration of black liquor and permeates was carried out by using NaOH solutions of 0.1 M and 0.2M at 40 °C for about 1 hour followed by rinsing with deionized water until neutral pH. The water fluxes before and after the filtration using the 50, 15 and 5 kDa membranes are depicted in Table 38. The water flux is seen as a measure of the efficiency of the cleaning process.

Table 38 - Water permeability obtained after and before the ultrafiltration using the 5, 15 and 50 kDa cut-off membranes, at 25 °C and flowrate set to 210 L.h⁻¹.

Membrane cut-off	L_p before (L.h ⁻¹ .m ⁻²)	L_p after (L.h ⁻¹ .m ⁻²)
50 kDa	89.7	76.2
15 kDa	74.5	70.3
5 kDa	39.4	34.7

The water permeability recovery (expressed in %) was determined for each membrane following the equation:

$$R(\%) = \frac{L_{p,\text{after}}}{L_{p,\text{before}}} \times 100 \quad (11)$$

where $L_{p,\text{after}}$ (L.m⁻².h⁻¹.bar⁻¹) corresponds to the water permeability of the membrane after the processing and the cleaning process and $L_{p,\text{before}}$ (L.m⁻².h⁻¹.bar⁻¹) corresponds to the initial permeability of the membrane.

For 15 kDa membrane, the water flux was restored to 94% of the initial value, while for 50 and 5 kDa membranes the cleaning was restored for 85 and 88% of the pure water flux, respectively. According to Satyanarayana et al. an irreversible fouling depends on feed solution-membrane interaction and also on the extent of washing (Satyanarayana et al., 2000). Moreover,

they confirm that a very efficient cleaning protocol may restore the original permeability of the membrane, if the feed solution-membrane interaction is very weak (Satyanarayana et al., 2000).

6.4 COMPOSITION AND STRUCTURE OF FRACTIONS AND ISOLATED LIGNINS

This study is focused on the correlation between the molecular weight cut-off of membranes and the molecular weight of lignin fractions, their composition, structure, and properties. It is well known that along with the molecular weight characteristics of lignin, its purity and structure are key factors that determine their utilization in different value-added applications. In this work, carbohydrate and inorganic material content were determined in order to evaluate the purity of the lignin fractions and isolated lignins. NO and NMR analyses were also performed on isolated lignins. The kraft liquor and the corresponding isolated lignin were also characterized for comparison.

6.4.1 Composition of ultrafiltration fractions

The composition with respect to TDS, density, carbohydrates, and inorganics of the different fractions obtained from the ultrafiltration of kraft liquor are shown in Table 39. The inorganics and carbohydrates contents were determined in the freeze-dried fractions and liquor.

Table 39 - Composition of the kraft liquor and the different fractions (retentates and permeate) obtained from the ultrafiltration process; values presented in %w/w.

	kraft liquor	lignin fraction			
		R50kDa	R15kDa	R5kDa	P5kDa
pH	12.7	12.4	12.1	11.5	11.4
Density (kg/m ³)	1.09	1.10	1.09	1.09	1.07
Total dissolved solids (TDS)	17.6	20.9	16.5	15.7	12.1
Inorganic matter (%w/w)*	49.1	42.5	51.8	55.2	64.6
Carbohydrates (%w/w)*	4.02	8.37	1.27	1.24	0.69
Lignin (%w/w)*	46.9	49.1	46.9	43.6	34.7

* Inorganic matter, carbohydrates and lignin contents referred to TDS.

A graphic representation of the composition of each fraction as well as the kraft liquor considering the percentage of inorganic material, carbohydrates and lignin (all referred to TDS) is shown in Figure 49.

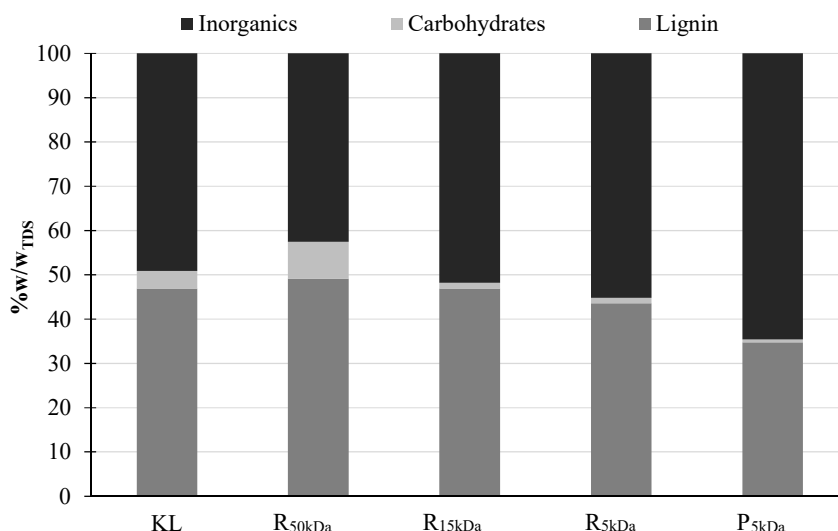


Figure 49 – Composition of lignin fractions obtained from the processing of kraft liquor with 50, 15 and 5kDa ceramic membranes.

As expected, the percentage of TDS decreased as the cut-off was smaller. Density data also corroborate this observation. On the other hand, the content of inorganics referred to the TDS increases along with the decrease of the membrane cut-off. This is related with the high fraction of inorganics of low molecular weight that pass through the membranes of lower cut-offs. It is also possible to observe that in general, the percentage of inorganic matter in lignin fractions and kraft liquor was higher than the organic matter (lignin content). According to the literature, the high content of inorganics is related with cooking chemicals accumulated during the pulping process (Toledano et al., 2010a; Zinovyev et al., 2016). From pH it can be seen that all the fractions are alkaline mainly due to kraft process conditions. It is also observed a slightly decrease in the pH with the liquor processing.

For lignin content, similar percentages were obtained in R_{50kDa}, R_{15kDa} and R_{5kDa} fractions and also in kraft liquor (KL), in the range 44-49 %W/W_{solids}. Permeate from 5 kDa membrane presents the lowest lignin content (35 %W/W_{solids}) confirming that there is a preferential retention of lignin in this membrane.

Carbohydrates presented a similar behavior to that found for TDS, with a decrease of the total sugar content in the fractions obtained from the lower membrane cut-off, membrane of 5 kDa. On the other hand, the fraction R_{50kDa} presents the highest content of carbohydrates. This is supported by literature where some authors referred that the carbohydrates are linked to highest molecular mass fraction of the kraft lignin (Brodin et al., 2009). All of these observations confirm that ultrafiltration is not only a fractionation process and could be also used as purification process.

6.4.2 Composition of isolated lignins

Lignins were isolated directly from ultrafiltration fractions as well as from rough kraft liquor by acid precipitation with yields of 66, 92, 64, 29, and 7.5% for LKL, LR_{50kDa}, LR_{15kDa}, LR_{5kDa}, and LP_{5kDa}, respectively. The isolation yields were calculated with reference to the TDS on the respective fractions and liquor.

Despite the isolation process, all the isolated lignins include contaminants, mainly inorganic compounds and carbohydrates. The contaminants contribution, in %w/w_{isolated material}, found for each lignin (LKL, LR_{50kDa}, LR_{15kDa}, LR_{5kDa}, and LP_{5kDa}) is depicted in Table 40.

Table 40 – Contaminants content of isolated lignins, presented as %w/w_{isolated material} (dry weight).

	isolated lignins				
	LKL	LR _{50kDa}	LR _{15kDa}	LR _{5kDa}	LP _{5kDa}
Inorganic matter (%w/w _{isolated material})	37.5	44.5	20.1	18.7	11.8
Carbohydrates (%w/w _{isolated material})	3.51	8.20	0.32	0.29	0.20

The evaluation and comparison of lignins content in each fraction and in the correspondent isolated material is shown in Figure 50.

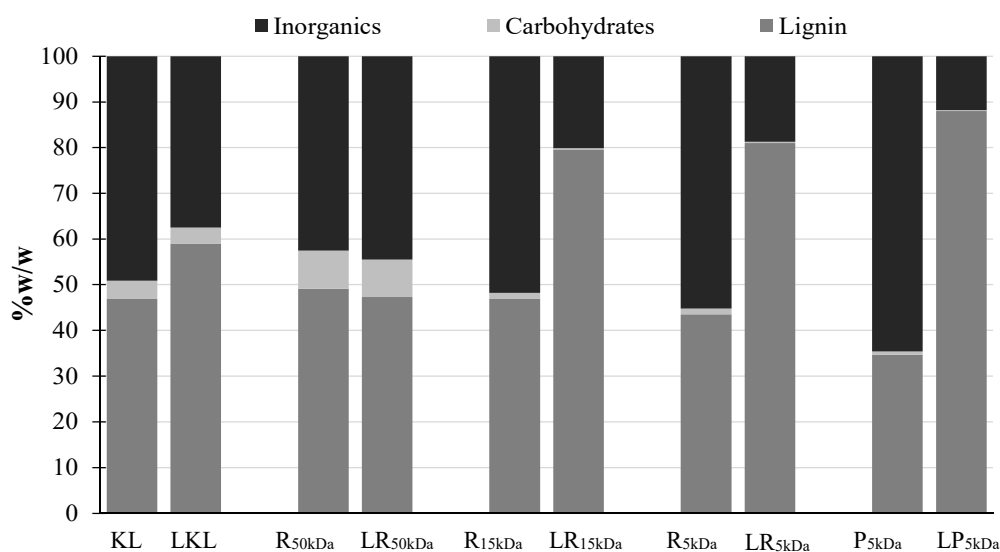


Figure 50 - Composition of fractions, in %w/w_{TDS}, and isolated lignins, referred to %w/w_{isolated material}, obtained from the ultrafiltration process of kraft liquor.

The resulting material from the isolation process of R_{15kDa}, R_{5kDa} and P_{5kDa} are almost composed by lignin (80–88%), but in the case of R_{50kDa} and even KL this value is about 47% of the isolated material.

The results show that lignin content increased with the cut-off decrease reaching a maximum of 88% in LP_{5kDa}. Moreover, it is possible to observe that the isolation process leads to a final material with lower content of inorganics and carbohydrates than the ultrafiltration fractions, except for LR_{50kDa}. This lignin shows a similar content of contaminants in the isolated lignin and in the corresponding fraction before isolation. The difference between lignin and inorganics content in isolated lignins and in the corresponding fractions is related with the molecular weight of the contaminants. In the lower molecular weight fractions the contaminants are dissolved and removed with the supernatant during the isolation process and only the high molecular weight fragments/compounds precipitated along with lignin. As expected, low molecular weight lignin fractions result in less contaminated lignins. This is in accordance with previous studies (Helander et al., 2013; Sevastyanova et al., 2014). It is also reasonable to infer that the carbohydrates found in LR_{50kDa} could be part of LCC that are large size complexes and consequently are retained in lower cut-off membranes. Considering the isolated lignins from R_{15kDa}, R_{5kDa} and P_{5kDa} there is no significant differences between their carbohydrates content.

6.4.3 Nitrobenzene oxidation of isolated lignins

The aim of NO is to evaluate the relative proportion between the aromatic moieties H, G and S in the non-condensed fraction of lignin. Results are based on the yields and types of simple phenolic aldehydes and acids produced in the oxidation. Condensation degree is inversely correlated with NO total yield because aryl–aryl covalent linkages are resistant to the depolymerization induced by NO. The evaluation of this parameter is important since the frequency of C-C linkages is also inversely related with lignin reactivity.

The yield of NO products, Hy, V, Sy, VA, and SA, are reported on total lignin weight free of ashes and carbohydrates, as depicted in Table 41. Therefore, the results refer to lignin and allow a direct comparison and evaluation of ultrafiltration process.

Table 41 - Yields of monomeric phenolic products obtained by NO of isolated lignins from ultrafiltration fractions.

lignin	products, % w/w _{lignin} *					
	Hy	VA	SA	V	Sy	total yield
LKL	0.13	0.34	2.79	2.58	10.5	16.3
LR _{50kDa}	0.18	0.34	2.60	2.30	8.84	14.3
LR _{15kDa}	0.10	0.35	3.14	2.42	10.2	16.2
LR _{5kDa}	0.10	0.40	3.24	2.42	10.3	16.4
LP _{5kDa}	0.13	0.40	3.26	2.62	11.0	17.4

* reported to nonvolatile solids weight after deducting ashes and carbohydrates.

The main oxidation products are Sy and SA proving that all the lignins show a predominance of S units. Total yields on lignin basis are in the range 14.3–17.4% for isolated lignins. LP_{5kDa} present a lower fraction of condensed structures and consequently a higher NO yield than the other isolated lignins. LR_{15kDa} and LR_{5kDa} show the closest values among all the lignins; LR_{50kDa} denotes the lowest NO yield, confirming the presence of the highest content of high molecular weight condensed lignin fragments in this fraction.

6.4.4 NMR analysis of isolated lignins

6.4.4.1 ¹³C NMR

NMR was carried out in order to obtain important information about the chemical structure of the isolated lignins from ultrafiltration fractions. Lignins were analysed by ¹³C NMR, following the approach and calculations already detailed in section 3.4.2 (Chapter 3) concerning the application of these spectroscopic methods to *E. globulus* lignins.

The main functional groups, linkages and structures identified and quantified in isolated lignins are depicted in Table 42. The ¹³C NMR spectrum of each lignin is shown in Figure 51.

Table 42 - Assignments and quantification (number per aromatic ring) of the structures/linkages and functional groups identified by ¹³C NMR for isolated lignins from ultrafiltration fractions.

assignments (spectroscopic range)	amount (number per aromatic ring)				
	LKL	LR _{50kDa}	LR _{15kDa}	LR _{5kDa}	LP _{5kDa}
C _β in β-5 and β-β structures (δ 51.0-53.8 ppm)	0.12	0.19	0.13	0.11	0.14
Aromatic OCH ₃ (δ 54.3-57.3 ppm)	1.29	1.06	1.42	1.43	1.55
C _γ in β-O-4 structures without C _α =O (δ 59.3-60.8 ppm)	0.14	0.16	0.13	0.11	0.13
C _γ in β-5 and β-O-4 structures with C _α =O; C _γ in β-1 (δ 62.5-63.8 ppm)	0.12	0.11	0.06	0.05	0.06
C _α in β-O-4 structures; C _γ in pinosresinol/syringaresinol and β-β structures (δ 70.0-76.0 ppm)	0.65	0.65	0.35	0.29	0.36
C _β in β-O-4 structures; C _α in β-5 and β-β structures (δ 80.0-90.0 ppm)	0.38	0.37	0.32	0.29	0.37
Aromatic C _{Ar} -H (δ 103.0-123.0 ppm)	1.93	1.85	1.92	1.95	1.93
Aromatic C _{Ar} -C (δ 123.0-137.0 ppm)	1.64	1.86	1.76	1.81	1.67
C ₄ in H units (δ 157.0-162.0 ppm)	0.06	0.06	0.05	0.03	0.06
CHO in benzaldehyde structures (δ 191.0-192.0 ppm)	0.02	0.05	0.02	0.03	0.01
CHO in cinnamaldehyde structures (δ 193.5-194.5 ppm)	0.02	0.05	0.02	0.03	0.03

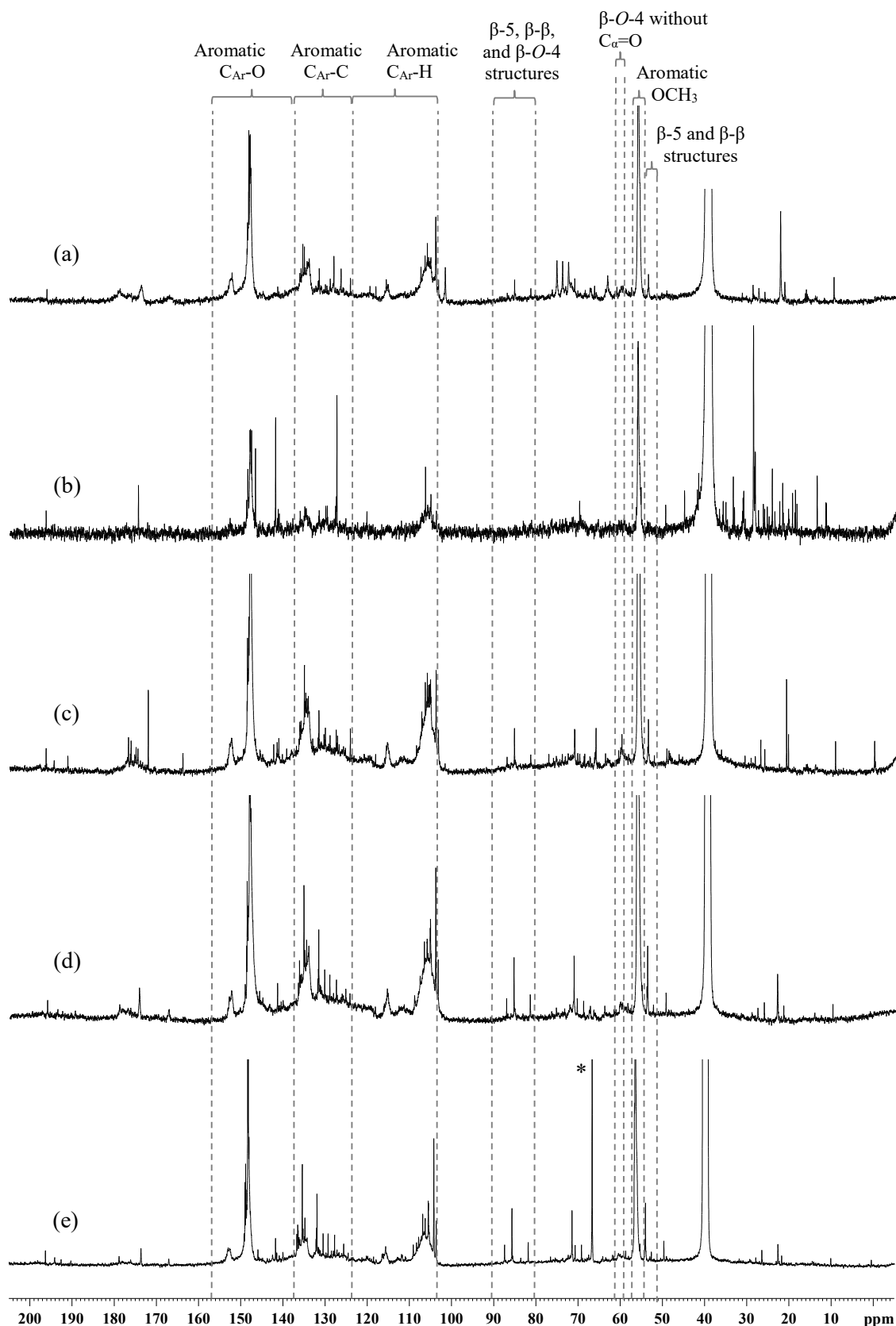


Figure 51 - Quantitative ^{13}C NMR spectra of (a) LKL, (b) LR_{50kDa}, (c) LR_{15kDa}, (d) LR_{5kDa}, and (e) LP_{5kDa} (in DMSO-d₆; * solvent peak (Hugo et al., 1997)).

The quantitative data from ^{13}C NMR also enables the determination of the main structural characteristics of each lignin (Table 43): content of β -O-4 structures (number per 100 aromatic rings), DC (degree of condensation in percentage) and S:G:H ratio.

Table 43 - β -O-4 structures content (number per 100 aromatic rings), DC and S:G:H ratio found for isolated lignins.

Lignins	β -O-4 structures	DC (%)	S:G:H
LKL	26	35	65:29:06
LR _{50kDa}	18	49	59:34:07
LR _{15kDa}	20	34	67:27:06
LR _{5kDa}	17	33	69:28:03
LP _{5kDa}	23	31	69:25:06

It can be noted that the isolated lignins from ultrafiltration fractions as well as from kraft liquor have higher content of S units than G units. The proportion of S structures and the ratio S/G of the isolated lignins slightly increase with cut-off decrease suggesting that the relative contents of S and G units in the different lignin fractions varied proportionally to lignin molecular weight.

In lignins, the number of C–C bonds between units could also have relation with the lignin molecular weight, mainly to the structures involving C₅ in the aromatic ring. G-type units are able to form this type of bonds, but this is not possible in S-type units as they have both C₃ and C₅ positions substituted by methoxyl groups (Alriols et al., 2010; Toledano et al., 2010a). As consequence, lignins mostly composed by G units and consequently with lower S/G ratio are expected to show high fractions of high molecular weight than those presenting high contents of S units. From ^{13}C NMR results it can be seen that LR_{50kDa}, the lignin with higher fractions of high molecular weight, shows the lowest content of S units and lowest S/G ratio, in opposition to the lignin with lower molecular weight, LP_{5kDa}. Aromatic OCH₃ content also confirms the decrease trend of lignins S/G ratio with the molecular weight: LP_{5kDa} > LR_{5kDa} \approx LR_{15kDa} > LKL > LR_{50kDa}.

In the side-chain region, different signals could be observed in the ultrafiltration fractions spectra that corresponds to classical lignin substructures such as β -O-4 and β -5; however, β -O-4 are the main linkage identified, although chemical shift in NMR spectra attributed to C α , C β or C γ in these structures have always interference of carbons from other environments. The content of β -O-4 structures found for the ultrafiltration fractions as well as the kraft liquor is between 17 and 26 per 100 ppu, denoting that the cleavage of these linkages is one of the main reactions in the delignification process. However, there is not a clear trend between β -O-4 content and the different cut-off membranes.

As already confirmed by NO total yields (Table 41) the lignin isolated from P_{5kDa} shows the highest content of uncondensed structures; ^{13}C NMR results also confirm this conclusion since this

lignin shows the lowest content of condensed structures, achieved by the low value of C_{Ar}-C structures, and DC. On the other hand, it can be concluded that LR_{50kDa} is the lignin with more condensed structures, noted by the highest DC value that is in accordance with the highest value of C_{Ar}-C linkages and also the lowest fraction of noncondensed structures evaluated by the low NO total yield of this lignin.

6.4.4.2 ³¹P NMR

Detailed quantitative ³¹P NMR data of isolated lignins are shown in Table 44; identification and quantification was performed as described in section 3.4.3 (Chapter 3). The spectrum of each lignin is presented in Figure 52. It was not possible to perform the ³¹P NMR analysis of the sample LR_{50kDa}; the high amount of inorganics in this lignin did not allow its dissolution in the NMR solvents.

From the data presented in Table 44 it is possible to conclude that high molecular weight lignins (LR_{15kDa} and LR_{5kDa}) contain larger amounts of phenolic structural units. Aliphatic, condensed and non-condensed phenolic units decrease as the membrane cut-off is smaller and consequently as the molecular weight lignin was lower.

Table 44 - Assignments and quantification of phenolic and aliphatic hydroxyl groups and carboxylic acids in lignins by ³¹P NMR.

Assignments	amount (mmol/g lignin)			
	LKL	LR _{15kDa}	LR _{5kDa}	LP _{5kDa}
Aliphatic OH	3.59	4.11	2.38	1.35
Carboxylic acids	2.34	3.33	0.46	0.59
Total phenolic units	7.72	18.9	14.1	6.56
Condensed phenolic units	2.05	3.75	2.38	0.99
Non-condensed phenolic units				
S phenolic units	4.59	11.8	9.85	4.51
G phenolic units	1.04	3.25	1.77	1.05
H phenolic units	0.04	0.12	0.05	0.01

The results show that the high molecular weight lignin fractions (R_{15kDa} and R_{5kDa}) have the highest content of total and aliphatic phenolic units, proving that these types of OH units are present in the structures and/or fragments with high molecular weight mainly retained in these fractions. The low molecular weight lignin fractions, on the other hand, probably preserved less side chains and more β-O-4 linkages, and hence exhibit less free phenolic groups and aliphatic hydroxyls. LP_{5kDa} also shows the lowest content of condensed phenolic units what is in accordance with the highest yield of monomeric phenolic products in the non-condensed fraction of this lignin, found by NO. The content of carboxylic groups was also affected by the fractionation. Isolated

lignins obtained from the lowest cut-off membrane (R_{5kDa} and P_{5kDa}) were found to contain small amounts of these functional groups.

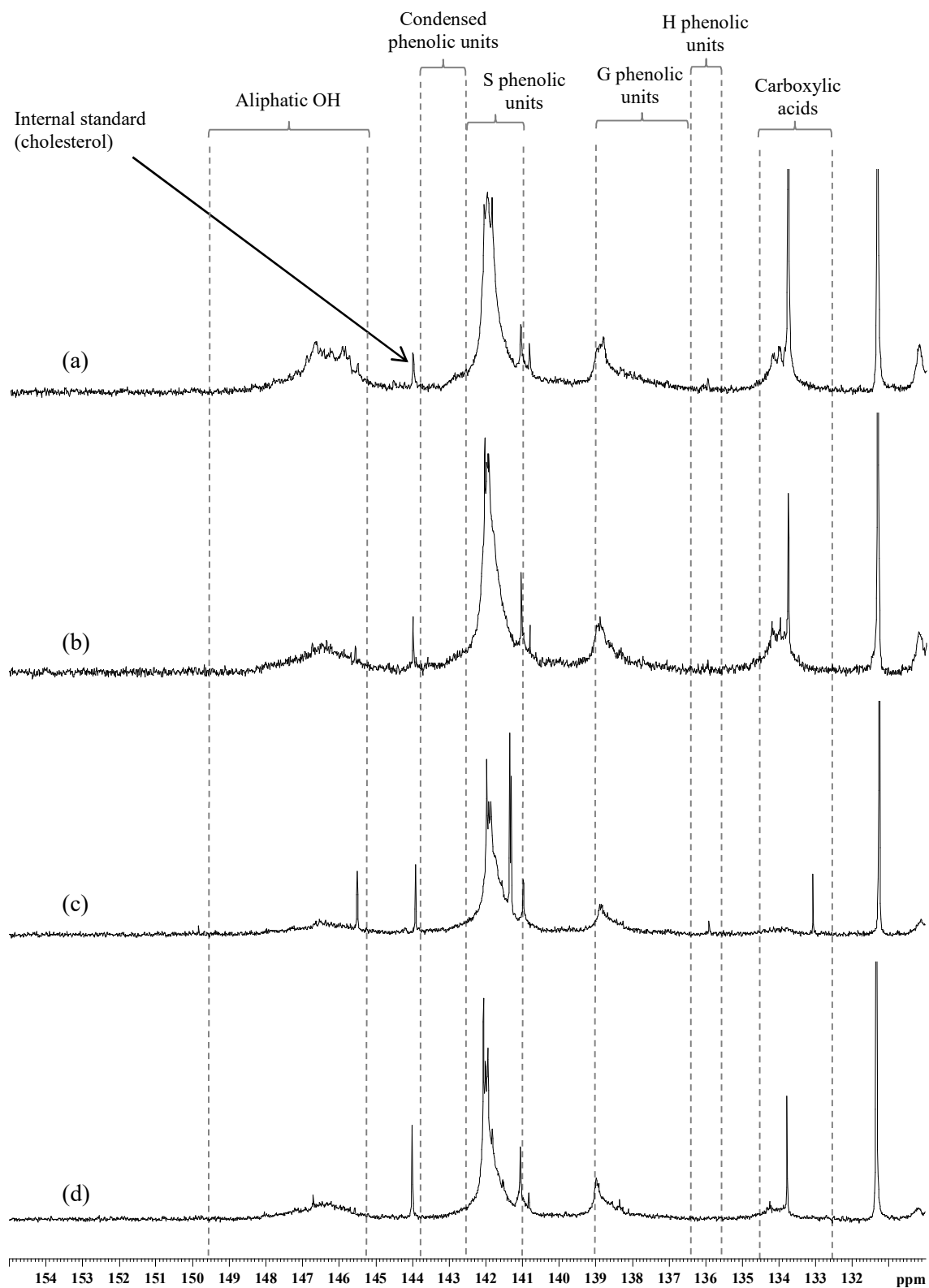


Figure 52 - Quantitative ^{31}P NMR spectra (δ 155-130 ppm) of phosphitylated lignins: (a) LKL, (b) LR_{15kDa} , (c) LR_{5kDa} , and (d) LP_{5kDa} (in $CDCl_3$).

Data from ^{31}P NMR clearly demonstrate that there was a direct relation between the obtained isolated lignins from ultrafiltration fractions and its functionality. Moreover, high functionality implies high reactivity of obtained lignin fractions; a significant number of phenolic groups in kraft lignins provides high reactivity and thus makes the lignin an attractive product for utilization in various applications (Sevastyanova et al., 2014).

6.4.5 Molecular weight distribution of isolated lignins by GPC

The molecular weight distribution of the lignins isolated from the ultrafiltration fractions and the black liquor was determined using GPC. In Figure 53 GPC chromatograms of lignins were normalized to unity and overlaid. Weight-average (Mw) and number-average (Mn) molecular weight and also the polydispersity index (Mw/Mn) of each lignin are shown in Table 45.

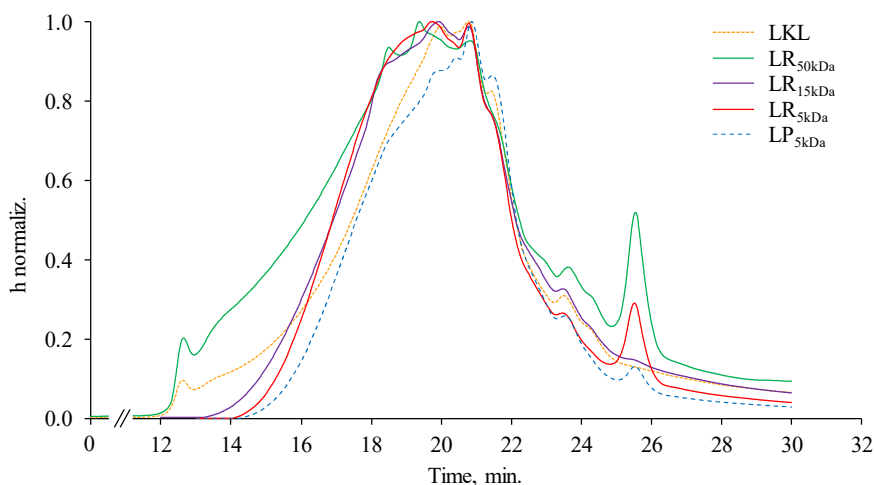


Figure 53 – Normalization of molecular weight distribution curves obtained by GPC analyses of isolated lignins; analyses were performed at 70 °C and a flow rate of 0.8 mL.min⁻¹ using DMF with LiCl 0.5%.

In this work the obtained values are relative to polystyrene standards. It is important to point out that without suitable standards for GPC calibration the analysis of lignins only provides relative molecular weight values. Moreover, structural differences between linear polymer standards and branched lignin macromolecules are a known source of error in the determination of molecular weight (Ringena et al., 2006). The lack of standardization and the difficulties associated with accurate lignin molar weight determination were already stated in previous studies in literature (Baumberger et al., 2007; Constant et al., 2016; Lin and Dence, 1992; Sevastyanova et al., 2014). The determination of the molecular weight by GPC strongly depends on the experimental set-up used, including the type of column and eluent, as well as on the calibration standards, lignin pretreatment, and methods applied for molecular weight determination, including peak integration approach and chromatogram corrections (Constant et al., 2016; Sevastyanova et al., 2014).

Figure 53 shows that the chromatographic profiles of isolated lignins progressively shift from low elution volumes to higher ones upon successive decrease of membranes cut-off. From the data presented in Table 45 it is possible to observe a clear trend of the decrease of the Mw and Mn values of the isolated lignins as the membranes cut-off used was smaller. Furthermore, it is also observed a decrease of the polydispersity with the pore-size.

Table 45 - Weight-average (Mw) and number-average (Mn) molecular weight and polydispersity (Mw/Mn) of isolated lignins analysed by GPC.

Lignins	Mw (g.mol ⁻¹)	Mn (g.mol ⁻¹)	Mw/Mn
LKL	10323	8768	1.19
LR _{50kDa}	12029	9577	1.26
LR _{15kDa}	9576	8335	1.15
LR _{5kDa}	9641	8552	1.13
LP _{5kDa}	8879	8030	1.11

Polydispersity of isolated fractions was reduced as a result of fractionation, indicating that ultrafiltration results in more homogeneous materials with narrower molecular weight distributions, as already found by other authors (Brodin et al., 2009; Toledano et al., 2010a). According to Toledano and their co-workers the polydispersity could also be related with the content of G units of lignins; the authors found that if the G content increases the polydispersity follows the same behavior (Toledano et al., 2010a). As already found through ¹³C NMR results (section 6.4.4.1), the S/G ratio in the different isolated lignins decrease as the cut-off and consequently the lignin molecular weight was greater (Figure 54).

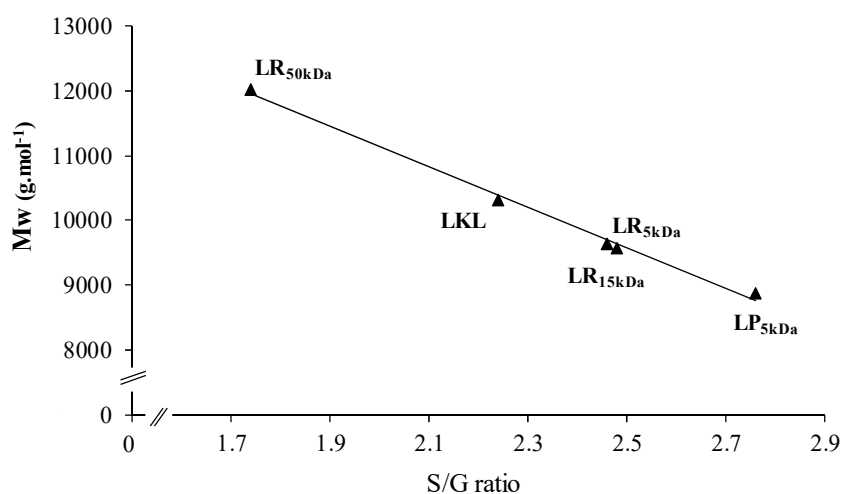


Figure 54 - Plot of Mw (g.mol⁻¹) versus S/G ratio, from ¹³C NMR, obtained for ultrafiltration fractions and kraft liquor.

LR_{50kDa} shows the lowest S/G ratio and the highest value of polydispersity, what is coherent with the presence of higher fractions of high molecular weight in this lignin.

The molecular weight distribution curve for LR_{5kDa} lignin (Figure 53) shows a peak in the low molecular weight region that corresponds to a high elution time. The same peak was found in the LP_{5kDa} lignin, with lower intensity. The presence of these similar lignin fragments in both samples, albeit in different intensities, indicated that small amounts of low molecular weight fragments are present in these lignin fractions. On the other hand, in LKL and LR_{50kDa} chromatograms is observed a peak in a very high molecular weight region. This peak could correspond to LCC, since these lignins have the highest amount of carbohydrates, as shown in Table 40 and discussed in section 6.4.2. The presence of these peaks is in accordance with lignins molecular weight distribution obtained by other authors (Humpert et al., 2016; Sevastyanova et al., 2014; Toledano et al., 2010a). However, it is difficult to compare the obtained Mn and Mw values with the data available in the literature since the molecular weight distribution of kraft lignins is strongly dependent upon the isolation procedure, the nature of the lignin samples and the uncertainties related to the GPC analysis itself, as already stated in this section.

As referred previously, the reactivity of lignins with high fractions of low molecular weight have different applications than those with high molecular weight due to the different reactivity. In literature it has been reported that lignins with high fraction of low molecular weight are suitable to be used as an extender or as component of phenol-formaldehyde resins because of their high reactivity, in comparison with lignins with high percentages of high molecular weight molecules (Ahvazi et al., 2016; Toledano et al., 2010a; Toledano et al., 2010b).

6.5 RADAR CLASSIFICATION OF ISOLATED LIGNINS FROM ULTRAFILTRATION FRACTIONS

The values of the key parameters selected for radar representation of isolated lignins were depicted in Table 41 and Table 43. The radar plots of isolated lignins are presented in Figure 55.

Radar plots confirm the structural differences found in the previous sections for the isolated lignins. The representation of isolated lignin key descriptors allows to observe that the permeate obtained from the membrane cut-off of 5 kDa benefits from its higher intensity of β -O-4 linkages and NCS when compared with the other lignins. The high content of these types of structures leads to a higher reactivity of this lignin; consequently, LP_{5kDa} stands out as a better choice for oxidative depolymerization, since it shows the higher aptitude to produce phenolic aldehydes, as V and Sy. On the other hand, LR_{50kDa} stands out as the lignin with lower potential to produce phenolic monomers, mainly due to its high content of condensed structures.

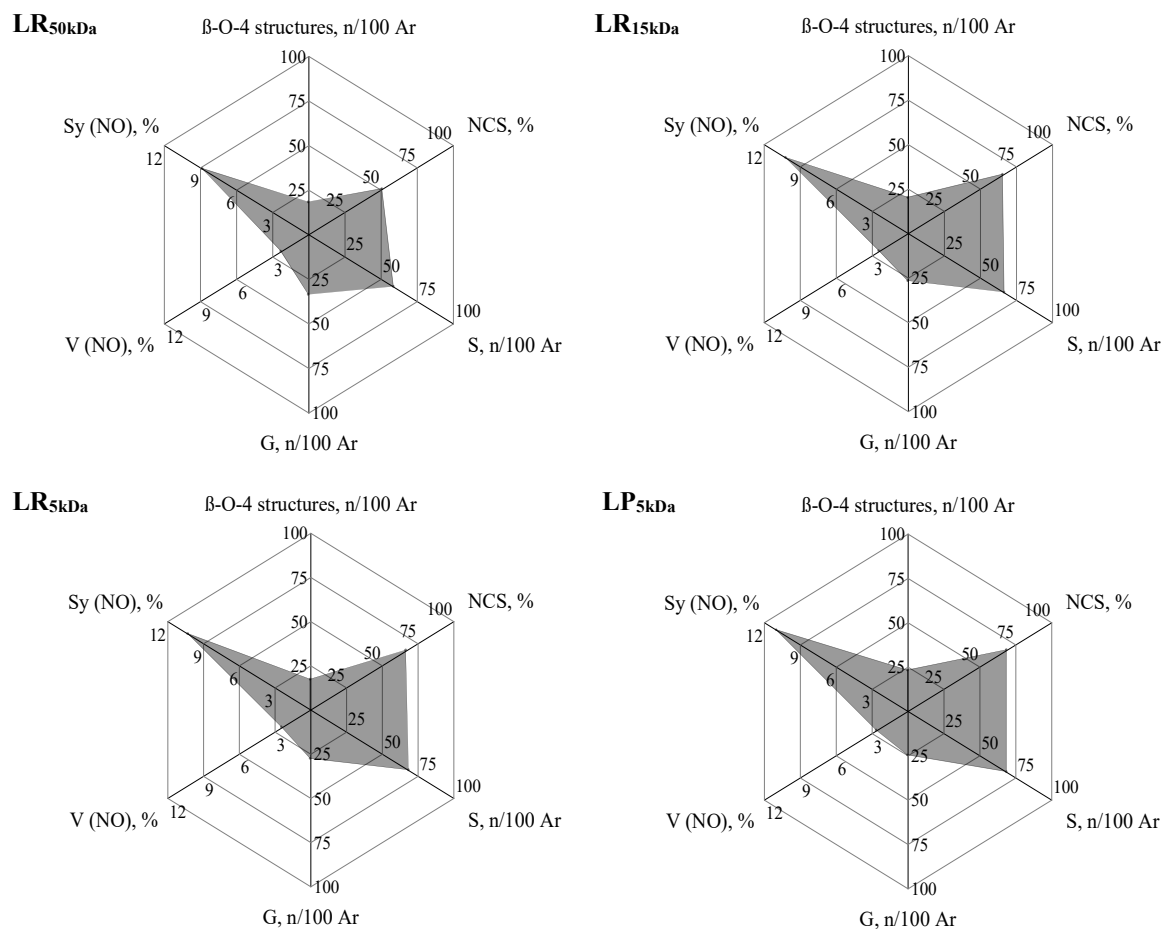


Figure 55 - Radar classification for lignins isolated from fractions obtained from the ultrafiltration of *E. globulus* kraft liquor.

6.6 CONCLUSIONS

Ultrafiltration showed to be an effective technique for lignin fractionation and allowed to find that kraft lignin in black liquor is nonhomogeneous not only with respect to its molecular weight, but also with respect to the frequency of functional groups. Selecting the right cut-off of the membrane, the weight-average molecular weight could be controlled as confirmed by the data obtained by GPC. The obtained ultrafiltration fractions presented lower polydispersity than kraft liquor, especially the lowest molecular weight fraction, suggesting that the ultrafiltration process led to more homogeneous materials with narrower molecular weight distributions. The lignins isolated from 5 and 15 kDa membranes fractions were less contaminated with carbohydrates and inorganic content. Furthermore, the lignins from permeate and retentate of 5 kDa membrane present a fraction of low molecular weight that is not visible in the other isolated lignins. The R_{50kDa} fraction is a highly contaminated fraction, with a high amount of inorganic material and also higher content of carbohydrates. The isolated lignin from this fraction shows a similar tendency, being the

lignin with lower purity. The different retention observed between lignin and carbohydrates also provides a mean of separating these two components by ultrafiltration. It was also found that increasing molecular size, the different lignin fractions tend to exhibit an increasing number of total phenolic and aliphatic hydroxyl groups. By NO it was found that LP_{5kDa} shows the highest content of uncondensed structures; ¹³C NMR results also confirm this conclusion since this lignin shows the lowest content of condensed structures and DC percentage.

The ultrafiltration lignin fractions with different molecular weight and structural characteristics could be used for specific industrial applications as value-added products. Lignins with higher molecular weight and more contaminated could be considered for usage as dispersant or as chelating agent. Lignin fractions with lower molecular weight could be used as adhesives where low molecular weight and purity are important factors to take into account. This type of lignins could also represent an important source of phenolic monomers, as V and Sy, through oxidative depolymerization.

6.7 REFERENCES

- Ahvazi, B., Cloutier, É., Wojciechowicz, O., Ngo, T.D. Lignin profiling: A guide for selecting appropriate lignins as precursors in biomaterials development. *ACS Sustainable Chemistry & Engineering* 2016, 4, 5090-5105.
- Alriols, M.G., García, A., Llano-Ponte, R., Labidi, J. Combined organosolv and ultrafiltration lignocellulosic biorefinery process. *Chem. Eng. J.* 2010, 157, 113-120.
- Arkell, A., Olsson, J., Wallberg, O. Process performance in lignin separation from softwood black liquor by membrane filtration. *Chem. Eng. Res. Des.* 2014, 92, 1792-1800.
- Baumberger, S., Abaecherli, A., Fasching, M., Gellerstedt, G., Gosselink, R., Hortling, B., Li, J., Saake, B., de Jong, E. 2007. Molar mass determination of lignins by size-exclusion chromatography: towards standardisation of the method. in: *Holzforschung*, pp. 459-468.
- Brodin, I., Sjöholm, E., Gellerstedt, G. 2009. Kraft lignin as feedstock for chemical products: The effects of membrane filtration. in: *Holzforschung*, pp. 290-297.
- Constant, S., Wienk, H.L.J., Frissen, A.E., Peinder, P.d., Boelens, R., van Es, D.S., Grisel, R.J.H., Weckhuysen, B.M., Huijgen, W.J.J., Gosselink, R.J.A., Bruijninx, P.C.A. New insights into the structure and composition of technical lignins: A comparative characterisation study. *Green Chemistry* 2016, 18, 2651-2665.

- Cui, C., Sun, R., Argyropoulos, D.S. Fractional precipitation of softwood kraft lignin: Isolation of narrow fractions common to a variety of lignins. *ACS Sustainable Chemistry & Engineering* 2014, 2, 959-968.
- Dafinov, A., Font, J., Garcia-Valls, R. Processing of black liquors by UF/NF ceramic membranes. *Desalination* 2005, 173, 83-90.
- Helander, M., Theliander, H., Lawoko, M., Henriksson, G., Zhang, L., Lindström, M.E. Fractionation of technical lignin: molecular mass and pH effects. *Bioresources* 2013, 8, 2270-2282.
- Hugo, E.G., Vadim, K., Abraham, N. NMR chemical shifts of common laboratory solvents as trace impurities. *J. Org. Chem.* 1997, 62, 7512-7515.
- Humpert, D., Ebrahimi, M., Czermak, P. Membrane technology for the recovery of lignin: A Review. *Membranes* 2016, 6, 42.
- Jönsson, A.S., Nordin, A.-K., Wallberg, O. Concentration and purification of lignin in hardwood kraft pulping liquor by ultrafiltration and nanofiltration. *Chem. Eng. Res. Des.* 2008, 86, 1271-1280.
- Keyoumu, A., Sjö Dahl, R., Henriksson, G., Ek, M., Gellerstedt, G., Lindström, M.E. Continuous nano- and ultra-filtration of kraft pulping black liquor with ceramic filters: A method for lowering the load on the recovery boiler while generating valuable side-products. *Ind. Crop. Prod.* 2004, 20, 143-150.
- Lin, S.Y., Dence, C.W. *Methods in lignin chemistry*; Springer-Verlag, 1992.
- Ringena, O., Lebioda, S., Lehnen, R., Saake, B. Size-exclusion chromatography of technical lignins in dimethyl sulfoxide/water and dimethylacetamide. *J. Chromatogr. A* 2006, 1102, 154-163.
- Satyanarayana, S.V., Bhattacharya, P.K., De, S. Flux decline during ultrafiltration of kraft black liquor using different flow modules: A comparative study. *Sep. Purif. Technol.* 2000, 20, 155-167.
- Sevastyanova, O., Lange, H., Crestini, C., Dobele, G., Helander, M., Chang, L., Lindström, M.E. 2014. Selective isolation of technical lignin from the industrial side-streams - structure and properties. *NWBC - Nordic Wood Biorefinery Conference*, Stockholm.

- Tolbert, A., Akinosho, H., Khunsupat, R., Naskar, A.K., Ragauskas, A.J. Characterization and analysis of the molecular weight of lignin for biorefining studies. *Biofuels, Bioproducts and Biorefining* 2014, 8, 836-856.
- Toledano, A., García, A., Mondragon, I., Labidi, J. Lignin separation and fractionation by ultrafiltration. *Sep. Purif. Technol.* 2010a, 71, 38-43.
- Toledano, A., Serrano, L., Garcia, A., Mondragon, I., Labidi, J. Comparative study of lignin fractionation by ultrafiltration and selective precipitation. *Chem. Eng. J.* 2010b, 157, 93-99.
- Zabkova, M., Borges da Silva, E.A., Rodrigues, A.E. Recovery of vanillin from lignin/vanillin mixture by using tubular ceramic ultrafiltration membranes. *J. Membr. Sci.* 2007, 301, 221-237.
- Zinovyev, G., Sumerskii, I., Korntner, P., Sulaeva, I., Rosenau, T., Potthast, A. Molar mass-dependent profiles of functional groups and carbohydrates in kraft lignin. *J. Wood Chem. Technol.* 2016, 1-13.

7

Final conclusions and suggestions for future work

7.1 FINAL CONCLUSIONS

The lignins characterization accomplished in this thesis led to the identification and quantification of different functional groups and interunit linkages that would be related with the ability to produce functionalized aldehydes. Several lignins from different species, morphological parts of the same species and subjected to different delignification processes were studied through their composition in inorganic material and sugars and characterized by NO, NMR, and FTIR spectroscopy.

The structural characterization of industrial *E. globulus* lignins from kraft and organosolv process showed a higher DC and a lower NO yield than mild acidolysis lignin, demonstrating that the delignification process induces significant structural transformations in lignins. The structural transformations are more accentuated in lignin from kraft process; kraft pulping increases degradation reactions and consequently reduces lignin potential to produce phenolic monomers. Lignin from wood and bark of *E. globulus* were also studied. These two lignins do not show noteworthy differences for the main types and contents of interunit linkages and functional groups, demonstrating that *E. globulus* lignins structure from wood and bark are similar. The overall results showed that organosolv process would be a preferable process to obtain lignin from *E. globulus* wood or bark when the objective is the valorization towards production of functionalized aldehydes.

The characterization of *in situ* and mild acidolysis lignins from two morphological parts (stalks and roots) of corn, cotton, sugarcane, and tobacco showed that the differences found between species exceeded the differences between morphological parts confirming the lignin specificity of each species. These results have an important contribution to the diversification of the biomass feedstock supply for bio-based products and for the design of effective deconstruction strategies for biorefinery purposes.

Taking advantage of all the results about lignins structural characterization, a radar classification tool was established for screening industrial or pre-industrial lignins for their potential as sources of Sy and V. Radars are an important tool for the design of processes to convert the agro-industrial waste materials into lignin-based high added-value products, since they are developed from key descriptors that may demystify the complexity of lignin and direct process variable selection to achieve maximum valorization of lignin.

The evaluation of the potential of *E. globulus* lignin as source of Sy and V was also studied through the oxidation with O₂ in alkaline medium of lignins from two pulping processes (kraft and sulfite) and three kraft liquor processing stages. The results showed that sulfite liquor is the raw-material with better performance toward oxidation considering the production of Sy and V. Among kraft liquors, weak kraft liquor shows higher potential than the concentrated kraft liquors.

However, using isolated lignin from this liquor as the raw material for oxidation, an increment in Sy and V yields were achieved. Oxidation with O₂ in alkaline medium was also performed in two tobacco lignins from butanol and ethanol organosolv under the same conditions and the results confirmed the qualitative differences of yields predicted by the radar classification. Based on the radar classification, the tobacco lignin from ethanol organosolv process showed higher production of V and Sy.

A kinetic study of V and Sy production from alkaline oxidation with O₂ of tobacco organosolv lignin was also carried out. The effect of process parameters (temperature, *p*O₂, lignin initial concentration) on the yield of V and Sy was evaluated; moreover, the kinetic parameters of the lignin oxidation process to produce these phenolic monomers were also achieved.

The ultrafiltration showed to be an effective technique for lignin fractionation and has demonstrated that kraft lignin in black liquor is nonhomogeneous not only with respect to its molecular weight, but also with respect to the quantity of functional groups. As the molecular size increase, the different lignin fractions tend to exhibit an increasing number of total phenolic and aliphatic hydroxyl groups. Membranes with lower cut-off led to lignin fractions with lower content of contaminants and also lower polydispersity. The set of results from ultrafiltration studies are particularly important in the field of lignin valorization since the lignin fractions obtained, with different molecular weight and structural characteristics, once optimized, could be used for specific industrial applications as added-value products.

Finally, the results presented in this thesis together with the on-going activities of different research groups worldwide will contribute to the better knowledge about lignin and the development of economical viable lignin valorization routes for the production of value-added chemicals and products.

7.2 SUGGESTIONS FOR FUTURE WORK

As already stated all over this thesis, lignin is one of the main constituents in lignocellulosic biomass and is nowadays available in large quantities as a pulp and paper industries by-product. Lignin polymer has valuable properties for numerous potential applications that could represent several economic and environmental benefits. However, lignin complex and highly non-uniform structure is a huge challenge for its efficient valorization. Adding to its inherent complexity, the structure of native lignin depends strongly on the plant species and could present local and seasonal variations; moreover, the pretreatment or pulping process performed on lignocellulosic material also causes considerable changes in the native lignin structure. Considering all these variation sources the ideal compromise is to select a lignin type and an isolation process adapted to the best lignin structure and properties required for a particular application.

7.2.1 Lignin as a polymer component

Currently, the majority of lignin is valorized in energy recovery streams by burning the black liquors in the pulp production industry, and only a small amount is isolated from spent pulping liquor and commercialized (about 2%), despite the existence of a great number of potential applications of high added-value. The application of lignin in biomaterials has been long considered for manufacturing of polymers, phenol formaldehyde resins, rubber compounds, carbon fibers, and a variety of chemicals, all currently sourced from petroleum (Figure 56).

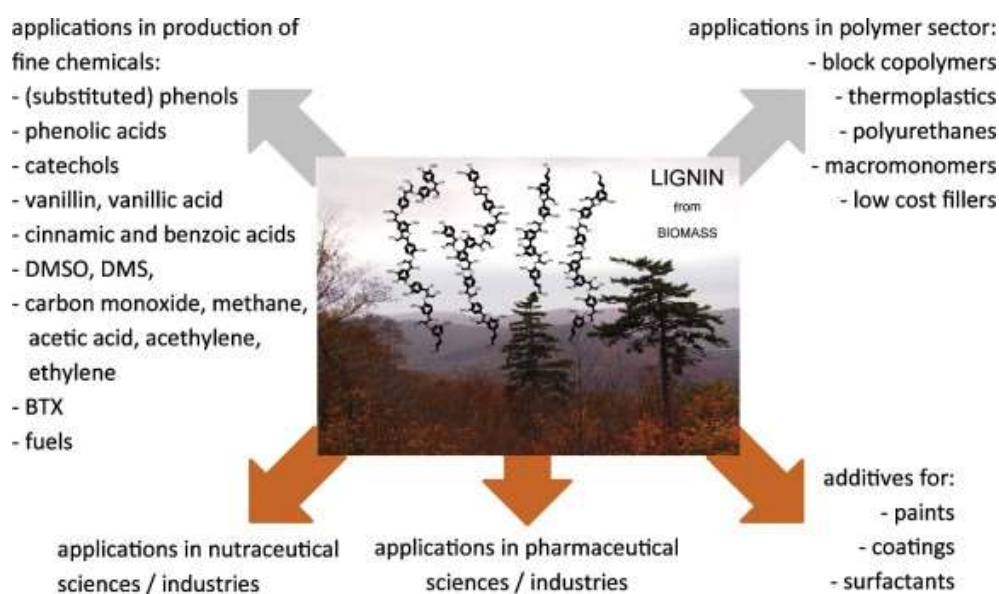


Figure 56 - Potential applications of lignin as renewable resource from biomass (DMSO - dimethyl sulfoxide; DMS - dimethyl sulfide; BTX - benzene, toluene, xylene) (Lange et al., 2013)

Particularly, lignin is a promising compound to be used in polymers due to its phenolic base structure, which could lead to an improvement of the mechanical properties when incorporated in a plastic. Lignin derivatives could be used to functionalize different polymers which have different applications in a variety of fields such as films and coatings formation, adhesive resin, plastic and rigid foam formation. However, lignin incorporation in polymers is not limited only by the reactivity of its various chemical, composition and functional groups but rather by other complex factors such as solubility, molecular weight, rheology, dispersity, and morphology (Ahvazi et al., 2016).

The control of lignin functionality appears to be one of the most important challenges for the development of this type of value-added materials. Detailed and precise knowledge of the macromolecular structure of lignin and their initial functional groups content will be the key to study their reactivity.

The incorporation of lignin into polymers has been intensively investigated in order to improve the mechanical properties of copolymers or environmental behavior of formulations (Cateto et al., 2008; Faruk and Sain, 2015; Laurichesse and Avérous, 2014; Mahmood et al., 2016). Several studies have revealed that rigid polyurethane foams obtained from lignin-based polyols present insulating properties, dimensional stability, and accelerated aging properties very similar to those prepared with commercial counterparts. Moreover, it was also proved that the natural properties of lignin will also contribute to an improvement of moisture and flame resistance (Cateto et al., 2009).

Some applications in polymers synthesis can afford a direct use of lignin, without any need for chemical modifications. In these cases, lignin could be directly incorporated into polymers formulations due to the presence of aliphatic and aromatic hydroxyl groups in the structure as the reactive sites. However, native lignin has much lower reactivity not only because it has less reactive sites, but also because the reactive positions of the macromolecule of lignin or its fragments have lesser accessibility due to the steric hindrance (Mahmood et al., 2016). While some potential applications can afford a direct use of lignin without any need for chemical modifications, many polymer applications require a previous functionalization of the lignin macromolecule in order to improve their reactivity. The reactivity of lignin is evaluated based on distinct structural features: the presence of free ortho position on the phenolic ring, the presence of multiple OH groups, and their ability for various chemical modifications (Duval and Lawoko, 2014). An effective way to improve lignin's reactivity is through depolymerization into oligomeric products with reduced molecular weight and increased content of hydroxyl groups, facilitating their utilization in bio-polymers preparation (Duval and Lawoko, 2014).

A study conducted by Mahmood and co-workers evaluated the effect of process parameters on the overall yield and molecular weight of lignin fragments obtained by depolymerization via hydrolysis (Mahmood et al., 2013). The effect on the mechanical and thermal characteristics of the polymeric materials with the incorporation of lignin before and after the depolymerization was also studied by these authors. The authors have verified that the direct incorporation of kraft lignin in polyurethane foams improves the mechanical characteristics of rigid polyurethane foams. However, the lignin percentage increase to above 30% had a negative effect on the foam rigidity. The authors also found that the percentage of bioreplacement in polyurethane foams could be improved if lignin was previously depolymerized, that results in the production of bio-polymers with lower Mw and better reactivity. Depolymerized products were effectively utilized for the preparation of rigid bio-based polyurethane foams without any modification achieving 50% of polymers replacements. The resulting foams showed good mechanical and thermal characteristics with improved physical and thermal stability compared with commercial foams (Mahmood et al., 2013). These results are quite

motivating, providing emphasis to the need for further research in this field allowing lignin valorization through its incorporation into polymeric materials.

7.2.2 Future research lines

A starting point for a future research line will include a study of an efficient process of depolymerization of a selected lignin in order to achieve specific lignin fragments to be used and valorized as precursors on polymeric materials. The lignin depolymerization process selected will be the oxidation with O₂ in alkaline medium, taking advantage of all the experience and work accomplished during this thesis in this field. Lignin oxidation will be conducted with controlled reaction conditions (temperature, pressure, alkaline charge) in order to obtain fragments of molecular weight within specified intervals with suitable characteristics that could be used according to the final applications. The ultrafiltration process will be worked up for the separation of the different oxidation products. It is well known that many polymer properties such as glass transition temperature, modulus and tensile strength are directly dependent upon their molecular weights. It is also important to differentiate between the aliphatic (primary or secondary) and the phenolic hydroxyls (condensed or non-condensed) content present in the lignin macromolecules resulting from oxidation, since these functional groups have direct influence in their reactivity. Moreover, a complete and comprehensive chemical and physical characterization of lignins and the resulting oxidation products should be attained.

A next step will be focused in the improvement of lignin depolymerization through catalytic oxidation. The use of catalysts, mainly transition metal salts, has been referred to increase the yields of the oxidation products. However, in this case the effect of the catalytic oxidation of lignin in the reactivity and functionality of the resulting macromolecules should be also studied; this promising research field was not explored so far.

All of these research lines could be considered important evaluators of lignin physical and chemical structural characteristics aimed to identify the better properties in view of partial and/or complete substitution of petroleum-based polymers during the production of biomaterials. Value-added utilization of lignins is critical for the accelerated development and deployment of the biorefinery.

7.3 REFERENCES

- Ahvazi, B., Cloutier, É., Wojciechowicz, O., Ngo, T.D. Lignin profiling: A guide for selecting appropriate lignins as precursors in biomaterials development. *ACS Sustainable Chemistry & Engineering* 2016, 4, 5090-5105.
- Cateto, C.A., Barreiro, M.F., Rodrigues, A.E., Belgacem, M.N. Optimization study of lignin oxypropylation in view of the preparation of polyurethane rigid foams. *Ind. Eng. Chem. Res.* 2009, 48, 2583-2589.
- Cateto, C.A., Barreiro, M.F., Rodrigues, A.E., Brochier-Salon, M.C., Thielemans, W., Belgacem, M.N. Lignins as macromonomers for polyurethane synthesis: A comparative study on hydroxyl group determination. *J. Appl. Polym. Sci.* 2008, 109, 3008-3017.
- Duval, A., Lawoko, M. A review on lignin-based polymeric, micro- and nano-structured materials. *React. Funct. Polym.* 2014, 85, 78-96.
- Faruk, O., Sain, M. Lignin in polymer composites; Elsevier Science, 2015.
- Lange, H., Decina, S., Crestini, C. Oxidative upgrade of lignin – Recent routes reviewed. *Eur. Polym. J.* 2013, 49, 1151-1173.
- Laurichesse, S., Avérous, L. Chemical modification of lignins: Towards biobased polymers. *Prog. Polym. Sci.* 2014, 39, 1266-1290.
- Mahmood, N., Yuan, Z., Schmidt, J., Xu, C. Depolymerization of lignins and their applications for the preparation of polyols and rigid polyurethane foams: A review. *Renew. Sust. Energ. Rev.* 2016, 60, 317-329.
- Mahmood, N., Yuan, Z., Schmidt, J., Xu, C. Production of polyols via direct hydrolysis of kraft lignin: Effect of process parameters. *Bioresour. Technol.* 2013, 139, 13-20.